NORTHWESTERN UNIVERSITY

Studies Directed Towards the Total Synthesis of Okilactomycin and Chrolactomycin

A DISSERTATION

SUBMITTED TO THE GRADUATE SCHOOL IN PARTIAL FULFILLMENT

OF THE REQUIREMENTS

for the degree

DOCTOR OF PHILOSOPHY

Field of Chemistry

By

William Joseph Morris

EVANSTON ILLINOIS

December 2007

ABSTRACT

Synthetic Studies Directed Towards the Total Synthesis of Okilactomycin and Chrolactomycin

William Joseph Morris

Okilactomycin and chrolactomycin are antitumor antibiotics isolated in 1987 and 2001, respectively. These tetracyclic natural products possess a unique 6-5 fused tetrahydro-γ-pyrone-γ-butyrolactone. The spirocenter is part of a highly functionalized cyclohexene ring, which together with the aforementioned 6-5 system compose the core of these molecules. A six carbon, 1,3-dialkyl-substituted carbon chain tethers the tetrahydro-γ-pyrone and cyclohexene ring giving rise to a rigid macrocycle. Both okilactomycin and chrolactomycin possess antiproliferative activity against a spectrum of human tumor cell lines as well as activity against Gram-positive bacteria. The biological profile in conjunction with the unprecedented molecular architecture renders these molecules important synthetic targets. To date, no total synthesis of these natural products has been reported.

This dissertation describes various approaches towards the synthesis of these interesting molecules. During the course of these studies, a novel Lewis acid catalyzed

cyclization methodology was developed, which provides rapid access to highly substituted pyanones.

The salient features of this synthesis include a streoselective anti-aldol reaction, a stereoselective Diels-Alder reaction and a novel cascade reaction that serves to join the principal fragments of the synthesis. Following the fragment coupling reaction, a silicate-mediated conjugate addition was used to form the pyranone ring. Following the presumed completion of the synthesis, it was determined that a diastereomer of the okilactomycin was actually prepared. We found through extensive experimentation that the silicate-mediated conjugate addition step was under thermodynamic control, which resulted in the formation of undesired diastereomers. Based on these data, we report preliminary studies on a third generation synthesis, which seeks to carry out the key conjugate addition under kinetic control.

_____

Thesis Advisor: Professor Karl A. Scheidt

Acknowledgements

First, I wish to extend my deepest gratitude to my research advisor, Professor Karl A. Scheidt. I consider myself fortunate to have had the opportunity to work in your group and benefit from your tireless pursuit of excellence. Your mentorship has enriched my graduate experience and for this, I am forever grateful.

I would also like to thank Professor Richard Silverman for his insightful questions and helpful suggestions during my time at Northwestern. I would like to acknowledge Dr. Daniel Appella, and Professor Frederick Lewis for their advice during my graduate studies. I would also like to acknowledge Professor Regan Thomson for his helpful discussions, most notably about the finer points of an asymmetric Diels–Alder reaction. I would also like to thank Dr Steve Wittenberger for his constant motivation and genuine interest in helping not only me, but the entire Scheidt group.

During my time in the Scheidt lab, I had the opportunity to work with several talented individuals. I would first like to thank my fellow Blue Team member, Dan Custar. Your hard work and dedication to the project is reflected in this document. I want thank my fellow office-mates, Chris Galliford, Anita Mattson, Audrey Chan and Brooks Maki for their friendship, interesting conversation and constant support.

I also want to acknowledge the A lab for making my experience memorable. I want to especially thank Troy Reynolds for allowing me to be a member of his social club. Rob Lettan, Dr. Margaret Biddle and Dr. Manabu Wadamoto have been valued coworkers who are always willing to offer helpful suggestions. I would also like to acknowledge Eric Phillips who has brought so much to the group in a short period of time.

I also want to thank the newest members of the laboratory, Dr. Alex Mathies, Dustin Raup, Antoinette Nibbs, and Tom (I am a real doctor) Zabawa for informative and entertaining discussions.

I would be remiss if I did not acknowledge Dr. Ashwin Bharadwaj for his continued friendship. I will always hold the work you did in this laboratory in the highest regard. Additionally, I want to thank Jon Pokorski. The beginning of graduate school was challenging for so many reasons and I'm not sure I would have made it past the first year without your friendship.

Finally, I want to thank my family and friends. Your constant support during this endeavor will not be forgotten.

List of Abbreviations

4Å MS	4 angstrom molecular sieves
Ac	acetyl
BHT	butylated hydroxytoluene
Bn	benzyl
Bu	butyl
°C	degrees Celsius
Cy	cyclohexyl
DBU	1,8-diazabicyclo[5.4.0]undec-7-ene
δ	chemical shift (parts per million)
DET	diethyl tartrate
DIBAL-H	diisobutylaluminum hydride
DMAP	4-dimethylaminopyridine
DMDO	dimethyldioxirane
DMF	dimethylformamide
DMS	dimethylsulfide
DMSO	dimthyl sulfoxide
dr	diastereomeric ratio
ee	enantiomeric excess
equiv	equivalents
Et	ethyl
Et_2O	diethyl ether

EtOAc	ethyl acetate
EtOH	ethanol
g	gram
HDA	hetero Diels-Alder
IMDA	intramolecular Diels-Alder
IR	infrared spectrum
J	coupling constant
KHMDS	potassium hexamethyldisilazane
LDA	lithium diisopropylamide
LiHMDS	lithium hexamethyldisilazane
LRMS	low resolution mass spectrometry
M	molar (concentration)
Me	methyl
MeCN	acetonitrile
MeOH	methanol
Mes	mesityl
mg	milligram
mL	milliliter
NaHMDS	sodium hexamethyldisilazane
NBS	*N*-bromosuccinamide
NIS	*N*-iodosuccinamide
NMO	*N*-methyl morpholine-*N*-oxide
NMR	nuclear magnetic resonance

NOE	nuclear Overhauser effect
OTf	trifluoromethanesulfonate
Ph	phenyl
PPTS	pyridinium *p*-toluenesulfonic acid
RCM	ring closing metathesis
TAS-F	tris(dimethylamino)sulfonium-difluorotrimethylsilicate
TBAF	tetrabutylammonium fluoride
TBAT	tetrabutylammonium triphenyldifluorosilicate
TBDPS	*tert*-butyldiphenylsilyl
TBHP	*tert*-butyl hydrogen peroxide
TBS	*tert*-butyldimethylsilyl
TES	triethylsilyl
TFA	trifluoroacetic acid
THF	tetrahydrofuran
THP	tetrahydropyran
TLC	thin layer chromatography
TMS	trimethylsilyl
TMSCN	trimethylsilyl cyanide
Tol-BINAP	2,2'-bis(di-*p*-tolylphosphino)-1,1'-binaphthyl
TPAP	tetra-*N*-propylammonium perruthenate

Dedication

To Mom and Dad

Table of Contents

1.1 Introduction 17
1.2 Isolation and Characterization 17
1.3 Tetronic Acid Natural Products 18
1.3.1 (–)-Chlorothricolide 19
1.3.2 Quartromicin D_3 21
1.3.3 Abyssomicin C 23
1.4 Biosynthesis 25
1.4.1 Okilactomycin Biosynthesis 26
1.5 Biological Activity of Okilactomycin and Chrolactomycin 28
1.5.1 Antimicrobial activity 28
1.5.2 Antitumor Activity 28
1.5.3 Telomerase and Cancer 30
1.6 Previous Studies Directed Towards the Synthesis of Okilactomycin and Chrolactomycin 31
1.6.1 Takeda's Biomimetic Approach 31
1.6.2 Paquette's Approach 33
2.1 Okilactomycin and Chrolactomycin as Synthetic Targets 38
2.2 Tetrohydropyran and Tetrahydropyranone Heterocycl**es** 38
2.2.1 Hetero Diels-Alder Reaction 39
2.2.2 The Prins Cyclization 40
2.2.3 The Petasis-Ferrier Rearrangement 41
2.2.4 Intramolecular Strategies 42
2.3 First Generation Approach Towards the Synthesis of Okilactomycin & Chrolactomycin 42
2.3.1 Retrosynthetic Analysis 43
2.3.2 Tandem Aldol/Conjugate Addition Model Studies 44
2.3.3 Revisions to the Synthetic Plan 50
2.4 Target-Inspired Method Development 52
2.4.1 Optimization of Dioxinone Addition to Aldehydes 55
2.4.2 Evaluation of the Aldehyde Scope 56

2.4.3 Multicomponent Approach 57
2.4.4 Mechanistic Considerations 58
2.4.5 Synthetic Utility 59
2.5 Second Generation Approach 62
2.5.1 Revised Retrosynthesis 62
2.5.2 Model Study 62
2.6 Synthesis of Principal Fragments 63
2.6.1 Synthesis and Elaboration of Dioxinone Fragment **II-51** 63
2.6.2 Synthesis and Elaboration of **II-52** 67
2.6.3 Diels–Alder Approach to Cyclohexene Fragment 71
2.6.4 Revised Model Study 77
2.6.5 Novel Fragment Assembly 78
2.6.6 Intramolecular Conjugate Addition 82
2.7 Completion of the Synthesis 91
2.7.1 Formation of the Macrocycle 91
2.7.2 Stereochemical Studies 94
2.7.3 NMR Spectroscopic Analysis of **II-104** 96
2.8 Completion of the Synthesis 98
2.8.1 Manipulation of the C18 Oxidation State 99
2.8.2 Protecting Group Strategy 99
2.8.3 Reduction Studies 102
2.8.4 Installation of the Exomethylene Unit 106
2.8.5 Reconsidering the End Game Strategy 108
2.9 Revised Diels-Alder Route 109
2.9.1 Syntheis of New α-hydroxy aldehyde 110
2.10 Discussion 112
2.11 Third Generation Approach Towards the Synthesis of Okilactomycin and Chrolactomycin 117
2.12 Conclusion 118
2.13 Experimental Section 119
2.13.1 General Procedure for $Sc(OTf)_3$-catalyzed cyclizations 120

2.13.2 General Procedure for One-pot cyclization/Ring Opening 120
2.13.3 Preparation of β-hydroxy-dioxinone **II-28** 121
2.13.4 Pyran Characterization 121
2.13.5 Pyranone Characterization Data 126
2.13.6 Characterization Data for Selected Intermediates 131
2.13.7 Select NMR Spectra 161

List of Tables:

Table 2-1. Optimization of Reaction Conditions 56
Table 2-2. Aldehyde Scope 57
Table 2-3. One Pot Cyclization/Ring Opening 58

List of Schemes:

Scheme 1-1. Yoshii's Approach Towards (–)-Chlorothricolide 20
Scheme 1-2. Roush's Approach to (–)-Chlorothricolide 21
Scheme 1-3. Roush's Synthesis of the Spirotetronate Monomers 23
Scheme 1-4. Sorensen's Approach Towards Abyssomicin C 25
Scheme 1-5. Yoshii's Approach Towards Okilactomycin 32
Scheme 1-6. Yoshii's [2+2] Model Result 33
Scheme 1-7. Paquette's Synthesis of Aldehyde **I-42** 35
Scheme 1-8. Completion of Aldehyde I-42 35
Scheme 1-9. Paquette's Approach Towards Cyclohexene **I-43** 36
Scheme 2-1. Preparation of Model Substrate 45
Scheme 2-2. Synthesis of New Acylation Partner 46
Scheme 2-3. Acylation of Tertiary Alcohol **II-7** 47
Scheme 2-4. Synthesis of the α-Hydoxy Aldehyde Coupling Partner 48
Scheme 2-5. Evaluation of Intermolecular Variant 49
Scheme 2-6. Tandem Knöevenagel/Conjugate Addition 51
Scheme 2-7. Tandem Knöevenagel/Conjugate Addition Model Studies 51
Scheme 2-8. Competing Side Reactions 52
Scheme 2-9. Tandem Knöevenagel/conjugate addition with $Sc(OTf)_3$ 53

Scheme 2-10. Synthetic Utility 60
Scheme 2-11. Diversity Oriented Synthesis from Pyran Bicycle 61
Scheme 2-12. Model System for $Sc(OTf)_3$ Catalyzed Cyclization 63
Scheme 2-13. Synthesis of Non-Racemic Aldehyde **II-53** 65
Scheme 2-14. Anti-Aldol Reaction 66
Scheme 2-15. Elaboration of the Dioxinone Fragment 67
Scheme 2-16. Attempt to Generate the Vinylidine Carbene 68
Scheme 2-17. Synthesis of Enone **II-69** via C–H Insertion 69
Scheme 2-18. Cuprate Addition to Enone **II-69** 70
Scheme 2-19. Circumventing the Allyl Cuprate Problem 71
Scheme 2-20. Alkylation Problems 71
Scheme 2-21. Synthesis of Diene **II-55** 74
Scheme 2-22. Stereoselective Diels-Alder Reaction 74
Scheme 2-23. Synthesis of α-Hydroxy Aldehyde **II-74** 76
Scheme 2-24. Revised Model Study 78
Scheme 2-25. Model for Novel Fragment Assembly 78
Scheme 2-26. Key Fragment Assembly 80
Scheme 2-27. Thermal Decomposition of β-Keto Ester **II-93** 81
Scheme 2.28. Modified Fragment Assembly Conditions 82
Scheme 2-29. Deprotection of the Butenolide 83
Scheme 2-30. Acid Survey 84
Scheme 2-31. Base Survey 85
Scheme 2-23. Lewis acid Survey 86
Scheme 2-33. Thiourea Survey 86
Scheme 2-34. Transition Metal Survey 87
Scheme 2-35. Silicate-Mediated Conjugate Addition 88
Scheme 2-36. Survey of Fluoride Sources 89
Scheme 2-37. Survey of Acid Additives 90
Scheme 2-38. Prepartion of the Tetracyclic Core 92
Scheme 2-38. Alkylation at C11 93
Scheme 2-40. Rizzacasa's Synthesis of (–)-Apicularen 94

Scheme 2-41. Synthesis of C8 Epimer 95
Scheme 2-42. Synthesis of C8 Epimer Continued 96
Scheme 2-43. Manipulation of the C18 Oxidation State 99
Scheme 2-44. Preparation of Model Pyranone **II-119** 100
Scheme 2-45. Me_3SnOH in Organic Synthesis 101
Scheme 2-45. Competition Experiment 102
Scheme 2-47. Reduction of Model Olefin **II-126** 103
Scheme 4-48. Reduction of Model Olefin Suing Diimide 104
Scheme 2-49. Protection of the Carboxylic Acid **II-116** 104
Scheme 2-50. Attempted Reduction of **II-128** 105
Scheme 2-51. Reduction of Macrocyclic Olefin Using PtO_2 106
Scheme 2-54. Installation of the Exomethylene Group 108
Scheme 2-55. Completion of the Synthesis 109
Scheme 2-56. Revised Synthesis of α-hydroxy aldehyde **II-74** 111
Scheme 2-57 Determination of Optical Purity 114
Scheme 2-58. Potential Outcomes of the Conjugate Addition 116
Scheme 2-59 Third Generation Approach 118

List of Figures:

Figure 1-1. Okilactomycin and Chrolactomycin 18
Figure 1-2. Tetronic Acid Substitution Patterns 19
Figure 1-3. Quartromicin D_3 21
Figure 1-4. Proposed Biosynthesis of Abyssomicin C 24
Figure 1-5. Claisen Condensation Step in Polyketide Biosynthesis 26
Figure 1-6. Proposed Biosynthesis of Okilactomycin and Chrolactomycin 27
Figure 1.7. Biological Activity of Okilactomycin and Chrolactomycin 29
Figure 1-8. Telomeres and Telomerase 31
Figure 1-9. Paquette's Retrosynthetic Analysis 34
Figure 2-1. Okilactomycin and Chrolactomycin 38
Figure 2-2. Tetrahydropyranones Using the Hetero Diels-Alder Reaction 39
Figure 2-3. Tetrahydropyran Synthesis Using the Prins Reaction 40
Figure 2-4. Tetrahydropyanone Synthesis Using the Petasis-Ferrier Rearrangement 41

Figure 2-5. Alternative Methods for the Synthesis of Pyrans.....42
Figure 2-6. Proposed Tandem Aldol/Conjugate Addition Reaction.....43
Figure 2-7. Retrosynthetic Analysis.....44
Figure 2-8. Dioxinones as β-Ketoester Precursors 46
Figure 2-9. Thermodynamic Equilibrium.....49
Figure 2-10. Revised Synthetic Plan 50
Figure 2-11. Potential Reaction Pathways.....54
Figure 2-12. Tetrahydropyranones from Dioxinones and Aldehydes.....55
Figure 2-13. Proposed Reaction Pathway.....59
Figure 2-14. Revised Retrosynthetic Analysis.....62
Figure 2-15. Proposed Reactive Conformer in Pseudoephedrine Alkylations 64
Figure 2-16. Proposed Mechanism for Anti-Aldol Reaction.....66
Figure 2.17. Proposed Mechanism for Conversion of **II-67** to **II-66** 69
Figure 2-18. Revised Retrosynthetic Analysis.....72
Figure 2-19. Model for Stereoinduction using Chiral Oppolzer Sultam.....75
Figure 2-20. Mechanism for the Formation of Butenolide **II-90**.....79
Figure 2-21. Conjugate Addition Considerations 82
Figure 2-22. Tenative Structural Assignment of Minor Diastereomer 94
Figure 2-23. Key NOE Signals of **II-104**.....97
Figure 2-24. Key NOE Sgnals for **II-104**.....97
Figure 2-25. Mechanism of Hydrogenation by $(Ph_3P)_3RhCl$ 105
Figure 2-26. Potential Outcomes of Diels-Alder Reaction..... 111
Figure 2-27. Analysis of ^1H NMR Spectra of Butenolides 113
Figure 2-28 Proposed structure of minor product from Diels Alder Reaction..... 115

Chapter 1

Okilactomycin and Chrolactomycin Overview

1.1 Introduction

Nature has supplied the synthetic chemist with a variety of targets for total synthesis. The plethora of molecular architectures supplied from nature's biosynthetic machinery provides the forum to push forward the current limitations associated with synthetic methodology. In addition to driving the evolution of synthetic methods, natural products serve as starting points for the development of chemotherapeutic agents. A recent report reveals that natural products have led to over 60% of the small molecule drugs brought to the market over the past 20 years.[1] Furthermore, natural products have emerged as powerful tools for studying cellular biology.[2,3] By using large libraries composed of natural product-like compounds, the intricate signaling network of cells is being dissected. Undeniably, organic synthesis continues to fuel our understanding of biological systems by providing access to new and diverse molecular structures.

1.2 Isolation and Characterization

In 1987, a research group at Yamanouchi Pharmaceuticals reported the basic structure of a new antibiotic okilactomycin **I-1** isolated from a specific strain of *Streptomyces griseoflavus* that was originally cultured from an Okinawan soil sample.[4,5] In 2001, a separate group at the Pharmaceutical Research Institute of the Kyowa Hakko Kogyo Company described the isolation of the natural product chrolactomycin **I-2** from a different strain of *Streptomyces*.[6] The structure of okilactomycin was determined by a combination of spectroscopic and X-ray crystallographic studies. Chrolactomycin was elucidated using NMR techniques and by comparison to okilactomycin. Notably, chrolactomycin possesses the same basic core structure and relative stereochemistry as

okilactomycin. The difference between **I-1** and **I-2** is a single modification of the C11 position (Figure 1-1). The absolute stereochemistry of these interesting natural products remains unknown. These tetracyclic natural products possess a unique 6-5 fused tetrahydro-γ-pyrone-γ-butyrolactone ring system that is unprecedented in the literature. The C13 spirocenter is part of a highly functionalized cyclohexene ring, which together with the aforementioned 6-5 system compose the core of these molecules. A six carbon, 1,3-dialkyl-substituted carbon chain tethers the tetrahydro-γ-pyranone and cyclohexene ring giving rise to a rigid 11-membered macrocycle. The spirocyclic portion of okilactomycin and chrolactomycin evokes comparison to the spirotetronic acid natural products (e.g. kijanolide, chlorothricolide and quartromycin). The key difference between **I-1** and **I-2** and the spirotetronates is that the tetronic acid has been functionalized giving rise to the tetrahydro-γ-pyranone. Additionally, the relative stereochemistry of the cyclohexene of **I-1** and **I-2** is different from many of the related spirotetronic acids.

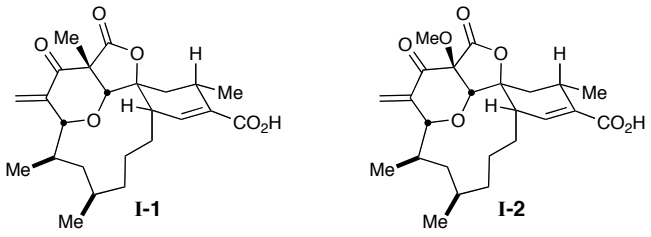

Figure 1-1. Okilactomycin and Chrolactomycin

1.3 Tetronic Acid Natural Products

The structures of okilactomycin and chrolactomycin are reminiscent of several other spirotetronate natural products. A subclass of these spirotetronate natural products are tetronic acids. These structures are characterized by a five-membered vinylogous acid

ring. The ubiquitous nature of these compounds in bioactive natural products has inspired interest from the synthetic community. Many of these targets exhibit antibiotic, antitumor, anticoagulent, antiepileptic, antifungal, analgesic, and anti-inflammatory properties. The synthetic efforts directed towards the synthesis of spirotetronate natural products has recently been reviewed.[7]

There are 4 classes of tetronic acids, which are typically classified by the substitution at C5 (Figure 1-2). These include 5-ylidene tetronic acids, 5-monosubstituted tetronic acids, 5,5-disubstituted tetronic acids, and 5-unsubstituted tetronic acids. The progress made in the area of 5,5-disubstituted tetronic acids will be discussed briefly focusing on natural products that possess structures similar to that of **I-1** and **I-2**.

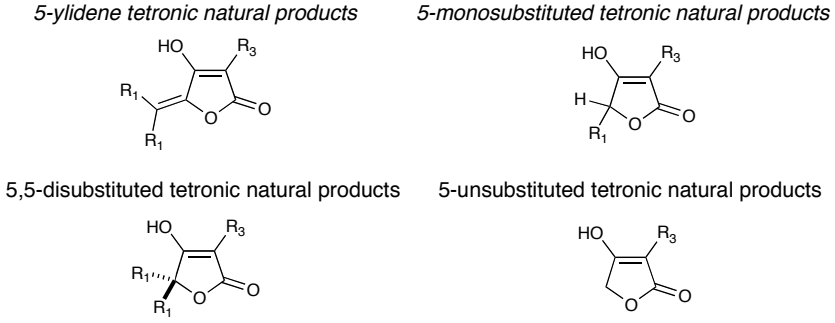

Figure 1-2. Tetronic Acid Substitution Patterns

1.3.1 (–)-Chlorothricolide

In 1969 chlorothricin and its aglycon chlorothricolide **I-3**, were isolated from *Streptomyces antibioticus*.[8] These interesting structures inspired a variety of synthetic efforts directed towards their synthesis.[9]

In 1990 Yoshii reported the first synthesis of (±)-chlorothricolide as its 24-*O*-methyl derivative **I-4**.[10] An intramolecular Diels–Alder reaction was used to prepare the octalin ring system. After further manipulations, Diels–Alder precursor **I-5** was heated to 180 °C and provided the desired cycloadduct **I-6** in 9% after chromatography. There were no subsequent reports from this laboratory describing the synthesis of **I-3**.

Scheme 1-1. Yoshii's Approach Towards (–)-Chlorothricolide

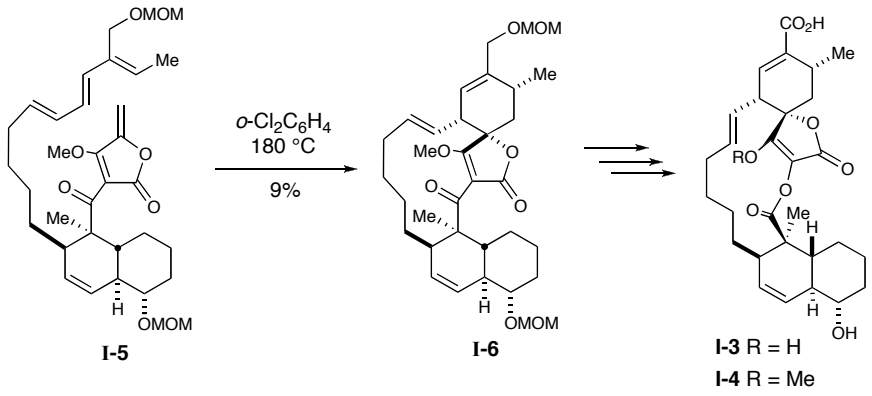

Roush and co-workers were eventually able to complete the total synthesis of **I-3** in 1994.[11] The enantioselective total synthesis was completed via an elegant, tandem inter- and intramolecular Diels–Alder (IMDA) reaction of hexaenoate **I-7** and the chiral dienophile (*R*)-**I-8** (Scheme 1-2). This remarkable reaction establishes 7 asymmetric centers in a single operation. The stereochemical outcome of the IMDA is largely dictated by the C9-trimethylsilyl group, which promotes formation of the trans-fused octalin ring system. The intermolecular Diels–Alder reaction is highly diastereofacial and exo selective.

Scheme 1-2. Roush's Approach to (–)-Chlorothricolide

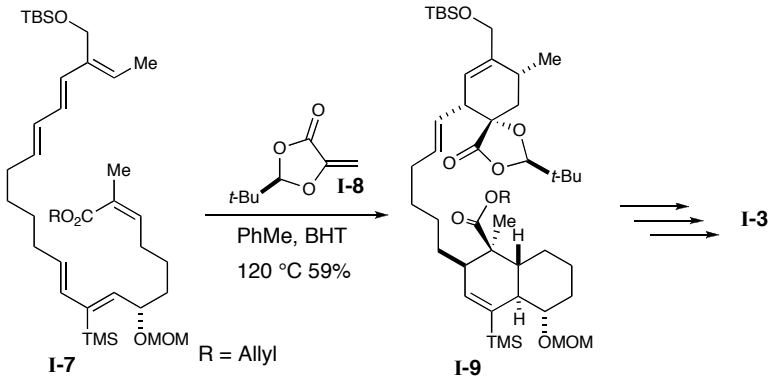

1.3.2 Quartromicin D_3

The quartromicins are a group of tetrameric natural products isolated from *actinomycetes* species in 1991.[12,13] One such member of this class of natural products is Quartromicin D_3 **I-10** (Figure 1-3). This imposing target possesses a 32-member carbocyclic core, which is made up of four spirotetronic acid units linked by substituted enones in a head-to-tail manner. The structural complexity of this molecule is magnified by the fact that the tetramer is made up of two distinct spirotetronate units that are epimeric at the spiro linkage.

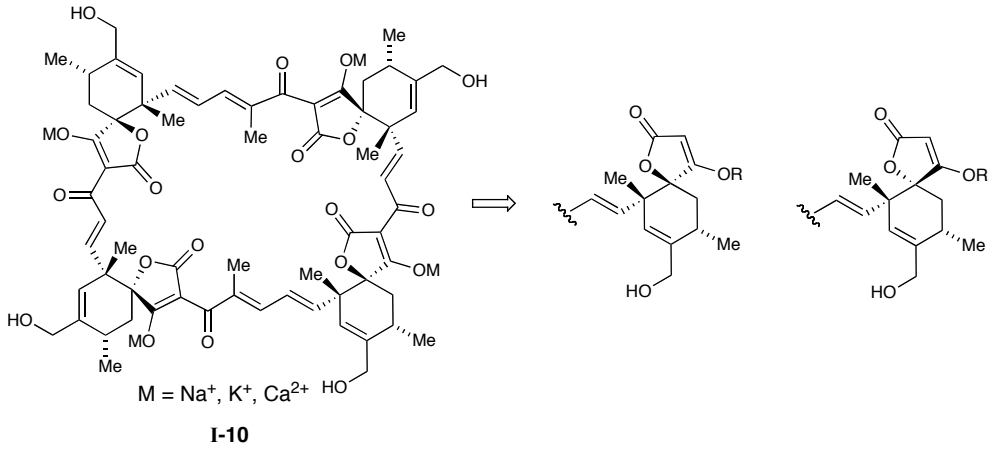

Figure 1-3. Quartromicin D_3

The quartromicin natural products possess potent inhibitory activity against herpes simplex virus (HSV), influenza, and human immunodeficiency virus (HIV). This biological activity combined with the unique structure makes these molecules very interesting targets for total synthesis.

The Roush group[14-18] has been actively pursuing the quartromicins, focusing on strategies to prepare the individual monomers of **I-10** and related structures. Their earliest reports focused on a stereoselective methylaluminum dichloride promoted Diels-Alder reaction between chiral *N*-acryloyl sultam **I-11** and diene **I-12** (Scheme 1-3). The resulting cycloadduct is reduced to aldehyde **I-13** and ultimately converted to spirotetronate **I-14**. A similar strategy was employed to access the epimeric spirotetronate monomer. A stereoselective [4+2] cycloaddition between diene **I-12** and non-racemic dienophile **I-15** produced the endo adduct with acceptable levels of stereocontrol (5:1). The auxiliary was removed under reductive conditions to produce diol **I-16**, which was ultimately converted to the epimeric monomer **I-17** (Scheme 1-3).

Scheme 1-3. Roush's Synthesis of the Spirotetronate Monomers

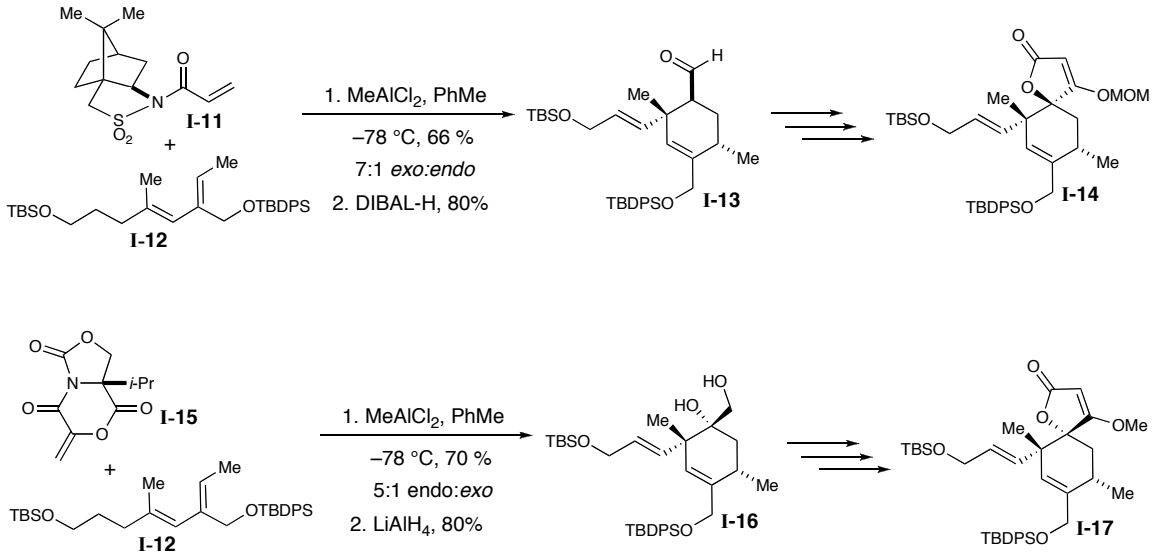

1.3.3 Abyssomicin C

Abyssomicin C **I-18** was recently isolated from a sediment sample collected at a depth 289 m beneath the surface of the Sea of Japan.[19] Abyssomicin C can inhibit Gram-positive bacteria, including pathogenic methicillin-resistant and vancomycin-resistant-*Staphylococcus aureus* strains. In addition to its antibiotic activity, abyssomicin C is an inhibitor of tetrahydrofolate biosynthesis by blocking the conversion of chorismate to *para*-amino-benzoic acid (pABA). Consequently, abyssomicin C is an attractive lead for the development of new antibacterial drugs.

The absyssomicins are spirotetronates with a novel level of structural complexity. The spirotetronic acid bridges the cyclohexene ring giving rise to a tricyclic ring system with a oxabicyclo[2.2.2]octane ring.

From a biosynthetic perspective the *anti* relationship between the hydroxyl group and the oxygen bridge of the oxabicyclo[2.2.2] octane core could potentially arise from transannular epoxide ring opening by the spirotetronic acid **I-19** (Figure 1-4). It has also

been proposed that the epoxide precursor **I-20** could arise biosynthetically from an intramolecular Diels–Alder reaction. These biosynthesis proposals have guided the synthetic efforts towards this molecule.

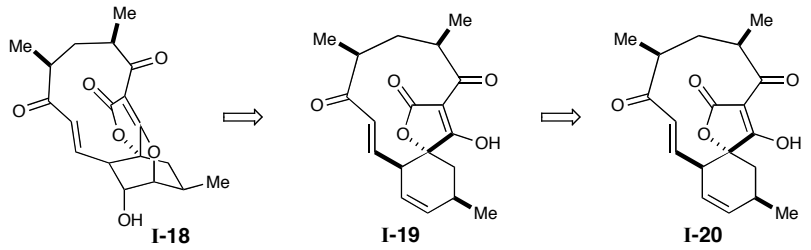

Figure 1-4. Proposed Biosynthesis of Abyssomicin C

Sorensen and co-workers reported the first total synthesis of (–)-abyssomicin C.[20,21] Their route was based largely on the biosynthetic proposal discussed previously. The IMDA precursor (**I-21**) was heated to 100 °C in the presence of $La(OTf)_3$ (Scheme 1-4). The desired cycloadduct **I-22** was formed in good yield as a single diastereomer. The late stage epoxidation was carried out in the presence of DMDO and was followed by nucleophilic demethylation to give tetronic acid **I-23**. The synthesis was completed by warming a solution of **I-23** in MeCN with TsOH and LiCl to furnish abyssomicin C.

Scheme 1-4. Sorensen's Approach Towards Abyssomicin C

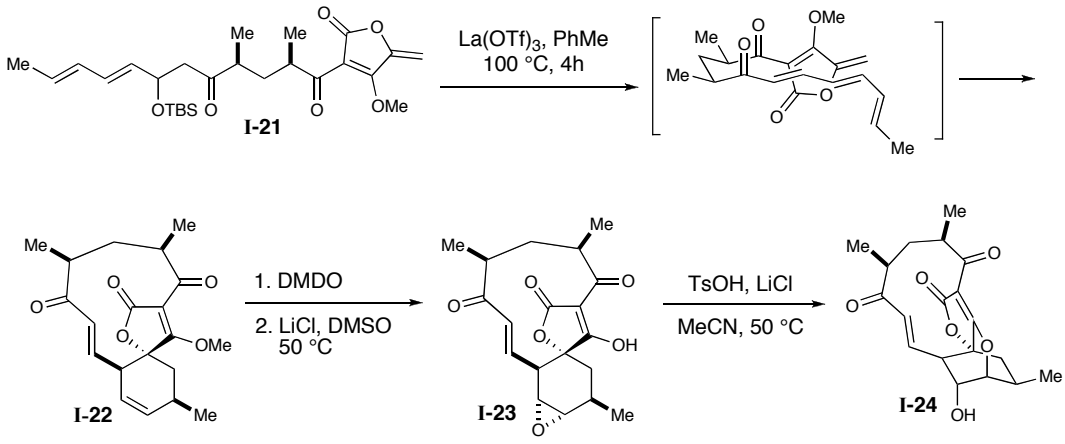

Following this report, the research groups of Snider,[22] Couladourus[23] and Nicolaou[24] presented formal total syntheses of abyssomicin C.

1.4 Biosynthesis

Polyketides are a structurally diverse class of natural products.[25] In recent years, many of the genes encoding a number of polyketide biosynthetic pathways have been studied leading to a general understanding of how nature constructs these fascinating secondary metabolites. Nature utilizes a decarboxylative Claisen condensation with malonic acid half thioesters as ester enolates as the key carbon-carbon bond forming step in polyketide and fatty acid biosynthesis.

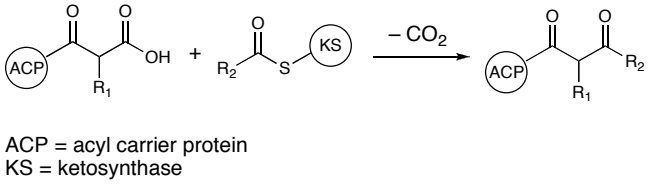

Figure 1-5. Claisen Condensation Step in Polyketide Biosynthesis

The enzymes involved in polyketide biosynthesis are responsible for the stepwise chain elongation and are known as polyketide synthtases. The growing polyketide chain is anchored on a ketosynthase (KS) via a thioester linkage. The acyl transferase (AT) is responsible for transferring an α-carboxylated nucleophilic extender unit from the acyl-CoA to the acyl carrier protein (ACP). The acyl-KS and the acyl-ACP catalyze C–C bond formation leading to a β-ketoacyl-ACP intermediate. After enzymatic modification the newly elongated chain is now transferred to a different KS and a new chain elongation cycle may begin.

1.4.1 Okilactomycin Biosynthesis

Shortly after the isolation and characterization of okilactomycin, Omura and co-workers used ^{14}C labeling experiments to identify the polyketide nature of okilactomycin.[26] The authors did not use this data to propose a biosynthesis for okilactomycin. Based on these experiments by Omura in conjunction with recent reports[27] describing the biosynthesis of spirotetronate natural products, we have proposed a partial biosynthesis of okilactomycin (Figure 1.6).

An acyclic precursor is built iterativly using the model for polyketide biosynthesis described previously (Figure 1-6). Once the desired length is achieved the ACP bound β-keto thioester is cleaved from the ACP by the hydroxyl group of enol pyruvate **I-25**. The resulting β-keto ester **I-26** undergoes cyclization to form the characteristic tetronic acid **I-27**. An intramolecualr Diels-Alder macrocyclization[28] then takes place to form the fully elaborated spirotetronic acid **I-28**.

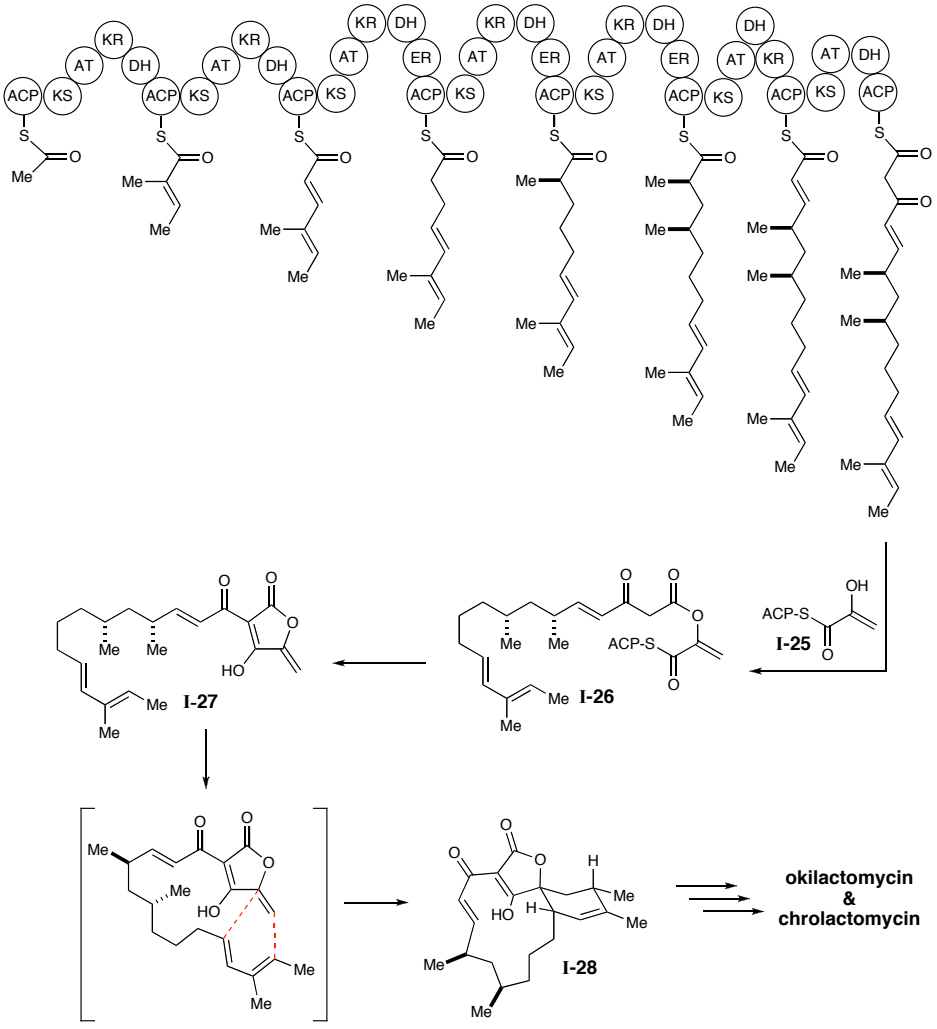

Figure 1-6. Proposed Biosynthesis of Okilactomycin and Chrolactomycin

1.5 Biological Activity of Okilactomycin and Chrolactomycin

1.5.1 Antimicrobial activity

Okilactomycin exhibited weak antimicrobial activity against Gram-positive organisms with MIC (minimum inhibitory concentration) ranging from 12.5 to 50 μg/ml. There was no observed activity against Gram-negative organisms.

Chrolactomycin possesses activity against Gram-positive bacteria such as *Staphylococcus aureus, Bacillus subtilis*, and *Enterococcus hirae*, but is not active against Gram-negative bacteria.

1.5.2 Antitumor Activity

Okilactomycin possess cytotoxic activity against lymphoid leukemia L1210 and leukemia P388 with IC_{50} values of 0.09 and 0.037 μg/ml respectively. Additionally, okilactomycin exhibited antitumor activity against Ehrlich ascites carcinoma, suggesting that it may also have antitumor activity *in vivo*.

Chrolactomycin exhibited antiproliferative activity against human tumor cell lines with IC_{50} values ranging from 0.45-1.6 μM. The antiproliferative activity was comparable to that of VP-16 (etoposide), a chemotherapy for a variety of cancers.

Okilactomycin

Antimicrobial		Antiproliferative	
Test Organism	MIC (μg/ml)	Cell Lines	IC_{50} (μg/ml)
Staphylococcus aureus	25	L1210	0.09
S. epidermidis	12.5	P388	0.037
Streptococcus pyogenes	12.5		

Chrolactomycin

Antimicrobial		Antiproliferative	
Test Organism	MIC (μg/ml)	Cell Lines	IC_{50} (μM)
Staphylococcus aureus	5.2	ACHN	1.2
Bacillus subtilis	5.2	A431	1.6
Enterococcus hirae	10.4	MCF-7	0.69
		T24	0.45

Figure 1.7. Biological Activity of Okilactomycin and Chrolactomycin

Recently, Nakai and coworkers identified chrolactomycin as a telomerase inhibitor.[29] The authors propose that this highly electrophilic[30] exomethylene group covalently modifies telomerase via addition of a sulfhydryl group from a cysteine residue. This result suggests okilactomycin and chrolactomycin may be valuable lead structures for the development of novel cancer therapies acting on human telomerase. This could possibly represent the mode of action of this compound and warrants a brief discussion of the relationship between telomerase and cancer.

1.5.3 Telomerase and Cancer

Weinberg has suggested that limitless replicative potential is one of the six hallmarks of cancer.[31] Many mammalian cells are programmed to limit the number of replication cycles in a lifetime. Once the cells have progressed through a certain number of replication cycles, they stop growing and enter a state of senescenece. This takes place when telomeres,[32] repetitive DNA sequences at the ends of chromosomes that protect the termini from being recognized as double-strand breaks, reach a critically shortened length and enter irreversible growth arrest (Figure 1-8). Telomeres progressively shorten in human cells during replication as a result of incomplete replication of the lagging strand DNA synthesis (the 'end replication problem'). Telomeres have thus been described as molecular clocks that count the number of times a cell has divided, and determine when cellular senescence occurs.

In contrast to normal cells, tumor cells typically have shortened telomeres that never reach the critical length to enter growth arrest. This suggests telomere stability is required for cells to replicate indefinitely. This telomere maintenance that is common to malignant cells is carried out by the enzyme telomerase.[33,34] Telomerase is a ribonucleoprotein enzyme complex that maintains the telomeric ends by adding G-rich strands of telomere repeats. Consequently, telomerase activation is the main pathway by which cells become immortal.

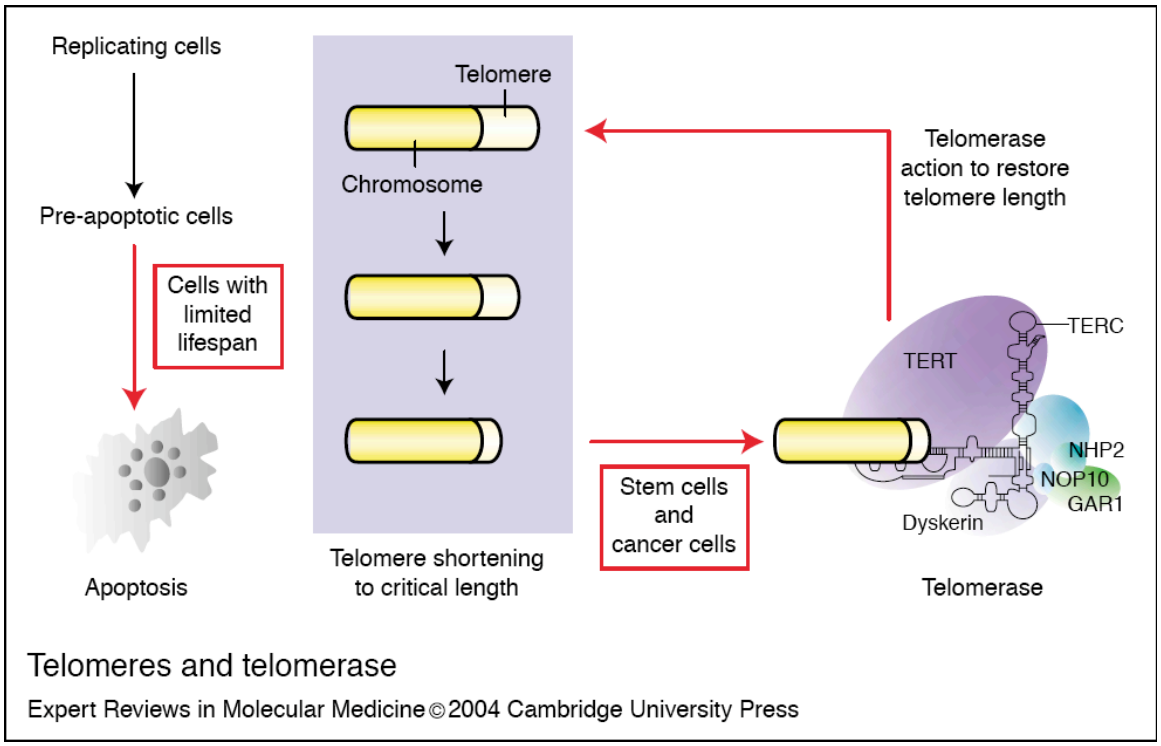

Figure 1-8. Telomeres and Telomerase

1.6 Previous Studies Directed Towards the Synthesis of Okilactomycin and Chrolactomycin

1.6.1 Takeda's Biomimetic Approach

In 1992, Takeda and coworkers disclosed the first report related to the synthesis of okilactomycin.[35] They were interested in utilizing an intramolecular Diels-Alder reaction to construct the macrocycle and the cyclohexene rings in a single synthetic operation. A similar strategy was successfully applied to the synthesis of (±)-24-*O*-methylchlorothricolide **I-4** in 1990.

Takeda chose to prepare a model substrate in order to test the feasibility of this approach. The synthesis of the model substrate is outlined in Scheme 1-5. The allylic sulphone **I-29** was condensed with THP protected aldehyde **I-30** to afford diene **I-31**

after reductive removal of the suulphone. The THP group was removed under acidic conditions, the resulting alcohol was oxidized to the corresponding aldehyde and homologated via Horner-Wadsworth Emmons olefination. The methyl ester **I-32** was hydrolyzed and subsequently converted to the acid chloride. The magnesium complex **I-33** was added to the acid chloride to afford the β-keto ester **I-34**. The β-keto ester was acylated, and the acetonide was cleaved under acidic conditions. The pyranone was formed under acidic conditions and the dieneophile was treated sequentially with HCl and DCC/CuCl to furnish the model substrate **I-36**.

Scheme 1-5. Yoshii's Approach Towards Okilactomycin

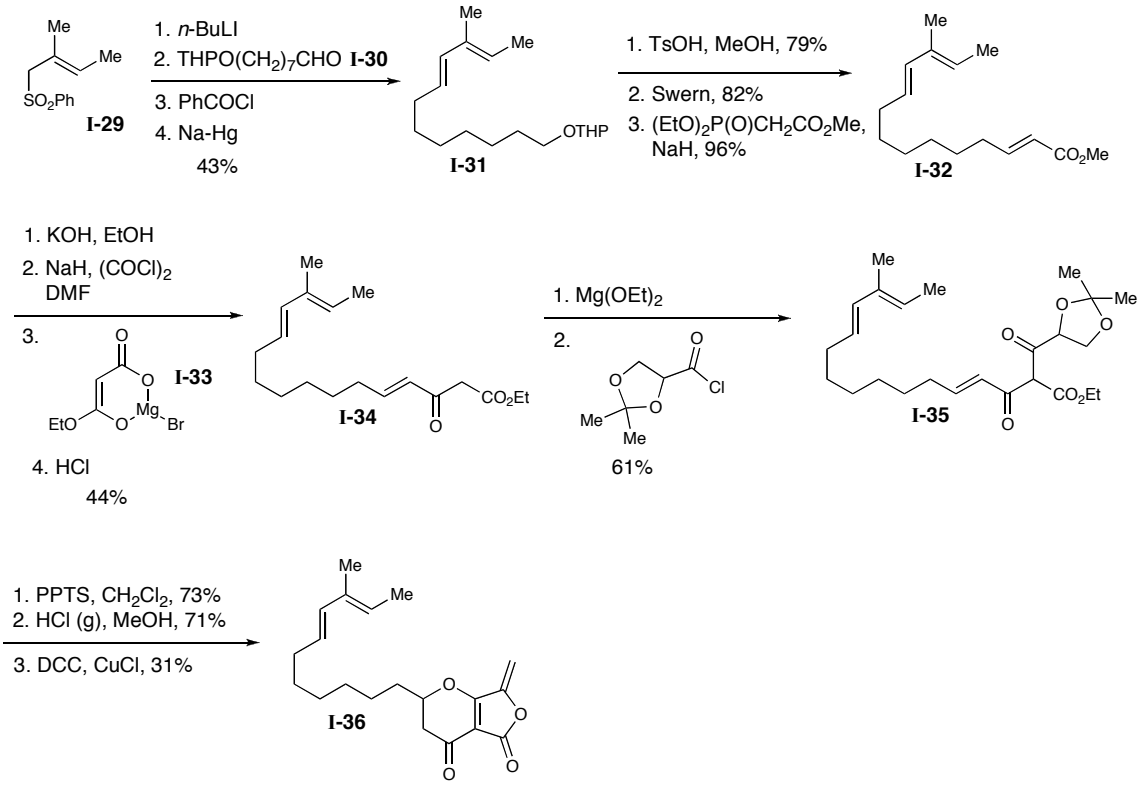

The model substrate **I-36** was treated with $SnCl_4$ at –80 °C (Scheme 1-6). Unexpectedly, four diastereomeric [2+2] cycloadducts (**I-37-I-40**) were formed instead of the desired [4+2] cycloadducts. This outcome was confirmed by x-ray crystallographic analysis.[36] There were no subsequent reports from the Takeda group regarding work in this area.

Scheme 1-6. Yoshii's [2+2] Model Result

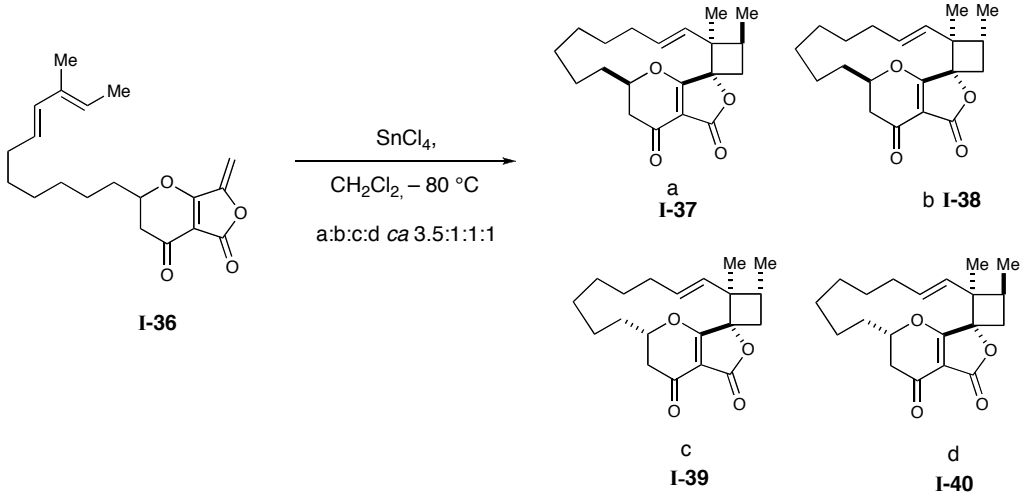

1.6.2 Paquette's Approach

Paquette and coworkers followed the seminal report by Takeda with back-to-back reports describing their strategy to okilactomycin in 2002.[37,38] Their approach involved a late stage tandem Knovenagel-Michael reaction sequence to prepare the γ-pyranone ring (Figure 1-9). The precursor for this reaction (**I-41**) would be prepared from aldehyde **I-42** and cyclohexene **I-43**. The reports describe their efforts to prepare these fragments.

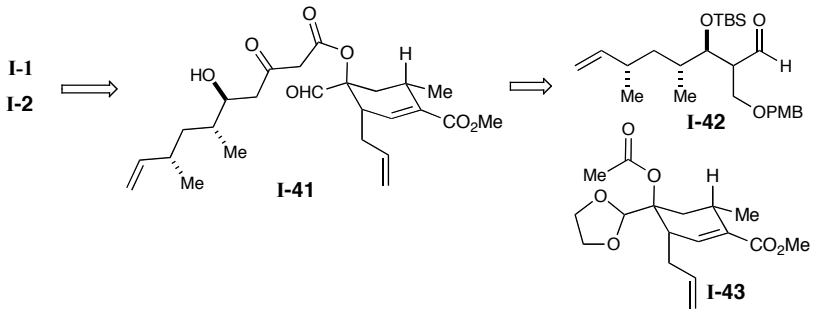

Figure 1-9. Paquette's Retrosynthetic Analysis

In the 1st article, the preparation of aldehyde **I-42** was outlined. The base catalyzed Michael addition of diethyl methylmalonate to methyl methacrylate afforded triester **I-44**. Hydrolysis and decarboxylation gave a pair of diastereomeric diacids. The diacids were cyclized under dehydrative conditions and the *meso*-anhydride **I-45** isolated after recrystallization. The anhydride **I-45** was treated with (*S*)-(–)-α-methylbenzylamine and the ring opened acid was reduced with borane•THF to give alcohols **I-46**. Carbinol **I-46** was cyclized under acidic conditions to give lactone **I-47**. The lactone was reduced to the lactol with DIBAL-H and subjected directly to Wittig olefination conditions. The primary alcohol **I-48** was oxidized under Swern conditions and homologated using ethyl (triphenylphosphoranylidene)acetate. The resulting ester was reduced and a Sharpless epoxidation yielded epoxy alcohol **I-50**.

Scheme 1-7. Paquette's Synthesis of Aldehyde **I-42**

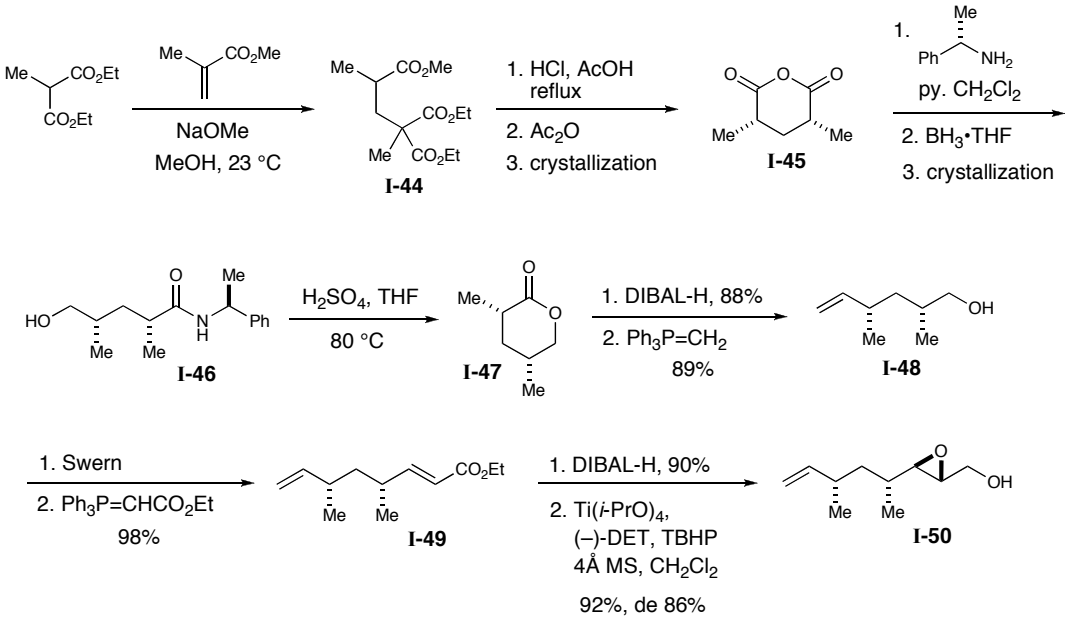

The epoxide **I-50** was opened regioselectivly by a dithiane anion. The resulting diol was orthogonally protected to afford ditiane **I-52**. The dithiane group was removed under oxidative conditions to afford aldehyde **I-42**.

Scheme 1-8. Completion of Aldehyde **I-42**

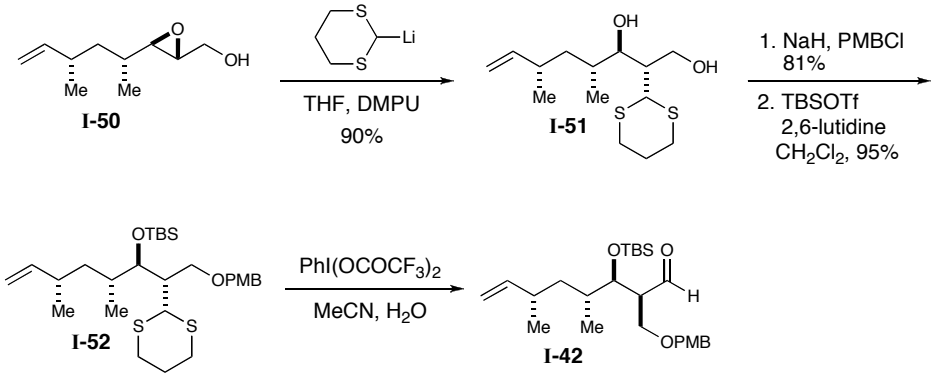

In the accompanying paper, a metathesis-based approach was outlined to prepare the cylohexene ring **I-43**. The cuprate derived from the Grignard **I-54** was added to enoyl sultam **I-53** in excellent yield and diastereoselectivity. Enolization of **I-55** with KHMDS followed by the addition of allyl iodide gave the alkylated derivative **I-56** in 64% yield and excellent diastereoselectivity. The PMB group was removed under oxidative conditions. The resulting diene was treated with Grubbs catalyst (**I-58**) providing the cyclohexene **I-59** in excellent yield. The cyclohexenyl alcohol was epoxidized under Sharpless conditions providing epoxy alcohol **I-60** as a single diastereomer. All attempts to open this epoxide with using allyl organmetallic reagents or intramolecualr allyl transfer were unsuccessful (**I-60 → I-61**).

There has not been any further report from the Paquette laboratory regarding the synthesis of okilactomycin.

Scheme 1-9. Paquette's Approach Towards Cyclohexene **I-43**

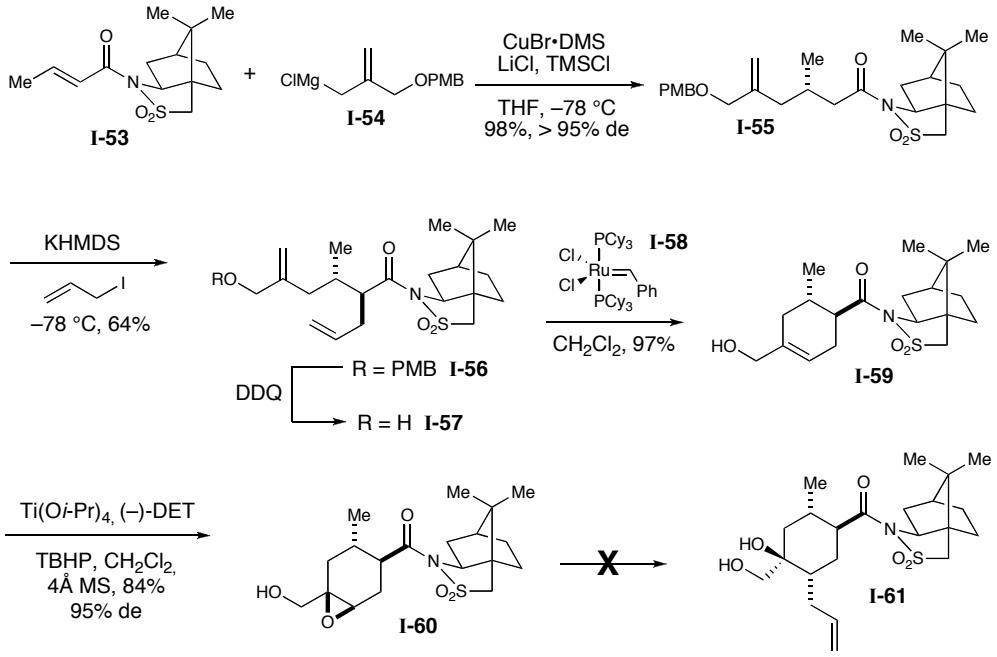

Chapter 2

Approaches Toward the Synthesis of Okilactomycin and Chrolactomycin

Portions of this chapter appear in the following publication:

Morris, W. J.; Custar, D. W.; Scheidt, K. A. "Stereoselective Synthesis of Tetrahydropyran-4-ones via a One-Pot Scandium(III) Triflate-Catalyzed Cyclization/Ring-Opening Strategy," *Org. Lett.* **2005**, *7,* 1113-1116.

2.1 Okilactomycin and Chrolactomycin as Synthetic Targets

We chose okilactomycin **II-1** and chrolactomycin **II-2** for total synthesis due to their fascinating structures and interesting biological activity. From a synthetic perspective, these tetracyclic molecules have an interesting topology and the overall structural complexity provides a significant challenge to organic synthesis. A synthesis of these molecules would provide the forum to discover new methods for organic synthesis and provide the material necessary to further elucidate their biological mode of action.

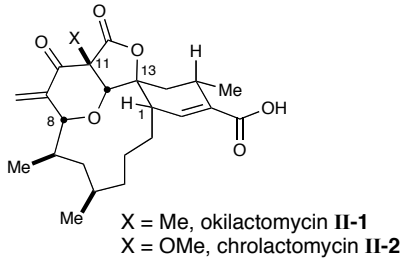

Figure 2-1. Okilactomycin and Chrolactomycin

After thorough inspection of these targets, we felt the 6-5 fused ring system would provide the greatest synthetic challenge. Consequently, we undertook a survey of the current methods available to prepare substituted pyrans in order to assess the potential of these approaches for the synthesis of okilactomycin and chrolactomycin.

2.2 Tetrohydropyran and Tetrahydropyranone Heterocycles

The large number of substituted tetrahydropyran (THP) structures in bioactive natural products has inspired the development of many strategies from many laboratories to synthesize these six membered heterocycles. The most common means to access these

structures are the hetero Diels–Alder reaction, the Prins cyclization, the Petasis–Ferrier rearrangement and etherification reactions.

2.2.1 Hetero Diels-Alder Reaction

The hetero Diels–Alder (HDA) reaction between a 2-silyloxydiene and aldehyde was pioneered by Danishefsky[39] and provides the desired six membered cycloadduct directly after aqueous work (Figure 2-2).[40-42] This HDA approach has seen broad utility in many natural product syntheses including most recently FR182877[43-45] and ambruticin.[46]

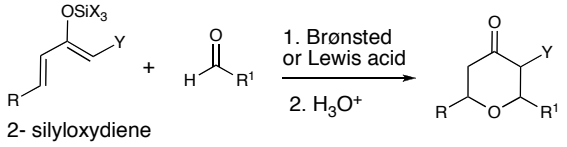

Figure 2-2. Tetrahydropyranones Using the Hetero Diels–Alder Reaction

Many laboratories, including those of Mikami,[47] Keck,[48] Jacobsen,[49,50] Kobayashi,[51,52] and Doyle[52] have developed enantioselective variants of this cycloaddition using chiral Lewis acids. Most recently, Rawal[53] and Yamamoto have reported elegant chiral Brønsted acid-catalyzed HDA reactions. For all of its utility, the hetero Diels–Alder reaction does have limits regarding selectivity and substrate scope. The silyloxydiene component must be synthesized with complete control over the alkene geometry. Additionally, the selective formation of one enolsilane can be challenging for complex substrates. Most importantly in the context of synthesizing **II-1** and **II-2**, the placement of electron withdrawing substituents on the diene significantly attenuates its

reactivity**.** These perturbations of the electronic characteristics of the diene can have a significant negative impact on reactivity and stereoselectivity of the HDA process.

2.2.2 The Prins Cyclization

The second major convergent strategy for the synthesis of pyrans is the Prins reaction between an oxocarbenium ion and a double bond (Figure 2-3).[54] The execution of this approach usually entails the combination of a homoallylic alcohol with an aldehyde under acidic conditions.

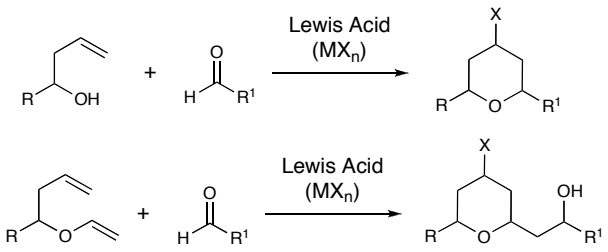

Figure 2-3. Tetrahydropyran Synthesis Using the Prins Reaction

The Prins strategy can be seriously compromised by the intervention of oxonia-Cope manifolds. In many cases, these rearrangements can promote complete or partial scrambling of homoallylic and aldehydic components as well as scramble the stereochemical information prior to the cyclization.[55-58] In efforts to control these unwanted processes during "standard" Prins process, a number of intramolecular variants have been developed at the expense of convergency. Many researchers, including Overman,[59] Speckamp,[60] Marko,[61] Keck,[62] Panek,[63,64] Li[65] and Roush[58] have all effectively utilized tethered allyl metal functionality, such as an allylsilane, in the presence of Lewis acids to intercept the oxocarbenium ion formed *in situ*. Rychnovsky

has developed elegant "segment-coupling Prins" methods to access the essential oxocarbenium ion for this reaction from either α-acetoxy ethers or by a remarkable cascade strategy involving a Mukaiyama aldol reaction with a vinyl ether.[66-68] The attack of the vinyl ether on the activated aldehyde promotes formation of the oxocarbenium that subsequently undergoes a Prins reaction with the pendant alkene. This methodology was elegantly applied in Rychnovsky's synthesis of leucascandrolide A. The use of all of these Prins-type strategies have been applied to the syntheses of numerous tetrahydropyran-containing complex natural products, most recently the synthesis of dactylolide by Floreancig.[69]

2.2.3 The Petasis–Ferrier Rearrangement

The Petasis–Ferrier rearrangement[70] (Figure 2-4) is a stereoselective bond forming sequence employed by the Smith laboratory in the syntheses of phorboxazole,[71] zampanolide,[72] and kendomycin.[73]

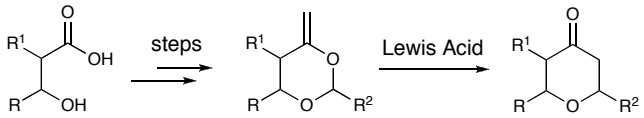

Figure 2-4. Tetrahydropyanone Synthesis Using the Petasis-Ferrier Rearrangement

The execution of a Petasis-Ferrier sequence includes the formation of vinyl acetals followed by treatment with Lewis acids to induce the stereoselective rearrangement. Although the execution of this rearrangement establishes the THP core,

the multiple steps necessary to convert an initial β-hydroxy acid to the corresponding tetrahydropyrone limit the overall efficiency of this strategy.

2.2.4 Intramolecular Strategies

There are many additional intramolecular strategies to synthesize tetrahydropyran rings with 2,6-*cis* stereochemistry (Figure 2-5). Early examples include Masamune's synthesis of bryostatin 7[74] and Evans's synthesis of antibiotic X-206,[75] which utilize stereoselective oxymercuration reactions. The conjugate addition of an alcohol to an enone has been used by White in the total synthesis of polycavernoside A[76] and Rizzacasa in the synthesis of apicularen.[77,78]

Although the established strategies for tetrahydropyran construction have been extensively utilized for organic synthesis, they all possess limitations that can have an adverse impact on retrosynthetic strategy and execution.

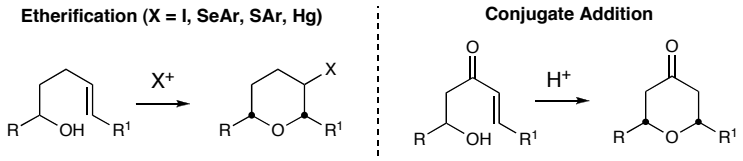

Figure 2-5. Alternative Methods for the Synthesis of Pyrans

2.3 First Generation Approach Towards the Synthesis of Okilactomycin & Chrolactomycin

Although the utility of the aforementioned methods has been clearly demonstrated within the context of total synthesis, we were concerned that the limitations of these approaches would compromise the total synthesis of okilactomycin and cholactomycin.

The hetero Diels-Alder and Prins cyclizations can have electronic requirements that preclude many potentially useful substitution patterns (e.g. electron withdrawing groups). The Petasis-Ferrier rearrangement lacks convergency and can require extensive functional group manipulation. Consequently, our initial approach focused on a novel strategy focused on a highly convergent cascade reaction.

2.3.1 Retrosynthetic Analysis

The structures of okilactomycin and chrolactomycin are particularly interesting in that they offer several potential sites for retrosynthetic bond disconnections. We were interested in assembling the carbon framework of both natural products and introducing the C11 substituent late in the synthesis. We chose to remove the highly reactive exomethylene unit and install it at the end of the synthesis.

We were intrigued by the possibility of forming the unprecedented 6-5 fused bicycle in a single synthetic operation from an aldehyde precursor such as **II-3**. We envisioned treatment of **II-3** with a mild base would promote an intramolecular aldol reaction that would be followed by a 1,4-conjugate addition of the resulting alkoxide to the α,β-unsaturated ketone (Figure 2-6).

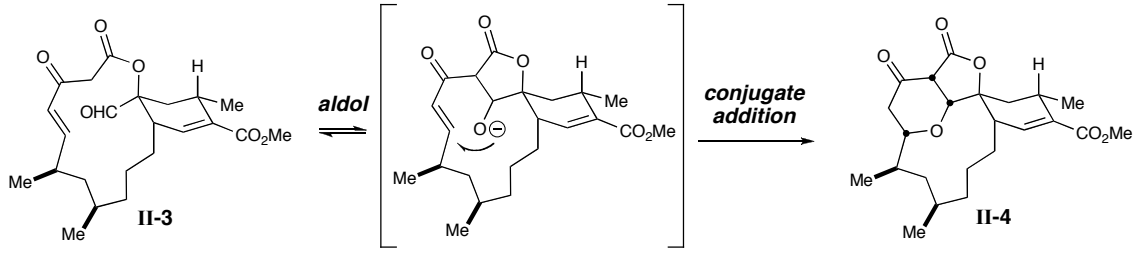

Figure 2-6. Proposed Tandem Aldol/Conjugate Addition Reaction

We could potentially arrive at aldehyde **II-3** via acylation of tertiary alcohol **II-5** with β-keto ester **II-6** and a ring closing metathesis (Figure 2-7). Given the complexity and the timing of the key step in the synthesis, we sought to develop a model system for this cascade reaction prior to beginning the synthesis of fragments **II-5** and **II-6**.

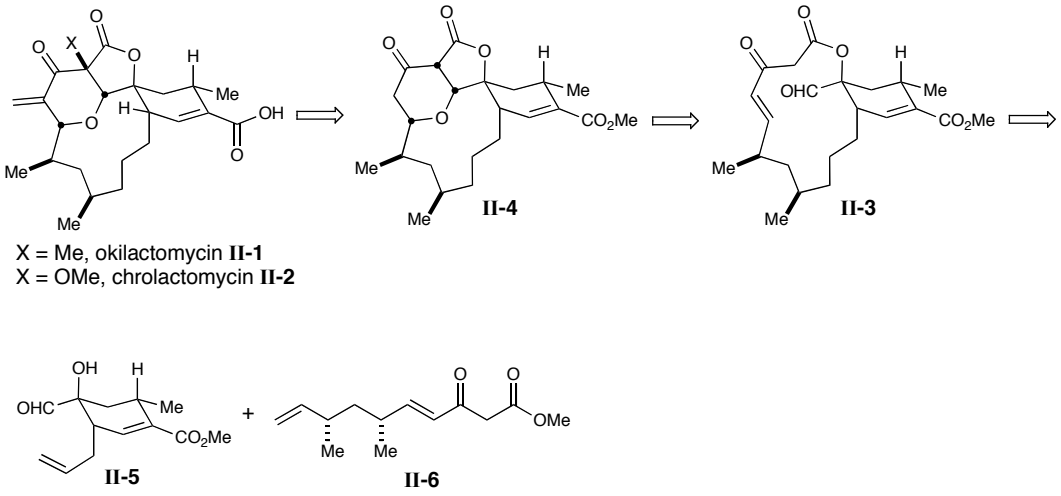

Figure 2-7. Retrosynthetic Analysis

2.3.2 Tandem Aldol/Conjugate Addition Model Studies

The synthesis of our model substrate began with a catalytic dihydroxylation of the commercially available methylene cyclohexane with OsO_4 (Scheme 2.1). The resulting primary alcohol was mono-protected as the TBS ether to provide the model tertiary alcohol **II-7** in 93% yield over the two steps.

The preparation of the β-ketoester coupling partner began with bromination of ethyl acetoacetate (Scheme 2-1). The exposure of the bromo-ketone **II-8** to the anion of diethyl phosphite provided the phosphonate **II-9** in 43% yield over 2 steps. The

phosphonate was treated with NaHMDS followed by hydrocinnamaldehyde to provide the desired β-ketoester **II-10** as a single olefin isomer in 60% yield.

Scheme 2-1. Preparation of Model Substrate

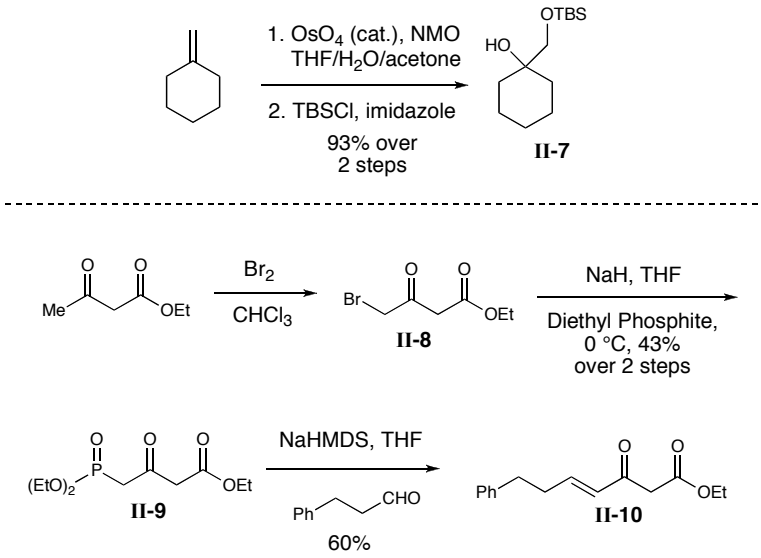

We were disappointed to find that the transesterification between **II-10** with **II-7** failed to provide the desired β-ketoester. After extensive experimentation we concluded that tertiary alcohol of **II-7** was too sterically hindered to transesterify ethyl ester **II-10**. We reasoned that if we could generate a more reactive electrophile, the poor nucleophilicity of the tertiary alcohol could be accommodated. We turned our attention to dioxinones, which are useful surrogates for β-ketoesters.[79] Dioxinones are known to undergo a retro-[4+2] cycloreversion when heated to 110 °C. This results in the extrusion of acetone and the generation of a highly electrophilic acyl ketene (Figure 2-8).

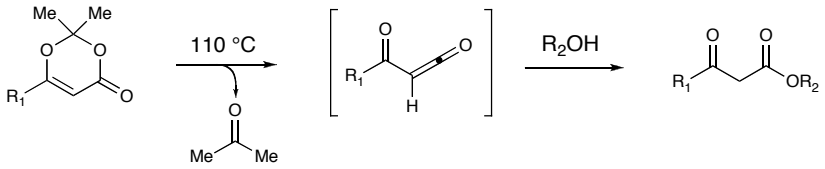

Figure 2-8. Dioxinones as β-Ketoester Precursors

This modification required that the synthesis of **II-10** be adjusted to allow for the installation of the dioxinone ring.[80] The dioxinone **II-11** was treated with LDA followed by hexachlorethane to furnish chlorodioxinone **II-12** in 75% yield. The chloride was displaced with the anion of diethyl phoshite to afford the phosphonate **II-13** in 70% yield. The Horner-Wadsworth Emmons olefination was carried out in the presence of *t*-BuOK to provide dioxinone **II-14** in 79% yield.

Scheme 2-2. Synthesis of New Acylation Partner

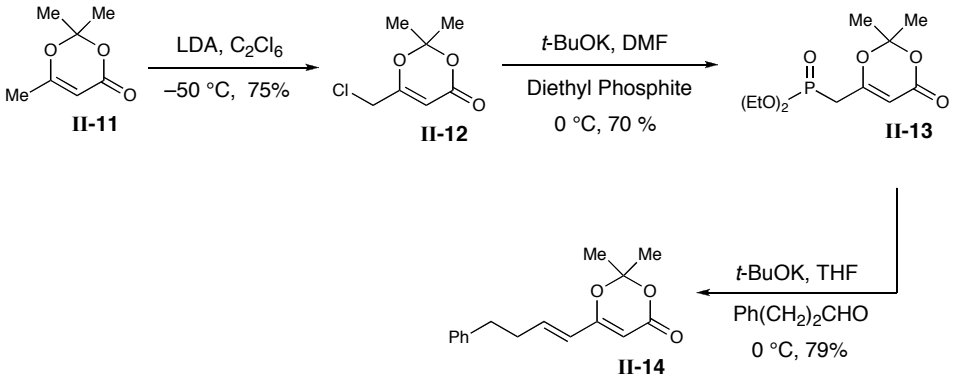

The alcohol **II-7** and dioxinone **II-14** were combined and heated to 110 °C to provide the desired acylated product **II-15** in 80% yield (Scheme 2-3). The TBS protecting group was removed with PPTS to provide primary alcohol **II-16** in 98% yield.

Unfortunately, alcohol **II-16** was resistant to all oxidation conditions surveyed. These included PCC, Dess-Martin,[81,] TPAP,[82] Swern[83] and Parikh-Doering[84] conditions. We speculated that the nucleophilic nature of the enol tautomer of **II-16** had a deleterious effect on the oxidation.

Scheme 2-3. Acylation of Tertiary Alcohol **II-7**

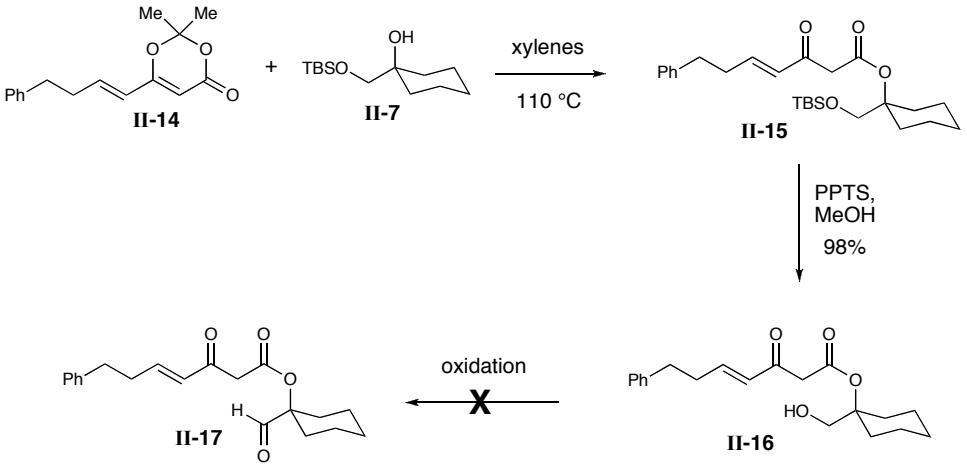

The inability to oxidize **II-16** forced us to evaluate alternative strategies. We considered a scenario where the aldehyde is brought into the acylation step in its correct oxidation state. To evaluate this proposal, cyclohexanone was treated with TMSCN in the presence of ZnI_2 to provide the trimethylsilyl cyanohydrin **II-18**.[85] The nitrile was reduced with DIBAL-H and the α-siloxy aldehyde **II-19** was isolated following hydrolysis of the intermediate imine. The removal of the TMS protecting group proved to be challenging. Under most conditions surveyed, the α-siloxy aldehyde dimerized irreversibly. After extensive experimentation, we found that the combination of AcOH/THF/H_2O (3/1/1) removed the TMS group without generating the dimerization product. These conditions appeared to be unique and will be reported on in the future.

Scheme 2-4. Synthesis of the α-Hydoxy Aldehyde Coupling Partner

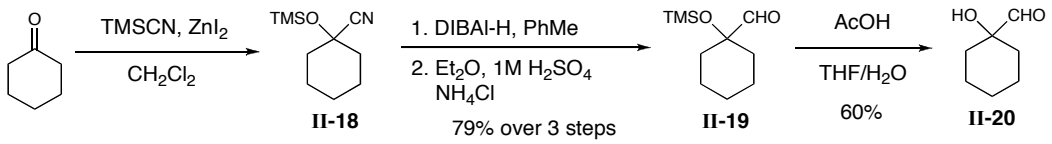

Unfortunately, when **II-20** and **II-14** were combined and heated to 110 °C the desired product **II-17** was not isolated.

Given the obstacles encountered with the model studies up until this point, we chose to evaluate the intermolecular variant of the proposed tandem reaction (Scheme 2-5). We found that exposure of β-ketoester **II-10** to bases such as *t*-BuOK, DBU, NaOEt, LDA and K_2CO_3 led to quantitative recovery of starting materials. We then exposed the enol silane (**II-21**) to a variety of Lewis acids in the presence of cyclohexanecarboxaldehyde. Again, we observed recovery of cyclohexanecarboxaldehyde and **II-10**.

Scheme 2-5. Evaluation of Intermolecular Variant

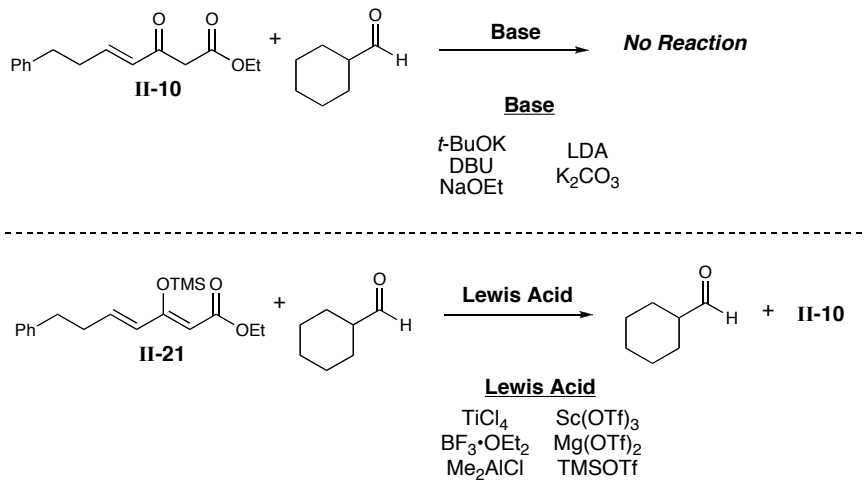

We attribute the apparent lack of reactivity to the reversibility of malonyl aldol reactions[86] and a rational for this observation could be based on anion stability. Specifically, the pKa of a 1,3-dicarbonyl compound is approximately 13 where the pKa of the alkoxide is approximately 16 (Figure 2-9). It should be noted that there are very few examples of this transformation.

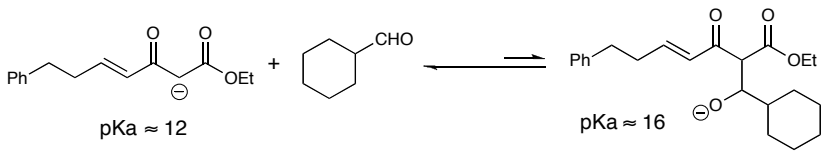

Figure 2-9. Thermodynamic Equilibrium

The results of these model studies provided compelling evidence that our proposed tandem aldol/conjugate addition cascade reaction was not the optimal approach towards the synthesis of okilactomycin and chrolactomycin. Consequently, we chose to revise our strategy at this stage of the project.

2.3.3 Revisions to the Synthetic Plan

Based on the results of the aforementioned model studies, we reasoned that a conjugate addition that resulted in formation of a more stable anion than an alkoxide would likely lead to the desired pyranone ring. Using the previous model study as a guide, we thought moving the conjugate acceptor between the two carbonyl units would lead to a more stable anion after conjugate addition and increase the electrophilicity of the 4-position based on the presence of a second electron withdrawing group (Figure 2-10).

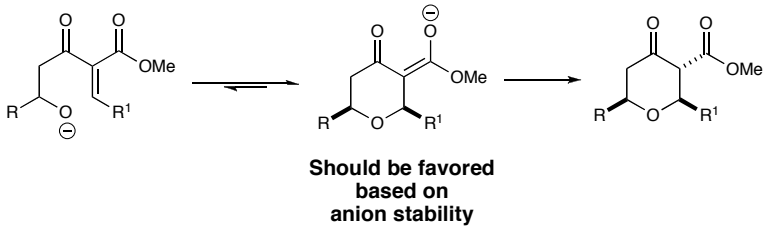

Figure 2-10. Revised Synthetic Plan

Fortunately at this time, we discovered two independent reports describing a tandem Knöevenagel/conjugate addition reaction promoted by Lewis acids (Scheme 2-6).[87,88] The authors proposed that a δ-hydroxy-β-ketoester such as **II-22** undergoes a Knöevenagel condensation with an aldehyde to generate a highly reactive electrophile *in situ*. Under the Lewis acidic conditions, the internal hydroxyl group would undergo 6-endo-trigonal cyclization to furnish desired pyranone **II-23**.

Scheme 2-6. Tandem Knöevenagel/Conjugate Addition

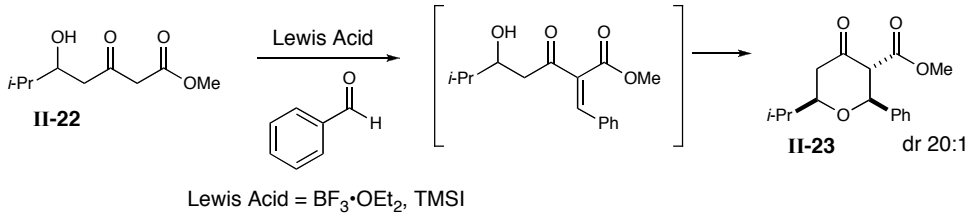

In order to evaluate this approach, δ-hydroxy-β-ketoester **II-24** and α-siloxy aldehyde **II-19** were exposed to TMSI (prepared *in situ* from TMSCl and NaI) (Scheme 2-7). We were pleased to find that pyranone **II-25** was isolated in 30% yield. Lactonization was carried out in the presence of *t*-BuOK and DMAP and provided the desired lactone **II-26** in 80% yield.

Scheme 2-7. Tandem Knöevenagel/Conjugate Addition Model Studies

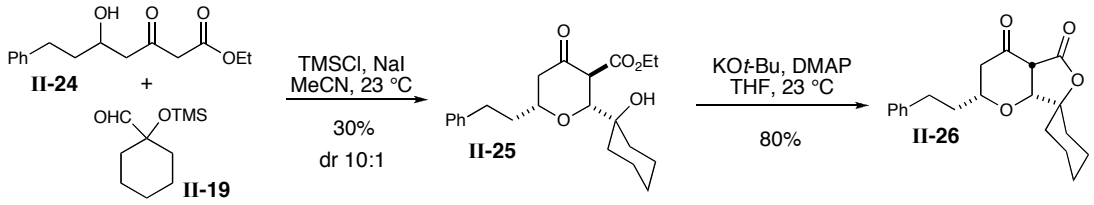

Although we were pleased with this result, we were interested in understanding why the yield of **II-25** was low. The major side products were isolated and provided evidence for a pair of competing side reactions that greatly reduced the efficiency of this process (Scheme 2-8). The first of these reactions was the dehydration of the starting δ-hydroxy-β-ketoester **II-24**. We found reports indicating that this process was known to occur under the reaction conditions (TMSI).[89] Presumably, the dehydration product was not identified by Clarke and Sabitha because the rate of dehydration was significantly

slower than the rate of the Knöevenagel/conjugate addition sequence. In our model reaction, the sterically encumbered nature of α-siloxy-aldehyde **II-19** retarded the initial Knöevenagel condensation allowing for the dehydration to become competitive. The second competing side reaction produced the cycloheptanone **II-27**. This product likely arises from the well precedented ring expansion of α-siloxy-aldehydes via a 1,2-alkyl shift.[90]

Scheme 2-8. Competing Side Reactions

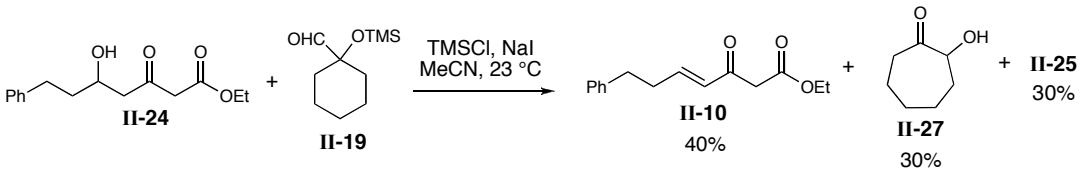

These competing side reactions greatly reduce the overall efficiency of this reaction. Given that this would be the key fragment assembly reaction in our total synthesis, we considered this an opportunity to use the information we had gathered and develop a new method for organic synthesis.

2.4 Target-Inspired Method Development

Main group Lewis acids consisting of silicon, aluminum, or boron typically exhibit high levels of reactivity due to the strongly electropositive nature of the metal center. We suspected the competitive side reactions taking place in our model studies were a result of this strong Lewis acidity. Thus, we required a Lewis acid that was less reactive in order to eliminate the side reactions, yet strong enough to promote the desired reaction. Additionally, we also were interested in rendering this tandem Knöevenagel/conjugate addition reaction catalytic in Lewis acid.

We initially considered the lanthanide triflates,[91,92] such as $Yb(OTf)_3$, $Eu(OTf)_3$, $Sm(OTf)_3$ and $La(OTf)_3$ as well as $CeCl_3 \bullet 7H_2O$. These Lewis acids promoted the tandem Knöevenagel/conjugate addition reaction between **II-24** and cyclohexanecarboxaldehyde, but did so in poor yield (< 40%). These results also made rendering this reaction catalytic highly unlikely. We continued our search for Lewis acids that promoted this reaction and were pleased to find that $Sc(OTf)_3$[65,93-95] did so in 75% yield. Interestingly, catalytic quantities of Lewis acid (10 mol %) could be employed without any deleterious effects to the yield.

We next turned our attention to applying this result to the model α-siloxy-aldehyde **II-19**. Unfortunately we found that when the new $Sc(OTf)_3$ conditions were applied to the model reaction, ring expansion product **II-27** was the only product obtained. This observation is consistent with literature reports showing that Knöevenagel condensations with tertiary aldehydes are rare, typically requiring highly reactive, main group Lewis acids.

Scheme 2-9. Tandem Knöevenagel/conjugate addition with $Sc(OTf)_3$

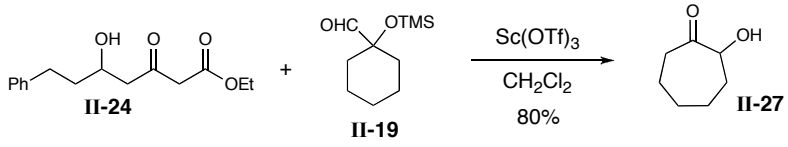

The inability to control the competing side reactions left us to consider alternative mechanistic pathways. We envisaged a scenario where the combination of an aldehyde, an alcohol and a Lewis acid would generate an oxocarbenium ion (Path B) rather than a Knövenagel intermediate (Path A) (Figure 2-11). The enol tautomer of the β-keto ester would add to the oxocarbenium to form the pyranone. This process would eliminate the need for a tertiary aldehyde to undergo a Knövenagel condensation reaction.

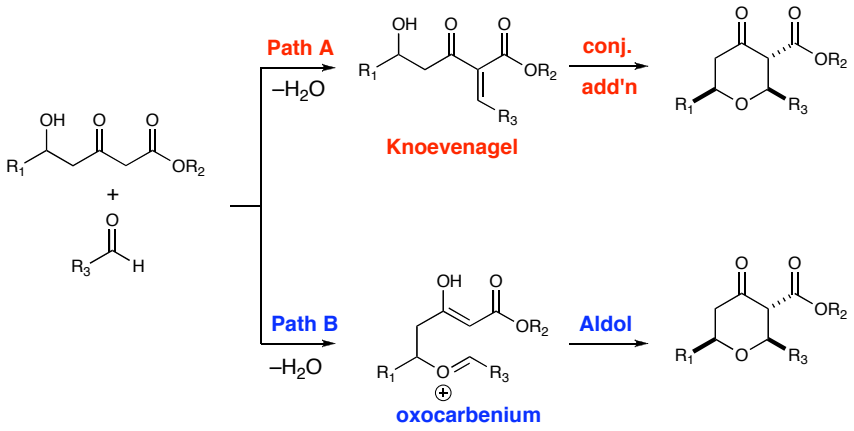

Figure 2-11. Potential Reaction Pathways

In order to access Path B, the β-ketoester would have to be protected to preclude Knöevenagel condensation from initially taking place. We had previously found that dioxinones were useful surrogates for β-ketoesters and could potentially serve as our protecting group. A closer evaluation of the dioxinone structure reveals an embedded enol ether moiety that could potentially serve as a latent nucleophile. We were surprised to find that few examples exist utilizing this intrinsic property of dioxinones and we sought to develop a novel synthetic methodology focused on exploiting this under-utilized property of dioxinones.[96,97]

Towards this end, we found that the combination of β-hydroxy-dioxinones and aldehydes under Lewis acid catalysis provided isolable, bicyclic pyranone products (Figure 2-12). These novel structures could be converted to 3-carboxy-pyranones by the addition of a metal alkoxide directly to the reaction flask.[98]

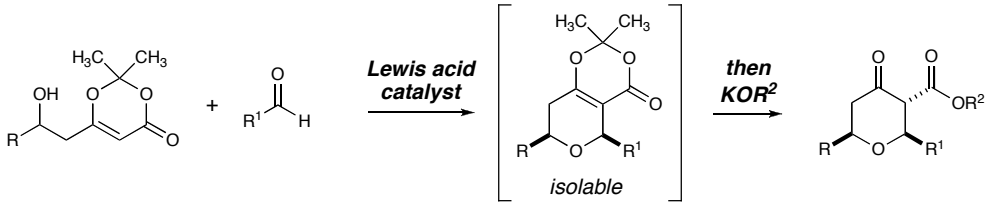

Figure 2-12. Tetrahydropyranones from Dioxinones and Aldehydes

We felt this method could potentially alleviate the problems we encountered during our previous model work such as ring expansion and undesired dehydration reactions. Additionally, this reaction represented a powerful new approach towards the synthesis of substituted pyranones in a highly convergent manner. We felt strongly about the potential utility of this transformation and thus, decided to conduct a thorough evalution of the reaction scope.

2.4.1 Optimization of Dioxinone Addition to Aldehydes

Our initial investigations focused on identifying optimal carbon–carbon bond–forming conditions to generate pyranone **II-29** from β-hydroxy-dioxinone **II-28** and hydrocinnamaldehyde (Table 2-1). While stoichiometric quantities of BF_3•OEt_2 promoted the cyclization of β-hydroxy-dioxinone **II-28** and hydrocinnamaldehyde (entry 1), we were delighted to discover that catalytic amounts of $Sc(OTf)_3$ afforded high yields of the desired heterocycle **II-29** (entries 2-5). Gratifyingly, the diastereoselectivity of the

overall process is excellent (20:1) affording the 2,6-cis relative stereochemistry as determined by NOE analysis. A survey of the catalyst loadings indicated that 10 mol% of $Sc(OTf)_3$ was optimal in terms of yield and reaction time. The use of other metal triflate salts in the reaction (not shown) did not provide significant quantities of **II-29**. It is important to note that the choice of dehydrating agent ($CaSO_4$)[99] is crucial for obtaining high yields of the pyran products under catalytic conditions.

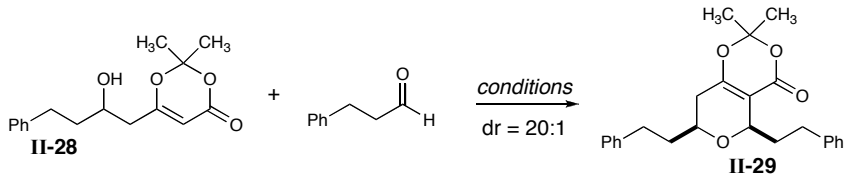

II-28 **II-29**

entry	Lewis acid	Solvent (Additive)	temperature & time	yield (%)[b]
1	2 equiv BF_3•OEt_2	CH_2Cl_2 (none)	0 °C, 2 h	51
2	20 mol% $Sc(OTf)_3$	MeCN (4Å MS)	0 °C, 3 h	45
3	20 mol% $Sc(OTf)_3$	CH_2Cl_2 ($CaSO_4$)[c]	–20 °C, 3 h	93
4	10 mol% $Sc(OTf)_3$	CH_2Cl_2 ($CaSO_4$)[c]	–20 °C, 4 h	80
5	5 mol% $Sc(OTf)_3$	CH_2Cl_2 ($CaSO_4$)[c]	–20 to 23 °C, 24 h	79

[a] Reactions performed at 0.2 M. [b] Isolated yield. [c] anhydrous.

Table 2-1. Optimization of Reaction Conditions

2.4.2 Evaluation of the Aldehyde Scope

With efficient Lewis acid-catalyzed conditions identified, the influence of aldehyde structure on the transformation was probed (Table 2-2). Saturated aldehydes participated in the cyclization, with linear systems (entries 1, 2, 8) being superior to α-branched substrates (entry 9) in terms of yield.

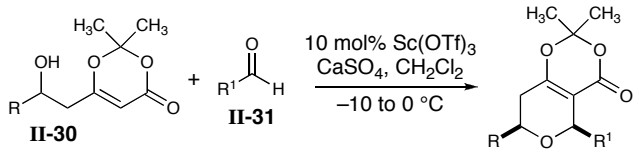

entry	R	R^1	yield (%)[b]	dr (cis:trans)[c]	product
1	$Ph(CH_2)_2$	$Ph(CH_2)_2$	80	20:1	**II-29**
2	"	*n*-hexyl	85	20:1	**II-32**
3	"	Ph	71	6:1	**II-33**
4	"	4-Cl-Ph	73	20:1	**II-34**
5	"	4-Fl-Ph	83	20:1	**II-35**
6	"	4-MeO-Ph	54	2:1	**II-36**
7	"	1-Naphthyl	81	3:1	**II-37**
8	"	$BnO(CH_2)_3$	80	20:1	**II-38**
9	"	*i*-Pr	75	2:1	**II-39**
10	Ph	$Ph(CH_2)_2$	64	20:1	**II-40**
11	cyclohexyl	"	70	20:1	**II-41**

[a] Reactions performed at 0.2 M. [b] Isolated yield after chromatographic purification. [c] As determined by ^{1}H NMR (500 MHz).

Table 2-2. Aldehyde Scope

The overall diastereoselectivity was dependent on the structure of the aldehyde. For example, *p*-anisaldehyde, 1-naphthaldehyde, and isobutyraldehyde were not as selective as unbranched saturated or electron deficient substrates (entries 6, 7, 9). Additionally, dioxinones (**II-30**) with alkyl chains (linear and branched) or aromatic rings flanking the hydroxyl group are good substrates.

2.4.3 Multicomponent Approach

In a multicomponent reaction approach,[100] 3-carboxy pyran-4-ones can be produced from a single reaction vessel by direct addition of potassium alkoxide salts (Table 2-3). This one-pot sequential process efficiently assembles three reaction components and can accommodate various substitution on the dioxinone (**II-30**), aldehyde coupling partner (**II-31**), or alkoxide nucleophile (KOR^2). Increasing the

catalyst loading to 20 mol % promotes the overall process in less than 10 hours. Presumably, the delivery of alkoxide promotes fragmentation of the dioxinone ring *in situ* to afford ethyl, benzyl and TMSE esters in good yield (as keto/enol tautomers).

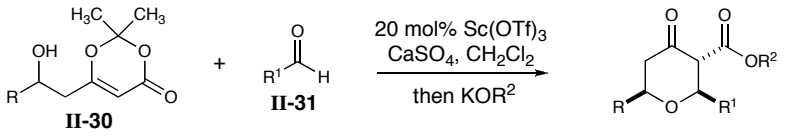

entry	R	R^1	R^2	yield (%)[b]: (cis/trans)[c]	product (keto:enol)[d]
1	$Ph(CH_2)_2$	$Ph(CH_2)_2$	Et	78 (95:5)	**II-42** (4:1)
2	cyclohexyl	$Ph(CH_2)_2$	Et	72 (95:5)	**II-43** (4:1)
3	Ph	$Ph(CH_2)_2$	Et	60 (95:5)	**II-44** (6:1)
4	$Ph(CH_2)_2$	Ph	Et	67 (93:7)	**II-45** (2:1)
5	$Ph(CH_2)_2$	$Ph(CH_2)_2$	$PhCH_2$	82 (94:6)	**II-46** (4:1)
6	$Ph(CH_2)_2$	$Ph(CH_2)_2$	$Me_3Si(CH_2)_2$	72 (95:5)	**II-47** (3:1)

[a] Reactions performed from –10 to 0 °C at 0.2 M; 4 equiv of KOR^2 added directly to reaction after conversion of **II-30**. [b] Isolated yield after chromatographic purification. [c] 2,6 relationship. [d] Enol/keto ratio determined by ^1H NMR Spectroscopy (500 MHz).

Table 2-3. One Pot Cyclization/Ring Opening

2.4.4 Mechanistic Considerations

Our current working model of the reaction begins with the Lewis acid-catalyzed formation of oxocarbenium ion **II-A** (Figure 2-13). Presumably, C–C bond formation proceeds via a chair-like arrangement to afford dioxinone intermediate **II-B**. The elimination of a proton from this oxocarbenium species affords the bicyclic 2,6-cis-dioxinone **II-29**. The addition of an alkoxide nucleophile (such as KOEt) to the reaction fragments the dioxinone ring and protonation of the resulting enolate (**II-C**) generates the thermodynamically favored equatorial ester **II-42**. Gratifyingly, the original stereocenter of the β-hydroxy-dioxinone is completely conserved in **II-29** when enantioenriched **II-30** is utilized in the reaction. This stereochemical fidelity provides the foundation to

synthesize desired optically active bicycles (such as **II-29**) or carboxy-substituted tetrahydropyran-4-ones (such as **II-42**) from enantioenriched β-hydroxy-dioxinones.

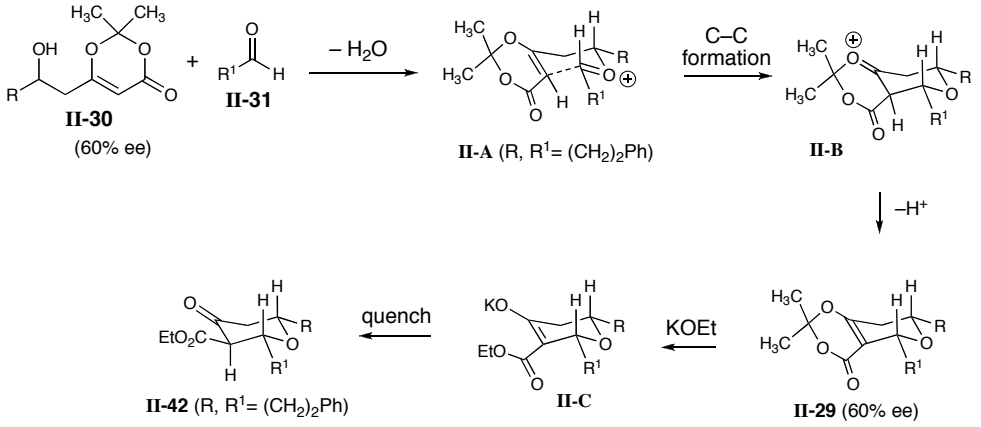

Figure 2-13. Proposed Reaction Pathway

2.4.5 Synthetic Utility

A significant advantage of this new methodology is that the dioxinone products **II-29** and **II-32-II-41** are highly versatile platforms for further synthetic manipulations (Scheme 2-10). One avenue of transformation employs the exposure of the dioxinone core to heat, which presumably generates a reactive acylketene (A) via thermal reversion. Differentially trapping the acylketene from **II-29** cleanly affords either unsubstituted tetrahydropyran-4-one **II-48** (71%) or β-keto amide **II-49** (63%) without affecting the diastereoselectivity established in **II-29**. Interestingly, compounds such as **II-29** and **II-32-41** have not been reported in the literature and a full investigation of the synthetic potential of these rigid reaction scaffolds should provide access to significant chemical diversity initiated by this new cyclization methodology.

Scheme 2-10. Synthetic Utility

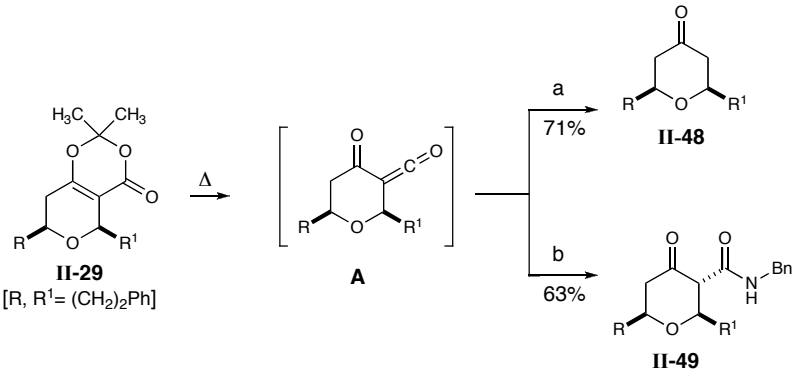

a) DMSO, H_2O, 130 °C; b) xylenes, reflux, H_2NCH_2Ph.

The intermediate pyrans could also serve as a versatile scaffold for diversity oriented synthesis (Scheme 2-11).[101] The variety of functional groups present in structures such as **II-29** offer the potential to carry out a wide range of transformations beyond manipulating the dioxinone ring. Specifically, we found that treatment of **II-29** with LDA and MeI provided a moderate yield of the alkylated derivative **II-50** with acceptable levels of stereocontrol. The Scheidt group is currently using this methodology in a variety of synthetic projects and we are confident the pyranones such as **II-29** will find broad utility in organic synthesis.

Scheme 2-11. Diversity Oriented Synthesis from Pyran Bicycle

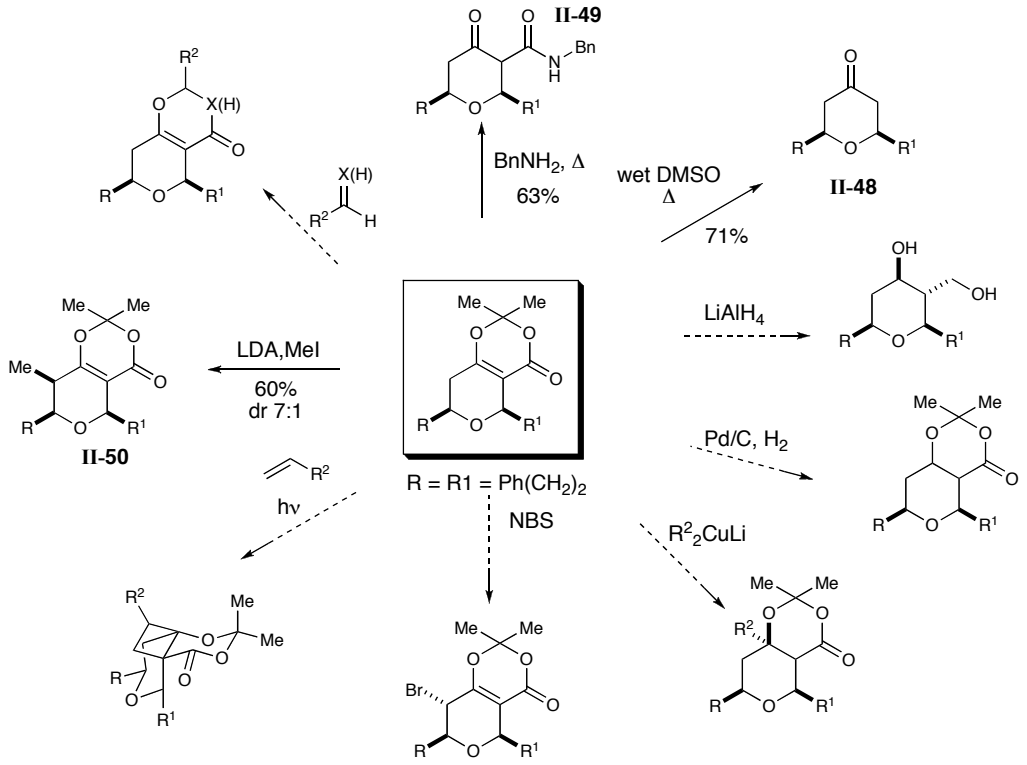

In summary, β-hydroxy-dioxinones and aldehydes undergo mild and stereoselective cyclizations in the presence of catalytic amounts of $Sc(OTf)_3$. This novel construction of the pyrone heterocycle capitalizes on the intrinsic, yet previous unexploited, nucleophilicity of the dioxinone moiety. The direct addition of a range of alkoxide nucleophiles to the reaction flask can convert the resulting bicyclic pyrans into carboxy-substituted tetrahydropyran-4-ones, thereby accessing a highly efficient three-component process. Alternatively, the intermediate pyrans can be isolated in good yield and converted into the related carboxamide or unsubstituted pyranones by trapping the easily generated acylketenes.

2.5 Second Generation Approach

The unprecedented ring system of okilactomycin and chrolactomycin provided the impetus for the development of the novel synthetic methodology described above. This method served to address the issues that arose during our model studies.

2.5.1 Revised Retrosynthesis

In order to apply our novel cyclization method to the synthesis of okilactomycin and chrolactomycin our retrosynthetic analysis had to be adjusted accordingly. The only notable change is that a secondary alcohol must be incorporated at the C8 position. In order to do so we envisaged an aldol disconnection between C8 and C9 to provide enol silane **II-54** and aldehyde **II-53**.

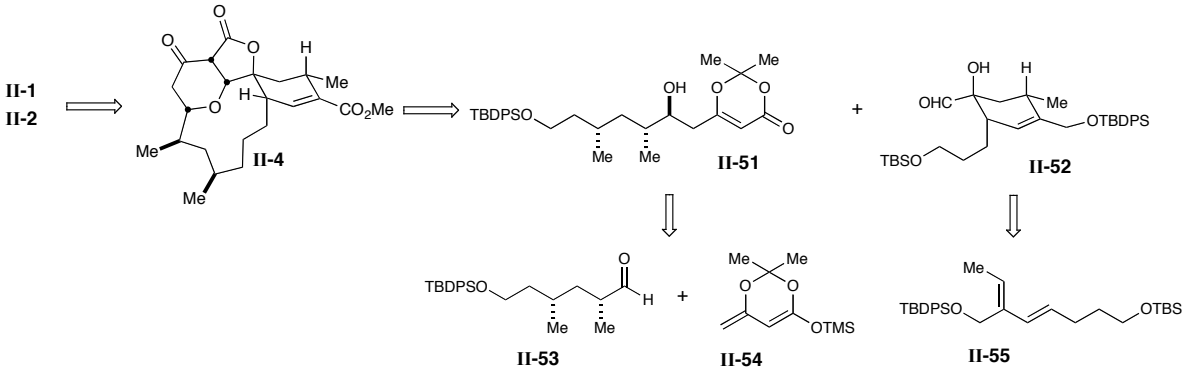

Figure 2-14. Revised Retrosynthetic Analysis

2.5.2 Model Study

Keeping in mind that the novel cyclization methodology was developed for the total synthesis of **II-1** and **II-2**, we were pleased to observe that when our reaction was applied to hindered aldehyde **II-56** the desired pyran **II-57** was obtained as a single diastereomer. Although the yield was less than optimal, the mass balance was primarily

unreacted starting materials **II-28** and **II-56**. This model system result was considered to be acceptable for us to pursue the total synthesis of okilactomycin and chrolactomycin using our novel cyclization method.

Scheme 2-12. Model System for $Sc(OTf)_3$ Catalyzed Cyclization

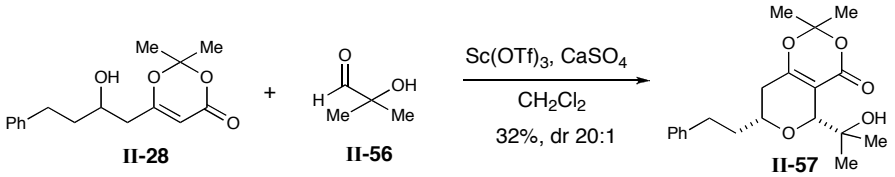

We turned our attention towards preparing the prinicpal fragments **II-51** and **II-52**. The goal was to establish an efficient, stereocontrolled route that would provide multigram quantities of intermediates **II-51** and **II-52**. It was important that the routes be flexible, should the need for modification arise unexpectedly late in the synthesis.

2.6 Synthesis of Principal Fragments

2.6.1 Synthesis and Elaboration of Dioxinone Fragment II-51

The synthesis of dioxinone **II-51** relied on Myers-chiral amide alkylation methodology[102-105] to install the 1,3-syn stereochemistry of the ansa chain (Scheme 2-13). The (–)-pseudoephedrine derived chiral propionamide **II-58** was alkylated with TBDPS protected iodoethanol to generate the desired extended amide **II-59** in 90% yield and high diastereoselectivity (20:1). The proposed model for stereoselectivity involves a reactive conformer such as that shown in Figure 2-15. In this conformation, the lithium alkoxide and the THF molecules that have aggregated to the lithium cation block the β-face of the

(*Z*)-enolate forcing alkylation to occur from the α-face.[103] The authors suggest the pseudoephedrine side chain adopts a staggered conformation in which the C–H bond α to the nitrogen lies in plane with the enolate oxygen, in accordance with allylic strain arguments.

Figure 2-15. Proposed Reactive Conformer in Pseudoephedrine Alkylations

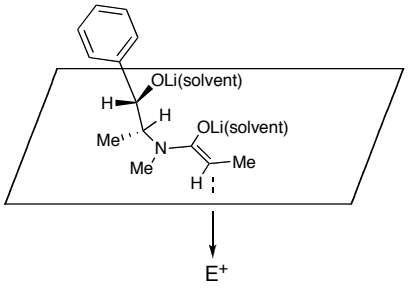

The amide **II-59** underwent reduction with lithium amidotrihydroborate[106] to provide the primary alcohol **II-60** in 92% yield. This reducing reagent is an alternative to typical metal hydrides that favor the formation of the tertiary amine product. The primary alcohol **II-60** was converted to primary iodide **II-61** using I_2 and PPh_3. The alkylation sequence was repeated (alkylation, amide reduction) and the resulting alcohol **II-62** was oxidized to aldehyde **II-53** using 10 mol % of tetrapropylammonium perruthenate (TPAP)[82] and NMO.

Scheme 2-13. Synthesis of Non-Racemic Aldehyde **II-53**

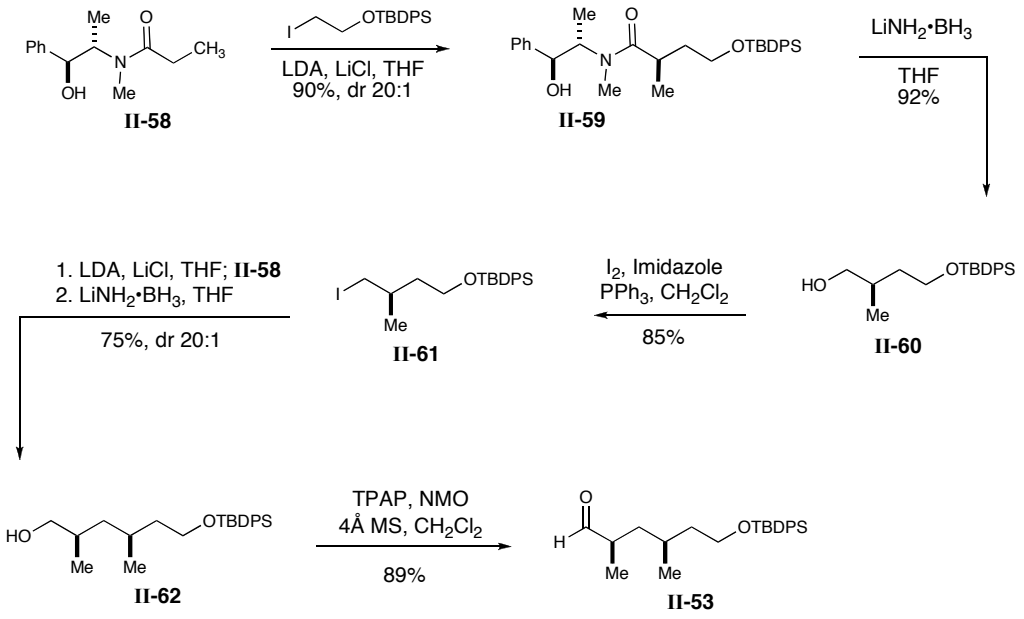

We considered an aldol reaction the most direct way to install the required C8 hydroxyl group. The anti relationship between the C7 methyl substituent and the C8 hydroxyl group required careful consideration. We speculated that the methyl substituent would not impact the facial selectivity of the aldol reaction. This speculation was verified by exposing aldehyde **II-53** and enol silane **II-54** to achiral Lewis acids such as $TiCl_4$ and BF_3•OEt_2. In each case, the resulting aldol adduct was isolated as a 1:1 mixture of syn and anti diastereomers. Based on these data, we were confident we could employ asymmetric catalysis to install the correct absolute stereochemistry at C8. We were pleased to find Carreira's copper(II)-catalyzed aldol methodology[107] with (*R*)-tol-BINAP as the ligand provided a 7:1 mixture favoring the anti diastereomer.

Scheme 2-14. Anti-Felkin Aldol Reaction

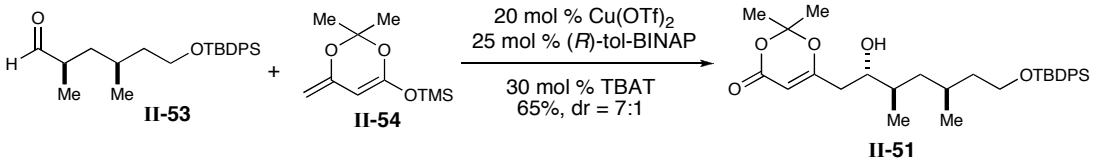

The proposed mechanism for this transformation is shown in Figure 2-16. A chiral copper fluoride complex **II-A** is initially generated *in situ* followed by exposure to the enol silane and aldehyde. The authors propose that TBAT promotes desilylation of the enol silane to a generate a chiral enolate **II-B**. This chiral enolate undergoes an asymmetric aldol reaction to form copper alkoxide **II-C**. This alkoxide is rapidly silylated by the starting enol silane **II-54** to afford the trimethylsiloxy dioxinone product **II-D** and regenerate the chiral enolate **II-B** to continue the catalytic cyle.

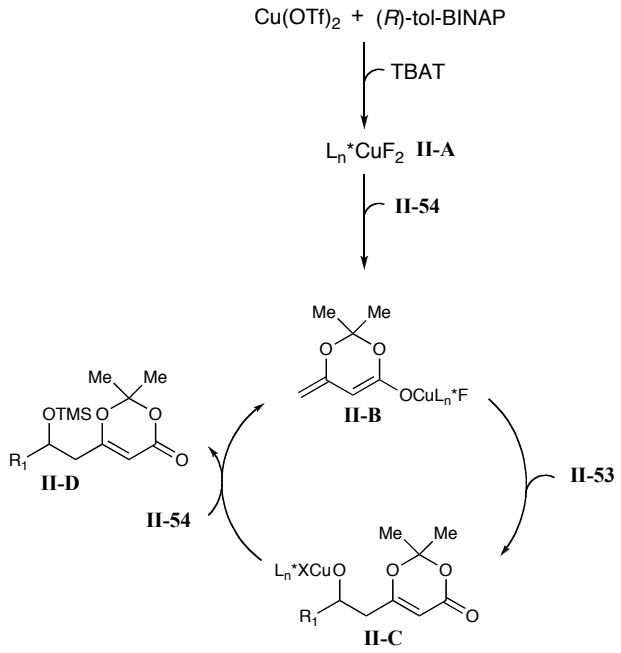

Figure 2-16. Proposed Mechanism for Anti-Felkin Aldol Reaction

The newly formed secondary alcohol **II-51** was protected as the TBS ether and the TBDPS group was selectively removed with NH_4F[108] to furnish primary alcohol **II-63**. The terminal double bond was installed using Grieco's selenium elimination procedure.[109]

Scheme 2-15. Elaboration of the Dioxinone Fragment

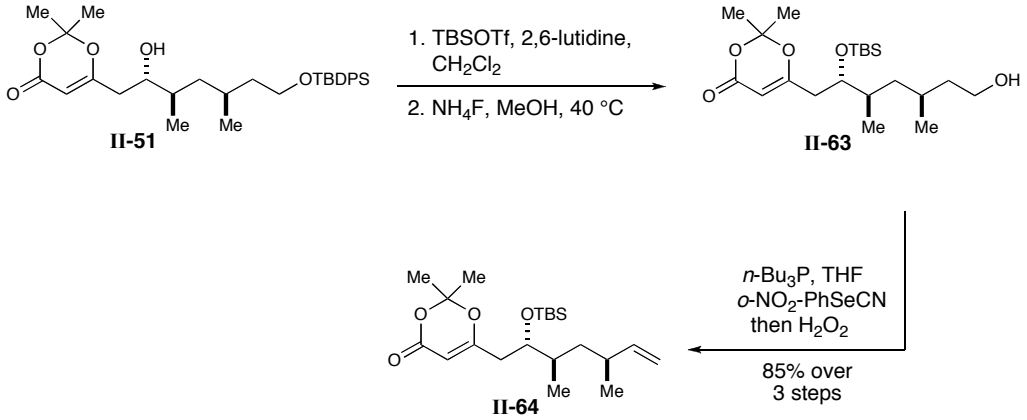

2.6.2 Synthesis and Elaboration of II-52

We were initially interested in utilizing chemistry developed by Taber and coworkers at the University of Delaware.[110-113] They describe using vinylidine carbenes to access substituted enones. This approach was attractive because it allowed us to set the stereochemistry at the critical α-hydroxy aldehyde stereocenter. We felt this streochemical information could then be used to establish the correct relative relationship of the substituents on the cyclohexene ring.

Commercially available (*S*)-glycidol was ring opened with methallyl Grignard and the resulting diol was immediately protected as the acetonide **II-65**. At this stage we attempted to reproduce a known procedure to transform acetonide **II-65** to cyclopentene **II-66** by treatment with with Br_2 and KHMDS. This procedure was intended to generate a

vinylidine carbene via the vicinal dibromide and insert into the methine C–H bond. Unfortunately, several attempts to reproduce this literature precedent were unsuccessful.

Scheme 2-16. Attempt to Generate the Vinylidine Carbene

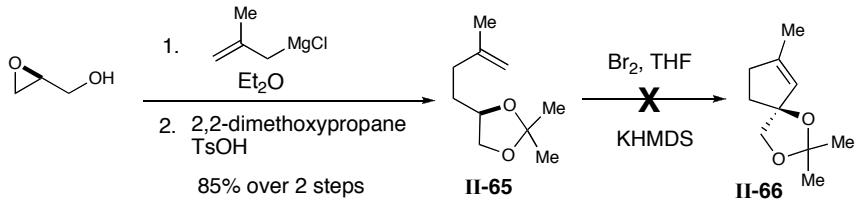

In order to to circumvent this problem we carried out an ozonolysis of the olefin **II-65** to provide ketone **II-67** (Scheme 2-17). The ketone **II-67** was treated with trimethylsilyldiazomethane[114] under basic conditions to provide the desired cyclopentene **II-66**. We believe that this reaction proceeds by nucleophilic addition to the carbonyl to form tetrahedral intermediate **II-A** (Figure 2-17). A Peterson olefination[115] ensues via **II-B**. The resulting vinyl diazonium intermediate **II-C** undergoes α-elimination of N_2 to generate the vinylidine carbene **II-D** which then inserts into the methine C–H bond to provide **II-66**. The cyclopentene was ozonolized to give the keto-aldehyde **II-68**. This compound was treated with KOH under biphasic conditions to provide a thermodyanamic mixture of enone **II-69** and β-hydroxy ketone **II-70**.

Scheme 2-17. Synthesis of Enone **II-69** via C–H Insertion

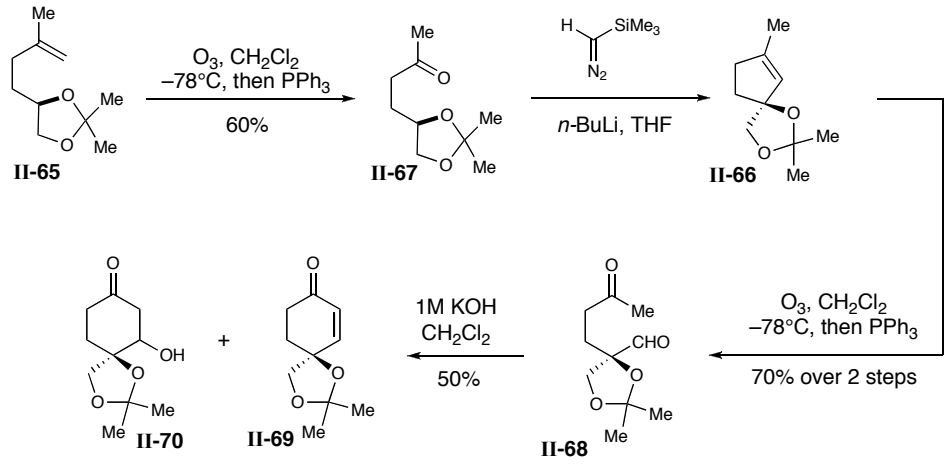

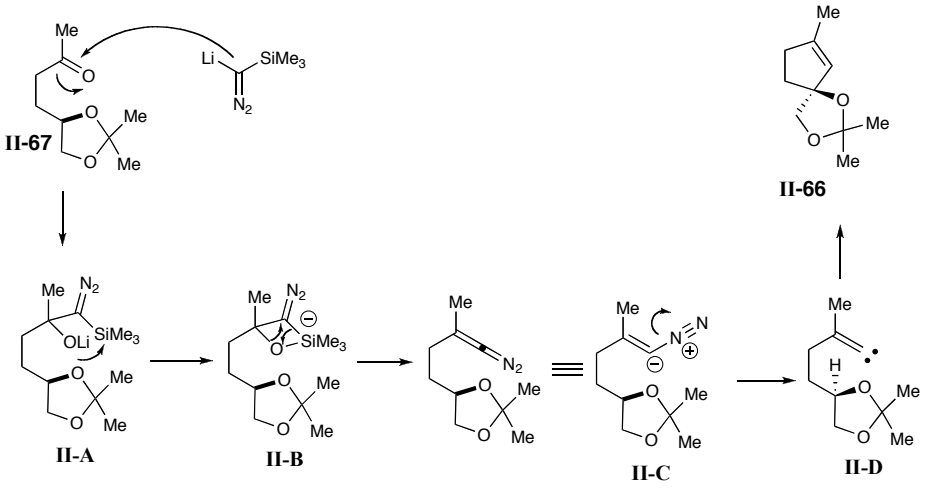

Figure 2.17. Proposed Mechanism for Conversion of **II-67** to **II-66**

With an established route in hand to access enone **II-69** we now sought to install the allyl group stereoselectively. Attempts to do so using the cuprate derived from allyl Grignard provided the 1,4-addition product **II-71** as a single diastereomer. This addition likely proceeds via the chair-like transition state to lead to the observed product.

Although the selectivity of this reaction was excellent, the poor yield (< 30%) prevented it from being synthetically useful within the context of multistep synthesis.

Scheme 2-18. Cuprate Addition to Enone **II-69**

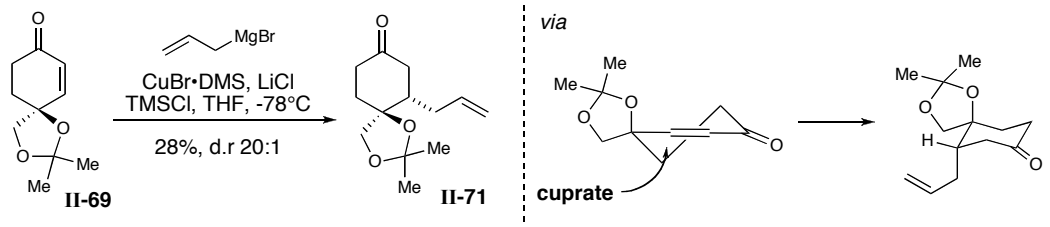

We attributed the poor yield to the capricious nature of allyl organometallic reagents.[116] In order to overcome this problem we considered a 2-step procedure involving the conjugate addition of a more stable cuprate followed by isomerization of a double bond to the desired position. This plan was easily executed as the cuprate derived from 4-bromo-but-1-ene underwent conjugate addition to provide ketone **II-72** in a 72% yield. The selectivity of this reaction was still excellent as the addition product was formed as a single diastereomer. The terminal double bond was isomerized[117,118] with $RhCl_3 \bullet XH_2O$ in EtOH to the more highly substituted olefin **II-73**. The extra carbon unit was not of concern as it would be extruded during the eventual ring closing metathesis.

Scheme 2-19. Circumventing the Allyl Cuprate Problem

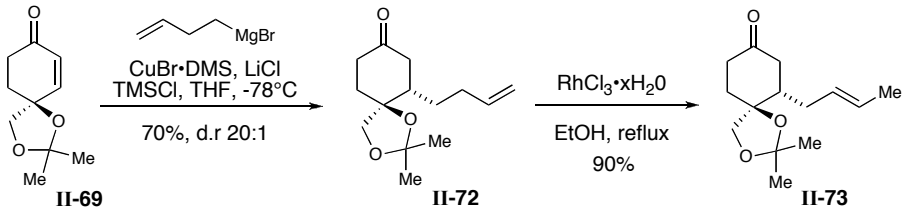

The next step was the introduction of the of the methyl substituent. We found that the site of enolization was difficult to control, ultimately leading to inseparable mixtures of alkylated regioisomers and diastereomers. Additionally, we found overalkylation to be a problem. These issues, taken together with our concerns for the efficiency of this route forced us to revise our strategy for the cyclohexene fragment.

Scheme 2-20. Alkylation Problems

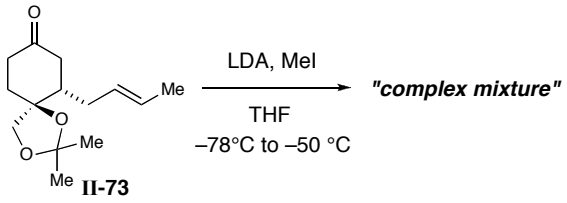

2.6.3 Diels–Alder Approach to Cyclohexene Fragment

The results of the previously described route to the cyclohexene fragment provided valuable information about its potential preparation. The vinylidine carbene based approach was inefficient and deviated from our goal of developing a route to access multigram quantities of the cyclohexene fragment. Additionally, using a substrate control approach to install the methyl and allyl substituents was not ideal.

After the previous route failed we investigated a series of papers by the Roush group describing their work in the area of spirotetronate natural products.[11,119-121] The

strategy employed by the Roush group for the synthesis of these molecules typically involved a Diels-Alder cycloaddition to prepare the spirotetronate portion of the target. Given the similaritites of the those natural products to our synthetic targets, we considered this a viable route after minor modifications.

From a retrosynthetic standpoint, we reasoned that the hydroxyl group of the α-hydroxy aldehyde **II-74** could be introduced through a diastereoselective Rubottom oxidation[122] of a silyl enol ether derived from aldehyde **II-75**. The aldehyde **II-75** could arise from reduction of acyl sultam **II-76**. This acyl sultam would serve as the auxillary for the key Diels–Alder reaction between diene **II-55** and dienophile **II-77**.

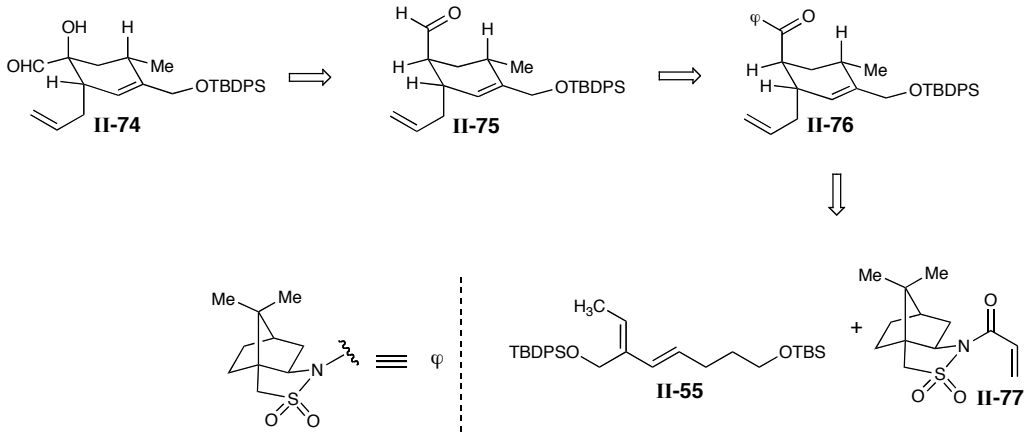

Figure 2-18. Revised Retrosynthetic Analysis

The synthesis of the requisite diene **II-55** for our Diels-Alder approach began with the hydrozirconation of TBS protected pentynol **II-78** with Schwartz's reagent[123] **II-79**. The resulting vinyl metal species was treated with NIS to afford the trans vinyl iodide **II-80** in 80% yield. It was detemined that the yield for this reaction could be maximized if the hydrometallation step was carried out at low temperature (0 °C). Separately, methyl

glycolate was protected as the TBDPS ether and converted to Weinreb amide **II-82** using isopropyl magnesium chloride.[124] Alternative procedures employing $AlMe_3$ failed to provide **II-82** in acceptable yields.

The transmetallation of vinyl iodide **II-80** with *n*-BuLi and addition to Weinreb amide **II-82** furnished the unsaturated ketone **II-83** in 76% yield. The next step was a Wittig olefination[125] to produce the desired diene. This step was critical because it would ultimately serve to establish the relative stereochemistry between the methyl and allyl substiuents on the final α-hydroxy aldehyde fragment. We required the (*Z*)-diene to be formed as this would ultimately lead to a syn relationship between the methyl and allyl substituents. We exposed ketone **II-83** to ethyl triphenylphosphonium bromide and KHMDS and were pleasantly surprised to observe the desired diene **II-55** was formed as a single alkene isomer in 91% yield. It has been proposed by Vedjes[126] that non-stabilized phosphorus ylides formed from bases with potassium counterions generally lead to the (*Z*)-olefin.

Scheme 2-21. Synthesis of Diene **II-55**

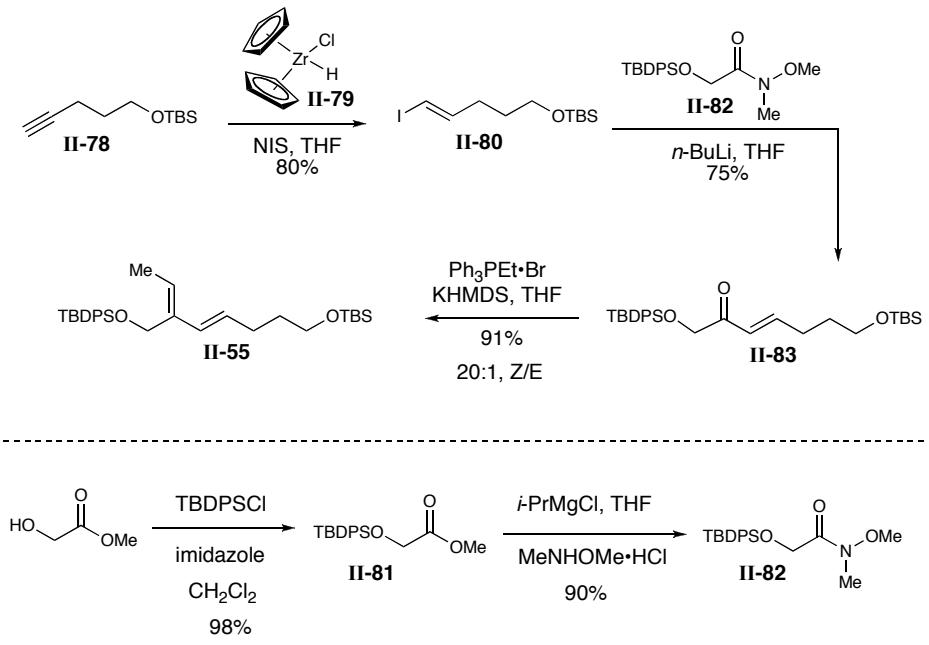

In a key reaction, the chiral Oppolzer[127,128] acrylamide **II-77** and diene **II-55** underwent a [4+2] cycloaddition in the presence of $MeAlCl_2$ producing a 7:1 mixture of diastereomers (Scheme 2-22). The major diastereomer (**II-84**) was assigned as the exo product based on an extensive NOE analysis (see experimental section).

Scheme 2-22. Stereoselective Diels-Alder Reaction

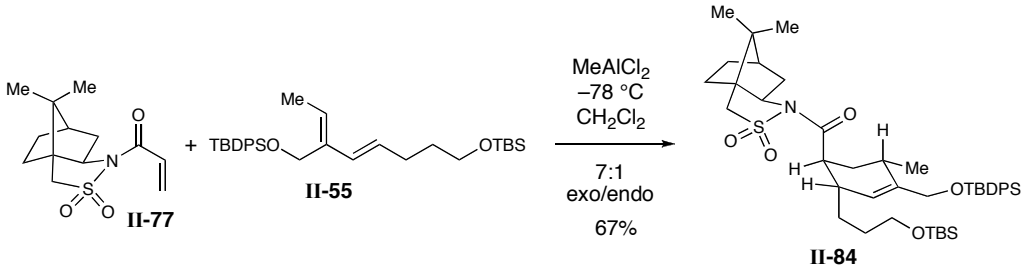

The use of the Oppolzer acrylamide in asymmetric Diels-Alder reactions is well documented. The proposed model for asymmetric induction begins with chelation of the Lewis acid by the carbonyl oxygen and one of the sulfonyl oxygens (Figure 2-19). The dieneophile adopts an *s*-cis orientation in order to minimize interaction with the norbornane ring. The diene approaches from the less sterically encumbered *Re* face, thereby avoiding undesirable steric interactions with the norbornane ring.[128]

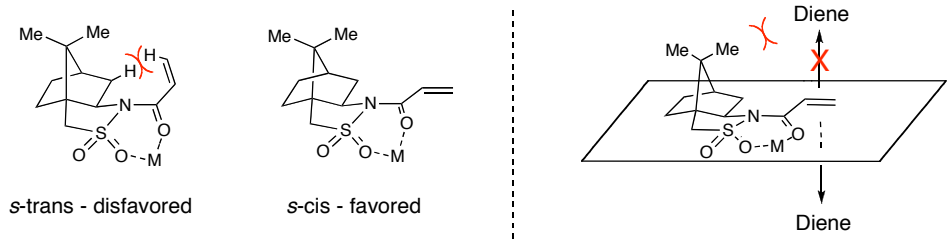

Figure 2-19. Model for Stereoinduction using Chiral Oppolzer Sultam

The next step in the synthetic sequence was the removal of the TBS ether and installation of the terminal double bond. The selective removal of the TBS ether in the presence of the TBDPS group was far more challenging than we had anticipated. After extensive experimentation, we found that 0.5% aqueous HCl selectively removes the TBS ether to provide alcohol **II-85** in 83% yield. The olefin **II-76** was prepared from **II-85** using Grieco's selenation/oxidation procedure.[109] The sultam auxiliary was removed with DIBAl-H to directly afford the aldehyde **II-75**. The aldehyde was then converted to the TBS enolsilane and immediately treated with DMDO to give α-hydroxy aldehyde **II-74** as a single diastreomer. The choice of silyl triflate during enol silane formation was critical to the success of this two step operation. We screened TMSOTf, TESOTf, and TBSOTf. The formation of the TMS silyl enol ether did not proceed to 100% completion

under any reaction conditions. This result limited its applicability in our synthesis as we did not want to recover starting materials in a seemingly simple two step transformation. We next chose to use the TES ether and found that the enol silane was formed smoothly, however, the subsequent Rubottom oxidation produced diastreomers. Gratifiyingly, we were pleased to find that the TBS enolsilane was formed in quantitative yield and the subsequent Rubottom oxidation produced a single diastereomer of the desired α-hydroxy aldehyde fragment. The relative stereochemistry of this intermediate was confirmed by NOE analysis (see experimental).

Scheme 2-23. Synthesis of α-Hydroxy Aldehyde **II-74**

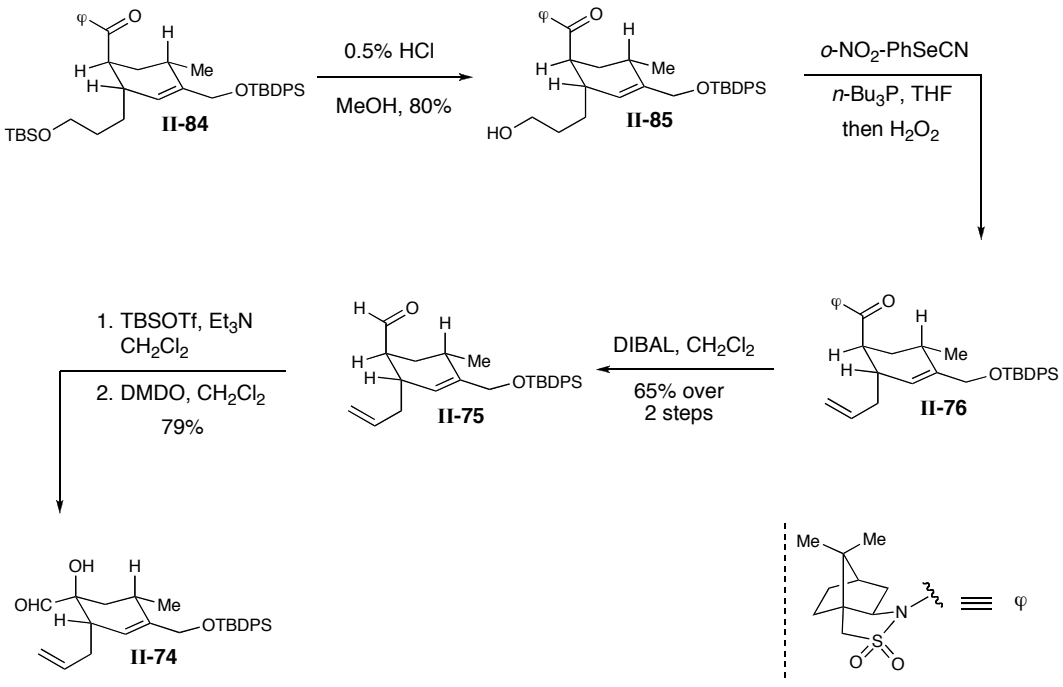

This route was completed in 10 steps in an overall yield of 19%. This route was found to be scalable, highly convergent, and reproducible. It provided access to gram

quantities of the desired α-hydroxy aldehyde **II-74** in optically enriched form and thus satisfied our objectives for fragment synthesis.

2.6.4 Revised Model Study

During the time that the asymmetric routes to the principal fragments **II-64** and **II-74** were being developed, we considered it prudent to conduct model studies using an α-hydroxy aldehyde that more closly resembled **II-74**. We combined the racemic α-hydroxy aldehyde **II-74** and β-hydroxy dioxinone **II-86** and subjected them to our novel $Sc(OTf)_3$ cyclization conditions (Scheme 2-24). Unfortunately, we did not observe formation of the desired pyran product **II-87**. The β-hydroxy dioxinone was recovered in quantitative yield but it appeared that the α-hydroxy aldehyde underwent undesired side reactions under the reaction conditions. We believe it is possible that a Prins reaction could potentially take place due to the proximity of the Lewis acid activated aldehyde and the terminal double bond. We attempted to mask the double bond as the TBS ether (**II-88**) but did not observe the formation of the desired pyran. We found that the reaction conditions caused removal of the TBS protecting group and caused hemiacetal formation (not shown). At this phase of the project, it now appeared our novel cyclization method was not going to be applicable to the total synthesis of **II-1** or **II-2**.

Scheme 2-24. Revised Model Study

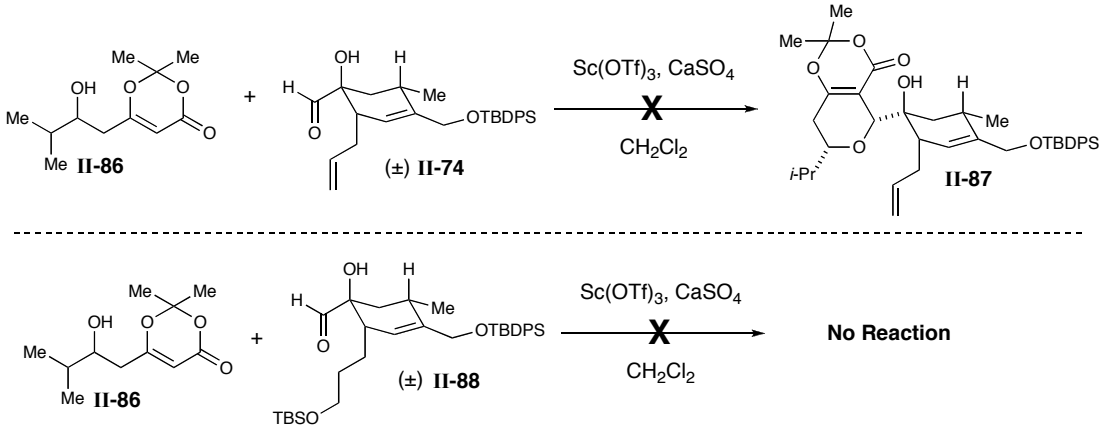

2.6.5 Novel Fragment Assembly

This result once again required us to find an alternative method for fragment assembly. Since the synthetic routes for fragments **II-64** and **II-74** were already established, we chose to evaluate coupling strategies that would utilize these fragments as opposed to manipulating the synthetic routes. We focused on using the dioxinone **II-64** to acylate the hindered tertiary alcohol of α-hydroxy aldehyde **II-74**. Towards this end, dioxinone **II-89** and α-hydroxy aldehyde **II-88** were heated to 130 °C for 90 minutes. Analysis by thin layer chromatography showed clean conversion to a single compound. This compound was isolated and identified as butenolide **II-90**.

Scheme 2-25. Model for Novel Fragment Assembly

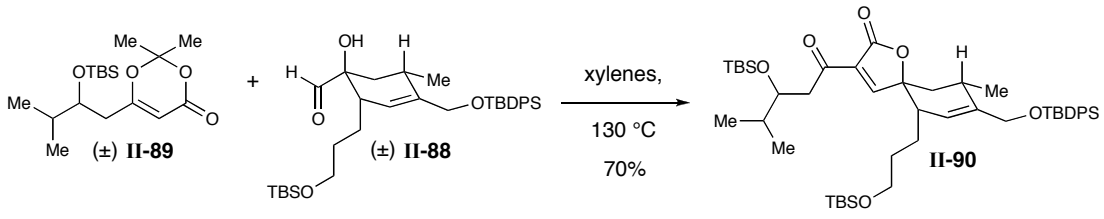

A proposed mechanistic pathway for the formation of butenolide **II-90** is shown in Figure 2-20. The reaction temperature initiates a [4+2] cycloreversion to generate acyl ketene **II-A**. The tertiary alcohol **II-88** is acylated by the highly reactive acyl ketene to form β-keto ester **II-B**. Under the reaction conditions the enol tautomer of **II-B** could serve as a nucleophile for the aldol addition to the aldehyde. This fleeting intermediate (**II-C**) is rapidly dehydrated to provide the butenolide product **II-90**.

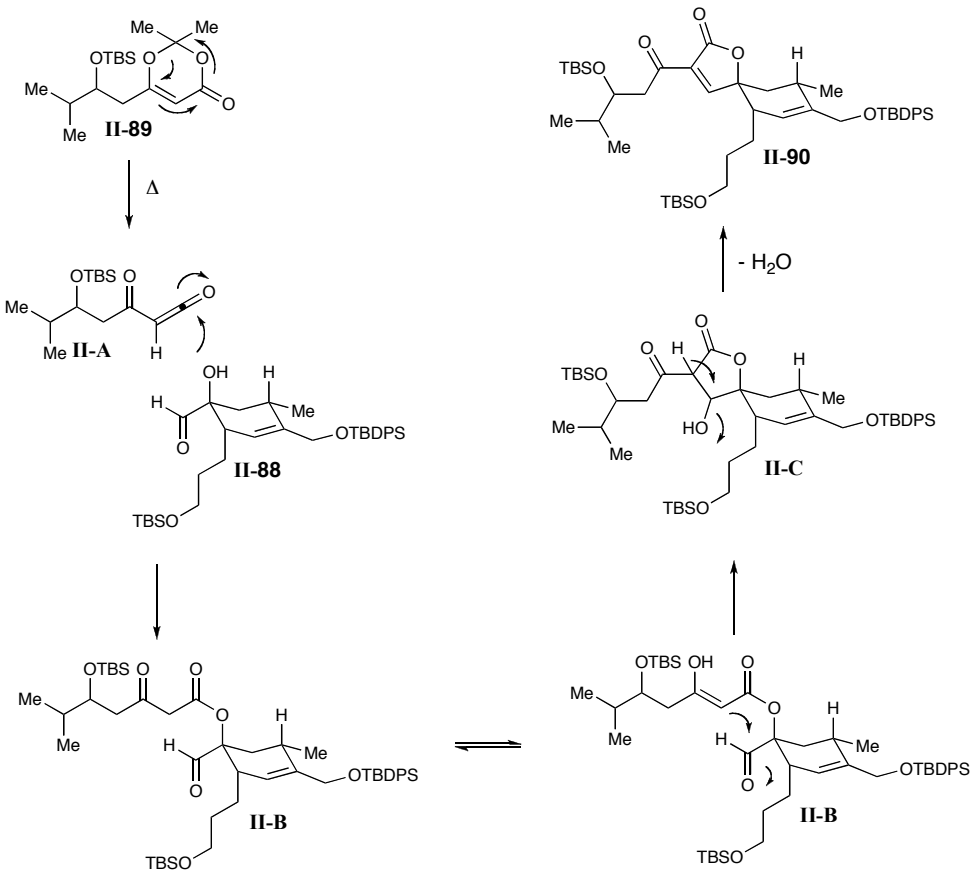

Figure 2-20. Mechanism for the Formation of Butenolide **II-90**

We found this result very promising. We considered the removal of the TBS group to be straightforward and we were confident the resulting alcohol would readily add to the newly formed conjugate acceptor. We attempted to reproduce the fragment coupling reaction using dioxinone **II-64** and α-hydroxy aldehyde **II-74**. Using the same reaction conditions described in Scheme 2-25, we were able to isolate the desired butenolide **II-91** and methyl ketone **II-92** (Scheme 2-26).

Scheme 2-26. Key Fragment Assembly

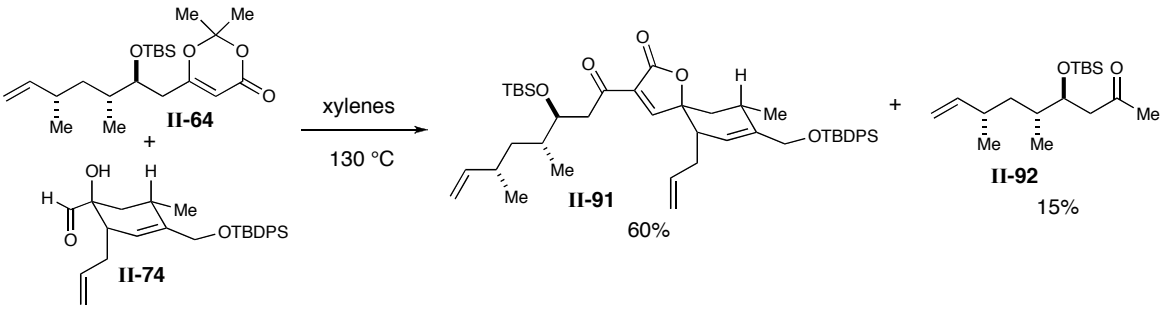

We suspected that water formed during the dehydration step could potentially add to the acyl ketene generated from the [4+2] cycloreversion and subsequently undergo decarboxylation to generate methyl ketone **II-92**. Operating under this hypothesis, we attempted to remove this water using a variety of drying agents such as 4Å molecular sieves, $CaSO_4$, $MgSO_4$ and Na_2SO_4. Unfortunately, these experiments resulted in similar product distributions for the butenolide **II-91** and the methyl ketone **II-92**. Next, we attempted to preclude the addition of H_2O to the acyl ketene by adding DMAP to the reaction mixture. We reasoned DMAP would be more nucleophilic than the adventitious H_2O and the resulting acyl pyridinium intermediate would be the reactive acylating agent.

Unfortunately, the DMAP additive provided similar product distributions for the butenolide **II-91** and the methyl ketone **II-92**.

At this time we began to consider the possibility that the methyl ketone **II-92** was formed via product decomposition. We became aware of a report by Witzeman[129,130] and co-workers who showed that *tert*-butyl acetoacetate eliminates to an acyl ketene intermediate 15 fold faster than ethyl acetoacetate. In addition to this report by Witzeman, we found that Roush and co-workers encountered similar problems in their work towards the synthesis of kijanolide.[131,132] In these studies, it was found that heating β-keto ester **II-93** to 130 °C led to the formation of methyl ketone **II-94**.

Scheme 2-27. Thermal Decomposition of β-Keto Ester **II-93**

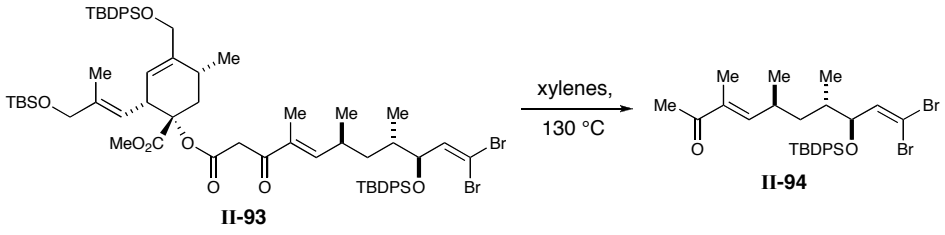

II-93 **II-94**

Based on the Witzeman and Roush reports, we we chose to lower the reaction temperature in an effort to reduce the (presumed) product decomposition. We were pleased to find that by reducing the reaction temperature to 113 °C and the reaction time to 75 minutes, the butenolide could be accessed in 85-95% yield with only minor amounts of methyl ketone.

Scheme 2.28. Modified Fragment Assembly Conditions

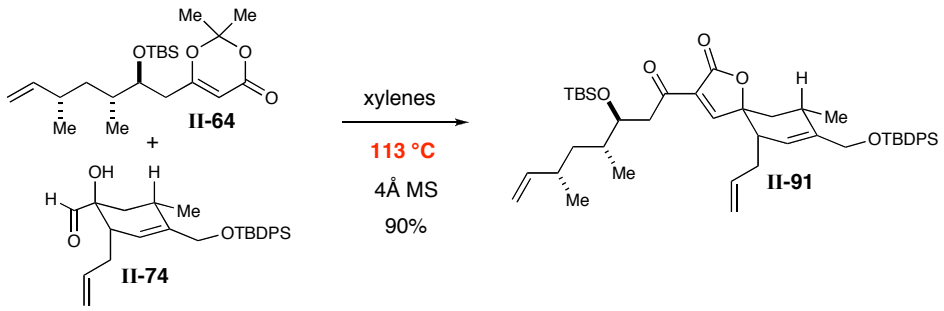

2.6.6 Intramolecular Conjugate Addition

With the optimized fragment coupling conditions now secured, our attention shifted towards developing a method to promote the conjugate addition of the C8 hydroxyl group onto our newly formed conjugate acceptor. Similar types of cyclizations are precendented in the literature utilizing a variety of conditions, however, the conjugate addition typically takes place on an α,β-unsaturated ketone (Figure 2-21). We reasoned that our conjugate acceptor was more electrophilic due to the additional electron withdrawing group present and therefore felt confident about its potential for success.

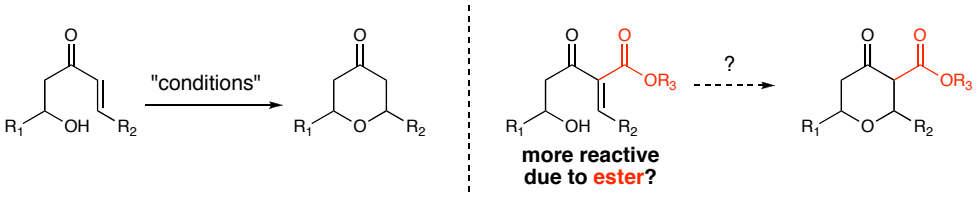

Figure 2-21. Conjugate Addition Considerations

The first step towards successfully executing this conjugate addition was to remove the TBS protecting group. Given the lability displayed by the TBDPS group during the synthesis of the α-hydroxy aldehyde fragment (**II-74**) we suspected it would

be difficult to selectively remove the TBS ether in the presence of the TBDPS ether. Consequently, we chose to expose the butenolide to tetrabutylammonium fluoride (TBAF), hoping to achieve global desilylation. These conditions did remove both silyl groups but did so in poor yield (< 60%). We thought the hydroxide content of the TBAF was responsible for this poor yield although no identifiable byproducts were obtained to confirm this suspicion. To attenuate this presumed basicity, AcOH was added prior to the addition of TBAF. These reaction conditions led to a new product distribution (Scheme 2-29). The first product was the TBDPS deprotected material **II-96**. We were also able to isolate the diol **II-95**. Finally, we were pleased to find that the desired pyranone **II-97** was formed in 18% yield. It appeared that the cyclized product was a 4:1 mixture of inseparable diastereomers. The identity of this minor diastereomer will be discussed at a later time. The relative stereochemistry of the C8, C11, and C12 protons of **II-97** was confirmed by NOE analysis (see expermiental section).

Scheme 2-29. Deprotection of the Butenolide

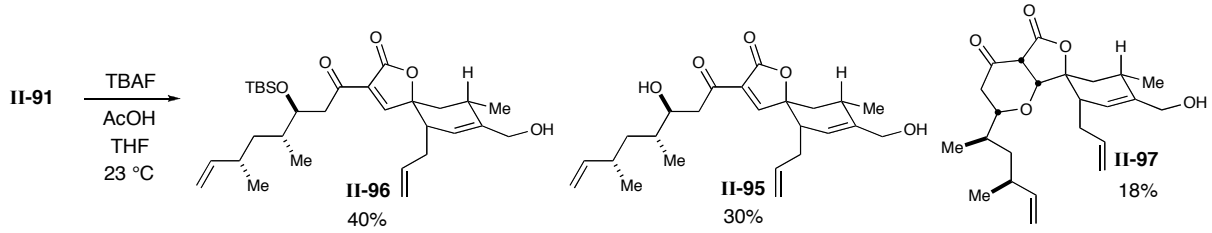

This result seemed to validate the proposed route to our target molecules. We speculated that the AcOH served a duel role in this reaction. It acted to buffer any hydroxide content introduced to the reaction by the TBAF and it served to protonate the newly formed enolate following the conjugate addition.

In order to maximize the efficiency of this process, we searched for conditions to convert the diol **II-95** into the desired pyranone **II-97**. We began by evaluating Bronsted acids in the reaction (Scheme 2-30). We surveyed TsOH, PPTS, AcOH, HCl and Amberlyst exchange resin. The results of these expermients were poor, as we either observed elimination of the C8 hydroxyl group to provide **II-98**, no reaction, or decomposition of the starting material.

Scheme 2-30. Acid Survey

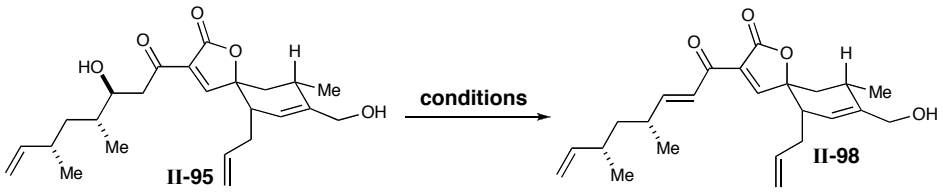

entry	conditions	Result (yield)
1	TsOH, THF, 0 °C to 23 °C	**II-98** (75%)
2	PPTS, MeOH. 0 °C to 23 °C	No Reaction
3	AcOH, THF, 23 °C	No Reaction
4	1M HCl (aqueous), 0 °C	**II-98** (50%)
5	Amberlyst Exchange Resin, MeOH	Decomposition

Concurrently, we surveyed a variety of bases in the reaction. The bases evaluated were NEt_3, DBU, *t*-BuOK, KHMDS and KOH. We found that the formation of **II-98** predominated under basic conditions.

Scheme 2-31. Base Survey

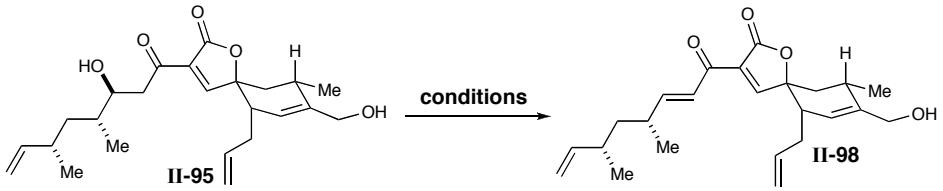

entry	conditions	Result (yield)
1	NEt_3, CH_2Cl_2, 23 °C	**II-98** (60%)
2	DBU, CH_2Cl_2, 23 °C	**II-98** (55%)
3	*t*-BuOK, THF, 0 °C	**II-98** (25%)
4	KHMDS, THF, –78 °C to 0 °C	**II-98** (40%)
5	KOH, THF/H_2O, 0 °C	**II-98** (60%)

Following the survey of acids and bases, we attempted to employ Lewis acids to promote the cyclization of **II-95** to pyranone **II-97**. We suspected that the low energy conformation of diol **II-95** had the 1,3-dicarbonyl functionality dipole minimized. We thought that a bis chelating Lewis acid would predispose the diol **II-95** towards cyclization.We attempted several Lewis acids such as $Mg(OTf)_2$, $Zn(OTf)_2$ $Sc(OTf)_3$, $Cu(OTf)_2$ and $TiCl_4$ to chelate the 2 carbonyl groups. Under these conditions we observed no reaction. When an amine base was added, we observed rapid formation of the elimination product **II-98** (Scheme 2-32).

Scheme 2-23. Lewis acid Survey

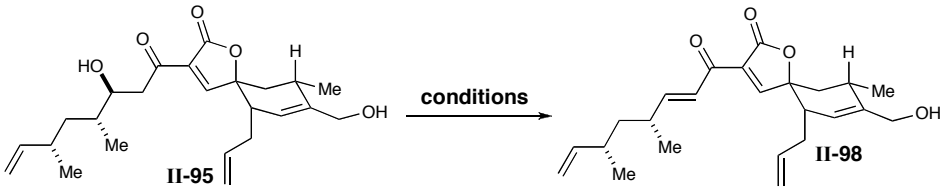

entry	conditions	additive	Result (yield)
1	$Mg(OTf)_2$, CH_2Cl_2, 23 °C	none	No Reaction
2	$Cu(OTf)_2$, CH_2Cl_2, 23 °C	none	No Reaction
3	$Sc(OTf)_3$ MeCN, 0 °C	none	No Reaction
4	$TiCl_4$, CH_2Cl_2, 0 °C	none	No Reaction
5	$Zn(OTf)_2$, CH_2Cl_2, 0 °C	none	No Reaction
6	$Mg(OTf)_2$, CH_2Cl_2, 23 °C	NEt_3	**II-98** (85%)
7	$TiCl_4$, CH_2Cl_2, 0 °C	NEt_3	**II-98** (82%)

After the Lewis acid survey, we turned to thioureas[133] to promote the conjugate addition. Thioureas serve to activate electrophiles (such as 1,3-dicarbonyl compounds) towards nucleophilic addition by acting as H-bond donors. Thioureas **II-99** and **II-100** provided no reaction. The thiourea derived from quinine (**II-101**) provided elimination product **II-98**.

Scheme 2-33. Thiourea Survey

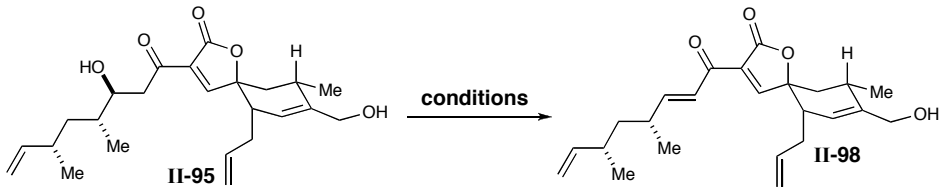

entry	conditions	Result (yield)
1	**II-99**, CH_2Cl_2, 23 °C	No Reaction
2	**II-100**, CH_2Cl_2, 23 °C	No Reaction
3	**II-101** CH_2Cl_2, 23 °C	**II-98** (70%)

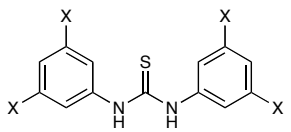

X = H **II-99**
X = CF_3 **II-100**

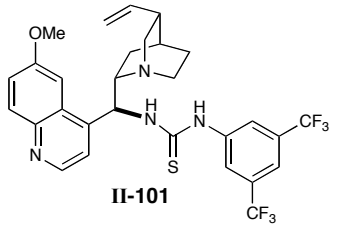

II-101

Our final attempts at accessing the pyranone **II-97** from the diol **II-95** focused on transition metal mediated processes. Gouverneur reported the use of $[Pd(MeCN)_4](BF)_4$ to promote the addition of oxygen nucleophiles to α,β-unsaturated ketones.[134,135] Additionlly, Floreancig[136] has shown a similar transformation could be carried out with $(Ph_3P)_3AuCl/AgSbF_6$. We attempted both conditions and found that decomposition to unidentifiable products took place.

Scheme 2-34. Transition Metal Survey

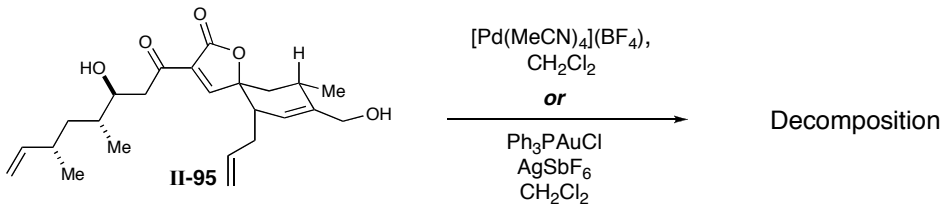

The reluctance of diol **II-95** to undergo cyclization forced us to reconsider the mechanism of this reaction. We began to speculate that the formation of a hypervalent silicate[137,138] was key to facilitating the desired conjugate addition reaction. We found that treating the TBS silyl ether **II-96** with TBAF and AcOH provided the pyranone **II-97** and the diol **II-95**. Given this data we shifted our focus towards finding the optimal combination of fluoride and acid that would improve the yield and product distribution.

Scheme 2-35. Silicate-Mediated Conjugate Addition

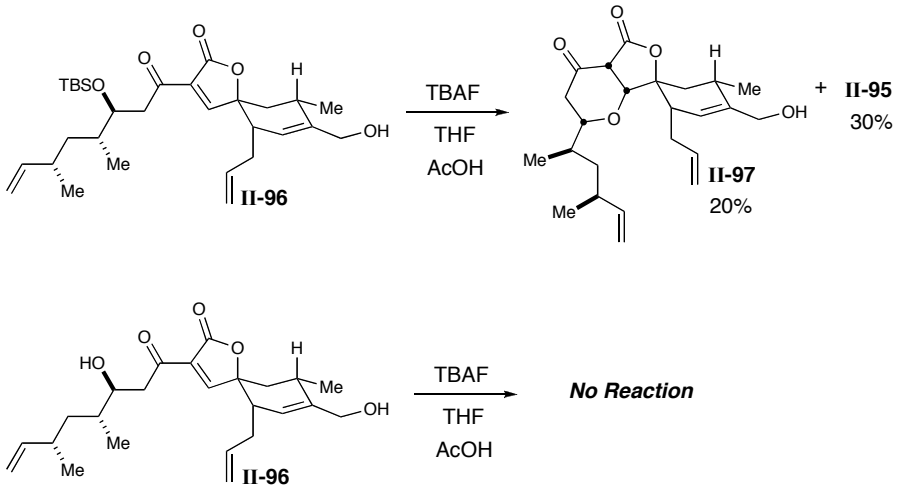

We began by screening various fluoride sources with AcOH. The results of this survey are shown in Scheme 2-36.We found that under most conditions, rapid desilylation of the TBDPS group was observed. In the case of tris(dimethylamino)sulfonium difluorotrimethylsilicate (TAS-F),[139-141] the conjugate addition took place to furnish pyranone **II-97**, but the yield was lower than when TBAF was used (15%).

Scheme 2-36. Survey of Fluoride Sources

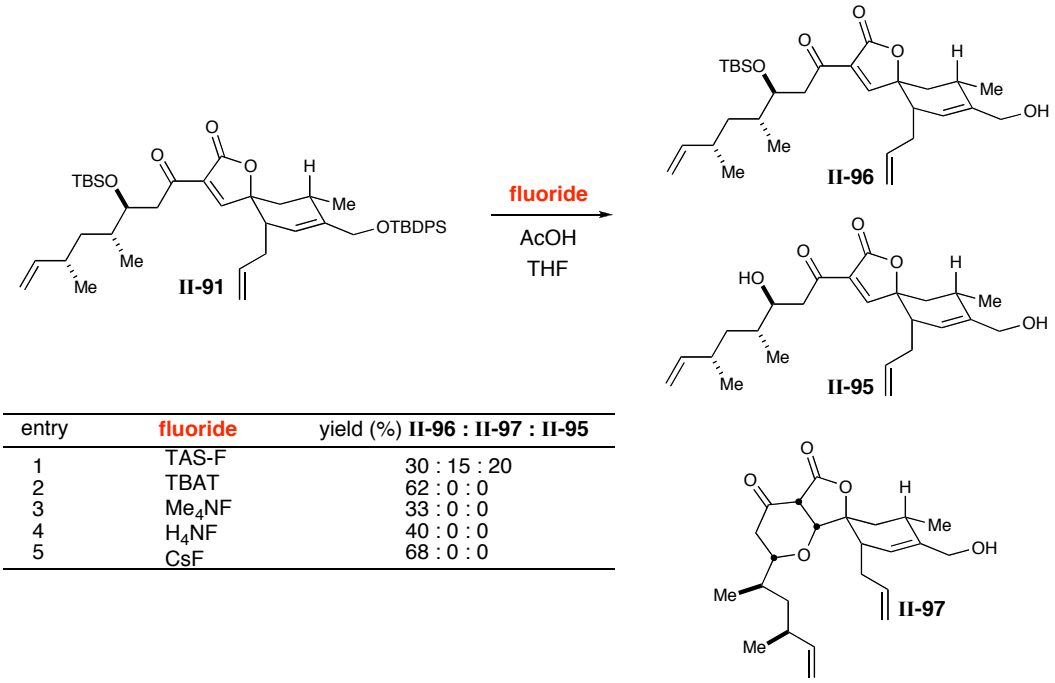

entry	fluoride	yield (%) **II-96 : II-97 : II-95**
1	TAS-F	30 : 15 : 20
2	TBAT	62 : 0 : 0
3	Me_4NF	33 : 0 : 0
4	H_4NF	40 : 0 : 0
5	CsF	68 : 0 : 0

We next considered if the pKa of the acid additive was important to the product distribution. After evaluating a variety of acids with TBAF as the fluoride source, we found acetic acid to be the optimal acid (Scheme 2-37).

Scheme 2-37. Survey of Acid Additives

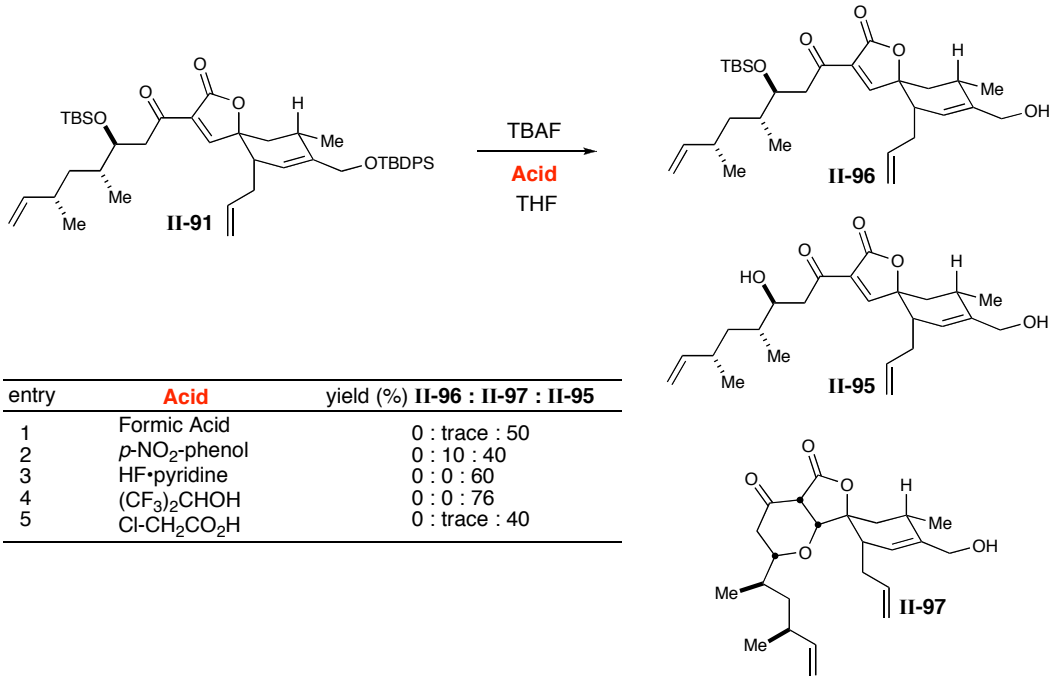

entry	Acid	yield (%) **II-96 : II-97 : II-95**
1	Formic Acid	0 : trace : 50
2	*p*-NO_2-phenol	0 : 10 : 40
3	HF•pyridine	0 : 0 : 60
4	$(CF_3)_2CHOH$	0 : 0 : 76
5	$Cl\text{-}CH_2CO_2H$	0 : trace : 40

After the *extensive* survey of reaction conditions we were convinced that the combination of TBAF and AcOH was optimal for the cyclization reaction.

Once we established TBAF/AcOH was the optimal reagent combination, we focused on finding the optimal reaction time and temperature. We determined that the TBDPS group was removed at 0 °C over 5 hours. The reaction did not proceed further unless it was warmed to 23 °C, at which time the diol **II-95** and pyranone **II-97** began to form (TLC analysis). We found that extension of the reaction times generally provided similar levels of conversion and yields. We were surprised to find that the diastereomeric ratio was dependent on reaction time. If the reaction was allowed to stir for 10 hours (5 hours at 0 °C and 5 hours at 23 °C), we observed a 4:1 ratio of diastereomers. If the reaction mixture was allowed to stir for 20 hours (5 hours at 0 °C and 15 hours at 23 °C), we observed a 2:1 mixture of diastereomers. Unfortunately, the extensive optimization

studies yielded very little improvement from our initial results. At this stage of the project, we chose to move forward with the synthesis and planned on revisting this reaction at a later time.

2.7 Completion of the Synthesis

2.7.1 Formation of the Macrocycle

We began by protecting the allylic alcohol of **II-97** as the TBDPS ether. The next step of the synthesis was the formation of the macrocycle via ring-closing metathesis (RCM).[142-144] It should be noted that the RCM could not be carried out successfully until the pyranone ring was formed. This effectively brought the two reacting dienes in close proximity to undergo ring closure. We exposed diene **II-102** to the first generation Grubbs catalyst, the first generation Grubbs–Hoveyda catalyst,[145] second generation Grubbs catalyst, and the second generation Grubbs–Hoveyda catalyst. We found the second generation Grubbs catalyst to be superior in terms of yield and reaction rate. We found that heating the reaction to 40 °C in the presence of 40 mol % of the second generation Grubbs catalyst for 4 hours provided a 65% yield of the 11-membered macrocycle **II-103**. The diastereomers formed during the conjugate addition step were not able to be separated after the macrocycle was closed.

Scheme 2-38. Preparation of the Tetracyclic Core

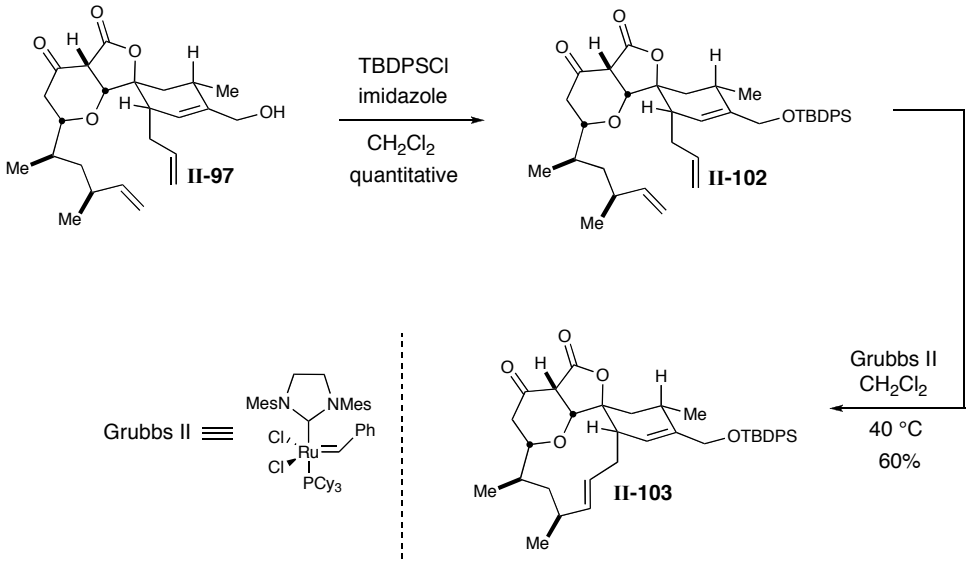

The tetracycle **II-103** was the differentiation point in our synthesis. The next step in our synthesis was to install the C11 substituent. We felt that pursuing okilactomycin was more practical because the installation of the C11 methyl substituent could be carried out in a single synthetic operation. The C11 methoxy group of chrolactomycin would require no less than two steps.

In previous model work we found that treating 3-carboxy substituted pyranones with strong bases such as NaH and *t*-BuOK led to decomposition of the starting material (data not shown). We believe that the formation of the enolates and subsequent retro-aldol type processes are responsible for the observed decomposition. We reasoned that if we used a mild base (K_2CO_3) in conjunction with higher reaction temperatures we could alkylate the C11 position without undergoing retro-aldol mediated decomposition. We were pleased to find that treatment of **II-103** with K_2CO_3 and MeI in MeCN provided the alkylated product in excellent yield (90%) as a single diastereomer (20:1). The

diastereoselectivity was confirmed based on NOE analysis (see experimental). The selectivity of this reaction can be rationalized by considering electrophile approach to the less hindered, convex face of the 6-5 ring system.

Scheme 2-38. Alkylation at C11

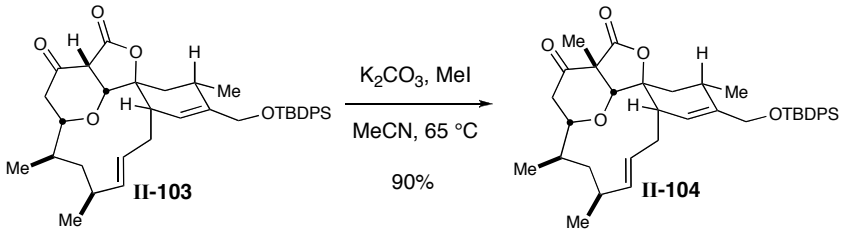

Additionally, we were pleased to find that the diastereomers we had been carrying through since the conjugate addition reaction were able to be separated at this step. We tentatively assigned the major diastereomer as our desired product, ie. **II-104**. This was based on an NOE analysis where the C8, C12 and newly installed methyl group were on the same face of the molecule. In the case of the minor diastereomer **II-105**, we were surprised to find that when the C12 proton was irradiated, we observed an NOE signal between the C11 methyl group *and* the C8 methine proton. This led us to consider that the C8 stereocenter had epimerized under the TBAF/AcOH reaction conditions.

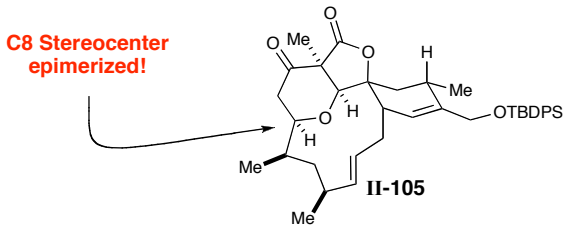

Figure 2-22. Tentative Structural Assignment of Minor Diastereomer

This type of epimerization has been precedented. Rizzacasa and coworkers found a similar epimerization in their synthesis of (–)-apicularen.[77,78] In this work, a transannular conjugate addition is used to form pyranone **II-106**. The authors found that the stereochemistry at C9 and C13 ((–)-apicularen numbering) could scramble via a conjugate addition/elimination equilibration sequence. Thus, under thermodynamic conditions, the absolute stereochemistry at C13 was inconsequential.

Scheme 2-40. Rizzacasa's Synthesis of (–)-Apicularen

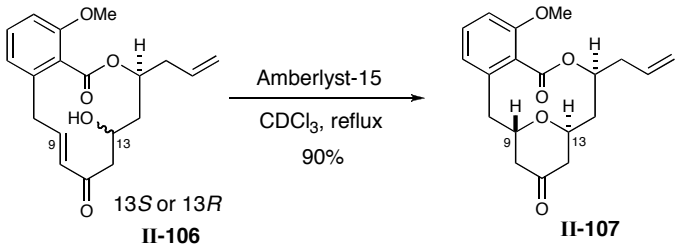

2.7.2 Stereochemical Studies

In order to verify the structure of **II-105** we prepared the C8 epimer of fragment **II-64**. The syn-aldol adduct was prepared from aldehyde **II-53** and enolsilane **II-54**. *The chiral ligand was changed to (S)-tol-BINAP which led to the formation of the syn-aldol product* ***II-108*** *with high levels of diastereocontrol (>30:1)*. The newly formed

secondary alcohol was protected as the TBS silyl ether in quantitative yield. The TBDPS group was selectively removed with NH_4F, and the resulting primary alcohol was converted to the terminal olefin **II-109** using Grieco's procedure.

Scheme 2-41. Synthesis of C8 Epimer

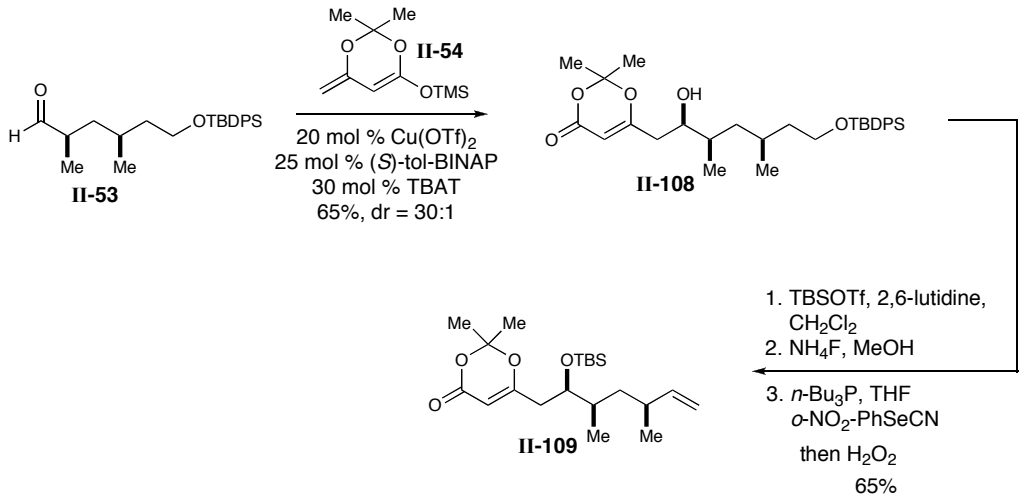

Dioxinone **II-109** was condensed with the α-hydroxy aldehyde **II-74** using our optimized fragment coupling procedure. The resulting butenolide **II-110** was treated with TBAF/AcOH in THF to form pyranone **II-111**. It should be noted that the yield was slightly higher, and the pyranone was formed as a single diastereomer. The allylic alcohol **II-111** was reprotected as the TBDPS ether and subjected to ring closing metathesis conditions. The desired macrocyle **II-112** was formed as a single olefin isomer. The tetracycle **II-113** was treated with K_2CO_3 and MeI to provide the alkylated pyranone.

The NMR spectrum of this compound matched the NMR spectrum of the minor diastereomer from when the C8 stereocenter was installed using (R)-tol-BINAP. This result provided compelling evidence that the C8 position is epimerizable under the

reaction conditions employed for the cyclization from the butenolide **II-91** to the pyranone **II-97**.

Scheme 2-42. Synthesis of C8 Epimer Continued

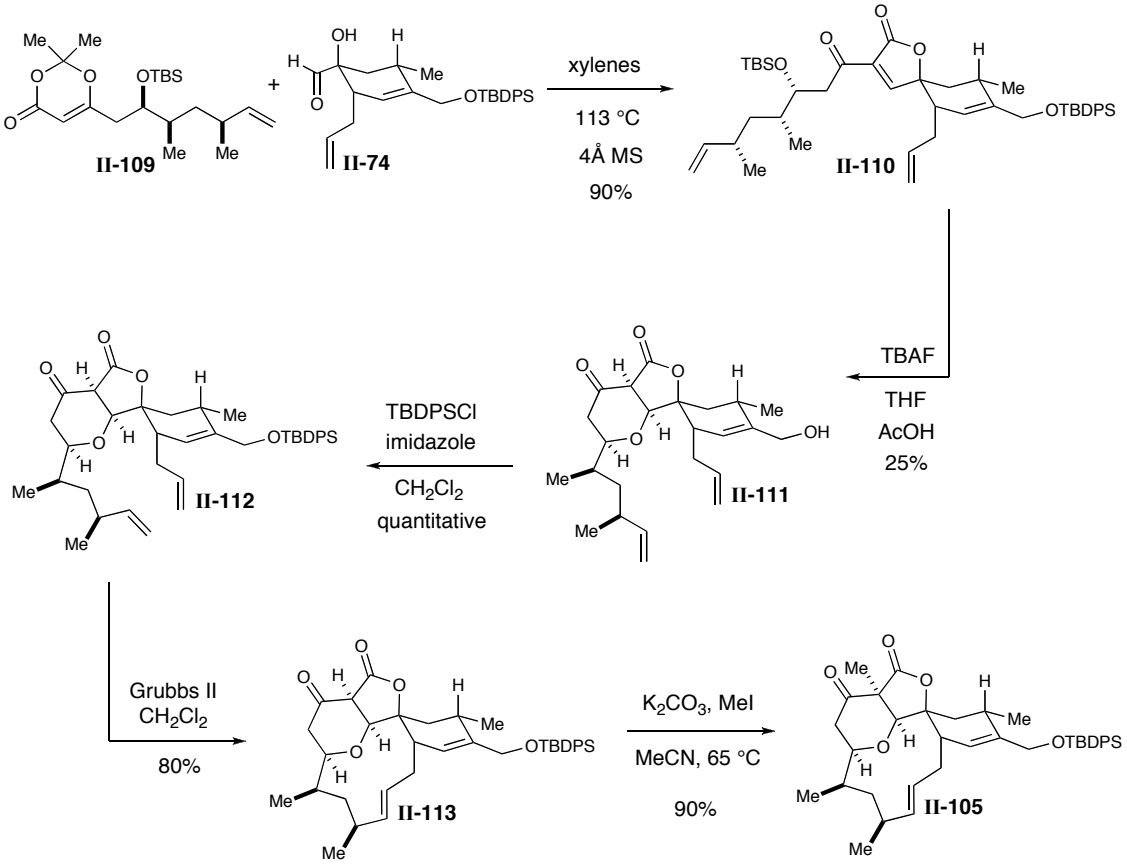

2.7.3 NMR Spectroscopic Analysis of II-104

Given the structural complexity of these advanced intermediates we felt it would be prudent to gather as much structural information as possible on tetraycle **II-104**. At this stage of the synthesis we could not access enough material to grow a crystal suitable for single crystal analysis. As an alternative, a series of 1D and 2D NMR spectroscopy

techniques were used in an attempt to verify the structure of **II-104**. We had previously established that the C11 methyl group, the C12 methine proton and the C8 methine proton were on the same face of the pyranone ring via 1D NOE analysis. An NOE between the C8 methine and the C23 methyl group indicated the correct relative stereochemistry at C7 and C8 (Figure 2-23).

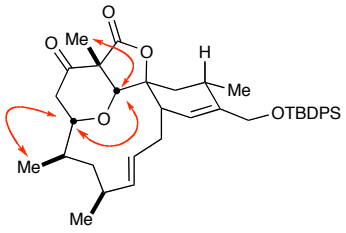

Figure 2-23. Key NOE Signals of **II-104**

We next sought to establish if there was a through space interaction between the C12 methine proton and the C1 methine proton. The isolation report indicates that there is an NOE signal between these 2 protons in the natural product. *We were unable to observe the same signal in our advanced intermediate* (Figure 2-24). We did, however, see correlation to the C14 proton.

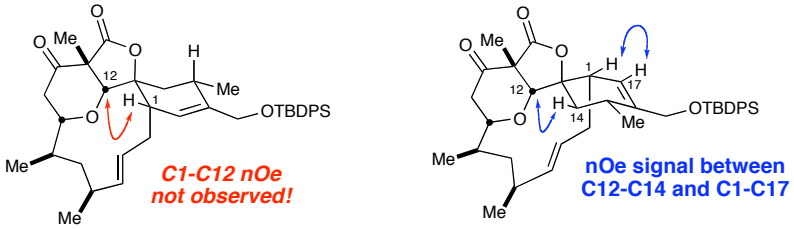

Figure 2-24. Key NOE Signals for **II-104**

Based on these signals, we considered the possibility that we had prepared the enantiomer of α-hydroxy aldehyde **II-74**. It should be noted that we did not have X-ray crystal data for any intermediate to verify the absolute streochemistry of the α-hydroxy aldehyde **II-74**. Therefore, the synthetic sequence used to prepare the α-hydroxy aldehyde **II-74** was repeated using the enantiomer the chiral auxilary **II-77**. These results will be discussed later.

Concurrently, we decided to move forward using *reassigned* **II-104**. We felt we could use this intermediate to gather valuble information about how to complete the final steps of the synthesis. The following sections will discuss the end game strategy. Following this discussion we will describe the results of using the enantiomer of α-hydroxy aldehyde **II-74**.

2.8 Completion of the Synthesis

The steps that remained to complete the synthesis involved: 1. Manipulation of the C18 oxidation state 2. Selective reduction of the C3-C4 double bond resulting from the ring closing metathesis and 3. Installation of the exomethylene unit. We felt the installation of the exomethylene unit should be one of the final steps in the synthesis given its highly electrophilic nature. We also recognized that we could increase the potential for selective reduction of the macrocyclic double bond in the presence of the trisubstituted olefin by making the trisubstituted olefin electron deficient. This works well within the context of the synthesis as the trisubstituted olefin will eventually become part of an α,β-unsturated carboxylic acid. Thus, our plan at this stage of the synthesis was to manipulate the oxidation state of C18 (using a suitable protecting group for the

carboxylic acid), reduce the macrocyclic olefin in the presence of the trisubstituted olefin, install the exomethylene unit and deprotect the carboxylic acid.

2.8.1 Manipulation of the C18 Oxidation State

To begin our manipulation of the C18 oxidation state the TBDPS ether **II-104** was treated with HF•pyridine providing the allylic alcohol **II-114** in quantitative yield (Scheme 2-43). The alcohol **II-114** was oxidized to aldehyde **II-115** using Dess–Martin periodinane.[81] The aldehyde **II-115** was oxidized with $NaClO_2$ under biphasic conditions to the carboxylic acid **II-116** in 65% yield.[146]

Scheme 2-43. Manipulation of the C18 Oxidation State

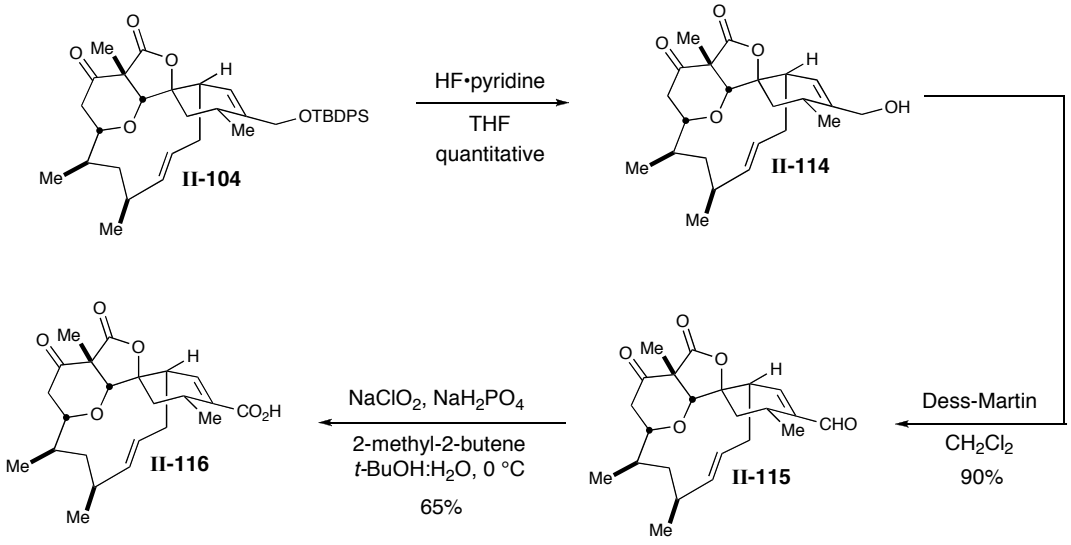

2.8.2 Protecting Group Strategy

The final steps of our synthesis involved the installation of the highly reactive exomethylene unit followed by the subsequent removal of the carboxylic protecting group. The selection of this protection required careful consideration because it would

have to be removed under conditions compatible with the exomethylene unit. Given this requirement a model system was developed to evaluate suitable candidates.

The first carboxylic acid protecting group chosen for evaluation was the methyl ester. This was initially considered because its preparation from carboxylic acid **II-116** would be straightforward and there are numerous conditions available for its conversion to the carboxylic acid.[147] In order to evaluate potential protecting groups, a model of the 6-5 bicycle was prepared. Pyranone **II-117** was alkylated using our established K_2CO_3/MeI conditions. The resulting β-keto ester **II-118** was treated with LiHMDS at –78 °C followed by Eschenmoser's salt[148] to furnish pyranone **II-119**.

Scheme 2-44. Preparation of Model Pyranone **II-119**

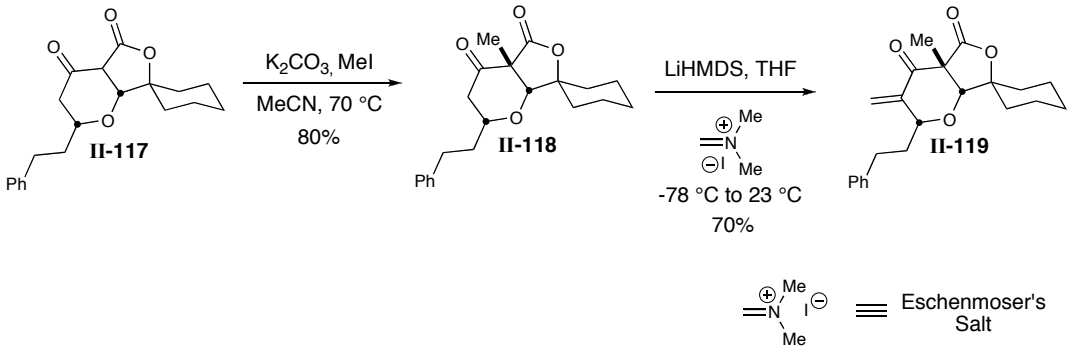

Our initial experiments involved subjecting the model intermediate **II-119** to the proposed reaction conditions required for methyl ester cleavage. In order for this protecting group strategy to be viable we needed the exomethylene group to be unreactive under the proposed deprotection conditions. We initially surveyed basic conditions such as KOH, LiOH, and NaOH. Under all of these conditions rapid decomposition of the exomethylene was observed (TLC analysis). We shifted our

attention to acidic conditions such as dilute aqueous HCl and rapid decomposition was observed again. Given these results, we sought a neutral alternatives for methyl ester cleavage. We found that TMSOK[149] was a neutral alternative for cleaving methyl esters on acid and base sensitive substrates. Despite these precedents, we did not find these conditions to be compatible with our model substrate **II-119**.

While continuing with our search for neutral conditions to cleave methyl esters, we became aware of a report by Ellman[150] and co-workers utilizing Me_3SnOH to convert bis-methyl ester **II-120** to bis-carboxylate **II-121**. Additionally, Nicolaou[151] used similar conditions to convert the sensitive methyl ester **II-122** to α-keto acid **II-123**.

Scheme 2-45. Me_3SnOH in Organic Synthesis

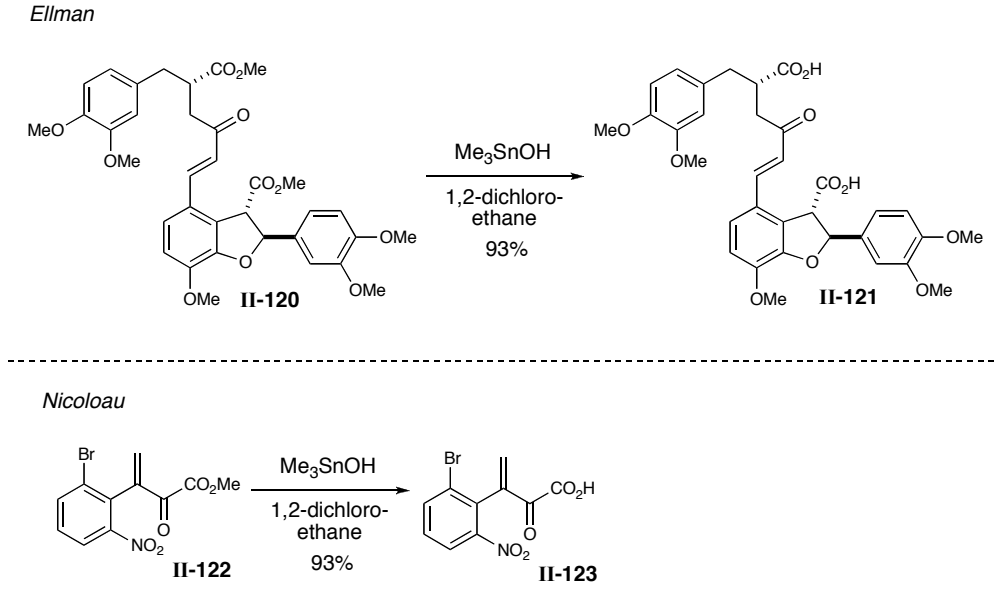

We subjected our exomethylene model substrate **II-119** to Me_3SnOH deprotection conditions and were able to recover the starting material in quantitative yield. We then

attempted a competition experiment where methyl ester **II-124** was introduced into the reaction mixture. We were pleased to observe conversion to the carboxylic acid **II-125** while the model exomethylene **II-119** remained unaffected.

Scheme 2-45. Competition Experiment

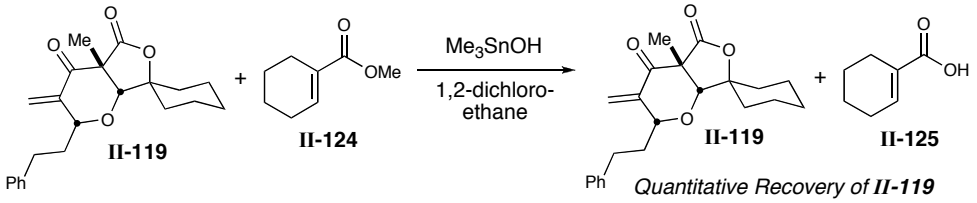

In the event that Me_3SnOH failed to work on the real system, we wanted to have a contingency plan in place. We felt silyl esters[152] were an attractive option due to the ease of preparation from carboxylic acids and the mild methods for their removal. When we subjected our model exomethylene substrate **II-119** to HF•pyridine (typical conditions for removal of silyl esters), we were able to recover the starting material unchanged. With two protecting group strategies in hand, we decided to move forward with the reduction studies.

2.8.3 Reduction Studies

The classic example of selective reduction of a double bond in the presence of an electron deficient double bond is the conversion of (+)-carvone to (+)-dihydrocarvone using Wilkinson's catalyst[153-155] or PtO_2.[156,157] We also considered diimide[158-160] an alternative to these methods because of the mild nature of the reagent.

Our initial thoughts were to avoid heterogenous catalysis, as we felt those were the most likely to be non-selective. Consequently our initial studies focused on Wilkinson's catalyst and diimide.

We prepared model olefin **II-126** and exposed it to Wilkinson's catalyst in benzene under a H_2 atmosphere (balloon) for 24 hours. This led to complete reduction of the double bond to the saturated system (**II-127**).

Scheme 2-47. Reduction of Model Olefin **II-126**

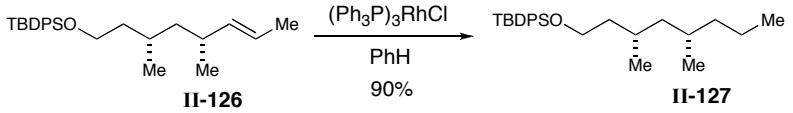

Simultaneously, we were evaluating diimide for the selective reduction of the macrocyclic double bond. Diimide reductions offer the advantage of being environmentally benign since N_2 gas is the only waste product. A widely precedented method for *in situ* generation of diimide is the decarboxylation of dipotassium azodicarboxylate **II-128**. The diimide reduction was carried out by adding a large excess (50 equiv) of dipotassium azodicarboxylate to a solution of olefin **II-126** in THF followed by AcOH. After 24 hours we were able to achieve a modest conversion of olefin **II-126** to the fully saturated system; however, it was clear even larger excess of the diimide precursors would be necessary. Although we were never able to achieve complete conversion to the fully saturated system **II-127** using diimide, we moved towards evaluating Wilkinson's catalyst and diimide on the real system.

Scheme 4-48. Reduction of Model Olefin Using Diimide

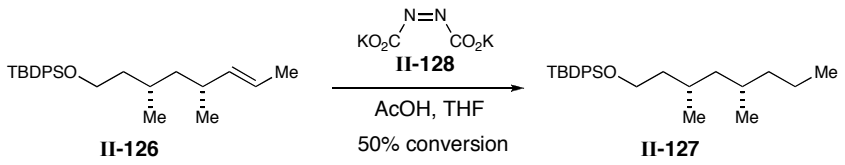

Prior to evaluating our reductions methods, we chose to protect the carboxylic acid **II-116** as the methyl ester. This was done by treating carboxylic acid **II-116** with MeI and K_2CO_3. The methyl ester **II-128** was obtained in quantitative yield.

Scheme 2-49. Protection of the Carboxylic Acid **II-116**

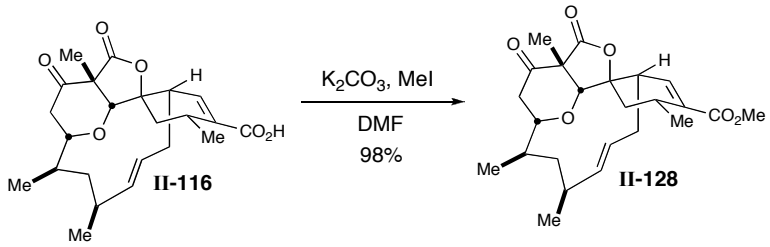

The methyl ester **II-128** was dissolved in benzene and treated with Wilkinson's catalyst under an H_2 atmosphere. Unfortunately, the starting material was recovered after 45 hours. A proposed mechanism for the hydrogenation of a double bond using Wilkinson's catalyst is shown in Figure 2-25 in order to understand why the model olefin **II-126** was reduced but olefin **II-128** was not. Presumably, the coordination step is slow due to the increased steric demand of **II-128** relative to **II-126**.

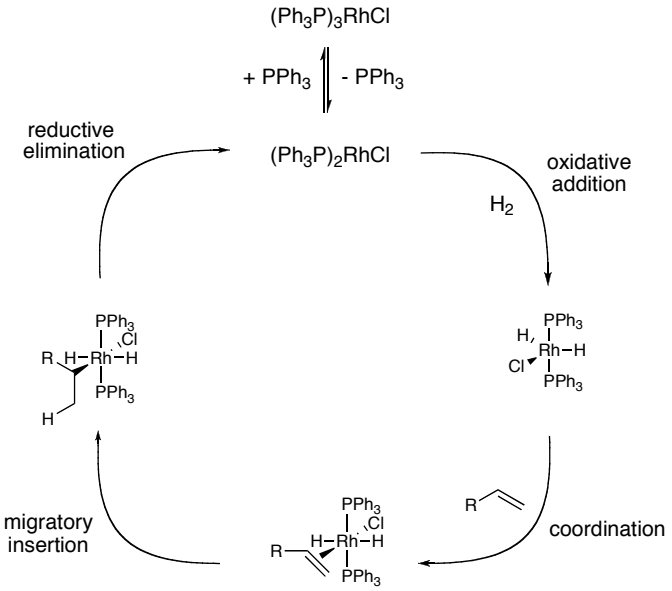

Figure 2-25. Mechanism of Hydrogenation by $(Ph_3P)_3RhCl$

We now hoped the diimide result described in Scheme 2-48 would translate well to the real system as our options were now more limited. We used the same procedure previously established during the model work and found no reduction. Again, we suspected steric hindrance was a problem. We attempted to add larger quantities of the diimide precursors but were discouraged to find that decomposition had taken place. Thus, our model work in the area of selective reduction ultimately proved unfruitful.

Scheme 2-50. Attempted Reduction of **II-128**

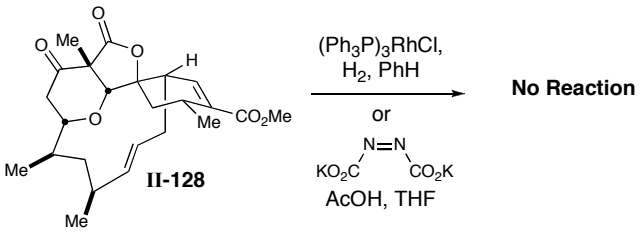

Given these poor results, we turned to heterogenous catalysis to reduce the macrocyclic olefin. The first reagent we evaluated was the Adam's catalyst, PtO_2. As previously mentioned, this catalyst has been used to selectivly reduce (+)-carvone to dihydrocarvone. A solution of our olefin **II-128** in EtOH was subjected to PtO_2 and H_2. We were pleased to find that *selective* reduction of the macrocyclic double bond had taken place to give tetracycle **II-129**.

Scheme 2-51. Reduction of Macrocyclic Olefin Using PtO_2

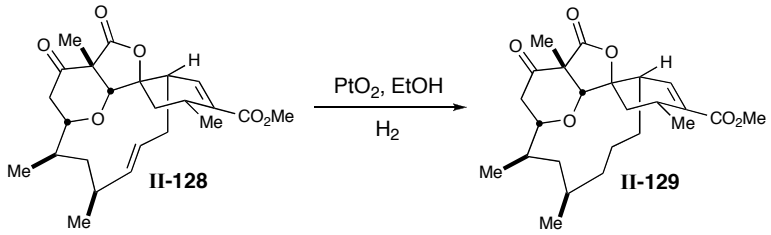

It should be mentioned that this initial result was difficult to reproduce. After extensive experimentation we were able to develop a reproducible procedure. The solvent was changed from EtOH to EtOAc due to increased substrate solubility. The key to obtaining reproducible results was to preactivate the PtO_2 with H_2 to form the active catalyst, "platinum black," prior to the addition of the substrate. We also found vigorous stirring helped to eliminate incomplete reduction problem by preventing aggregation of the heterogenous catalyst onto the stir bar.[156]

2.8.4 Installation of the Exomethylene Unit

The remaining steps in our synthesis involved the installation of the exomethylene unit and conversion of the methyl ester to the carboxylic acid of the natural product.

Exomethylene units are common motifs in natural products, and consequently, numerous methods have been developed to introduce them into organic molecules.[148,161-165]

In our previous model work, we found that treatment of pyranone **II-118** with LiHMDS followed by Eschenmoser's salt provided the desired α,β-unsaturated ketone **II-119**. We felt confident that this was an excellent model and thus attempted to install the exomethylene on pyranone **II-129** in the same manner. Unfortunately, decomposition to unidentifiable byproducts took place. We speculated that raising the reaction temperature to 23 °C (required due to the poor solubility of Eschenmoser's salt in THF) after formation of the enolate could potentially cause β-elimination and subsequent retro-aldol processes.

These results forced us to consider more mild conditions. It had previously been shown by Nicoloau[166] that exomethylene groups could be installed on acyclic aldehydes using Eschenmoser's salt and an amine base. Although this strategy had never been successfully reported on a cyclic ketone, we considered it ideal because of the mild reaction conditions. Consequently, methyl ester **II-129** was treated with NEt_3 and Eschenmoser's salt. After 24 hours at 23 °C, we were able to observe a small amount of desired product by NMR spectroscopic analysis. We reasoned that the reaction was sluggish due to the developling steric interaction between the vinyl protons of the new exomethylene group and C23 methyl substituent. When we attempted to heat the reaction to overcome this issue, we were pleased to find the product was formed in acceptable yield.

Scheme 2-54. Installation of the Exomethylene Group

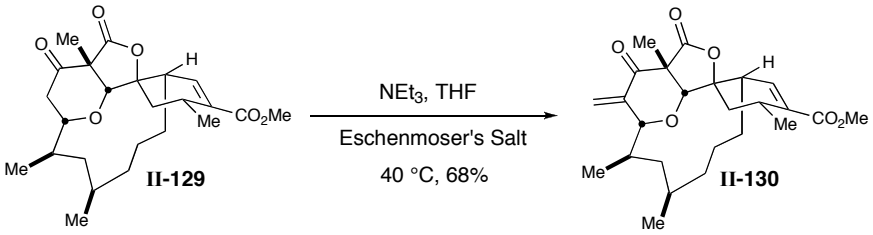

2.8.5 Reconsidering the End Game Strategy

During the time we were establishing conditions for the completion of the synthesis, we considered the possibilty that a protecting group was not required for the carboxylic acid. If the carboxylic acid was alkylated by the Eschenmoser's salt during the installation of the exomethylene group, the resulting hemiaminal would likely hydrolyze during the work up and furnish the natural product (or diastereomer of the natural product). Towards this end, olefin **II-116** was reduced under heterogenous conditions to provide carboxylic acid **II-131**. Exposure of **II-131** to Eschenmoser's salt and NEt_3 provided carboxylic acid **II-132**. It should be noted that we could not obtain an analytically pure (> 95% pure) NMR spectrum of **II-132**. Despite this issue, the characterization data obtained allowed us to confirm our suspicion, unequivocally, that we had failed to prepare the natural product **II-1**.

Scheme 2-55. Completion of the Synthesis

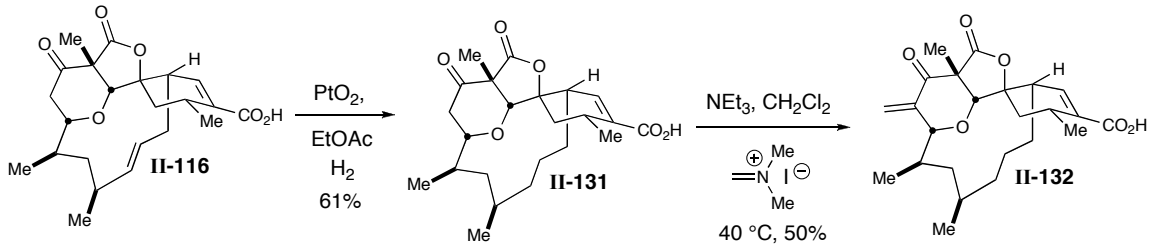

2.9 Revised Diels-Alder Route

(*Author's note: The structural assignment of the synthetic intermediates will be assigned as what we believed them to be at the time of their preparation. Their assignments are subject to change in the subsequent sections, and the reader will be informed of such change.*)

We had now established unambiguously that we had not prepared okilactomycin **II-1**. This required us to reevaluate our synthesis in order to establish the source of the discrepancy. The logical starting point for such an analysis was the principal fragments **II-64** and **II-74**. We felt confident about the structural assignment of the dioxinone fragment **II-64** because the methods used to establish the absolute stereochemistry were well precedented. Additionally, we had prepared both, the syn and anti aldol adducts (C8) and used coupling constant data to establish the relative configuration with respect to the C23 methyl substituent.

Given this level of certainty, we felt the α-hydroxy aldehyde **II-74** was the source of the structural discrepancy. Our NOE analysis of tetracycle **II-104** strongly suggested we had prepared the enantiomer of **II-74**. We assigned the major cycloadduct (**II-84**) as the exo diastereomer based on correlation to a similar[18] (but not identical) literature reference and our own NMR spectroscopic data that could potentially be construed as

ambiguous. If, in fact, the the Diels-Alder reaction had proceeded to give the endo cycloadduct, the elaboration of this intermediate would lead to the enantiomer of α-hydroxy aldehyde **II-74** (as drawn). This would account for the structural discrepancy that we observed. Thus, it seemed logical to change the enantiomer of the chiral auxiliary we used for the Diels-Alder reaction in order to access the correct enantiomer (based on our hypothesis) of the desired α-hydroxy aldehyde.

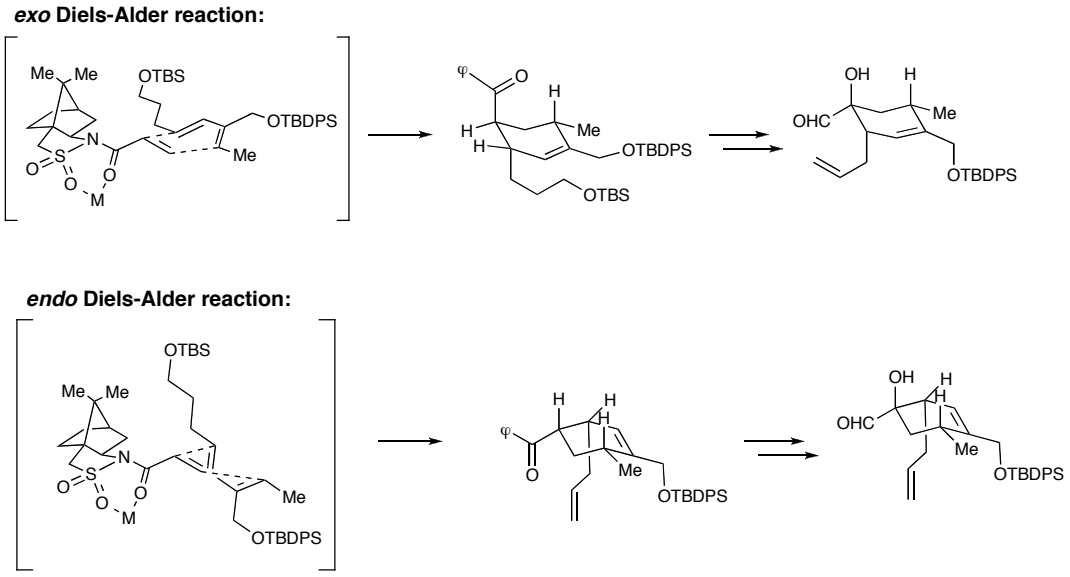

Figure 2-26. Potential Outcomes of the Diels-Alder Reaction

2.9.1 Syntheis of New α-hydroxy aldehyde

The Diels-Alder sequence was carried out as shown in Scheme 2-21, 2-22, and 2-23 using the chiral auxiliary **II-133**. The chemistry proceded uneventfully and ultimately provided what we believed to be the desired α-hydroxy aldehyde **II-74'** (Note: the prime notation indicates that we tentatively assigned the structures as intermediates that have already been presented in this text) We determined that we had indeed prepared the

enantiomer by comparing optical rotation data between both α-hydroxy aldehydes that were synthesized.

Scheme 2-56. Revised Synthesis of α-hydroxy aldehyde **II-74**

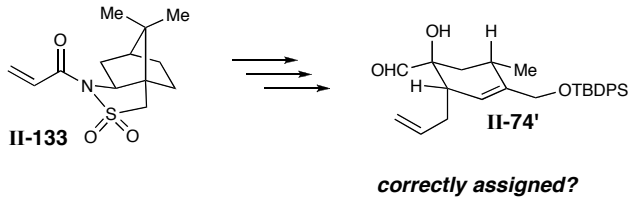

The fragment coupling reaction between dioxinone **II-64** and the newly prepared **II-74** provided the butenolide **II-91'**. The butenolide was exposed to TBAF and AcOH to provide a pyranone in 35% yield and as a single diastereomer. We were astonished to observe that the NMR spectrum of this pyranone matched the NMR spectrum of pyranone **II-97**! This result seemed counterintuitive, so we proceeded to elaborate the newly obtained pyranone to evaluate if the identical spectra represented an anomoly or we had in fact prepared **II-97** again. Towards this end, the newly prepared pyranone was protected as a TBDPS ether and we found that this intermediate had identical spectroscopic properties as **II-102**. After the ring closing metathesis and alkylation at C11 we found that the new tetracycle was identical to **II-104**. The synthetic sequence was completed and found to produce intermediates that had identical spectroscopic properties to the intermediates in Schemes 2-43 and 2-55.

2.10 Discussion

We were left to ask "*How could both enantiomers of the α-hydroxy aldehyde fragment ultimately lead to same cyclized pyranone (**II-97**)?*" After a detailed analysis of the data we were able to identify the cause of this seemingly bizarre turn of events.

The analysis began by comparing the NMR spectra of the two butenolides obtained from our fragment coupling reaction. A detailed inspection of the chemical shifts of the C9 (H_a and H_b) protons of the butenolide derived from the original α-hydroxy aldehyde (**II-74**, Scheme 2-23) showed that the product was formed as a 4:1 mixture of diastereomers (top spectra, Scheme 2-27). When the Diels-Alder route was repeated to give the new α-hydroxy aldehyde (**II-74'**, Scheme 2-56) the ratio of the diastereomers was reversed, as the minor product from the original butenolide formation was now the major one (bottom spectra, Scheme 2-27).

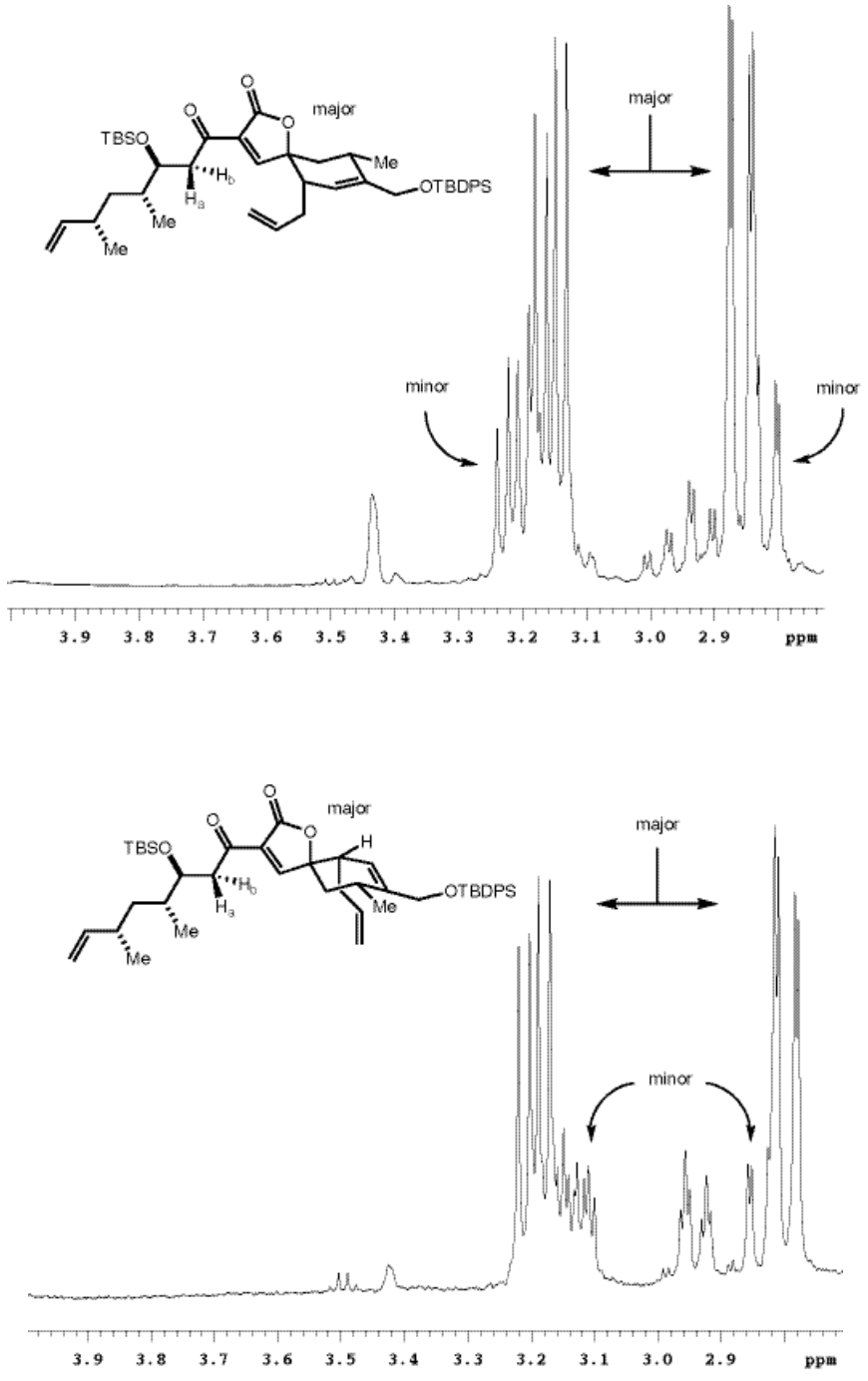

Figure 2-27. Analysis of ^{1}H NMR Spectra of Butenolides

These results strongly suggest that both α-hydroxy aldehydes had been prepared with reduced levels of optical purity. In order to test this hypothesis both α-hydroxy aldehydes (enantiomer of **II-74** now assigned as **II-137**) underwent reduction with $NaBH_4$ to afford the corresponding diols (**II-134** and **II-138** respectively). The diols were mono-acylated with (*R*)-(–)-α-methoxy-α-(trifluoromethyl)phenylacetyl chloride (**II-135**). The NMR spectra (see experimental section) of the resulting Mosher esters[167] (**II-136** and **II-139**) indicated that the enantiomeric excess was approximately 65% .

Scheme 2-57 Determination of Optical Purity

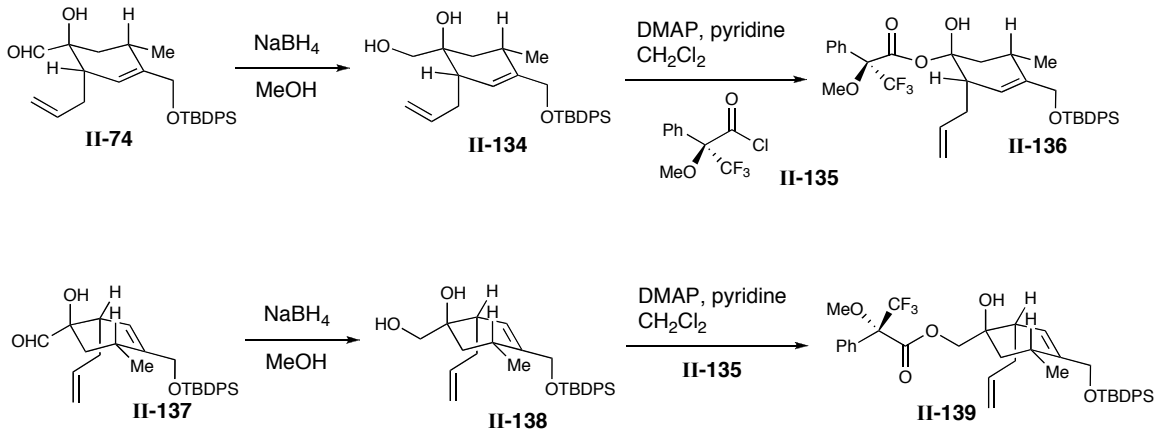

The reason for this reduced optical purity likely stems from the stereoselective Diels-Alder reaction described in Scheme 2-22. We now believe that the minor product was incorrectly assigned as the endo diastereomer. We suspect the minor product was the cycloadduct **II-140**. This would arise from an epimerization of the stereoecenter α to the carbonyl under the Lewis acid reaction conditions. Unfortunately, we suspect small amounts of the endo diastereomer were produced and were inseparable from the major cycloadduct **II-84**. Consequently, these diastereomers were carried forward to ultimately

produce **II-74** with diminished levels of optical purity. This would seem to explain the appearance of diastereomers after the fragment coupling step.

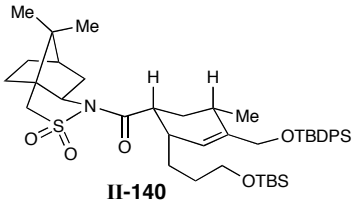

II-140

Figure 2-28 Proposed structure of the minor product from Diels Alder Reaction

This result also served to explain why both enantiomers of the α-hydroxy aldehyde produced the same pyranone **II-97**. *The data would strongly suggest that only one of the two butenolide diastereomers undergoes cyclization to form the pyranone*. Unfortunately, it was the undesired butenolide diastereomer. We also feel that the difference in yield for the TBAF/AcOH conjugate addition step provides empirical evidence for the structural assignments shown in Figure 2-27. Since the conjugate addition provides higher yields when butenolide **II-91'** is employed, it stands to reason that this mixture contains more of the undesired antipode of the α-hydroxy aldehyde (**II-137**). *Specifically, chiral auxiliary **II-77** leads to **II-74** (as the major enantiomer) and **II-133** leads to **II-137**.*

Our data suggests that *if* the conjugate addition takes place on the desired butenolide diastereomer, one of two scenarios takes place (Scheme 2-58): 1) The desired pyranone undergoes a retro-conjugate addition to form the diol (which we believe to be irreversible), or 2) The C8, C11, and C12 stereocenters epimerize via an unknown mechanism to provide pyranone **II-141**.

Scheme 2-58. Potential Outcomes of the Conjugate Addition

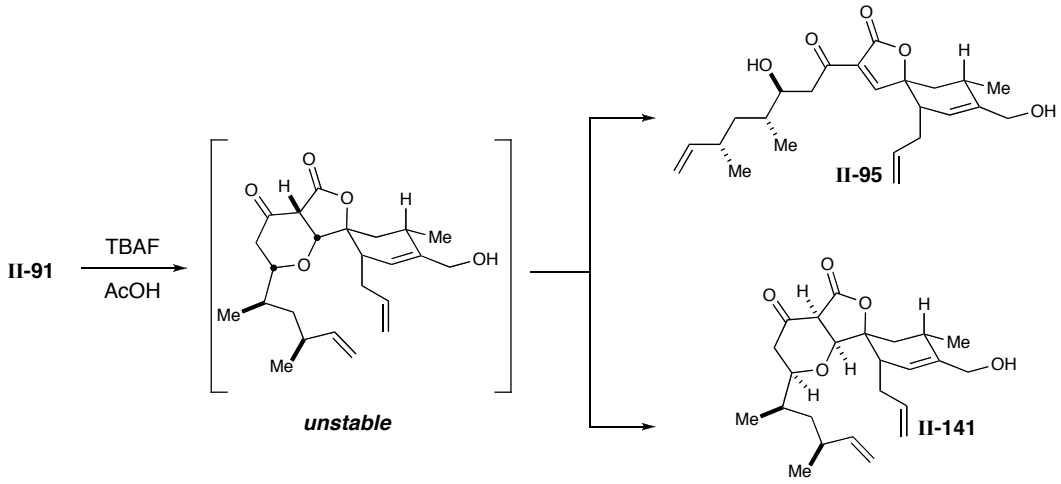

The data presented seems to suggest that the conjugate addition reaction which serves to form the pyranone ring is under thermodynamic control. Although no formal molecular modeling has been conducted to determine the ground state energies of the products, it seems accurate to say the desired pyranone (labeled as unstable in Scheme 2-58) is higher in energy than **II-95** or **II-141**. Using these results as a guide, we have begun work on a third generation approach towards the synthesis of **II-1** and **II-2**.

2.11 Third Generation Approach Towards the Synthesis of Okilactomycin and Chrolactomycin

The results described previously have inspired our current approach towards the synthesis of okilactomycin **II-1** and chrolactomycin **II-2**. In order for the total synthesis to be completed using a route similar to one described previously, two changes need to be made. First, an alternative synthesis of α-hydroxy aldehyde **II-74** must be developed. This new route must provide access to **II-74** as a single enantiomer. The second change is that we must devise a strategy such that the key conjugate addition reaction is under kinetic control.

With regard to the second issue, we reasoned that if the macrocycle was closed prior to the formation of the pyranone, the conjugate addition could likely be carried out under kinetic control. Thus, our third generation approach involves a transannular conjugate addition as the key step.

We began by treating α-hydroxy aldehyde **II-74** with $NaBH_4$ and protecting the resulting diol as the bis-trimethylsilyl ether (**II-143**). Dioxinone **II-64** and bis-trimethylsilyl ether **II-143** were treated with the second generation Grubbs catalyst to afford the cross metathesis product **II-143** in an acceptable yield after 2 resubjections. The TMS groups were removed under acidic conditions, and the primary alcohol was oxidized to aldehyde **II-144** under Parikh-Doering conditions. The aldehyde **II-144** was heated to 113 °C under dilute conditions to yield butenolide **II-145**. This represented the first intramolecular example of our novel butenolide-forming cascade reaction. We are currently evaluating means to remove the TBS protecting group and promote the conjugate addition.

Scheme 2-59 Third Generation Approach

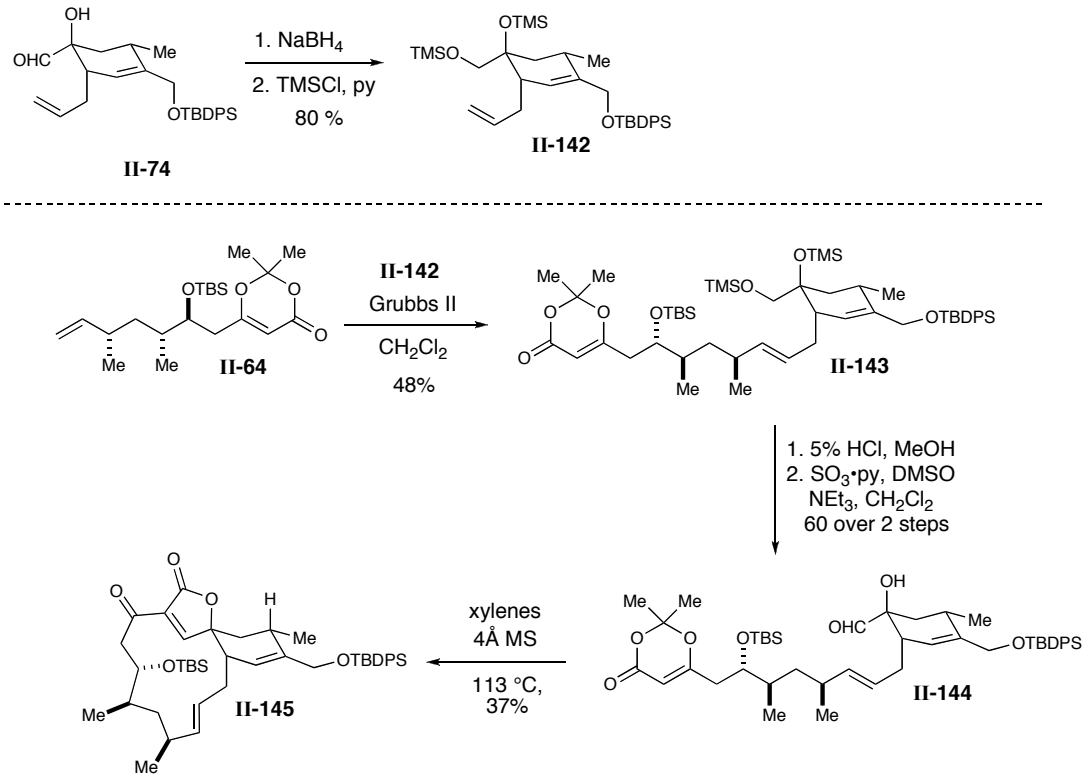

2.12 Conclusion

Several approaches to the synthesis of **II-1** and **II-2** have been described. Our first generation approach, though unsuccessful in the context of total synthesis, led to the development of a novel cyclization methodology. Ultimately, we discovered a novel cascade reaction that was employed to couple the principal fragments in our synthesis. After extensive experimentation, it was determined that our key conjugate addition reaction was under thermodynamic control, resulting in the formation of undesired diastereomers of key intermediates. These results have served to guide our most recent route, which seeks to exploit a transannular approach to maintain kinetic control during the conjugate addition. These results will be reported in due course.

2.13 Experimental Section

General Information. All reactions were carried out under a nitrogen atmosphere in flame-dried glassware with magnetic stirring. THF, Et_2O, CH_2Cl_2, DMF and toluene were purified by passage through a bed of activated alumina. $CHCl_3$ was purified by passage through a pad of alumina prior to use. Reagents were purified prior to use unless otherwise stated following the guidelines of Perrin and Armarego. Purification of reaction products was carried out by flash chromatography using EM Reagent silica gel 60 (230-400 mesh). Analytical thin layer chromatography was performed on EM Reagent 0.25 mm silica gel 60-F plates. Visualization was accomplished with UV light and anisaldehyde, ceric ammonium nitrate stain, potassium permangenate, or phosphomolybic acid followed by heating. Melting points were obtained on a Thomas Hoover capillary melting point apparatus and are uncorrected. Infrared spectra were recorded on a Bio-Rad Win FT-IR Pro spectrometer. ^{1}H-NMR spectra were recorded on a Varian Inova 500 (500 MHz) or Mercury 400 (400 MHz) spectrometer and are reported in ppm using solvent as an internal standard ($CDCl_3$ at 7.26 ppm). Data are reported as (ap = apparent, s = singlet, d = doublet, t = triplet, q = quartet, m = multiplet, b = broad; coupling constant(s) in Hz; integration. Proton-decoupled ^{13}C-NMR spectra were recorded on a Varian Inova 500 (125 MHz) or Mercury 400 (100 MHz) spectrometer and are reported in ppm using solvent as an internal standard ($CDCl_3$ at 77.0 ppm). Electrospray mass spectra (ESI-MS) were obtained using Micromass Quattro II Triple Quadrupole Mass Spectrometer.

2.13.1 General Procedure for $Sc(OTf)_3$-catalyzed cyclizations

A 10 mL round bottom flask was charged with powdered $CaSO_4$ (3 mmol, 15 equiv) and flame-dried prior to use. $Sc(OTf)_3$ (0.02 mmol, 0.1 equiv) was added to the flask followed by CH_2Cl_2 (1 mL). The aldehyde (0.21 mmol, 1.05 equiv) was added and the mixture was cooled to –10 °C. To this solution was added β-hydroxy-dioxinone (0.2 mmol, 1 equiv) in CH_2Cl_2 (0.5 mL). The reaction was allowed to stir for 4-24 hours before being quenched by the addition of brine (5 mL) and filtered through a short pad of Celite eluting with CH_2Cl_2. The layers were separated and aqueous layer was extracted with EtOAc (3 x 2 mL). Combined organic layers were dried over Na_2SO_4, filtered, concentrated in vacuo, and purified by flash chromatography to afford cyclized products **II-29**, **II-32-41**.

2.13.2 General Procedure for One-pot cyclization/Ring Opening

A 10 mL round bottom flask was charged with powdered $CaSO_4$ (3 mmol, 15 equiv) and flame-dried prior to use. $Sc(OTf)_3$ (0.04 mmol, 0.2 equiv) was added to the flask followed by CH_2Cl_2 (1 mL). The aldehyde (0.21 mmol, 1.05 equiv) was added and the mixture was brought to –10 °C. To this solution was added β-hydroxy-dioxinone (0.2 mmol, 1 equiv) in CH_2Cl_2 (0.5 mL). The reaction was allowed to stir until the b-hydroxy-dioxinone was consumed as visualized by TLC (1-5 hours) at which time the reaction was warmed to 0 °C and KOEt (0.8 mmol, 4 equiv) was added in one portion. The resulting solution stirred at 0 °C for 30 minutes and room temperature for 4 hours before being quenched by the addition of brine (5 mL) and filtered through a pad of Celite. The aqueous layer was extracted with EtOAc (3 x 3 mL) and the combined organic layers

were dried over Na_2SO_4, filtered and concentrated in vacuo. The residue was purified by flash chromatography to afford tetrahydropyran-4-ones **II-42-47**.

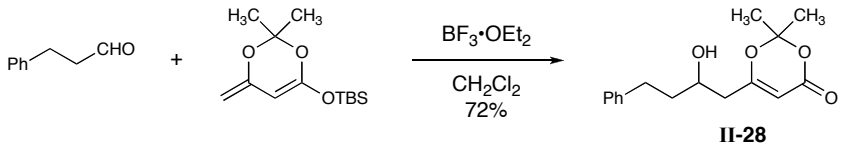

II-28

2.13.3 Preparation of β-hydroxy-dioxinone II-28

To a –78 °C solution of silyl dienol ether (600 mg, 2.34 mmol), and hydrocinnamaldehyde (0.1 mL, 0.76 mmol), in CH_2Cl_2 (4 mL) was added BF_3•OEt_2 (0.3 mL, 2.34 mmol) drop-wise over 2 minutes. Reaction was allowed to stir for 4 hours and was quenched with pH 7.0 phosphate buffer (8 mL). The resulting mixture was extracted with EtOAc (3 x 3 mL) and the combined organic layers were dried over Na_2SO_4, filtered, concentrated, and purified by flash chromatography to afford II-28. All additional b-hydroxy-dioxinones were prepared in the same manner.

2.13.4 Pyran Characterization

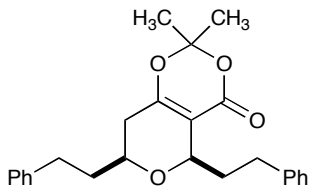

(**II-29**): Purified with 30% ethyl acetate/hexanes, yielding 78 mg (85%) of **II-29** as a yellow oil. R_f = 0.61 (30% ethyl acetate/hexanes); IR (film) 3079, 3059, 3026, 2999, 2927, 2858, 1724, 1647, 1495, 1452, 1403 cm^{-1}; ^1H NMR (500 MHz, $CDCl_3$) δ 7.33-7.21 (m, 10H); 4.43 (m, 1H), 3.51 (m, 1H); 2.88 (m, 2H); 2.79 (m, 2H); 2.50 (m, 1H); 2.22 (m, 1H); 1.98 (m, 2H); 1.85 (m, 2H); 1.70 (s, 3H); 1.69 (s, 3H); ^{13}C NMR (125 MHz, $CDCl_3$)

. δ 163.7, 159.2, 142.3, 141.6, 128.8, 128.7, 128.6, 128.5, 126.2, 125.9, 105.9, 105.1, 72.6, 71.5, 37.2, 35.9, 33.8, 31.7, 28.4, 27.8, 22.4; LRMS (ESI): Mass calculated for $C_{25}H_{28}O_4$ $[M+Na]^+$, 415.1. Found 415.7.

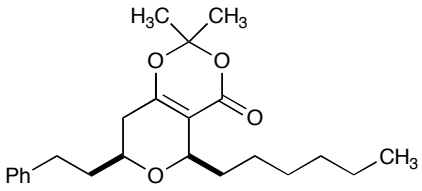

(**II-32**): Purified with 30% ethyl acetate/hexanes, yielding 54 mg (80%) of **II-32** as a yellow oil. R_f = 0.74 (30% ethyl acetate/hexanes); IR (film) 3061, 3026, 2997, 2927, 2857, 1727, 1650, 1495, 1403 cm^{-1}; ^1H NMR (500 MHz, $CDCl_3$) δ . 7.30-7.18 (m, 5 H); 4.35 (m, 1H); 3.44 (m, 1H); 2.80 (m, 1H); 2.74 (m, 1H); 2.18-2.04 (m, 2H); 1.94 (m, 1H); 1.80 (m, 1H); 1.68 (s, 3H); 1.66 (s, 3H); 1.58 (m, 4H); 1.47 (m, 2H); 1.30 (m, 4H); 0.89 (m, 3H); ^{13}C NMR (125 MHz, $CDCl_3$) δ 163.7, 159.8, 141.7, 128.7, 128.6, 126.2, 105.8, 105.5, 73.3, 71.3, 37.1, 34.2, 33.7, 32.2, 31.6, 29.5, 27.8, 25.5, 25.4, 22.9, 22.4; LRMS (ESI): Mass calculated for $C_{23}H_{32}O_4$ $[M+Na]^+$, 395.5 Found 395.1.

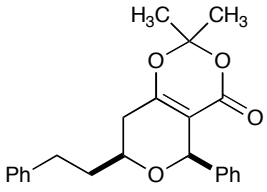

(**II-33**): Purified with 30% ethyl acetate/hexanes, yielding 78 mg (71%) of **II-33** as a yellow oil. R_f = 0.48 (30% ethyl acetate/hexanes); IR (film) 3030, 2999, 2936, 2858, 1729, 1652, 1403, 1275 cm^{-1}; ^1H NMR (500 MHz, $CDCl_3$) δ 7.45-7.11 (m, 10H); 5.36 (s, 1H); 3.69 (m, 1H); 2.76 (m, 2H); 2.44-2.24 (m, 2H); 2.02 (m, 1H); 1.86 (m, 1H); 1.69 (s, 3H); 1.68 (s, 3H) ^{13}C NMR (125 MHz, $CDCl_3$) δ 163.6, 159.2, 142.0, 140.1, 128.8, 128.7, 128.6, 128.5, 128.3, 126.3, 106.2, 76.1, 72.4, 36.8, 33.7, 31.5, 27.8, 22.9; LRMS (ESI): Mass calculated for $C_{23}H_{24}O_4$ $[M+Na]^+$, 387.4 Found 387.0.

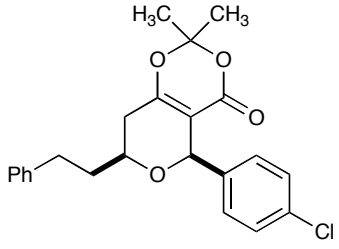

(**II-34**): Purified with 30% ethyl acetate/hexanes, yielding 56 mg (73%) of **II-34** as a yellow oil. R_f = 0.54 (30% ethyl acetate/hexanes); IR (film) 3059, 3027, 2997, 2938, 2858, 1728, 1649, 1403, 1275, 1202 cm^{-1}; ^1H NMR (500 MHz, $CDCl_3$) δ 7.38-7.16 (m, 9H); 5.32 (s, 1H); 3.68 (m, 1H); 2.77 (m, 2H); 2.38-2.24 (m, 2H); 2.03 (m, 1H); 1.86 (m, 1H); 1.66 (s, 3H); 1.65 (s, 3H) ^{13}CNMR (125 MHz, $CDCl_3$) δ 163.8, 159.1, 141.3, 139.1, 134.2, 129.6, 128.8, 128.7, 128.6, 126.3, 106.4, 105.1, 75.4, 72.5, 36.8, 33.6, 31.6, 27.8, 22.9; LRMS (ESI): Mass calculated for $C_{23}H_{23}ClO_4$ $[M+Na]^+$, 422.3 Found 422.1.

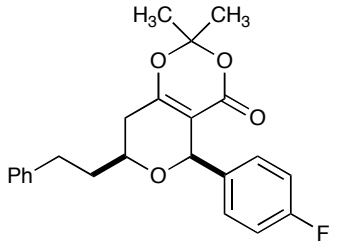

(**II-35**): Purified with 30% ethyl acetate/hexanes, yielding 59 mg (83%) of **II-35** as a yellow oil. R_f = 0.56 (30% ethyl acetate/hexanes); IR (film) 3060, 2999, 2935, 2858, 1728, 1649, 1510, 1400, 1275, 1219 cm^{-1}; ^1H NMR (500 MHz, $CDCl_3$) δ 7.40-7.03 (m, 9H); 5.34 (s, 1H); 3.69 (m, 1H); 2.80-2.72 (m, 2H); 2.38-2.25 (m, 2H); 2.01-1.98 (m, 1H); 1.86-1.85 (m, 1H); 1.67 (s, 6H); ^{13}CNMR (125 MHz, $CDCl_3$) δ 163.8, 159.1, 141.9, 136.5, 130.0, 129.9, 128.8, 128.7, 126.3, 115.6, 115.5, 106.3, 105.3, 75.4, 72.3, 36.9, 33.6, 31.5, 27.6, 22.9; LRMS (ESI): Mass calculated for $C_{23}H_{23}FO_4$ $[M+Na]^+$, 405.3 Found 405.2

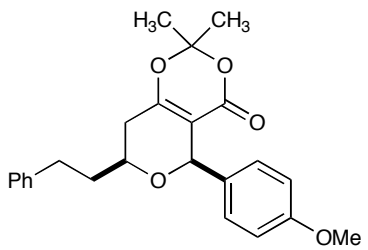

(**II-36**): Purified with 30% ethyl acetate/hexanes, yielding 44 mg (54%) of **II-36** as a yellow oil. R_f = 0.35 (30% ethyl acetate/hexanes); IR (film) 2931, 2859, 1728, 1652, 1512, 1403, 1273, 1248 cm^{-1}; ^1H NMR (500 MHz, $CDCl_3$) δ 7.36-7.26 (m, 3H); 7.23-7.18 (m, 4H); 6.92-6.89 (m, 2H); 5.32 (s, 1H); 3.80 (s, 3H); 3.67 (m, 1H), 2.80 (m, 2H); 2.40 (m, 1H); 2.27 (m, 1H); 1.99 (m, 1H); 1.77 (m, 1H); 1.69 (s, 3H); 1.67 (s, 3H); ^{13}CNMR (125 MHz, $CDCl_3$). δ. 163.5, 159.7, 158.9, 141.6, 132.8, 129.3, 128.7, 128.6, 128.5, 126.2, 114.1, 106.2, 75.6, 72.3, 55.5,36.8, 33.7, 31.5, 27.8, 22.8; LRMS (ESI): Mass calculated for $C_{24}H_{26}O_5$ $[M+Na]^+$, 417.4 Found 417.0

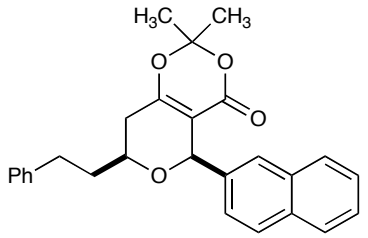

(**II-37**): Purified with 30% ethyl acetate/hexanes, yielding 62 mg (81%) of **II-37** as a yellow oil. R_f = 0.43 (30% ethyl acetate/hexanes); IR (film) 3057, 2998, 2930, 2858, 1727, 1651. 1403, 1267, 1403, 1267, 1203 cm^{-1}; ^1H NMR (500 MHz, $CDCl_3$) δ 7.95-7.20 (m, 12H); 5.55 (s, 1H); 3.77-3.74 (m, 1H); 2.83-2.75 (m, 2H); 2.41-2.29 (m, 2H); 2.06-2.02 (m, 2H); 1.71 (s, 3H); 1.68 (s, 3H); ^{13}C. NMR (125 MHz, $CDCl_3$). δ. 163.6, 141.5, 137.8, 133.6, 133.5, 128.8, 128.7 128.5, 128.4, 128.3, 128.0, 127.8, 126.3,126.2, 126.1,125.5, 106.2, 76.2, 72.4, 36.9, 33.7, 31.5, 27.8, 22.8; LRMS (APCI): Mass calculated for $C_{27}H_{26}O_4$ $[M]^+$, 414.5 Found 415.1

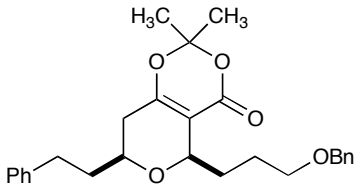

(**II-38**): Purified with 30% ethyl acetate/hexanes, yielding 64 mg (80%) of **II-38** as a yellow oil. R_f = 0.50 (30% ethyl acetate/hexanes); IR (film) 2929, 2856, 1724, 1647, 1403, 1267, 1204, 1101 cm^{-1}; ^1H NMR (500 MHz, $CDCl_3$) δ 7.36-7.17 (m, 10H); 4.53 (s, 2H); 4.41-4.40 (d, 1H); 3.55-3.44 (m, 3H); 2.81-2.78 (m, 1H); 2.75-2.71 (m, 1H); 2.18-2.10 (m, 3H); 1.93-1.73 (m, 5H); 1.68 (s, 3H); 1.66 (s, 3H); ^{13}CNMR (125 MHz, $CDCl_3$) δ 163.9, 159.7, 141.6, 138.8, 128.7, 128.6, 128.5, 127.9, 127.7, 126.2, 105.9, 105.0, 73.1, 72.9, 71.3, 70.7, 37.0, 33.7, 31.1, 30.7, 27.7, 25.7, 22.4; LRMS (APCI): Mass calculated for $C_{27}H_{32}O_5$ $[M+H]^+$, 436.5 Found 437.0

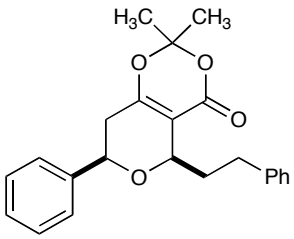

(**II-40**): Purified with 30% ethyl acetate/hexanes, yielding 48 mg (64%) of **II-40** as a yellow oil. R_f = 0.57 (30% ethyl acetate/hexanes); IR (film) 3061, 3028, 2998, 2926, 2855, 1725, 1650, 1402, 1271, 1204 cm^{-1}; ^1H NMR (500 MHz, $CDCl_3$) δ 7.44-7.16 (m, 10H); 4.67 (m, 2H); 2.86 (m, 2H); 2.50 (m, 3H); 2.10 (m, 1H); 1.73 (s, 3H); 1.72 (s, 3H); ^{13}CNMR (125 MHz, $CDCl_3$) δ 163.6, 159.6, 142.4, 140.9, 128.9, 128.8, 128.5, 128.2, 125.9, 125.8, 106.3, 104.9, 74.2, 73.1, 35.9, 35.5, 31.5, 27.6, 22.5; LRMS (ESI): Mass calculated for $C_{23}H_{24}O_4$ $[M+Na]^+$, 387.2 Found 387.4

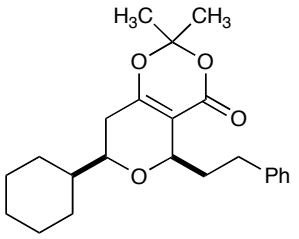

(**II-41**): Purified with 30% ethyl acetate/hexanes, yielding 52 mg (70%) of **II-41** as a yellow oil. R_f = 0.67 (30% ethyl acetate/hexanes); IR (film) 3060, 3026, 2998, 2926, 2853, 1727, 1649, 1402, 1267, 1203 cm^{-1}; ^1H NMR (500 MHz, $CDCl_3$) δ 7.28-7.16 (m, 5H); 4.36 (m, 1H); 3.25 (m, 1H); 2.82 (m, 1H); 2.78 (m, 1H); 2.43 (m, 1H); 2.21-2.05 (m, 2H); 1.88-1.71 (m, 2H); 1.68 (s, 6H); 1.58-1.02 (m, 10H); ^{13}C NMR (125 MHz, $CDCl_3$) δ 164.4, 159.1, 142.4, 128.8, 128.5, 125.9, 105.9, 105.2, 72.6, 42.6, 35.8, 31.6, 31.4, 29.0, 28.1, 27.6, 26.7, 26.2, 26.0, 22.4; LRMS (ESI): Mass calculated for $C_{23}H_{30}O_4$ $[M+Na]^+$, 393.2 Found 393.4

2.13.3 Pyranone Characterization Data

Note: For tetrahydropyran-4-ones **II-42-47** the reported ^{13}C NMR reflects a mixture of keto:enol tautomers. For ^1H spectra, the major constituent (keto tautomer) is reported.

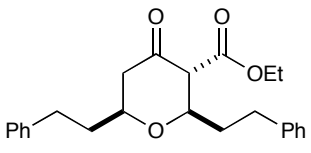

(**II-42**): Purified with 15% EtOAc/hexanes, yielding 88 mg (78%) of **II-42** as a yellow oil. R_f = 0.55 (25% ethyl acetate/hexanes); IR (film) 3026, 2926, 2861, 1741, 1716, 1651, 1603, 1494, 1452, 1126 cm^{-1}; ^1H NMR (500 MHz, $CDCl_3$) major:keto tautomer δ 7.32-7.21 (m, 10 H); 4.20 (m, 2H); 3.87 (m, 1H); 3.60 (m, 1H); 3.26 (d, J = 10.7 Hz, 1H); 2.99 (m, 1H); 2.89 (m, 1H); 2.79 (m, 2H); 2.42-2.20 (m, 2H); 2.06-1.81 (m, 4H); 1.26 (t, J = 7.3 Hz, 3H); ^{13}C NMR (125 MHz, $CDCl_3$) δ 202.3, 170.9, 168.3, 141.5, 141.4,

128.9, 128.7, 128.6, 128.4, 126.4, 125.4, 77.7, 75.9, 72.2, 70.9, 63.4, 61.4, 60.6, 47.6, 38.1, 36.9, 35.9, 31.9, 32.0, 31.7, 31.3, 14.3; LRMS (APCI): Mass calculated for $C_{24}H_{28}O_4$ $[M]^+$, 380.2. Found 380.9.

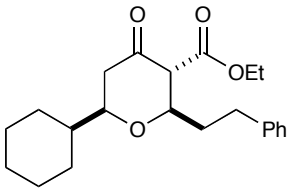

(**II-43**): Purified with 15% diethyl ether/hexanes, yielding 72 mg (72%) of **II-43** as a yellow oil. R_f = 0.60 (25% ethyl acetate/hexanes); IR (film) 3061, 3026, 2926, 2853, 1741, 1716, 1653, 1604, 1450 cm^{-1}; ^1H NMR (500 MHz, $CDCl_3$) major:keto tautomer δ 7.63–7.60 (m, 5H); 4.16 (m, 2H); 3.80 (m 1H); 3.38 (m, 1H); 3.23 (d, *J* = 10.6 Hz, 1H); 2.94 (m, 1H); 2.77 (m, 1H); 2.52 (m, 2H); 2.05 (m, 1H); 1.9-1.4 (m, 12H); 1.26 (t, *J* = 7.3 Hz, 3H); ^{13}C NMR (125 MHz, $CDCl_3$) δ 203.3, 171.4, 168.3, 142.9, 141.6, 128.8, 128.7, 128.4, 126.2, 125.7, 81.3, 76.5, 72.2, 63.7, 63.7, 61.3, 60.5, 45.0, 43.4, 42.6, 36.9, 33.1, 31.8, 31.2, 29.2, 29.0, 28.7, 26.7, 26.6, 26.1, 22.9, 14.3; LRMS (ESI): Mass calculated for $C_{22}H_{30}O_4$ $[M+Na]^+$, 381.1. Found 381.1

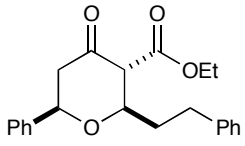

(**II-44**): Purified with 15% diethyl ether/hexanes, yielding 63 mg (60%) of **II-44** as a yellow oil. R_f = 0.50 (25% ethyl acetate/hexanes); IR (film) 3027, 2980, 2928, 2865, 1742, 1716, 1653, 1494, 1452, 1263 cm^{-1}; ^1H NMR (500 MHz, $CDCl_3$) major:keto tautomer δ 7.49-7.15 (m, 10H); 4.74 (dd, *J* = 2.4, 11.5 Hz, 1H); 4.20 (m, 2H); 4.09 (m 1H); 3.41 (d, *J* = 10.7 Hz, 1H); 2.97 (m, 1H); 2.81 (m, 2H); 2.60 (m, 1H); 2.04 (m, 2H); 1.25 (t, *J* = 7.0, Hz, 3H); ^{13}C NMR (125 MHz, $CDCl_3$) δ 202.0, 168.2, 141.5, 140.5, 128.9, 128.7, 128.4,

126.3, 125.9, 125.7, 78.5, 78.0, 63.2, 61.5, 48.9, 36.8, 31.7, 14.4; LRMS (ESI): Mass calculated for $C_{22}H_{24}O_4$ $[M+Na]^+$, 375.2. Found 375.1.

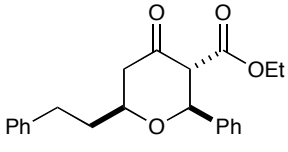

(**II-45**): Purified with 20% diethyl ether/hexanes, yielding 42 mg (67%) of **II-45** as a yellow oil. R_f = 0.45 (25% ethyl acetate/hexanes); IR (film) 3028, 2980, 2931, 2864, 1744, 1716, 1653, 1494, 1452cm^{-1}; ^{1}H NMR (500 MHz, $CDCl_3$) major:keto tautomer δ 7.49-7.15 (m 10H); 4.89 (d, J = 10.4 Hz, 1H); 4.10 (m, 2H); 3.84 (m, 1H); 3.60 (d, *J* = 10.4 Hz, 1H); 2.79 (m, 2H); 2.55-2.32 (m, 2H); 1.97-1.80 (m, 2H); 1.26 (t, *J* = 7.0 Hz, 3H); ^{13}C NMR (125 MHz) δ 202.0, 185.2, 170.6, 167.6, 141.3, 139.0, 128.9, 128.8, 128.7, 128.6, 128.4, 128.3, 128.0, 127.1, 126.3, 126.0, 81.0, 76.8, 76.4, 72.3, 64.7, 61.3, 60.3, 47.9, 47.2, 37.8, 36.9, 35.3, 31.4, 14.2; LRMS (ESI): Mass calculated for $C_{22}H_{24}O_4$ $[M+Na]^+$, 375.2. Found 375.0.

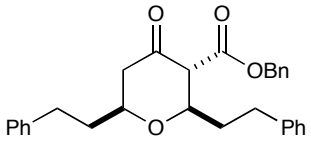

(**II-46**): Purified with 20% diethyl ether/hexanes, yielding 80 mg (82%) of **II-46** as a yellow oil. R_f = 0.48 (25% ethyl acetate/hexanes); IR (film) 3061, 3027, 2924, 2862, 1743, 1716, 1653, 1603, 1494, 1452, 1336, 1257, 1124 cm^{-1}; ^{1}H NMR (500 MHz, $CDCl_3$) major:keto tautomer δ 7.39-7.06 (m, 15H); 5.25 (d, A of AB system, *J* = 12.2 Hz, 1H); 5.14 (d, B of AB system, *J* = 12.2 Hz, 1H); 3.88 (m, 1H); 3.62 (m 1H); 3.32 (d, *J* = 10.7 Hz, 1H); 2.92 (m 2H); 2.74 (m, 2H); 2.47-2.20 (m, 2H); 2.00-1.80 (m, 4H); ^{13}CNMR (125 MHz, $CDCl_3$). δ 202.1, 168.1, 141.4, 141.3, 135.6, 128.9, 128.8, 128.7, 128.6,

128.5, 128.4, 126.7, 126.2, 77.8, 76.0, 67.2, 63.5, 47.4, 38.1, 36.8, 31.9, 31.7; LRMS (APCI): Mass calculated for $C_{29}H_{30}O_4$ $[M-H]^+$, 441.5. Found 441.1.

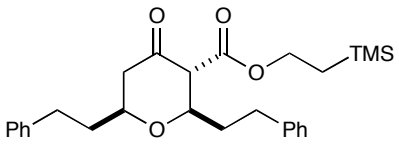

(**II-47**): Purified with 10% diethyl ether/hexanes, yielding 88 mg (72%) of **II-47** as a yellow oil. R_f = 0.53 (25% ethyl acetate/hexanes); IR (film) 3061, 3026, 2952, 2923, 2862, 1739, 1715, 1651, 1604 cm^{-1}; ^1H NMR (500 MHz, $CDCl_3$) major:keto tautomer δ 7.33-7.18 (m, 10 H); 4.24 (m, 2H); 3.88 (m, 1H); 3.64 (m, 1H); 3.25 (d, *J* = 10.4 Hz, 1H); 3.02-2.75 (m, 4H); 2.47-2.28 (m, 2H); 2.06-1.81 (m, 4H); 0.89 (t, 2H); 0.05 (s, 9H); ^{13}C NMR (125 MHz, $CDCl_3$) δ 202.1, 171.3, 170.7, 168.4, 142.8, 142.0, 141.5, 141.4, 140.2, 128.8, 128.7, 128.6, 128.5, 126.2, 126.1, 125.8, 100.8, 81.3, 77.8, 75.9, 72.3, 70.9, 63.8, 63.5, 62.9, 47.5, 38.1, 37.2, 36.9, 35.6, 31.9, 31.8, 31.7, 22.9, 17.7, 14.3, –1.2; LRMS (ESI): Mass calculated for $C_{27}H_{36}O_4Si$ $[M+Na]^+$, 475.3. Found 475.1.

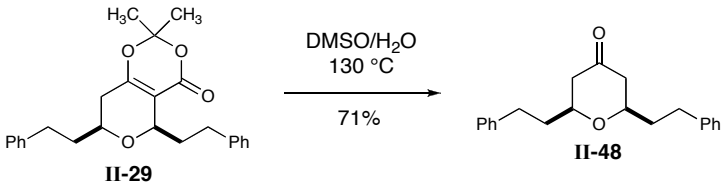

II-29 **II-48**

Preparation of tetrahydropyran-4-one **II-48:**

A solution of **II-29** (120 mg, 0.30 mmol) in DMSO (4 mL) and H_2O (0.5 mL) was heated to 130 °C (bath temperature) for 14 hours. The mixture was then cooled to room temperature and diluted with brine (10 mL) and extracted with EtOAc (3 x 3mL). The combined organic layers were filtered, concentrated and purified by flash

chromatography (15% ethyl acetate/hexanes) to yield 67 mg (71%) of **II-48** as a clear oil. R_f = 0.40 (25% ethyl acetate/hexanes); IR (film) 3061, 3028, 2924, 2856, 1717, 1494, 1452 cm^{-1}; ^1H NMR (500 MHz, $CDCl_3$) δ. 7.32-7.19 (m, 10H); 3.54 (m, 2H); 2.91 (m, 2H); 2.78 (m, 2H); 2.37-2.25 (m, 4H); 2.05 (m, 2H); 1.82 (m, 2H); ^{13}C NMR (125 MHz, $CDCl_3$). δ. 207.5, 141.7, 128.7, 128.6, 126.3, 76.0, 48.2, 38.3, 31.9; LRMS (EI): Mass calculated for $C_{21}H_{24}O_2$ $[M]^+$, 308.2. Found 308.0.

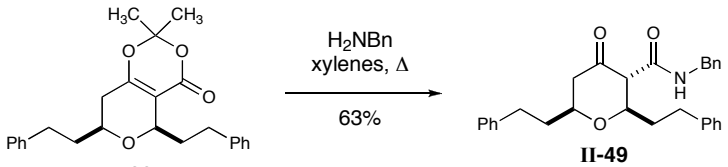

Preparation of Amide **II-49**:

A solution of **II-29** (75 mg, 0.20 mmol) and benzyl amine (0.4 mL, 3.68 mmol) in xylenes was vented and submerged into an oil bath that had been preheated to 150 °C. The reaction stirred for 1 hour before being concentrated *in vacuo*. The crude oil was purified by flash chromatography (30% ethyl acetate/hexanes) to yield 53 mg (63%) of **II-49** as a yellow oil. R_f = 0.36 (25% ethyl acetate/hexanes); IR (film) 3062, 3026, 2923, 2862, 1718, 1643, 1554, 1496, 1452, 1349 cm^{-1}; ^1H NMR (500 MHz, $CDCl_3$) major:keto tautomer δ. 7.40-7.15 (m, 15H); 6.17 (s, 1H); 4.51 (dd, A of AB system, J = 5.7, 14.9 Hz, 1H); 4.40 (dd, B of AB system, J = 5.7, 14.9 Hz, 1H); 3.97 (m, 1H); 3.65 (m, 1H); 3.00 (d, J = 10.1 Hz, 1H); 2.99 (m, 1H); 2.88 (m, 1H); 2.78 (m, 2H); 2.43 (m, 1H); 2.26 (m, 1H); 2.00 (m, 2H); 1.90 (m, 1H); 1.80 (m, 1H); ^{13}C NMR (125 MHz, $CDCl_3$). δ. 204.1, 167.2, 141.7, 141.5, 138.1, 128.9, 128.8, 128.7, 128.6, 127.9, 127.7, 126.3, 126.2, 78.3,

75.6, 63.7, 47.5, 43.8, 38.1, 36.9, 32.0, 31.8; LRMS (ESI): Mass calculated for $C_{29}H_{31}NO_3$ $[M]^+$, 442.3 Found 442.1.

Preparation of enantioenriched **II-28**:

Enantioenriched β-hydroxy dioxinone **II-28** was prepared by the procedure previously reported by Denmark.[168] Enantiomeric excess was determined by HPLC analysis (Chiralcel OD-H, 70:30 Hexanes/^{i}PrOH, 1 mL/min, 254 nm): (5*R*) enantiomer t_r = 8.7 min (major), (5*S*) enantiomer t_r = 6.4 min (minor).

2.13.6 Characterization Data for Selected Intermediates

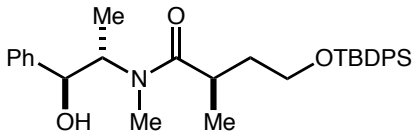

(**II-59**): To a –78 °C suspension of LiCl (21.8 g, 514 mmol) and diisopropylamine (25.7 mL, 183 mmol) in THF (123 mL) was added *n*-BuLi (82 mL, 172 mmol, 2.1 M solution in hexanes) via cannula. The resulting suspension was warmed to 0 °C briefly and then was cooled to -78 °C. An ice-cooled solution of amide II-58 (20.2 g, 91.5 mmol) in THF (300 mL) was added via cannula. The mixture was stirred at –78 °C for 1 h, at 0 °C for 15 min, and at 23 °C for 5 min. The mixture was cooled to 0 °C and a solution of TBDPS iodoethanol (23.5 g, 57.2 mmol) in THF (27 mL) was added via cannula. The mixture stirred for 18 hours in a water bath before being quenched by the addition of saturated NH_4Cl (300 mL). The organic layer was removed and the remaining aqueous layer was extracted with EtOAc (4 x 100 mL). The combined organic layers were combined and dried over Na_2SO_4, filtered and concentrated *in vacuo*. The residue

was purified by flash column chromatography (SiO_2, 75% Et_2O/hexanes) to afford **II-59** (30.4 g, 98%) as a viscous oil (dr 20:1). Analytical data for II-59: $[\alpha]_D^{25}$ = +36.4 (c 1, CH_2Cl_2); IR (film) 3379, 3062, 1959, 1890, 1824, 1770, 1618, 1107 cm^{-1}; ^1H NMR (3:1 rotamer ratio, only major rotamer reported, 500 MHz, C_6D_6) δ 7.69-7.65 (m, 5H), 7.4-7.0 (m, 10H), 4.56-4.53 (m,1H), 3.58-3.52 (m, 2H), 2,80-2.76 (m, 1H) 2.49 (s, 3H), 1.94-1.90 (m, 1H), 1.49-1.45 (m, 1H), 1.21-1.19 (m, 1H), 1.09 (s, 9H), 0.97-0.96 (d, *J* = 5.5 Hz, 3H), 0.96-0.95 (d, *J* = 6.7 Hz, 3H); ^{13}C NMR (125 MHz, C_6D_6) δ 177.6, 143.6, 135.9, 135.8, 135.7, 134.1, 129.9, 129.8, 128.2, 126.7, 76.1, 61.8, 37.0, 32.6, 27.1, 27.0, 19.3, 17.1, 14.2; LRMS (ESI): Mass calculated for $C_{31}H_{41}NO_3Si$ $[M+H]^+$, 504.75. Found 504.70.

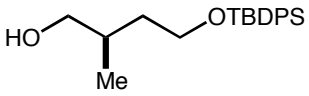

(**II-60**): To a –78 °C solution of diisopropylamine (33.1 mL, 234 mmol) in THF (233 mL) was added *n*-BuLi (103 mL, 217 mmol, 2.1 M solution in hexanes) via cannula. The resulting solution was stirred at –78 °C for 10 min, then warmed to 0 °C and held at that temperature for 10 min. Borane-ammonia complex (90%, 6.9 g, 223 mmol) was added in one portion , and the suspension was stirred at 0 °C for 15 min and then armed to 23 °C. After 15 min, the suspension was cooled to 0 °C and a solution of **II-59** (30.4 g, 55.7 mmol) in THF (140 mL) was added via cannula. The reaction mixture was warmed to 23 °C, held at this temperature for 2 h, and then cooled to 0 °C where excess hydride was quenched by the addition of 0.01 M aqueous HCl (500 mL). The mixture was stirred for 30 min at 0 °C and then extracted with EtOAc (4 x 150 mL). The combined organic extracts were washed with 0.1 m aqueous HCl (60 mL), 1 M NaOH (2 x 60 mL), and brine (50 mL). The organic layer was

dried over Na_2SO_4, filtered and concentrated. The residue was purified by flash column chromatography (SiO_2, 60% Et_2O/hexanes) to afford **II-60** (18.3 g, 96%) as a viscous oil. Analytical data for II-60: $[\alpha]_D^{25}$ = +6.3 (c 1.05, CH_2Cl_2); IR (film) 3351, 1959, 1890, 1824, 1773, 1465, 1427 cm^{-1}; ^1H NMR, (500 MHz, $CDCl_3$) δ 7.69–7.68 (m, 4H), 7.46–7.39 (m, 6H), 3.78–3.74 (m, 1H), 3.73-3.70 (m, 1H), 3.54-3.48 (m, 2H), 2.60 (br s, 1H), 1.88-1.85 (m, 1H), 1.64-1.62 (m, 1H), 1.57-1.49 (m, 1H), 1.06 (s, 9H), 0.92-0.91 (d, *J* = 7.02 Hz, 3H); ^{13}C NMR (125 MHz, $CDCl_3$) δ 135.8, 133.6, 129.9, 127.6, 68.4, 62.7, 37.0, 34.1, 27.0, 19.3, 17.4; LRMS (ESI): Mass calculated for $C_{21}H_{30}O_2Si$ $[M+Na]^+$, 365.5. Found 365.2.

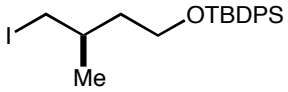

(**II-61**): To a solution of Ph_3P (16.8 g, 64.1 mmol) in CH_2Cl_2 (200 mL) was added imidazole (5.45 g, 80 mmol) and iodine (18.4 g, 72.1 mmol) at 23 °C. A solution of **II-60** in CH_2Cl_2 (24 mL) was added to this suspension via cannula. After 2 h, CH_2Cl_2 was removed *in vacuo*. The solid residue was purified by flash column chromatography (SiO_2, 10% EtOAc/hexanes) to afford **II-61** (20.2 g, 84%) as a colorless oil. Analytical data for II-61: $[\alpha]_D^{25}$ = +1.2 (c 1.2, CH_2Cl_2); IR (film) 1959, 1889, 1824, 1771, 1550 cm^{-1}; ^1H NMR, (500 MHz, $CDCl_3$) δ 7.68–7.66 (m, 4H), 7.44–7.38 (m, 6H), 3.71-3.69 (t, *J* = 6.23 Hz, 2H), 3.27-3.24 (dd, *J* = 9.7, 4.5 Hz, 1H), 3.18-3.15 (dd, *J* = 9.7, 4.5 Hz 1H), 1.76-1.71 (m, 1H), 1.70-1.63 (m, 1H), 1.48-1.43 (m, 1H), 1.07 (s, 9H), 0.98-0.96 (d, *J* = 6.58 Hz, 3H); ^{13}C NMR (125 MHz, $CDCl_3$) δ 135.8, 134.0, 129.9, 127.9, 61.8, 39.2, 31.6, 27.2, 20.9, 19.5, 18.4; LRMS (ESI): Mass calculated for $C_{21}H_{29}IOSi$ $[M–I]^+$, 325.5. Found 325.2.

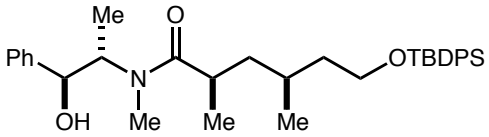

(**Not shown in text**) To a –78 °C suspension of LiCl (22.7 g, 535 mmol) and diisopropylamine (26.8 mL, 192 mmol) in THF (77 mL) was added *n*-BuLi (87 mL, 178 mmol, 2.05 M solution in hexanes) via cannula. The resulting suspension was warmed to 0 °C briefly and then was cooled to –78 °C. An ice-cooled solution of amide II-58 (20.8 g, 93.8 mmol) in THF (144 mL) was added via cannula. The mixture was stirred at -78 °C for 1 h, at 0 °C for 15 min, and at 23 °C for 5 min. The mixture was cooled to 0 °C and a solution of **II-61** (20.2 g, 44.6 mmol) in THF (10 mL) was added via cannula. The mixture stirred for 18 hours at 23 °C before being quenched by the addition of saturated ½ saturated NH_4Cl (300 mL). The organic layer was removed and the remaining aqueous layer was extracted with EtOAc (4 x 100 mL). The combined organic layers were combined and dried over Na_2SO_4, filtered and concentrated *in vacuo*. The residue was purified by flash column chromatography (SiO_2, 50% EtOAc/hexanes) to afford the desired amide (22.5 g, 93%) as a viscous oil (dr 20:1). Analytical data: $[\alpha]_D^{25}$ = +45.7 (c 0.9, CH_2Cl_2); IR (film) 3374, 1617, 1612, 1107 cm^{-1}; ^1H NMR (3:1 rotamer ratio, only major rotamer reported, 500 MHz, C_6D_6) δ 7.79-7.77 (m, 5H), 7.26-7.00 (m, 10H), 4.5-4.40 (m, 1H0, 3.78-3.70 (m, 2H), 2.40-2.35 (m, 1H), 2.25 (s, 3H), 1.82-1.80 (m, 1H), 1.61-1.59 (m, 1H), 1.25-1.20 (m, 1H), 1.15 (s, 9H), 1.05-1.02 (m, 1H), 0.96-0.94 (d, *J* = 8.4 Hz, 3H), 0.94-0.93 (d, J = 6.7 Hz, 3H), 0.90 (m, 1H), 0.85 (m, 1H), 0.65-0.64 (d, *J* = 6.2 Hz, 3H); ^{13}C NMR (125 MHz, C_6D_6) δ 178.2, 143.7, 135.9, 135.8, 134.3, 129.8, 128.5, 127.2, 126.5, 76.3, 62.2, 41.7, 40.1, 34.1, 27.5, 27.0, 26.3, 23.6, 19.8, 19.3, 17.9, 14.2; LRMS (ESI): Mass calculated for $C_{34}H_{47}NO_3Si$ $[M+H]^+$, 546.8. Found 546.6.

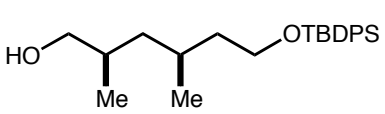

(**II-62**): To a –78 °C solution of diisopropylamine (24.5 mL, 173 mmol) in THF (170 mL) was added *n*-BuLi (80 mL, 160 mmol, 2.0 M solution in hexanes) via cannula. The resulting solution was stirred at -78 °C for 10 min, then warmed to 0 °C and held at that temperature for 10 min. Borane-ammonia complex (90%, 5.1 g, 165 mmol) was added in one portion, and the suspension was stirred at 0 °C for 15 min and then warmed to 23 °C. After 15 min, the suspension was cooled to 0 °C and a solution of amide (22.5 g, 41.2 mmol) in THF (103 mL) was added via cannula. The reaction mixture was warmed to 23 °C, held at this temperature for 2 h, and then cooled to 0 °C where excess hydride was quenched by the addition of 0.01 M aqueous HCl (500 mL). The mixture was stirred for 30 min at 0 °C and then extracted with EtOAc (4 x 150 mL). The combined organic extracts were washed with 0.1 m aqueous HCl (50 mL), 1 M NaOH (2 x 50 mL), and brine (40 mL). The organic layer was dried over Na_2SO_4, filtered and concentrated. The residue was purified by flash column chromatography (SiO_2, 40% Et_2O/hexanes) to afford **II-62** (14.3 g, 91%) as a colorless, viscous oil. Analytical data for II-62: $[\alpha]_D^{25}$ = +9.5 (c 0.95, CH_2Cl_2); IR (film) 3338, 1889, 1825, 1427, 1107 cm^{-1}; ^1H NMR, (500 MHz, $CDCl_3$) δ 7.69–7.68 (m, 4H), 7.45–7.38 (m, 6H), 3.74–3.68 (m, 2H), 3.51-3.48 (m, 1H), 3.40-3.35 (m, 1H), 1.73-1.69 (m, 2H), 1.68-1.63 (m, 2H), 1.32-1.26 (m, 2H), 1.06 (s, 9H), 0.93-0.91 (d, *J* = 6.7Hz, 3H), 0.86-0.84 (d, *J* = 6.71 Hz, 3H); ^{13}C NMR (125 MHz, $CDCl_3$) δ 135.8, 134.3, 129.7, 127.8, 68.6, 62.2, 41.2, 39.3, 33.3, 27.1, 26.9, 20.6, 19.4, 17.3; LRMS (ESI): Mass calculated for $C_{24}H_{36}O_2Si$ $[M+Na]^+$, 407.63. Found 407.26.

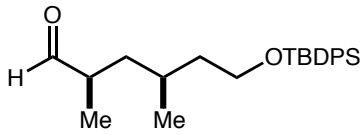

(**II-53**): To a suspension of powdered 4Å molecular sieves (8.4 g) and **II-62** (3.8 g, 9.89 mmol) in CH_2Cl_2 (68 mL) was added NMO (1.85 g, 15.8 mmol) followed by TPAP (172 mg, 0.49 mmol). After 45 min the green reaction mixture was filtered through Celite (eluting with CH_2Cl_2) and concentrated *in vacuo* to approximately 15 mL. The resulting material was filtered through SiO_2 (eluting with 40% Et_2O/hexanes, 300 mL). Removal of the solvent *in vacuo* afforded aldehyde **II-53** (3.45 g, 92%) as a colorless oil. Aldehyde **II-53** was used directly in the next step.

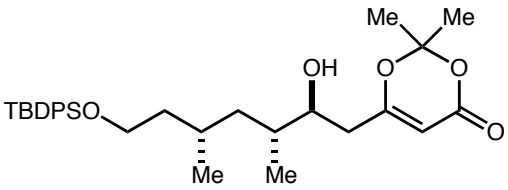

(**II-51**): A mixture of $Cu(OTf)_2$ (651 mg, 1.8 mmol) and (*R*)-Tol-BINAP (1.5 g, 2.25 mmol) in THF (58 mL) was stirred at room temperature under N_2 for 15 minutes to yield a clear yellow solution. A solution of $Bu_4NPh_3SiF_2$ (1.5 g, 2.7 mmol) in THF (16 mL) was added via cannula and the resulting solution was stirred for 15 minutes. The mixture was cooled to –78 °C and enol silane **II-54** (2.5 g, 11.7 mmol) was added dropwise followed immediately by a solution of **II-53** (3.45 g, 9.0 mmol) in THF (6.4 mL). The mixture was warmed to –50 °C and allowed to stir for 24 h. Trifluroacetic acid (3.6 mL) was added at -78 °C and the solution was allowed to warm to 23 °C. Stirring was continued for 1 h. The reaction mixture was diluted with EtOAc (90 mL) and saturated $NaHCO_3$ was added dropwise until gas evolution ceased. The organic layer was washed with brine (30 mL), dried over Na_2SO_4 and concentrated. The residue was purified by flash column chromatography (65% Et_2O/hexanes) to afford β-hydroxy-dioxinone **II-51** (2.90 g, 61%) as an inseperable

mixture of diastereomers (dr 7:1). Analytical data for **II-51**: $[\alpha]_D^{25} = -1.7$ (c 1, CH_2Cl_2); IR (film) 3453, 1718, 1631, 1384 cm^{-1}; ^1H NMR, (500 MHz, $CDCl_3$) δ 7.69–7.67 (m, 4H), 7.45–7.38 (m, 6H), 5.34 (s, 1H), 3.76-3.67 (m, 3H), 2.36-2.33 (dd, *J* = 14.3, 3.0 Hz, 1H), 2.28-2.23 (dd, *J* = 14.6, 9.7 Hz, 1H), 1.76-1.72 (m, 2H), 1.70 (s, 6H), 1.67-1.62 (m, 2H), 1.33-1.32 (m, 1H), 1.23-1.20 (m,1H), 1.06 (s, 9H), 0.93-0.92 (d, *J* = 6.7 Hz, 3H), 0.88-0.87 (d, *J* = 6.7 Hz, 3H); ^{13}C NMR (125 MHz, $CDCl_3$) δ 170.2, 161.3, 135.8, 134.2, 129.8, 127.8, 106.8, 95.2, 73.0, 62.1, 40.0, 38.7, 38.0, 36.6, 27.1, 25.6, 24.9, 20.9, 19.4, 15.5, 13.6; LRMS (ESI): Mass calculated for $C_{31}H_{44}O_5Si$ $[M+NH_4]^+$, 542.76. Found 542.51.

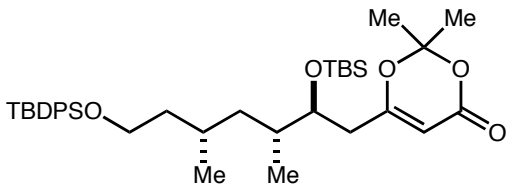

(**Not shown in text**): To a 0 °C solution of **II-51** (2.90 g, 5.49 mmol) in CH_2Cl_2 (58 mL) was added 2,6-lutidine (1.9 mL, 16.5 mmol) and TBSOTf (1.3 mL, 6.0 mmol). The resulting solution was stirred at 0 °C for 90 minutes and quenched by the addition of saturated $NaHCO_3$ (120 ml). The aqueous layer was extracted with EtOAc (3x 15 ml). The combined organic layers were dried over Na_2SO_4, filtered and concentrated. The resulting residue was purified by flash column chromatography (40% Et_2O/hexanes) to afford bis silyl ether (3.3 g, 92%) as a clear oil. Analytical data: $[\alpha]_D^{25} = -9.9$ (c 1, CH_2Cl_2); IR (film) 1736, 1636, 1461, 1384 cm^{-1}; ^1H NMR, (500 MHz, $CDCl_3$) δ 7.68–7.67 (m, 4H), 7.45-7.37 (m, 6H), 5.27 (s, 1H), 3.87-3.84 (ddd, *J* = 8.8, 6.7, 5.1 Hz, 1H), 3.75-3.66 (m, 2H), 2.24-2.22 (dd, *J* = 6.7, 1.5 Hz, 1H), 1.81-1.79 (m, 1H), 1.68 (s, 3H), 1.66 (s, 3H), 1.21-1.18 (dd, *J* = 13.4, 6.1, 1H), 1.06 (s, 9H), 1.02-0.97 (m, 1H), 0.89 (s, 9H), 0.87-0.86 (d, *J* = 6.7, 3H), 0.86-0.82 (m, 4H),

0.79-0.78 (d, *J* = 6.4 Hz, 3H), 0.06 (s, 3H), 0.03 (s, 3H) ; ^{13}C NMR (125 MHz, $CDCl_3$) δ 170.5, 161.3, 135.7, 134.2, 129.8, 127.8, 106.5, 95.4, 72.9, 62.1, 40.9, 39.2, 37.5, 36.3, 27.1, 26.1, 26.0, 24.4, 20.7, 19.4, 18.2, 14.5, –4.1, –4.5; LRMS (ESI): Mass calculated for $C_{37}H_{58}O_5Si_2$ $[2M+NH_4]^+$, 1294.6. Found 1294.03.

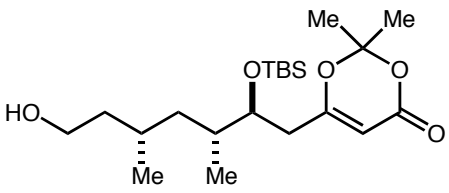

(**II-63**): To a 23 °C solution of bis silyl ether (3.3 g, 5.05 mmol) in MeOH (106 mL) was added NH_4F (18.7 g, 505 mmol). The resulting mixture was warmed to 40 °C for 24 h. The solvent was removed *in vacuo* and the resulting residue was purified by flash column chromatography (75% Et_2O/hexanes) to afford II-63 (1.9 g, 92%) as a clear oil. Analytical data for **II-63**: $[\alpha]_D^{25}$ = –22.7 (c 1, CH_2Cl_2); IR (film) 2931, 1715, 1635, 1461, 1384 cm^{-1}; ^{1}H NMR, (500 MHz, $CDCl_3$) δ 5.27 (s, 1H), 3.88-3.85 (ddd, *J* = 11.2, 7.6, 3.9 Hz, 1H), 3.72-3.64 (m, 2H), 2.25-2.24 (dd, J = 3.6, 1.2, Hz, 1H), 1.75 (m, 1H), 1.70 (s, 3H), 1.68 (s, 3H), 1.64-1.62 (m, 2H), 1.41 (br s. 1H), 1.30-1.29 (m, 1H), 1.28-1.25 (m, 1H), 1.05-1.00 (m, 1H), 0.95-0.94 (d, *J* = 6.4 Hz, 3H), 0.90-0.88 (d, *J* = 7.0 Hz, 3H), 0.87 (s, 9H), 0.05 (s, 3H), 0.02 (s, 3H); ^{13}C NMR (125 MHz, $CDCl_3$) δ 170.4, 161.3, 106.5, 95.4, 72.7, 61.0, 40.6, 39.4, 37.5, 36.3, 27.1, 26.0, 24.5, 20.8, 18.2, 14.7, –4.1, –4.5; LRMS (ESI): Mass calculated for $C_{21}H_{40}O_5Si$ $[2M+Na]^+$, 823.03. Found 823.62.

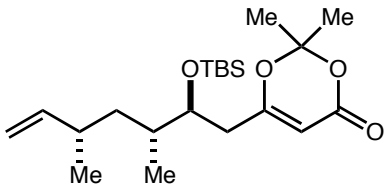

(**II-64**): To a 23 °C solution of **II-63** (1.9 g, 4.64 mmol) in THF (22.5 mL) was added 2-nitrophenylselenocyanide (1.7 g, 7.42 mmol) and *n*-Bu_3P (1.8 mL, 7.42 mmol). The resulting solution stirred at 23 °C for 30 min. The mixture was than passed through a short plug of SiO_2 (eluting with 60% Et_2O/ hexanes) and concentrated. The resulting residue was purified by flash column chromatography (40% Et_2O/hexanes) to afford the intermediate organoselenide as a yellow oil. This oil was dissolved in THF (39 ml) and cooled to 0 °C. Hydrogen peroxide (30%, 8.1 mL) was added slowly. The resulting mixture was allowed to stir for 12 h at 0 °C. The reaction was quenched by the slow addition of saturated Na_2SO_3 (50 mL) at 0 °C. The aqueous layer was extracted with EtOAc (3 x 15 ml) and the combined organic layers were dried over Na_2SO_4, filtered and concentrated. The resulting residue was purified by flash column chromatography (40% Et_2O/hexanes) to afford **II-64** oil (1.35 g, 76%) as a yellow oil. Analytical data for **II-64**: $[\alpha]_D^{25} = -22.1$ (c 1, CH_2Cl_2); IR (film) 1735, 1636, 1265 cm^{-1}; ^1H NMR, (500 MHz, $CDCl_3$) δ 5.58–5.51 (ddd, *J* = 17.1, 10.0, 8.8 Hz, 1H), 5.25 (s, 1H), 4.98-4.94 (d, *J* = 17.1 Hz, 1H), 4.94-4.93 (d, *J* = 10.0 Hz, 1H), 3.82-3.79 (ddd, *J* = 9.8, 6.4, 5.8 Hz, 1H), 2.26-2.25 (d, *J* = 6.1 Hz, 1H), 2.23-2.21 (m, 1H), 1.69 (s, 3H), 1.67 (s, 3H), 1.27-1.21 (m, 2H), 1.09-1.04 (m, 2H), 1.02-1.01 (d, *J* = 6.7 Hz, 3H), 0.87 (s, 9H), 0.84-0.83 (d, *J* = 7.0 Hz, 3H), 0.03 (s, 3H), 0.02 (s, 3H); ^{13}C NMR (125 MHz, $CDCl_3$) δ 170.2, 161.3, 144.2, 113.6, 106.5, 95.4, 73.5, 39.7, 37.9, 36.3, 36.1, 26.0, 24.5, 22.0, 18.2, 14.2, –4.1, –4.5; LRMS (ESI): Mass calculated for $C_{21}H_{38}O_4Si$ $[2M+Na]^+$, 787.4. Found 787.7.

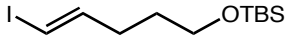

(**II-78**): To a 0 °C suspension of bis(cyclopentadienyl)zirconium chloride hydride (Schwartz Reagent) (15.0 g, 58.2 mmol) in THF (168 mL) was added TBS pentynol (10.9 g, 55.4 mmol) via cannula. The reaction stirred for 20 min then *N*-iodosuccinimide (13.1 g, 58.2 mmol) was added in one portion. The reaction was allowed to warm to 23 °C and stirred for 10 minutes. The mixture was diluted with hexanes (100 mL). The reaction mixture was filtered through Celite and the filter pad was rinsed with hexanes (400 mL). The filtrate was concentrated *in vacuo* and diluted with hexanes. The resulting heterogenous mixture was filtered through Florisil and the filter pad was rinsed with hexanes (400 mL). This filtrate was concentrated *in vacuo* to dryness to give **II-78** (15.9 g, 88%) as a pale yellow oil. The vinyl iodide is used in the next reaction without further purification. Analytical data for **II-78**: IR (film) 2930, 1261, 836 cm^{-}1; ^{1}H NMR ($CDCl_3$, 500 MHz) δ 6.55-6.50 (ddd, *J* = 14.2, 7.1, 7.1, 1H), 6.00 (d, *J* = 14.4. 1H), 3.62-3.59 (t, *J* = 6.2 Hz, 2H), 2.15-2.11 (dd, *J* = 14.2, 7.2 Hz, 2H), 1.63-1.58 (m, 2H), 0.90 (s, 9H), 0.05 (s, 6H); ^{13}C NMR (125 MHz, $CDCl_3$) δ 146.4, 74.9, 62.2, 32.7, 31.6, 29.9, 26.2, –5.1; LRMS (ESI): Mass calculated for $C_{11}H_{23}IOSi$ $[M+H]^+$, 327.05. Found 327.07.

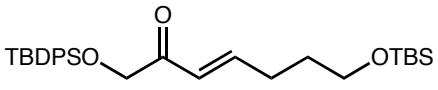

(**II-83**): To a –78 °C solution of vinyl iodide **II-78** (15.9 g, 48.8 mmol) in THF (455 mL) was added 1.85 M solution of *n*-BuLi in hexanes (29 mL, 53.7 mmol) over 3 min. A solution of Weinreb's amide **II-82** (19.1 g, 53.7 mmol) in THF (76 mL) was added rapidly via cannula. Following the addition, the cooling bath was removed and the reaction was allowed to stir for 90 minutes. The reaction mixture was recooled to –78 °C and

quenched with 0.1N HCl (150 mL). The mixture was poured into a mixture of 0.1N HCl (120 mL) and 1:1 hexanes-ether (500 mL). The aqueous layer was separated and extracted with EtOAc (40 mL). The combined organic extracts were dried over Na_2SO_4, filtered, and concentrated *in vacuo* to dryness. The residue was purified by flash column chromatography (2% Et_2O/hexanes) to afford enone **II-83** (18.3 g, 76%) as a clear oil. Analytical data for II-83: IR (film) 1693, 1624, 1471, 1427, 1107 cm^{-1}; ^1H NMR ($CDCl_3$, 500 MHz) δ 7.69-7.68 (m, 4H), 7.47-7.39 (m, 6H), 7.01-6.95 (ddd, J = 15.2, 6.7, 6.7 Hz, 1H), 6.49-6.46 (d, J = 15.5, 1H), 4.34 (s, 2H), 3.64-3.62 (t, J = 6.1 Hz, 2H), 2.32-2.27 (m, 2H), 1.70-1.65 (m, 2H), 1.12 (s, 9H), 0.91 (s, 9H), 0.06 (s, 6H); ^{13}C NMR ($CDCl_3$, 500 MHz) δ 197.8, 148.2, 135.7, 133.0, 130.1, 128.0, 125.6, 69.2, 62.3, 31.2, 29.3, 27.0, 26.1, 19.5, 18.5, –5.0; MS (ESI): mass calculated for $C_{29}H_{44}O_3Si_2$ $[2M+Na]^+$, 1015.4. Found 1015.5.

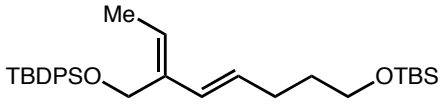

(**II-55**): To a –78 °C suspension of $Ph_3PEt^+Br^-$ (35.5 g, 95.7 mmol) in THF (258 mL) was added a 0.60 M solution of potassium hexamethyldisilylazide (KHMDS) in toluene (153 mL, 92 mmol). The reaction was allowed to warm to 0 °C and stir for 25 minutes. The reaction solution was recooled to –78 °C and soution of enone **II-83** (18.3 g, 36.8 mmol) in THF (102 mL) was added dropwise via cannula. The reaction mixture was allowed to warm to 0 °C and stir for 2 hours. The mixture was recooled to –78 °C and poured into a mixture of 0.1N HCl (200 mL) and 1:1 Et_2O/hexanes (300 mL). The aqueous layer was separated and extracted with EtOAc (3 x 40 mL). The combined organic extracts were washed with brine (200 mL), dried over Na_2SO_4, filtered, and concentrated *in vacuo* to dryness. The

residue was purified by flash column chromatography to afford diene **II-55** (16.4 g, 88%) as a clear oil. Analytical data for II-55: IR (film) 1470, 1427, 1253, 1109 cm^{-1}; ^1H NMR ($CDCl_3$, 500 MHz) δ 7.72-7.71 (m, 4H), 7.45-7.38 (m, 6H), 6.01-5.98 (d, *J* = 15.5 Hz, 1H), 5.84-5.78 (ddd, *J* = 14.3, 7.0, 7.0, 1H), 5.53-5.49 (q, *J* = 14.3, 7.0, 1H), 4.35 (s, 2H), 3.65-3.63 (t, *J* = 6.3 Hz, 2H), 2.17-2.13 (m, 2H), 1.66-1.60 (m, 2H), 1.53-1.51 (d, *J* = 7.0, 3H), 1.05 (s, 9H), 0.92 (s, 9H), 0.07 (s, 6H); ^{13}C NMR ($CDCl_3$, 500 MHz) δ 137.7, 136.0, 134.1, 132.5, 129.8, 128.7, 127.9, 126.9, 62.8, 59.0, 33.1, 29.7, 27.1, 26.3, 19.5, 14.4, 13.8, –4.9; MS (ESI): mass calculated for $C_{31}H_{48}O_2Si_2$ $[M+Na]^+$, 531.88. Found 531.98.

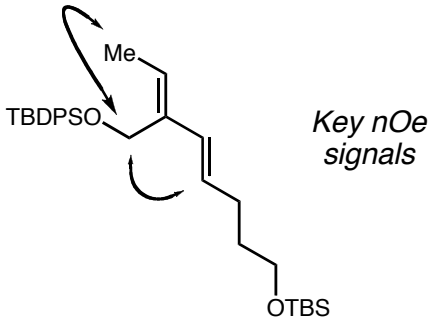

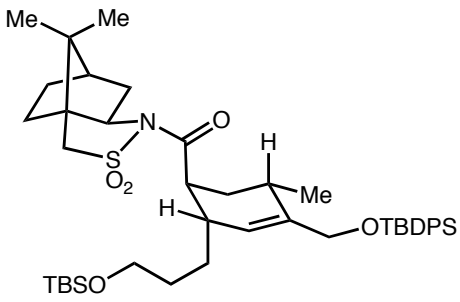

(**II-84**): To a –78 °C solution of diene **II-55** (3.0 g, 5.9 mmol) and acyl sultam **II-77** (1.59 g, 5.90 mmol) in CH_2Cl_2 (3.3 mL) was added a 1.0 M solution of $EtAlCl_2$ (10.6 mL, 10.6 mmol) dropwise over 3 min. The reaction was stirred at –78 °C for 1h. The reaction was allowed to warm to -20 °C and stir for 24 h. The reaction mixture was recooled to –78 °C and quenched with saturated $NaHCO_3$ (5 mL). The mixture was filtered through a frit funnel to remove the white precipitate. The white precipitate was washed with ether (30 mL). The mother liquor was then poured into saturated $NaHCO_3$ (100 mL). The aqueous layer was separated and extracted with ethyl acetate (50 mL). The combined organic layers were washed with brine, dried over

anhydrous Na_2SO_4, filtered and concentrated in vacuo to dryness. The residue was purified by flash chromatography (gradient) to give 4.13 g (90%) of **II-84** as a white foam. Analytical data for II-84: $[\alpha]_D^{25} = -21.4$ (c 1, CH_2Cl_2); IR (film) 3058, 2958, 2930, 1697, 1462, 1388, 1260, 997, 776 cm^{-1}; ^1H NMR ($CDCl_3$, 500 MHz) δ 7.70-7.67 (m, 4H), 7.43-7.39 (m, 6H), 5.57 (s. 1H), 4.16 (A of AB, *J* = 13.1 Hz, 1H), 4.09 (B of AB, *J* = 13.1Hz, 1H), 3.92 (t, *J* = 6.1 Hz, 1H), 3.61-3.55 (m, 2H), 3.52 (A of AB, *J* = 13.7 Hz, 1H), 3.44 (B of AB, *J* = 13.7 Hz, 1H), 3.06 (ap t, *J* = 10.1 Hz, 1H), 2.63 (m, 1H), 2.36-2.34 (m, 1H), 2.12 (d, *J* = 6.4 Hz, 1H), 1.95-1.88 (m, 5H), 1.84-1.78 (ddd, *J* = 12.5, 12.2, 5.5, 1H), 1.68-1.64 (m, 1H), 1.52-1.45 (m, 5H), 1.19 (s, 3H), 1.07 (s. 9H), 1.01 (d, *J* = 7.3 Hz, 3H), 0.99 (s, 3H), 0.89 (s, 9H), 0.03 (s, 6H); ^{13}C NMR ($CDCl_3$, 500 MHz) δ 176.3, 141.1, 135.8, 133.9, 129.8, 127.9. 123.9, 66.3, 65.7, 63.6, 53.5, 48.5, 47.9, 44.9, 42.1, 39.6, 39.0, 33.6, 33.2, 30.0, 29.3, 28.8, 27.1, 26.7, 26.2, 21.1, 20.1, 19.5, 19.4, 18.5, –5.0; MS (ESI): mass calculated for $C_{44}H_{67}NO_5SSi_2$ $[M+NH_4]^+$, 795.43. Found 795.61.

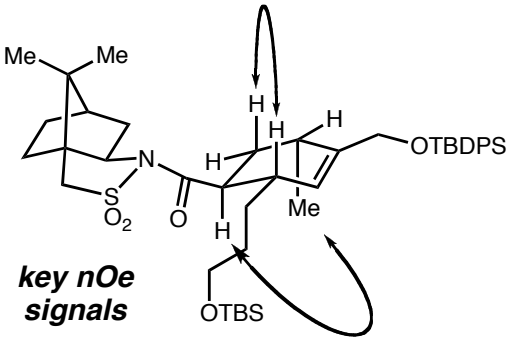

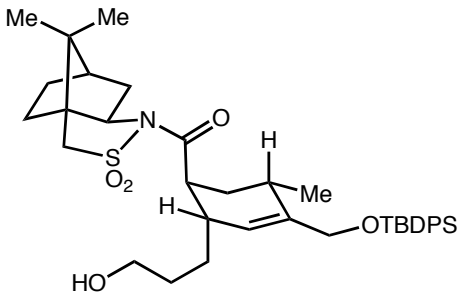

(**II-85**): To a 0 °C solution of cyclohexene **II-84** (4.13 g, 5..3 mmol) in MeOH (220 mL) was added a 0.5% HCl (9.6 mL). The reaction was allowed to warm to 23°C and stir for 10 h. The reaction mixture was quenched by addition of $NaHCO_3$ (330 mg). The mixture was then diluted with ethyl acetate (40 mL) and MeOH was removed

in vacuo. The mixture was then diluted with H_2O (150 mL) and extracted with ethyl acetate (4 x 50 mL). The combined organic layers were dried over anhydrous Na_2SO_4, filtered and concentrated in vacuo to dryness. The residue was purified by flash chromatography (30% EtOAc-hexanes) to give 2.9 g (83%) of **II-85** as a white foam. Analytical data for **II-85**: $[\alpha]_D^{25} = -12.6$ (c 1, CH_2Cl_2); IR (film) 2949, 2858, 1693, 1457, 1330, 1211, 1111, 1063 cm^{-1}; ^1H NMR ($CDCl_3$, 500 MHz) δ 7.69-7.66 (m, 4H), 7.42-7.38 (m, 6H), 5.52 (s, 1H), 4.16 (A of AB, *J* = 13.1 Hz, 1H), 4.09 (B of AB, *J* = 13.1Hz, 1H), 3.92 (t, *J* = 6.1 Hz, 1H), 3.58-3.54 (m, 2H), 3.52 (A of AB, *J* = 13.9 Hz, 1H), 3.44 (B of AB, *J* = 13.7 Hz, 1H), 3.09 (ap t, *J* = 10.3 Hz, 1H), 2.67 (m, 1H), 2.36-2.34 (m, 1H), 2.12 (d, *J* = 6.4 Hz, 1H), 1.94-1.88 (m, 5H), 1.85-1.79 (ddd, *J* = 12.2, 12.2, 5.1, 1H), 1.67-1.62 (m, 1H), 1.50-1.43 (m, 3H), 1.41-1.34 (m, 2H), 1.19 (s, 3H), 1.06 (s. 9H), 1.01-0.99 (d, *J* = 7.3 Hz, 3H), 0.98 (s, 3H); ^{13}C NMR ($CDCl_3$, 500 MHz) δ 176.3, 141.4, 135.8, 133.9, 129.8, 127.8, 123.7, 66.2, 65.7, 63.2, 53.4, 48.5, 47.9, 44.9, 41.6, 39.2, 39.0, 33.5, 33.2, 29.4, 28.8, 28.7, 27.0, 26.6, 21.0, 21.3, 19.5, 19.4; MS (ESI): mass calculated for $C_{38}H_{53}NO_5SSi$ $[M+NH_4]^+$, 681.34. Found 681.73.

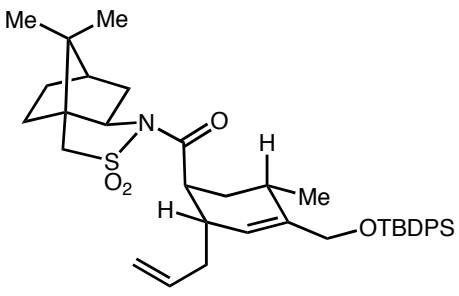

(**II-76**): To a solution of alcohol **II-85** (2.9 g, 4.4 mmol) in THF (22 mL) was added 2-nitrophenylselenocyanide (2.53 g, 11.1 mmol) in one portion. To the reaction mixture was added *n*-Bu_3P (2.76 mL, 11.1 mmol). After 1 h, the reaction was quenched by the addition of 1M NaOH. The mixture was extracted with ethyl acetate (50 mL). The combined organic layers were dried over anhydrous Na_2SO_4,

filtered and concentrated *in vacuo* to dryness. The residue was purified by flash chromatography (60% ether-hexanes) to give the intermediate selenide as a yellow foam. To a 0 ^{o}C solution of selenide (3.73 g, 4.4 mmol) in THF (97 mL) was added 30% H_2O_2 (15 mL) dropwise. After 12 h, the reaction was recooled to 0 ^{o}C and was quenched by careful addition of saturated Na_2SO_3. The mixture was extracted with ethyl acetate (50 mL). The combined organic layers were dried over anhydrous Na_2SO_4, filtered and concentrated in vacuo to dryness. The residue was purified by flash chromatography (gradient) to give 2.36 g (83%) of **II-76** as a yellow foam. Analytical data for **II-76**: $[\alpha]_D^{25}$ = –33.4 (c 1, CH_2Cl_2); IR (film) 2932, 2868, 1687, 1388, 1328, 1211, 1111, 1061 cm^{-1}; ^{1}H NMR ($CDCl_3$, 500 MHz) δ 7.69-7.66 (m, 4H), 7.44-7.38 (m, 6H), 5.76-5.70 (ddd, J = 17.0, 10.2, 7.1 Hz, 1H), 5.64 (s, 1H), 5.05 (d, J = 17.0, 1H), 5.02 (d, J = 10.2, 1H), 4.16 (A of AB, *J* = 12.8 Hz, 1H), 4.09 (B of AB, *J* = 13.3 Hz, 1H), 3.92 (t, *J* = 6.0 Hz, 1H), 3.52 (A of AB, *J* = 13.5 Hz, 1H), 3.43 (B of AB, *J* = 13.7 Hz, 1H), 3.05 (ap t, *J* = 11.3, Hz, 1H), 2.69 (m, 1H), 2.34-2.32 (m, 1H), 2.18 (m, 1H), 2.13 (d, *J* = 6.2 Hz, 1H), 1.98-1.88 (m, 5H), 1.84-1.78 (ddd, *J* = 12.2, 12.2, 5.1, 1H), 1.44-1.36 (m, 3H), 1.19 (s, 3H), 1.05 (s, 9H), 0.99-0.98 (d, *J* = 7.0 Hz, 3H), 0.98 (s, 3H) ; ^{13}C NMR ($CDCl_3$, 500 MHz) δ 176.1, 141.1, 135.9, 135.7, 133.8, 129.8, 127.8, 123.1, 117.3, 66.0, 65.7, 53.4, 48.5, 47.9, 44.9, 42.2, 39.6, 39.0, 38.3, 33.6, 33.2, 28.9, 27.0, 26.6, 21.1, 20.1, 19.4, 19.2; MS (ESI): mass calculated for $C_{38}H_{51}NO_4SSi$ $[M+Na]^+$, 668.33. Found 668.79.

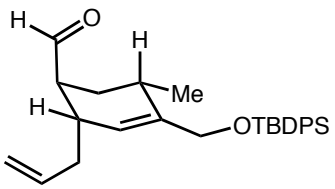

(**II-75**): To a –78 °C solution of cyclohexene **II-76** (2.55 g, 3.96 mmol) in CH_2Cl_2 (48 mL) was added 1.0 M solution of DIBAl-H in CH_2Cl_2 (19.8 mL, 19.8 mmol) dropwise down the side of the round bottom. The reaction mixture was allowed to stir at –78 °C for 1h. The reaction mixture was quenched with MeOH (8 mL) and 1N HCl (6 mL). The mixture was allowed to warm to room temperature and was then poured into a mixture of CH_2Cl_2 (100 mL) and H_2O (80 mL), the aqueous layer was extracted with CH_2Cl_2 (50 mL). The combined organic extracts were then washed with brine, dried over anhydrous Na_2SO_4, and concentrated *in vacuo* to dryness. The residue was purified by flash chromatography (30% EtOAc-hexanes) to give 1.62 g (95%) of **II-75** as a pale yellow oil. Analytical data for **II-75**: $[\alpha]_D^{25} = -9.5$ (c 0.65, CH_2Cl_2); IR (film) 3062, 2929, 1723, 1444, 1362, 1103, 1057 cm^{-1}; ^1H NMR ($CDCl_3$, 500 MHz) δ 9.70 (d, *J* = 1.6 Hz, 1H), 7.70-7.67 (m, 4H), 7.44-7.38 (m, 6H), 5.76-5.70 (ddd, J = 17.0, 10.2, 7.1 Hz, 1H), 5.64 (s, 1H), 5.05 (d, J = 17.0, 1H), 5.02 (d, J = 10.2, 1H), 4.16 (A of AB, *J* = 13.5 Hz, 1H), 4.09 (B of AB, *J* = 13.2 Hz, 1H), 2.62 (m, 1H), 2.42-2.36 (m, 2H), 2.26-2.21 (m, 1H), 2.13-2.06 (m, 1H), 1.78-1.72 (ddd, *J* = 12.9, 12.6, 5.5, 1H), 1.68-1.64 (m, 1H), 1.06 (s. 9H), 0.99-0.98 (d, *J* = 6.9 Hz, 3H); ^{13}C NMR ($CDCl_3$, 500 MHz) δ 205.0, 141.4, 136.0, 135.7, 133.9, 129.9, 127.9, 123.4, 117.5, 66.0, 47.7, 39.0, 34.6, 30.1, 28.1, 27.0, 19.6, 19.5; MS (ESI): mass calculated for $C_{28}H_{36}O_2Si$ $[M+Na]^+$, 455.67. Found 455.56.

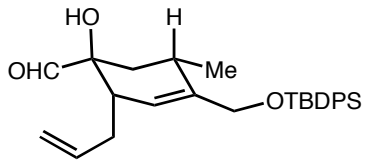

(**II-74**): To a solution of aldehyde **II-75** (1.50 g, 3.50 mmol) in CH_2Cl_2 (6.5 mL) was added Et_3N (6.4 mL, 46 mmol) followed by addition of TBSOTf (8.0 mL, 35 mmol) dropwise. The reaction mixture was stirred for 1h at 23 ^oC. The reaction was diluted with hexanes (10 mL) and saturated Na_2SO_3 (20 mL) was added. The mixture was extracted with hexanes (30 mL). The combined organic extracts were dried over anhydrous Na_2SO_4 and concentrated *in vacuo* to dryness to give the intermediate enol silane as a yellow oil, The enol silane was used in the next reaction without further purification. To a 0 ^oC solution of the enol silane (1.91 g, 3.50 mmol) in CH_2Cl_2 (70 mL) was added 0.075 M solution of DMDO in acetone (56 mL, 4.2 mmol) over 5 min. The reaction mixture was stirred at 0 ^oC for 5 min and then concentrated *in vacuo*. The mixture was diluted with EtOAc (20 mL) and recooled to 0 ^oC. To the mixture was added 0.1N HCl (12 mL) slowly. The aqueous layer was separated and extracted with EtOAc (50 mL). The combined organic extracts were dried over anhydrous Na_2SO_4 and concentrated *in vacuo* to dryness. The residue was purified by flash chromatography (gradient) to give 1.11 g (83% over 2 steps) of **II-74** as a yellow oil. Analytical data for **II-74**: $[\alpha]_D^{25}$ = +24.7 (c 1, CH_2Cl_2); IR (film) 3495, 3062, 2930, 1719, 1427, 1111, 1061 cm^{-1}; ^1H NMR ($CDCl_3$, 500 MHz) δ 9.70 (s, 1H), 7.72-7.70 (m, 4H), 7.46-7.38 (m, 6H), 5.78-5.71 (m, 2H), 5.10-5.08 (d, *J* = 9.2 Hz, 1H), 5.08-5.05 (d, *J* = 16.1 Hz, 1H), 4.26 (A of AB, *J* = 13.9 Hz, 1H), 4.22 (B of AB, *J* = 13.7 Hz, 1H), 3.42 (s, 1H), 2.60 (m, 1H), 2.40 (m, 1H), 2.39-2.35 (m, 1H), 2.03-1.99 (dd, J = 13.5, 6.7 Hz,

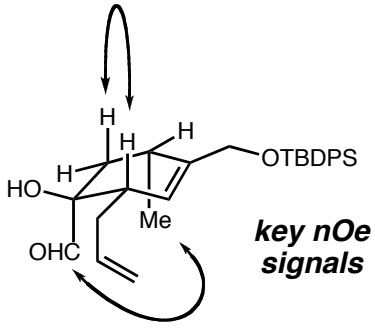

1H), 1.91-1.85 (m, 1H), 1.65-1.62 (dd, J = 13.7, 5.3 Hz, 1H), 1.10 (s. 9H), 1.01-0.99 (d, *J* = 7.3 Hz, 3H); ^{13}C NMR ($CDCl_3$, 500 MHz) δ 204.7, 140.5, 136.1, 133.8, 129.9, 128.5, 127.9, 121.3, 117.5, 78.7, 65.5, 43.8, 39.4, 35.0, 28.6, 27.1, 20.1, 19.5; MS (ESI): mass calculated for $C_{28}H_{36}O_3Si$ $[M+Na]^+$, 471.23. Found 471.87.

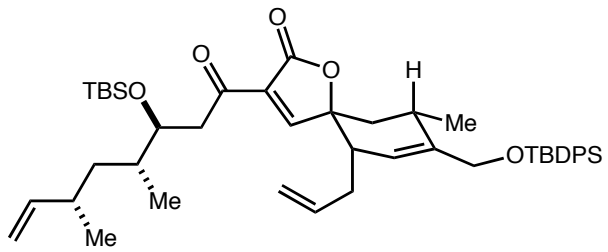

(**II-91**): To a solution of α-hydroxy-aldehyde **II-74** (175 mg, 0.39 mmol) and dioxinone **II-64** (85 mg, 0.22 mmol) in xylenes (0.4 mL) was added activated 4 Å molecular sieves (88 mg). The reaction mixture was submersed in an oil bath that had been preheated to 113 °C and allowed to stir for 75 minutes. The reaction mixture was then cooled to 23 °C and filtered through a short pad of silica gel (eluting with 60% Et_2O/hexanes). The filtrate was concentrated in *vacuo*. The residue was purified by flash column chromatography (10% Et_2O/hexanes) to afford butenolide **II-91** (141 mg, 86%) as a yellow oil. Analytical data for **II-91**: $[\alpha]_D^{25}$ = –32.1 (c 1, CH_2Cl_2); IR (film) 3072, 2954, 2895, 1766, 1693, 1617, 1460, 1377, 1253, 1107, 1072 cm^{-1}; ^{1}H NMR ($CDCl_3$, 500 MHz) δ 8.10 (s, 1H), 7.71–7.68 (m, 4H), 7.48-7.39 (m, 6H), 5.74-5.66 (m, 2H), 5.63-5.56 (ddd, *J* = 17.4, 10.0, 8.2 Hz, 1H), 5.10-5.08 (d, *J* = 10.0 Hz, 1H), 5.07-5.03 (d, *J* = 17.1, 1H), 5.00-4.96 (d, *J* = 17.4 Hz, 1H), 4.95-4.93 (d, *J* = 10.0 Hz, 1H), 4.26-4.23 (ddd, *J* = 9.1, 6.7, 3.0 Hz, 1H), 4.23-4.21 (A of AB, *J* = 14.0 Hz, 1H), 4.21-4.18 (B of AB, *J* = 14.0 Hz, 1H), 3.24-3.19 (dd, *J* = 15.8, 9.1 Hz, 1H), 2.83-2.79 (dd, *J* = 15.8, 3.0 Hz, 1H), 2.66-2.60 (m, 1H), 2.56-2.55 (m, 1H), 2.27-2.17 (m, 2H), 2.16-2.12 (dd, *J* = 13.7, 6.7 Hz, 1H), 1.88-1.82 (m, 1H), 1.76-1.68 (m, 1H), 1.66-1.62

(dd, *J* = 13.7, 6.1 Hz, 1H), 1.31-1.28 (m, 2H), 1.09 (s, 9H), 1.02-1.01 (d, *J* = 6.7 Hz, 3H), 0.99-0.98 (d, *J* = 7.0 Hz, 3H), 0.93-0.92 (d, *J* = 6.7 Hz, 3H), 0.85 (s, 9H), 0.06 (s, 3H), –0.01 (s, 3H); ^{13}C NMR ($CDCl_3$, 500 MHz) δ 194.2, 168.5, 164.0, 144.4, 140.4, 135.8, 135.3, 133.6, 132.2, 130.0, 127.9, 120.8, 117.8, 113.4, 87.8, 72.5, 65.3, 44.0, 43.2, 40.0, 39.3, 36.9, 36.4, 36.0, 29.2, 27.0, 26.1, 21.8, 19.6, 19.4, 13.9, –4.2, –4.4; MS (ESI): mass calculated for $C_{46}H_{66}O_5Si_2$ $[M+H]^+$, 755.44. Found 755.98.

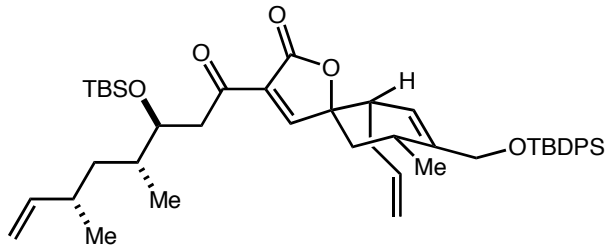

(**II-91'**):To a solution of α-hydroxy-aldehyde *ent*–(**II-74**) (344 mg, 0.90 mmol) and dioxinone **II-64** (192 mg, 0.50 mmol) in xylenes (0.90 mL) was added activated 4 Å molecular sieves (200 mg). The reaction mixture was submersed in an oil bath that had been preheated to 113 °C and allowed to stir for 75 minutes. The reaction mixture was then cooled to 23 °C and filtered through a short pad of silica gel (eluting with 60% Et_2O-hexanes). The filtrate was concentrated in *vacuo*. The residue was purified by flash column chromatography (10% Et_2O/hexanes) to afford butenolide **II-91'** (340 mg, 90%) as a yellow oil. Analytical data: $[\alpha]_D^{25}$ = –32.3 (c 1, CH_2Cl_2); IR (film) 3072, 2955, 2857, 1766, 1693, 1617, 1459, 1252, 1071 cm^{-1}; ^{1}H NMR ($CDCl_3$, 500 MHz) δ 8.12 (s, 1H), 7.71–7.68 (m, 4H), 7.48-7.39 (m, 6H), 5.74-5.66 (m, 2H), 5.63-5.56 (ddd, *J* = 17.4, 10.0, 8.2 Hz, 1H), 5.10-5.08 (d, *J* = 10.0 Hz, 1H), 5.07-5.03 (d, *J* = 17.1, 1H), 5.00-4.96 (d, *J* = 17.4 Hz, 1H), 4.95-4.93 (d, *J* = 10.0 Hz, 1H), 4.26-4.23 (ddd, *J* = 9.1, 6.7, 3.0 Hz, 1H), 4.23-4.21 (A of AB, *J* = 14.0 Hz, 1H), 4.21-4.18 (B of AB, *J* = 14.0 Hz, 1H), 3.17-3.13 (dd, *J* = 15.8, 9.1 Hz, 1H), 2.87-2.84 (dd, *J* = 15.8, 3.0 Hz, 1H),

2.66-2.60 (m, 1H), 2.56-2.55 (m, 1H), 2.27-2.17 (m, 2H), 2.16-2.12 (dd, *J* = 13.7, 6.7 Hz, 1H), 1.88-1.82 (m, 1H), 1.76-1.68 (m, 1H), 1.66-1.62 (dd, *J* = 13.7, 6.1 Hz, 1H), 1.31-1.28 (m, 2H), 1.09 (s, 9H), 1.02-1.01 (d, *J* = 6.7 Hz, 3H), 0.99-0.98 (d, *J* = 7.0 Hz, 3H), 0.93-0.92 (d, *J* = 6.7 Hz, 3H), 0.85 (s, 9H), 0.06 (s, 3H), –0.01 (s, 3H); ^{13}C NMR ($CDCl_3$, 500 MHz) δ 194.2, 168.5, 164.0, 144.4, 140.4, 135.8, 135.3, 133.6, 132.2, 130.0, 127.9, 120.8, 117.8, 113.4, 87.8, 72.5, 65.3, 44.0, 43.2, 40.0, 39.3, 36.9, 36.4, 36.0, 29.2, 27.0, 26.1, 21.8, 19.6, 19.4, 13.9, –4.2, –4.4; MS (ESI): mass calculated for $C_{46}H_{66}O_5Si_2$ $[M+NH_4]^+$, 773.18. Found 773.16.

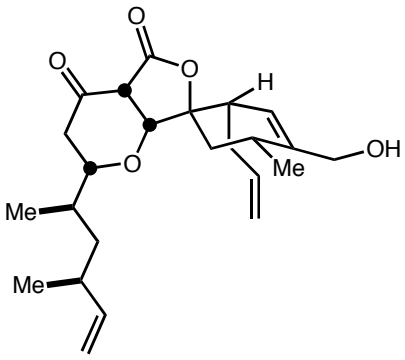

(**II-97**): To a solution of butenolide **II-91** (340 mg, 0.45 mmol) in THF (6 mL) was added AcOH (0.13 mL, 2.25 mmol). The reaction mixture was cooled to 0 °C and TBAF (1M in THF, 2.25 mL, 2.25 mmol) was added. The reaction was stirred for 5 hours at 0 °C then 5 hours at 23 °C. The reaction was quenched with saturated $NaHCO_3$ (8 mL). The aqueous layer was extracted with EtOAc (5 x 5 mL). The combined organic layers were dried over Na_2SO_4, filtered and concentrated. The residue was purified by flash column chromatography (50% EtOAc/hexanes) to afford pyranone **II-97** (45 mg, 25%) as a clear oil. Analytical data for **II-97**: $[\alpha]_D^{25}$ = – 109.5 (c 1.2, CH_2Cl_2); IR (film) 3525, 3075, 2959, 1773, 1718, 1641, 1454, 1292, 1178 cm^{-1}; ^{1}H NMR ($CDCl_3$, 500 MHz) δ 5.88-5.81 (ddd, J = 16.1, 11.2, 5.8, 1H), 5.80-5.79 (d, *J* = 4.3 Hz, 1H), 5.57-5.49 (ddd, *J* = 15.8, 10.1, 8.8 Hz, 1H), 5.10-5.07 (d, *J* = 16.1, 1H), 5.09-5.07 (d, *J* = 11.2 Hz, 1H), 4.99-4.96 (d, *J* = 15.8 Hz, 1H), 4.95-4.94 (d, *J* = 10.1, 1H), 4.23-

4.22 (d, *J* = 3.5 Hz, 1H), 4.17-4.15 (A of AB, *J* = 13.1 Hz, 1H), 4.09-4.07 (B of AB, *J* = 13.4 Hz, 1H), 3.70-3.69 (d, J = 3.5 Hz, 1H), 3.40-3.38 (ddd, *J* = 11.4, 11.4, 5.6, Hz, 1H), 2.70-2.65 (m, 2H), 2.55-2.54 (m, 1H), 2.45-2.42 (d, *J* = 11.4 Hz, 1H), 2.38-2.32 (d, *J* = 5.6 Hz, 1H), 2.20-2.18 (m, 1H), 1.91-1.85 (m, 1H), 1.73-1.69 (m, 2H), 1.53-1.47 (m, 2H), 1.11-1.09 (m, 1H), 1.10-1.09 (d, J = 7.0 Hz, 3H), 1.01-1.00 (d, *J* = 6.7 Hz, 3H), 0.91-0.90 (d, *J* = 7.0 Hz, 3H); ^{13}C NMR ($CDCl_3$, 500 MHz) δ 199.3, 169.5, 143.7, 140.7, 135.5, 123.6, 117.0, 114.0, 90.1, 80.4, 80.1, 64.9, 55.7, 43.1, 38.8, 38.7, 37.8, 35.8, 34.7, 28.2, 26.0, 22.1, 18.7, 15.0; MS (ESI): mass calculated for $C_{24}H_{34}O_5$ $[2M+Na]^+$, 827.4. Found 827.71.

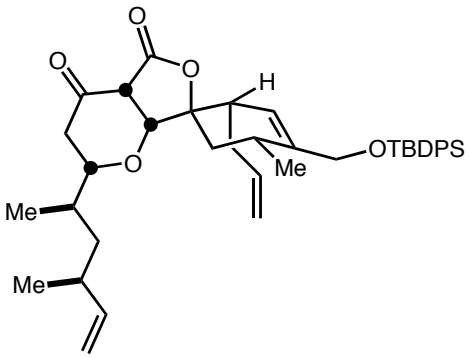

(**II-102**): To a solution of pyranone **II-97** (45 mg, 0.11 mmol) in CH_2Cl_2 (1.1 mL) was added imidazole (16 mg, 0.23 mmol) and TBDPSCl (0.17 mL, 2M solution). The reaction was stirred for 90 minutes at 23 °C. The reaction was quenched with saturated $NaHCO_3$ (5 mL). The aqueous layer was extracted with EtOAc (5 x 4 mL). The combined organic layers were dried over Na_2SO_4, filtered and concentrated. The residue was purified by flash column chromatography (50% EtOAc/hexanes) to afford pyranone **II-102** (43 mg, 60%) as a clear oil. Analytical data for **II-102**: $[\alpha]_D^{25}$ = – 94.9 (c 1.4, CH_2Cl_2); IR (film) 3071, 2958, 1719, 1641, 1459, 1427, 1294, 1203, 1177, 1074 cm^{-1}; ^{1}H NMR ($CDCl_3$, 500 MHz) δ 7.74–7.67 (m, 4H), 7.45-7.38 (m, 6H), 5.93-5.92 (d, *J* = 4.8, 1H), 5.90-5.82 (ddd, *J* = 15.2, 8.2, 5.8 Hz, 1H), 5.60-5.53 (ddd, *J* = 17.1, 9.4, 9.1 Hz, 1H), 5.12-5.09 (d,

J = 17.1, 1H), 5.10-5.08 (d, *J* = 9.4 Hz, 1H), 5.02-4.99 (d, *J* = 15.2 Hz, 1H), 4.99-4.97 (d, *J* = 8.2, 1H), 4.22 (d, *J* = 3.6 Hz, 1H), 4.19-4.17 (A of AB, *J* = 13.7 Hz, 1H), 4.16-4.13 (B of AB, *J* = 13.7 Hz, 1H), 3.69-3.68 (d, *J* = 3.6 Hz, 1H), 3.43-3.39 (ddd, *J* = 10.9, 10.2, 7.3, Hz, 1H), 2.77-2.76 (m, 1H), 2.71-2.69 (m, 1H), 2.51-2.48 (m, 1H), 2.46-2.44 (d, *J* = 7.3 Hz, 1H), 2.42-2.41 (d, *J* = 10.9 Hz, 1H), 2.25-2.18 (m, 1H), 1.95-1.88 (m, 1H), 1.77-1.72 (m, 1H), 1.69-1.66 (dd, J = 14.0, 5.4 Hz, 1H), 1.58-1.51 (m, 2H), 1.09-1.08 (m, 1H), 1.06 (s, 9H), 1.04-1.03 (d, J = 6.7 Hz, 3H), 1.01-1.00 (d, *J* = 7.0 Hz, 3H), 0.95-0.93 (d, *J* = 6.7 Hz, 3H); ^{13}C NMR ($CDCl_3$, 500 MHz) δ 199.4, 169.4, 143.7, 139.3, 135.7, 134.9, 133.8, 129.8, 127.8, 122.1, 116.8, 114.0, 90.0, 80.5, 80.2, 65.2, 55.9, 43.2, 38.8, 38.5, 37.9, 35.8, 35.7, 35.0, 28.5, 26.9, 22.1, 19.4, 18.8, 15.1; MS (ESI): mass calculated for $C_{40}H_{52}O_5Si$ $[M+NH_4]^+$, 658.21. Found 658.09.

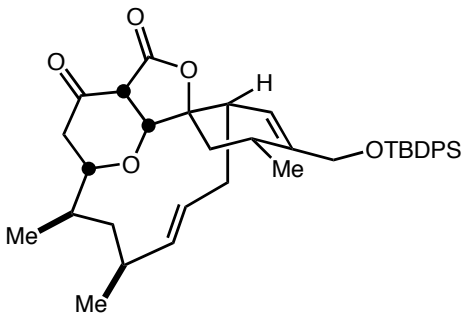

(**II-103**): To a solution of pyranone **II-102** (23 mg, 35.9 μmol) in CH_2Cl_2 (3 mL) was added Grubbs-2nd generation (9 mg, 10.6 μmol) in CH_2Cl_2 (0.5 mL). The reaction was warmed to 45 °C and allowed to stir for 4 hours. The reaction was cooled to 23 °C, passed through a short plug of SiO_2 (eluting with 60% EtOAc/hexanes) and concentrated. The residue was purified by flash column chromatography (15% EtOAc/hexanes) to afford tetracycle **II-103** (13.4 mg, 61%) as a clear oil. Analytical data for **II-103**: $[\alpha]_D^{25}$ = – 92.0 (c 0.6, CH_2Cl_2); IR (film) 2956, 1774, 1712, 1651, 1457, 1428, 1304, 1110 cm^{-1}; ^{1}H NMR ($CDCl_3$, 500 MHz) δ 7.71–7.69 (m, 4H), 7.45-7.39 (m, 6H), 5.92-5.91 (d, *J* = 4.2 Hz 1H), 5.56-5.51 (ddd, *J* = 18.6, 8.2, 7.9 Hz, 1H), 5.40-5.36 (dd, *J* = 18.6, 2.1 Hz,

1H), 4.19-4.16 (A of AB, *J* = 13.7 Hz, 1H), 4.15 (d, *J* = 3.6 Hz, 1H), 4.15-4.13 (B of AB, *J* = 13.7 Hz, 1H), 3.64-3.63 (d, *J* = 3.6 Hz, 1H), 3.24-3.19 (ddd, *J* = 11.2, 10.9, 1.8 Hz, 1H), 3.07-3.06 (m, 1H), 2.94-2.88 (m, 1H), 2.68-2.65 (dd, J = 15.8, 1.8 Hz, 1H), 2.61-2.48 (m, 1H), 2.34-2.29 (dd *J* = 15.8, 11.2 Hz, 1H), 2.23-2.19 (m, 1H), 1.79-1.75 (m, 1H), 1.73-1.69 (dd, *J* = 13.4, 5.8 Hz, 1H), 1.55-1.52 (m, 2H), 1.41-1.38 (m, 1H), 1.06 (s, 9H), 1.04-1.03 (d, *J* = 7.0 Hz, 3H), 1.03-1.01 (m, 1H), 1.01-1.00 (d, *J* = 6.7 Hz, 3H), 0.87-0.85 (d, *J* = 7.0 Hz, 3H); ^{13}C NMR ($CDCl_3$, 500 MHz) δ 199.0, 169.3, 142.4, 138.3, 135.7, 133.8, 129.8, 127.8, 124.2, 123.3, 90.4, 81.0, 79.5, 65.4, 55.8, 45.9, 45.2, 39.2, 38.6, 34.5, 32.8, 32.4, 28.7, 26.9, 22.5, 19.4, 18.9, 17.8; MS (ESI): mass calculated for $C_{38}H_{48}O_5Si$ $[M+NH_4]^+$, 630.87. Found 630.66.

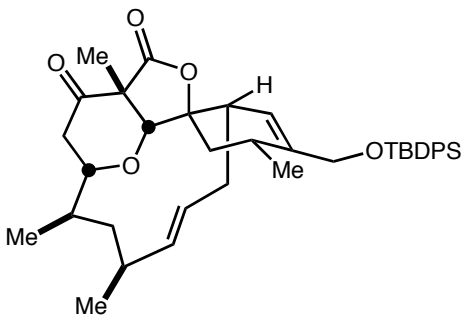

(**II-104**): To a solution of pyranone **II-103** (13.4 mg, 21.9 μmol) in MeCN (1.8 mL) was added K_2CO_3 (54 mg, 0.39 mmol) and MeI (66 μL, 2M solution in MeCN). The reaction was warmed to 70 °C and allowed to stir for 4 hours. The reaction was cooled to 23 °C, passed through a short plug of SiO_2 (eluting with 60% EtOAc/hexanes) and concentrated. The residue was purified by flash column chromatography (15% EtOAc/hexanes) to afford pyranone **II-104** (12 mg, 87%) as a clear oil. Analytical data for **II-104**: $[\alpha]_D^{25}$ = – 96.4 (c 0.5, CH_2Cl_2); IR (film) 2954, 1771, 1712, 1647, 1457, 1374, 1107 cm^{-1}; ^{1}H NMR ($CDCl_3$, 500 MHz) δ 7.72–7.69 (m, 4H), 7.45-7.38 (m, 6H), 5.93-5.91 (d, *J* = 5.4 Hz 1H), 5.60-5.55 (ddd, *J* = 18.3, 8.2, 7.6 Hz, 1H), 5.43-5.39 (dd, *J* = 18.3, 3.0 Hz, 1H), 4.19-4.17 (A of AB, *J* = 13.4 Hz, 1H), 4.15-4.13 (B of AB, *J* = 13.4

Hz, 1H), 3.90 (s, 1H), 3.33-3.29 (ddd, *J* = 11.2, 10.9, 2.7 Hz, 1H), 3.00 (m, 1H), 2.87-2.86 (m, 1H), 2.80-2.76 (dd, *J* = 16.7, 2.7 Hz, 1H), 2.63-2.58 (m, 1H), 2.50-2.42 (m, 1H), 2.40-2.35 (dd *J* = 16.7, 10.9 Hz, 1H), 2.09-2.05 (dd, *J* = 13.4, 5.8 Hz, 1H), 1.99-1.93 (m, 1H), 1.70-1.68 (m, 1H), 1.67 (s, 3H), 1.66 (m, 1H), 1.20 (m, 1H), 1.06 (s, 9H), 1.04-1.03 (d, *J* = 7.0 Hz, 3H), 1.03-1.02 (m, 1H), 1.01-1.00 (d, *J* = 6.7 Hz, 3H), 0.88-0.87 (d, *J* = 6.4 Hz, 3H); ^{13}C NMR ($CDCl_3$, 500 MHz) δ 200.7, 172.8, 141.7, 138.2, 135.7, 133.9, 129.8, 127.8, 124.6, 124.4, 89.9, 85.2, 81.1, 65.5, 57.8, 45.0, 44.3, 39.9, 39.8, 36.5, 33.5, 32.7, 28.9, 26.9, 21.9, 20.2, 19.4, 19.0, 18.4; MS (ESI): mass calculated for $C_{39}H_{50}O_5Si$ $[M+NH_4]^+$, 644.34. Found 644.69.

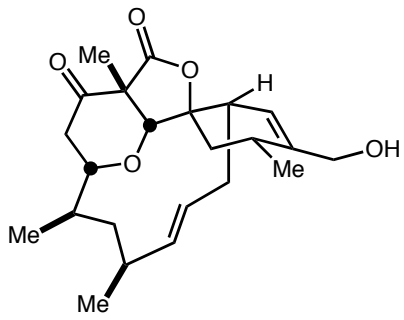

(**II-114**): To a 0 °C solution of pyranone **II-104** (12 mg, 19.2 μmol) in THF (0.4 mL) was added HF•pyridine (0.10 mL, 1.2 mmol). The reaction was warmed to 23 °C and allowed to stir for 2 hours. The reaction was quenched with saturated $NaHCO_3$ (3 mL) and the aqueous layer was extracted with EtOAc (3 x 4 mL). The combined organics were dried over Na_2SO_4, filtered and concentrated. The residue was purified by flash column chromatography (40% EtOAc/hexanes) to afford pyranone **II-114** (7 mg, 95%) as a clear oil. Analytical data for **II-114**: $[\alpha]_D^{25}$ = – 118.8 (c 0.25, CH_2Cl_2); IR (film) 3741, 2924, 1766, 1699, 1647, 1507, 1457, 1196 cm^{-1}; ^{1}H NMR ($CDCl_3$, 500 MHz) δ 5.87-5.86 (d, *J* = 5.2 Hz 1H), 5.62-5.57 (ddd, *J* = 18.3, 8.2, 7.6 Hz, 1H), 5.45-5.42 (dd, *J* = 18.3, 3.0 Hz, 1H), 4.19-4.17 (A of AB, *J* = 13.4 Hz, 1H), 4.10-4.08 (B of AB, *J* = 13.4 Hz, 1H), 3.93 (s, 1H), 3.34-3.30 (ddd, *J* = 11.2, 10.9, 2.7 Hz, 1H), 2.98 (m, 1H), 2.87-2.85 (m, 1H),

2.81-2.77 (dd, *J* = 16.7, 2.7 Hz, 1H), 2.66-2.62 (m, 1H), 2.50-2.49 (m, 1H), 2.40-2.35 (dd *J* = 16.7, 10.9 Hz, 1H), 2.10-2.08 (dd, *J* = 13.4, 5.8 Hz, 1H), 1.97-1.91 (m, 1H), 1.70-1.68 (m, 2H), 1.67 (s, 3H), 1.29-1.19 (m, 2H), 1.14-1.13 (d, *J* = 6.7 Hz, 3H), 1.01-1.00 (d, *J* = 6.7 Hz, 3H), 0.89-0.87 (d, *J* = 6.4 Hz, 3H); ^{13}C NMR ($CDCl_3$, 500 MHz) δ 200.4, 172.8, 141.8, 139.4, 125.6, 124.6, 89.7, 85.2, 81.2, 65.0, 57.7, 44.9, 44.1, 40.0, 39.9, 36.2, 33.3, 32.7, 28.6, 21.8, 20.3, 18.8, 18.4; MS (ESI): mass calculated for $C_{23}H_{32}O_5$ $[M+NH_4]^+$, 406.22. Found 406.56.

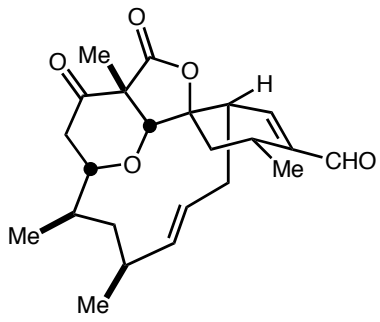

(**II-115**): To a 0 °C solution of alcohol **II-114** (7 mg, 18 μmol) in CH_2Cl_2 (0.30 mL) was added Dess-Martin Periodinane (19 mg, 45 μmol). The reaction was warmed to 23 °C and allowed to stir for 90 minutes. The reaction was quenched with saturated $NaHCO_3$ (1 mL) and 10% Na_2SO_3 (1 mL). After stirring for 20 minutes the aqueous layer was extracted with EtOAc (3 x 4 mL). The combined organics were dried over Na_2SO_4, filtered and concentrated. The residue was purified by flash column chromatography (20% EtOAc/hexanes) to afford pyranone **II-115** (6 mg, 87%) as a yellow oil. Analytical data for **II-115**: $[\alpha]_D^{25}$ = – 119.6 (c 0.25, CH_2Cl_2); IR (film) 2958, 1771, 1712, 1687, 1456, 1374, 1179, 1088 cm^{-1}; ^{1}H NMR ($CDCl_3$, 500 MHz) δ 9.41 (s, 1H), 6.87-6.86 (d, *J* = 4.8 Hz, 1H), 5.61-5.57 (ddd, *J* = 18.3, 8.2, 7.6 Hz, 1H), 5.53-5.49 (dd, *J* = 18.3, 3.0 Hz, 1H), 3.98 (s, 1H), 3.36-3.31 (ddd, *J* = 11.2, 10.9, 2.7 Hz, 1H), 2.86-2.85 (m, 2H), 2.80-2.76 (dd, *J* = 16.7, 2.7 Hz, 1H), 2.51-2.47 (m, 2H), 2.40-2.35 (dd *J* = 16.7, 10.9 Hz, 1H), 2.25-2.20 (dd, *J* = 13.4, 5.8 Hz, 1H), 2.17-2.11 (m, 1H), 1.68-1.65 (m, 2H), 1.67 (s, 3H), 1.31-

1.22 (m, 2H), 1.27-1.26 (d, J = 7.0 Hz, 3H), 1.04-1.02 (d, J = 6.7 Hz, 3H), 0.90-0.88 (d, J = 6.7 Hz, 3H); ^{13}C NMR ($CDCl_3$, 500 MHz) δ 199.9, 193.6, 171.0, 152.3, 143.3, 143.1, 122.9, 88.8, 84.9, 81.1, 57.5, 44.9, 44.4, 41.0, 39.9, 36.0, 33.0, 31.9, 26.6, 22.0, 20.1, 19.3, 18.3; MS (ESI): mass calculated for $C_{23}H_{30}O_5$ $[2M+Na]^+$, 795.4. Found 795.31.

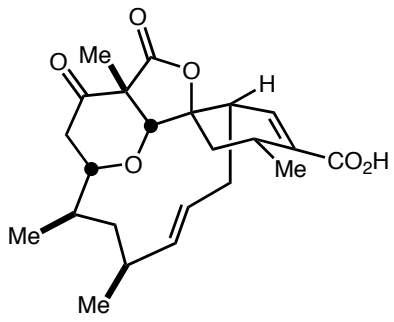

(**II-116**): To a 0 °C solution of aldehyde **II-115** (6 mg, 15.5 μmol) in *t*-BuOH/H_2O (5/1) (0.6 mL) was added 2-methyl-2-butene (75 μL, 0.7 mmol), NaH_2PO_4 (28 mg, 0.2 mmol) and $NaClO_2$ (42 mg, 0.36 mmol). The reaction was allowed to stir at 0 °C for 1 hour before being warmed to 23 °C for 90 minutes. The reaction was quenched with saturated NH_4Cl (3 mL). The aqueous layer was extracted with EtOAc (3 x 4 mL). The combined organics were dried over Na_2SO_4, filtered and concentrated. The residue was purified by flash column chromatography (20/1 $CHCl_3$/MeOH) to afford carboxylic acid **II-116** (3.9 g, 64%) as a white foam. Analytical data for **II-116**: $[\alpha]_D^{25}$ = – 177.8 (c 0.23, CH_2Cl_2); IR (film) 2923, 1769, 1716, 1686, 1639, 1455, 1376, 1278, 1192, 1078 cm^{-1}; ^{1}H NMR ($CDCl_3$, 500 MHz) δ 7.14-7.12 (d, J = 4.8 Hz, 1H), 5.62-5.58 (ddd, J = 18.3, 8.2, 7.6 Hz, 1H), 5.49-5.45 (dd, J = 18.3, 3.0 Hz, 1H), 3.96 (s, 1H), 3.33-3.29 (ddd, J = 11.2, 10.9, 2.7 Hz, 1H), 3.22 (m, 1H), 2.91-2.85 (m, 2H), 2.79-2.75 (dd, J = 16.7, 2.7 Hz, 1H), 2.45-2.40 (m, 1H), 2.39-2.33 (dd J = 16.7, 10.9 Hz, 1H), 2.25-2.21 (dd, J = 13.4, 5.8 Hz, 1H), 2.15-2.11 (m, 1H), 1.70-1.6 (m, 2H), 1.67 (s, 3H), 1.29-1.20 (m, 2H), 1.26-1.22 (d, J = 7.3 Hz, 3H), 1.02-1.02 (d, J = 6.7 Hz, 3H), 0.88-0.87 (d, J = 6.4 Hz, 3H); ^{13}C NMR ($CDCl_3$, 500 MHz) δ 200.1, 172.4, 171.4, 142.9, 142.8, 133.0, 123.2, 89.0, 84.9, 81.0,

57.7, 44.9, 44.6, 40.4, 39.9, 36.2, 32.9, 32.0, 28.0, 22.1, 20.3, 20.1, 18.4; MS (ESI): mass calculated for $C_{23}H_{30}O_6$ $[2M+Na]^+$, 827.4. Found 827.72.

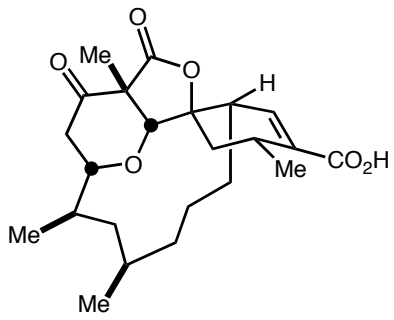

(**II-131**): To a heterogenous solution of PtO_2 (0.9 mg, 3.9 μmol) in EtOAc (0.30 mL) was added a H_2 (balloon) for 2 minutes. After 2 minutes, the PtO_2 had turned black in color indicating it was activated. A solution of carboxylic acid **II-116** (3.9 mg, 9.7 μmol) in EtOAc (0.4 mL) was added via cannula to the PtO_2 solution. The reaction was allowed to stir at 23 °C under an atmosphere of H_2 (balloon) for 50 minutes. The reaction was filtered through Celite (eluting with EtOAc) and the filtrate was concentrated. The residue was purified by flash column chromatography (20/1 $CHCl_3$/MeOH) to afford carboxylic acid **II-131** (2.8 mg, 71%) as a white foam. Analytical data for **II-131**: $[\alpha]_D^{25}$ = – 132.2 (c 0.09, CH_2Cl_2); IR (film) 3741, 2921, 1766, 1686, 1647, 1554, 1456, 1274, 1199, 1080 cm^{-1}; ^1H NMR ($CDCl_3$, 500 MHz) δ 7.17-7.15 (d, *J* = 5.8 Hz, 1H), 3.99 (s, 1H), 3.22-3.17 (dd, *J* = 11.9, 10.6 Hz, 1H), 2.91-2.90 (m, 1H), 2.85-2.83 (m, 1H), 2.72-2.69 (d, *J* = 15.8 Hz, 1H), 2.39-2.33 (dd *J* = 15.8, 11.9 Hz, 1H), 2.20-2.17 (dd, *J* = 13.4, 5.8 Hz, 1H), 1.97-1.95 (m, 1H), 1.87-1.81 (m, 1H), 1.81-1.78 (m, 1H), 1.72-1.69 (m, 1H), 1.67 (s, 3H), 1.59-1.55 (m, 2H), 1.44-1.42 (m, 1H), 1.30-1.29 (m, 2H), 1.23-1.22 (d, *J* = 6.4 Hz, 3H), 1.17-1.14 (m, 1H), 0.95-0.94 (d, *J* = 7.0 Hz, 3H), 0.90-0.88 (d, *J* = 6.4 Hz, 3H); ^{13}C NMR ($CDCl_3$, 500 MHz) δ 200.1, 172.3, 170.7, 143.0, 132.6, 89.6, 85.5, 81.6, 57.5, 44.6, 43.6, 39.5, 38.4, 36.7, 33.5, 33.1, 29.8, 28.4, 27.8, 21.0, 20.6, 20.3, 18.2; MS (ESI): mass calculated for $C_{23}H_{32}O_6$ $[2M+Na]^+$, 831.41. Found 831.63.

2.13.7 Select NMR Spectra

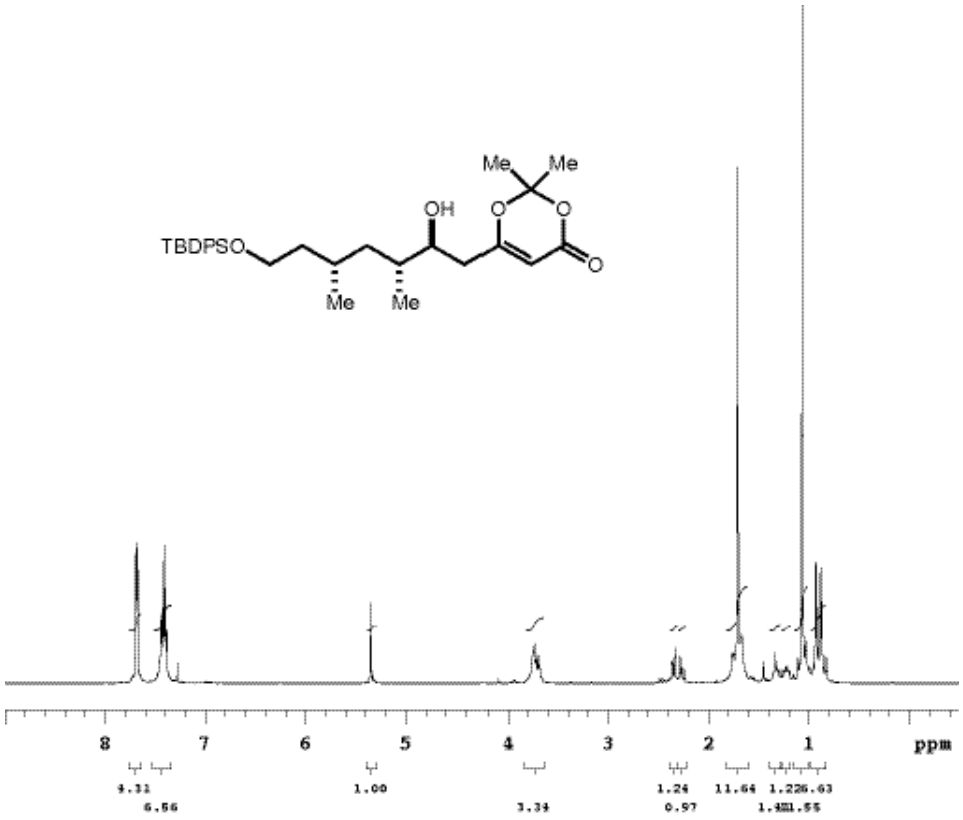

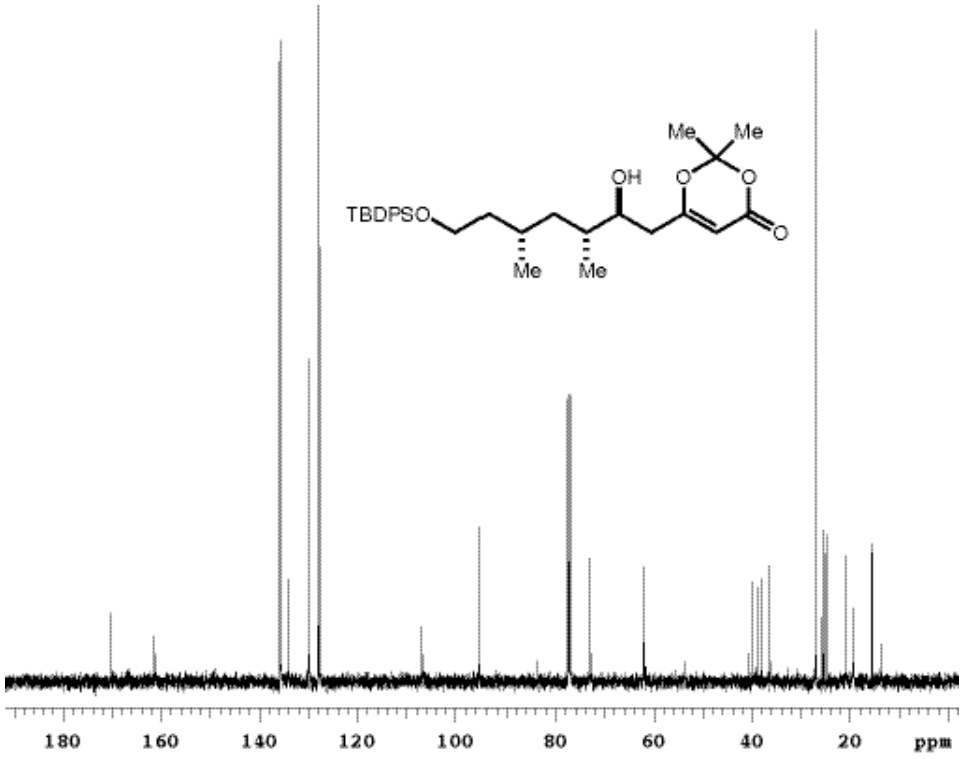

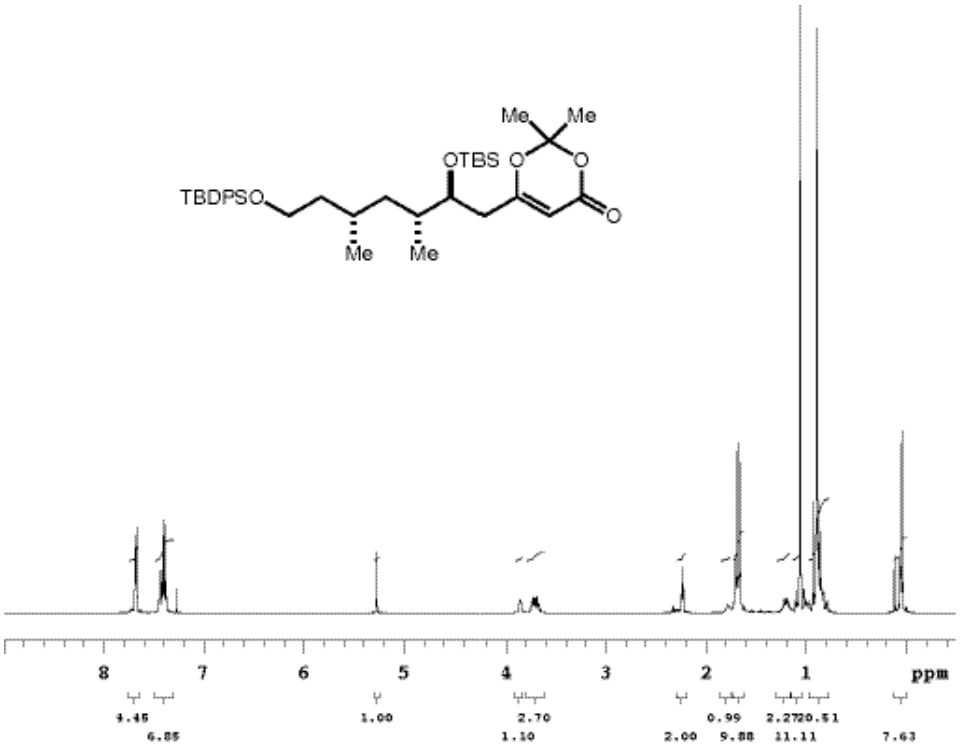
Me
Me
OTBS
O
O
TBDPSO
O
Me
Me
8
7
6
5
4
3
2
1
ppm
9.45
6.85
1.00
2.70
1.10
2.00
0.99
5.88
2.27
20.51
11.11
7.63

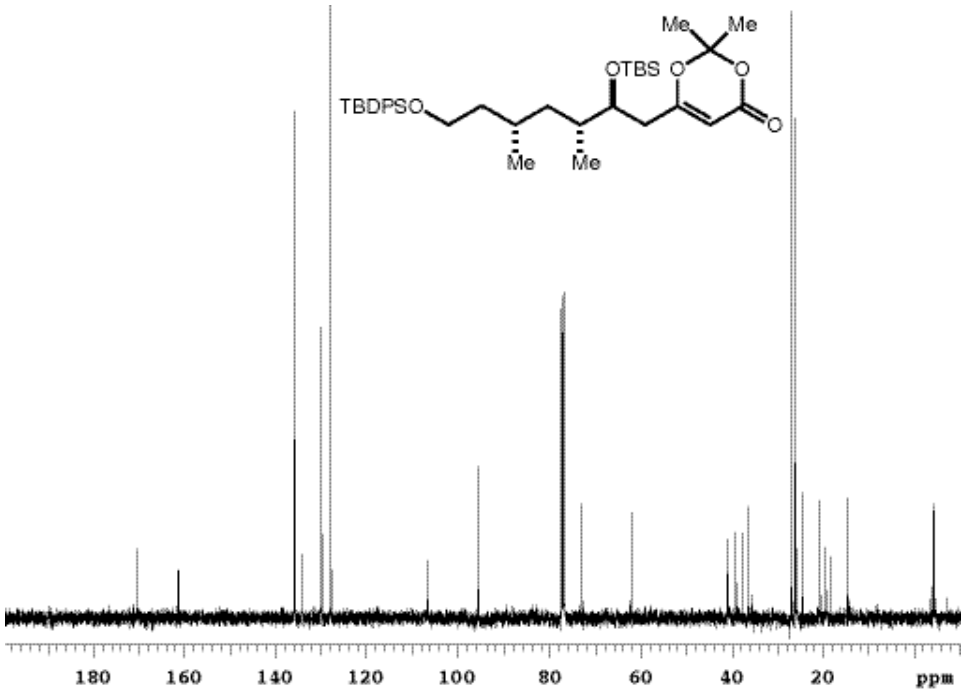
Me
Me
OTBS
O
O
TBDPSO
O
Me
Me
180
160
140
120
100
80
60
40
20
ppm

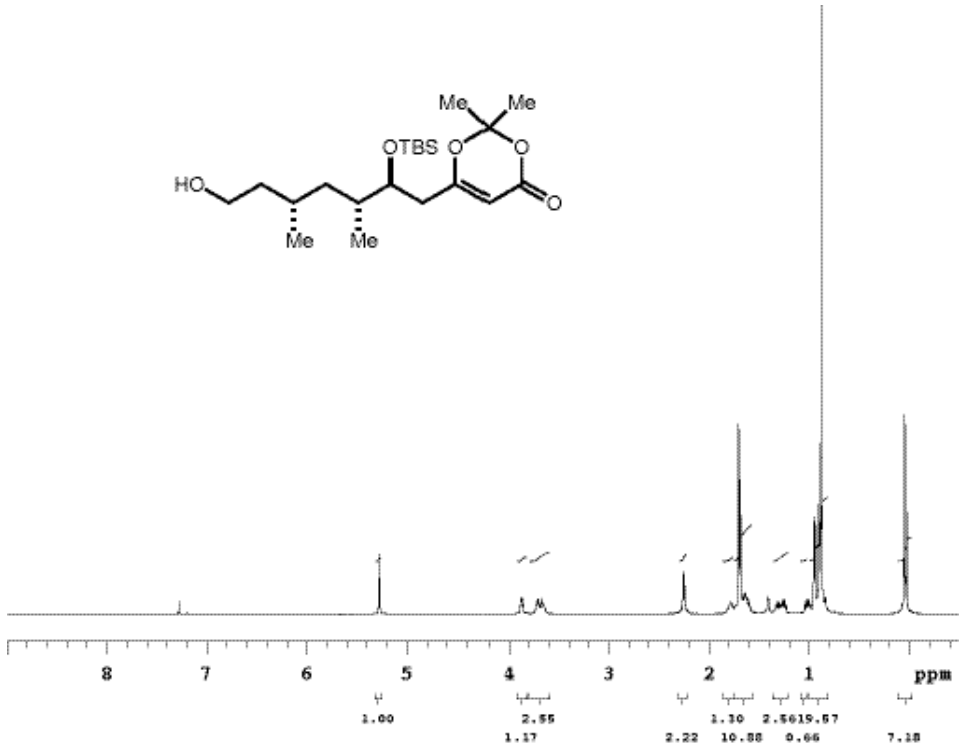
Me
Me
OTBS
O
O
HO
O
Me
Me
8
7
6
5
4
3
2
1
ppm
1.00
2.55
1.17
2.22
1.30
10.88
2.56
19.57
0.66
7.18

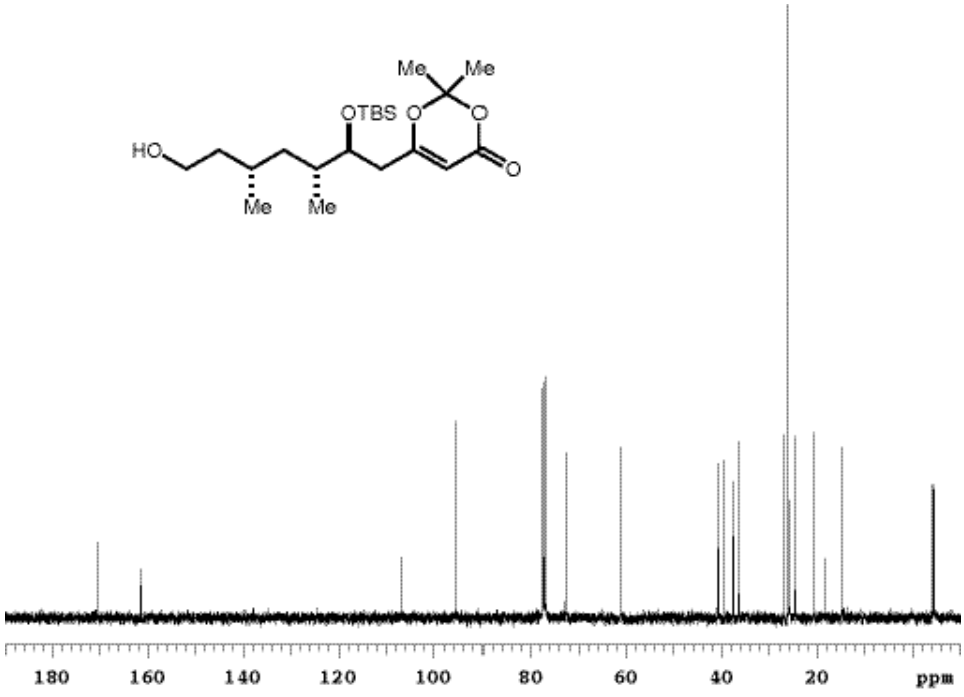
Me
Me
OTBS
O
O
HO
O
Me
Me
180
160
140
120
100
80
60
40
20
ppm

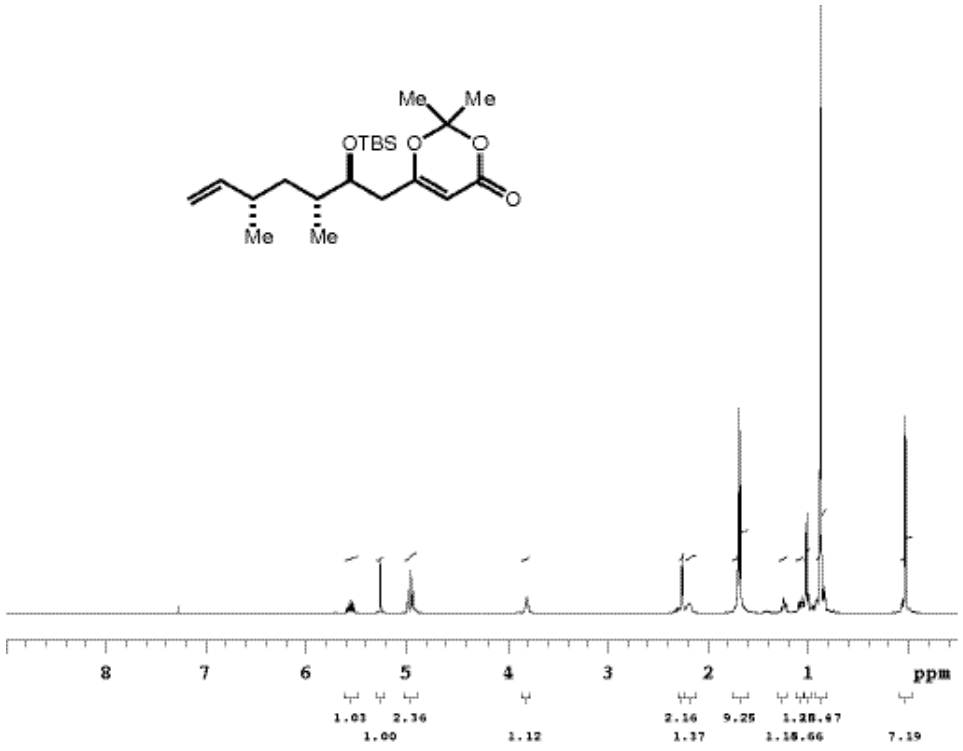
Me
Me
OTBS
O
O
O
Me
Me
8
7
6
5
4
3
2
1
ppm
1.03
2.36
1.00
1.12
2.16
1.37
9.25
1.28.67
1.18.66
7.19

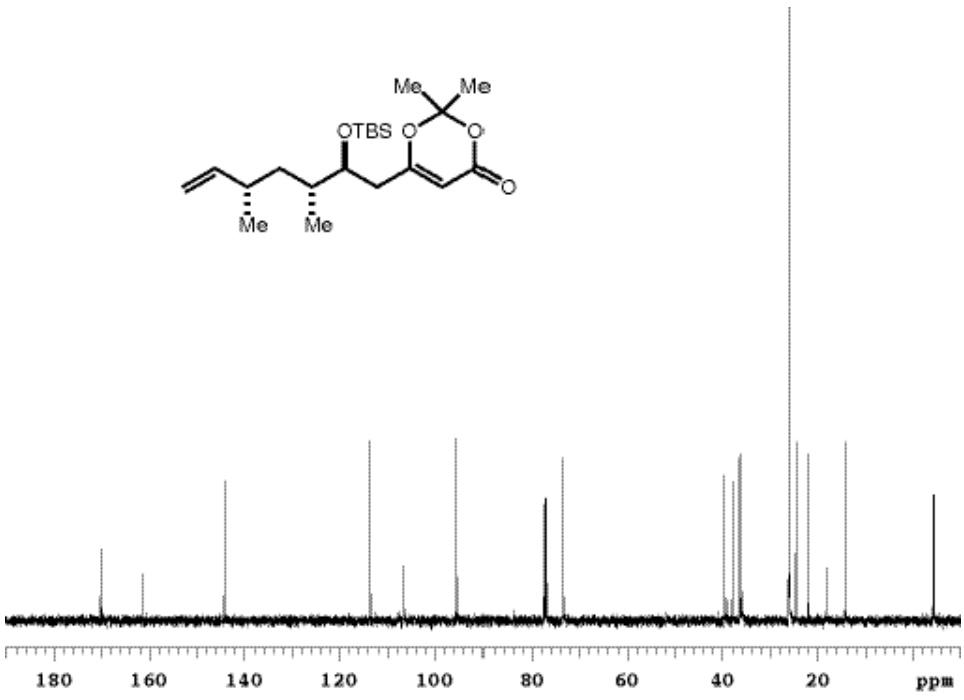
Me
Me
OTBS
O
O
O
Me
Me
180
160
140
120
100
80
60
40
20
ppm

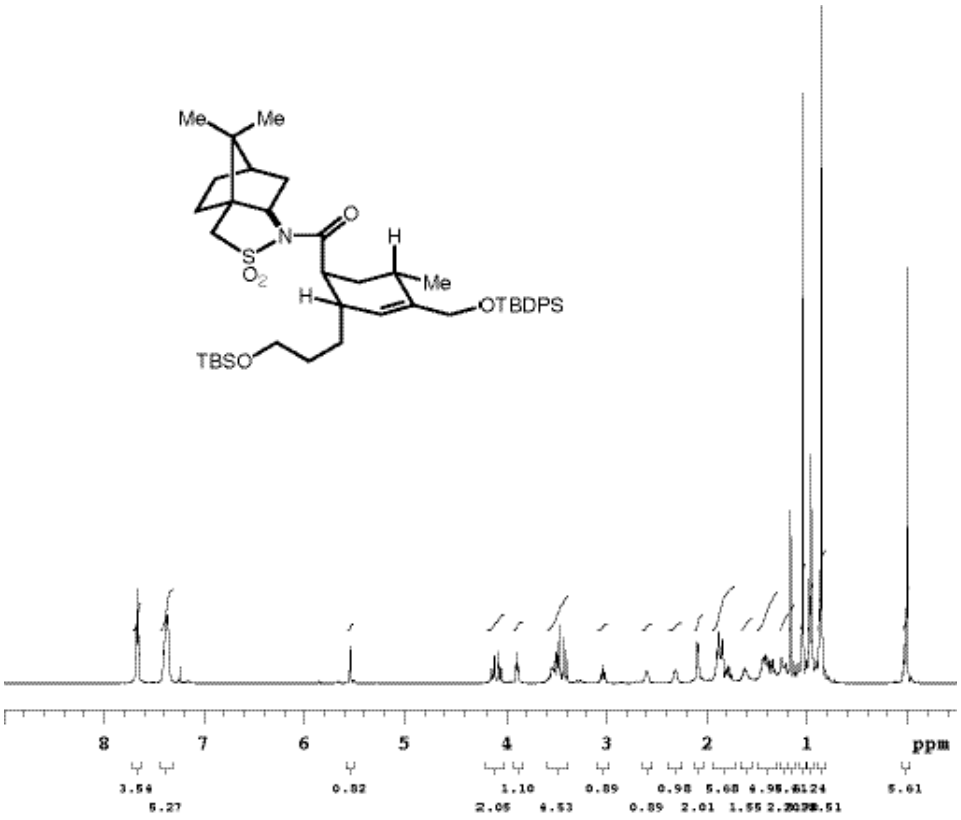
Me
Me
O
N
S
O2
H
Me
H
OTBDPS
TBSO
8
7
6
5
4
3
2
1
ppm

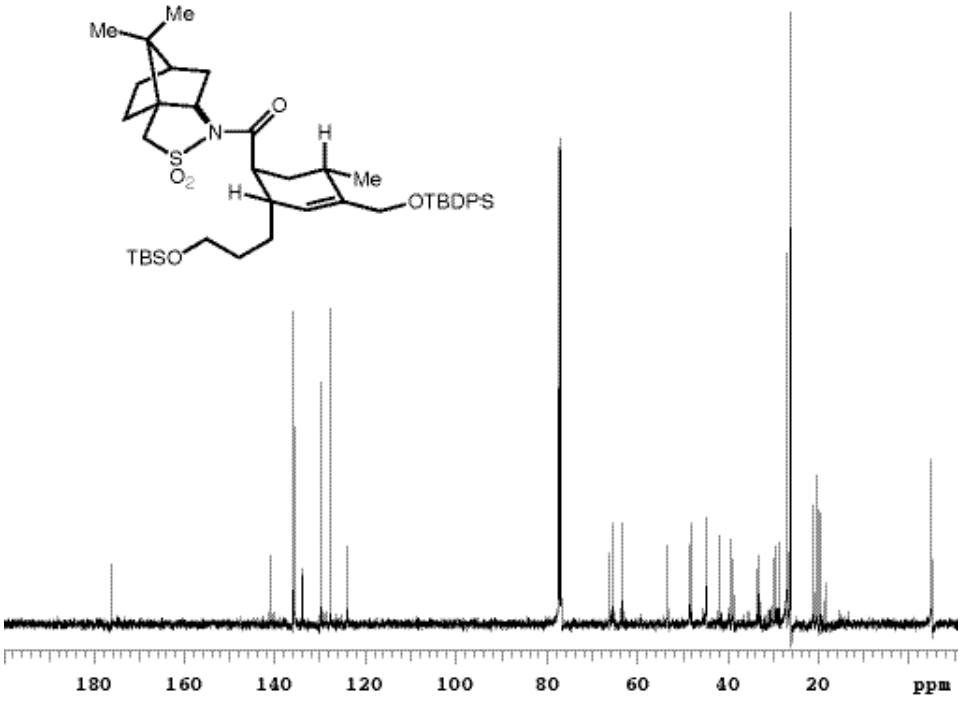
Me
Me
O
N
S
O2
H
Me
H
OTBDPS
TBSO
180
160
140
120
100
80
60
40
20
ppm

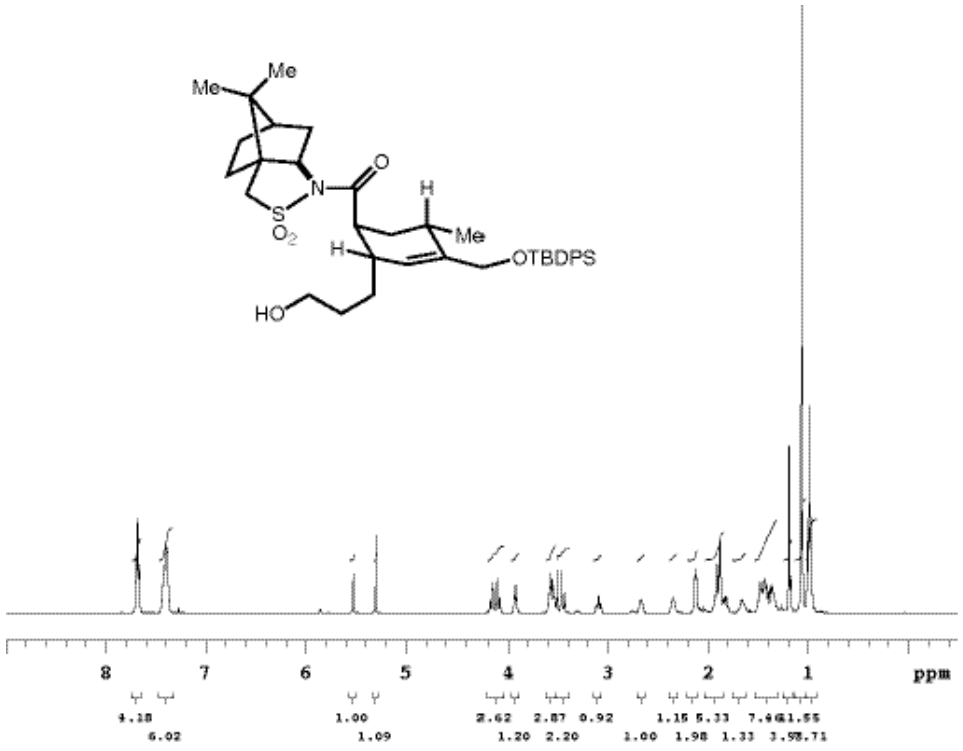
Me
Me
O
N
S
O2
H
Me
H
OTBDPS
HO
8
7
6
5
4
3
2
1
ppm
9.18
6.02
1.00
1.09
2.62
1.20
2.87
2.20
0.92
1.00
1.15
1.98
5.33
1.33
7.46
3.98
1.55
1.71

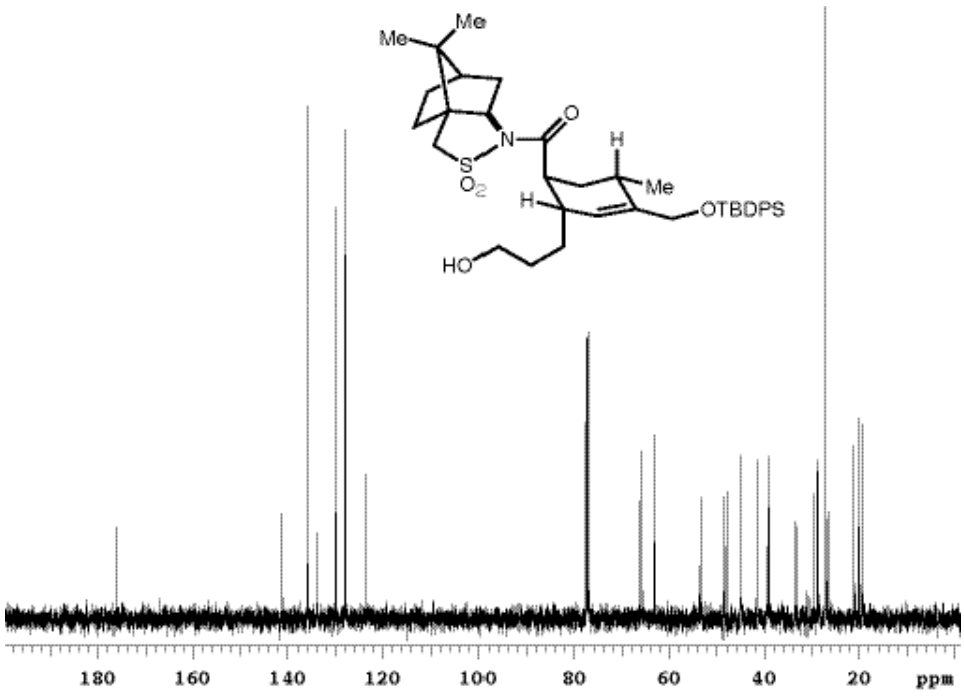
Me
Me
O
N
S
O2
H
Me
H
OTBDPS
HO
180
160
140
120
100
80
60
40
20
ppm

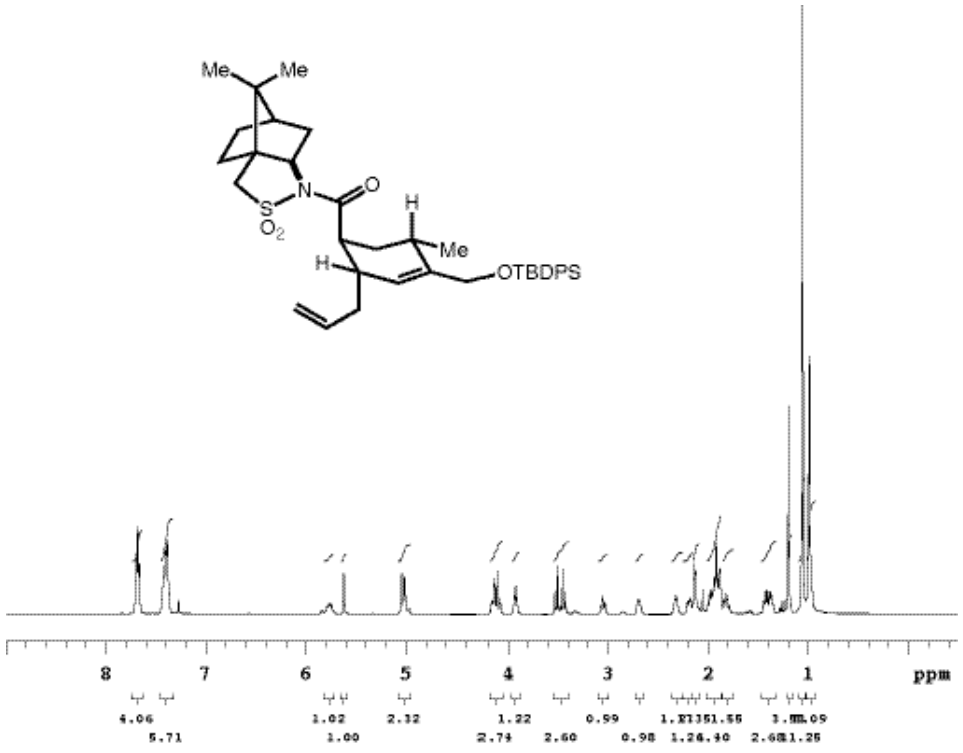
Me
Me
O
N
S
O2
H
Me
H
OTBDPS
8
7
6
5
4
3
2
1
ppm

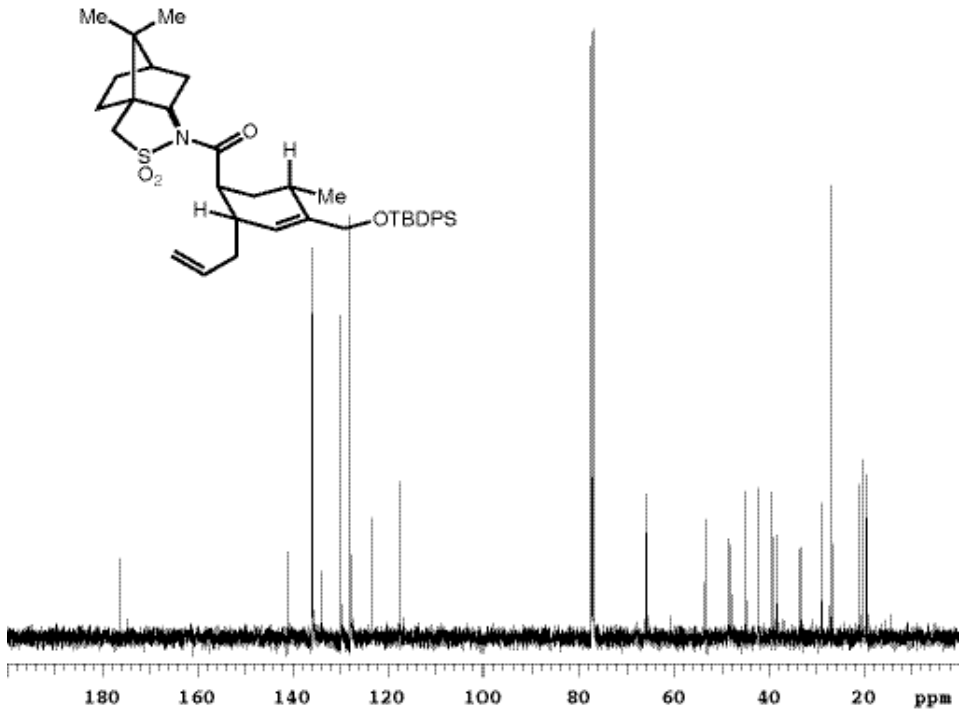
Me
Me
O
N
S
O2
H
Me
H
OTBDPS
180
160
140
120
100
80
60
40
20
ppm

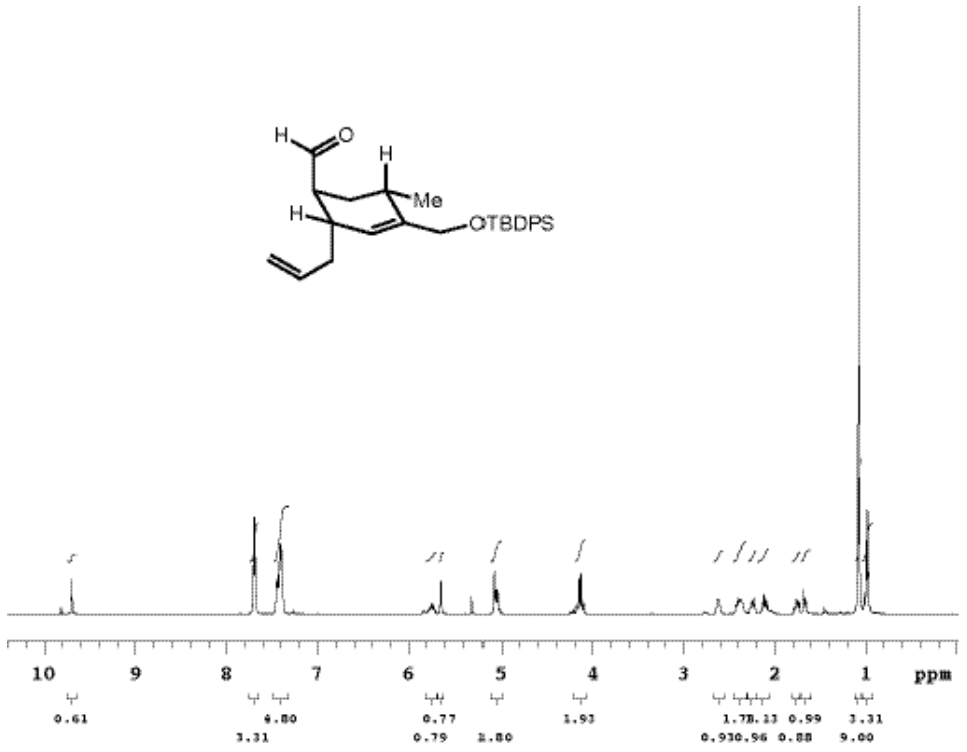
H
O
H
Me
H
OTBDPS
10
9
8
7
6
5
4
3
2
1
ppm
0.61
4.80
3.31
0.77
0.79
2.80
1.93
1.78
3.13
0.99
0.93
0.96
0.88
3.31
9.00

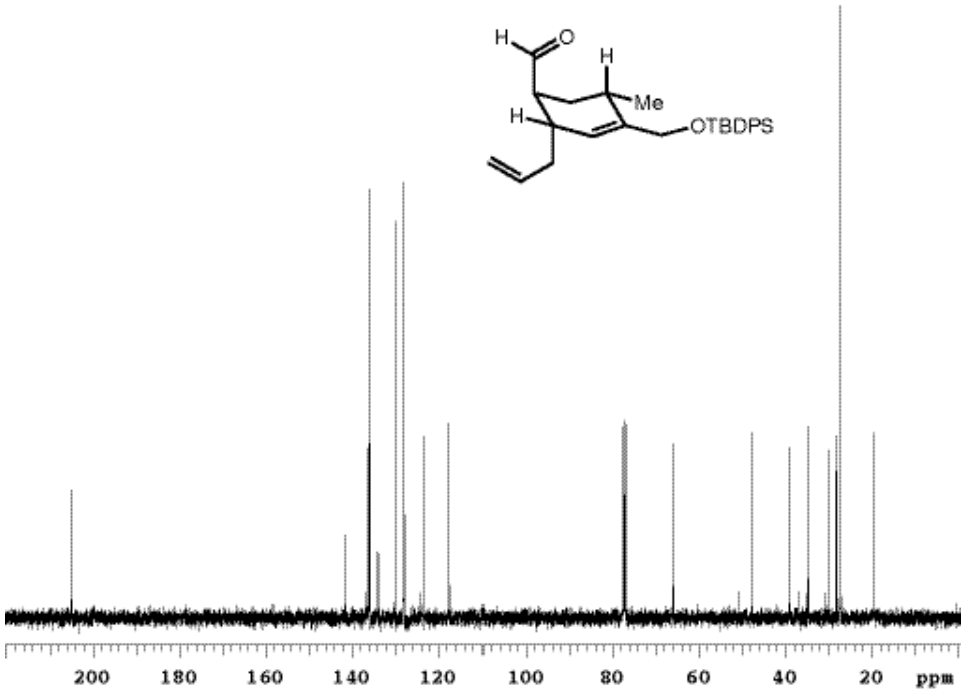
H
O
H
Me
H
OTBDPS
200
180
160
140
120
100
80
60
40
20
ppm

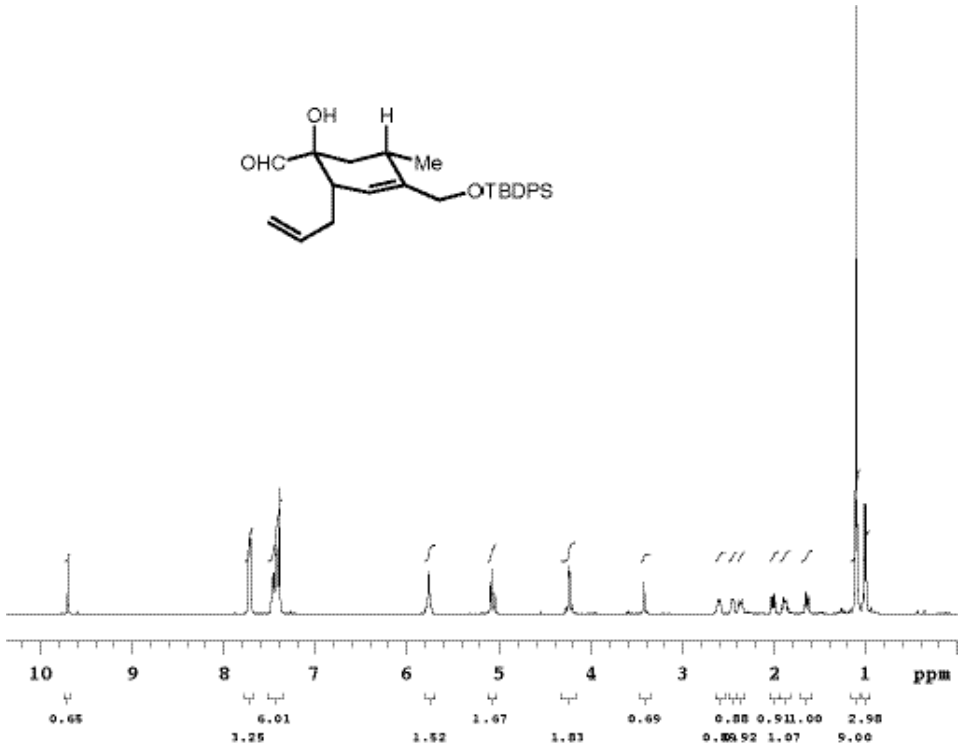
OH
H
OHC
Me
OTBDPS
10
9
8
7
6
5
4
3
2
1
ppm
0.65
6.01
3.25
1.52
1.67
1.83
0.69
0.88
0.92
1.07
1.00
2.98
5.00

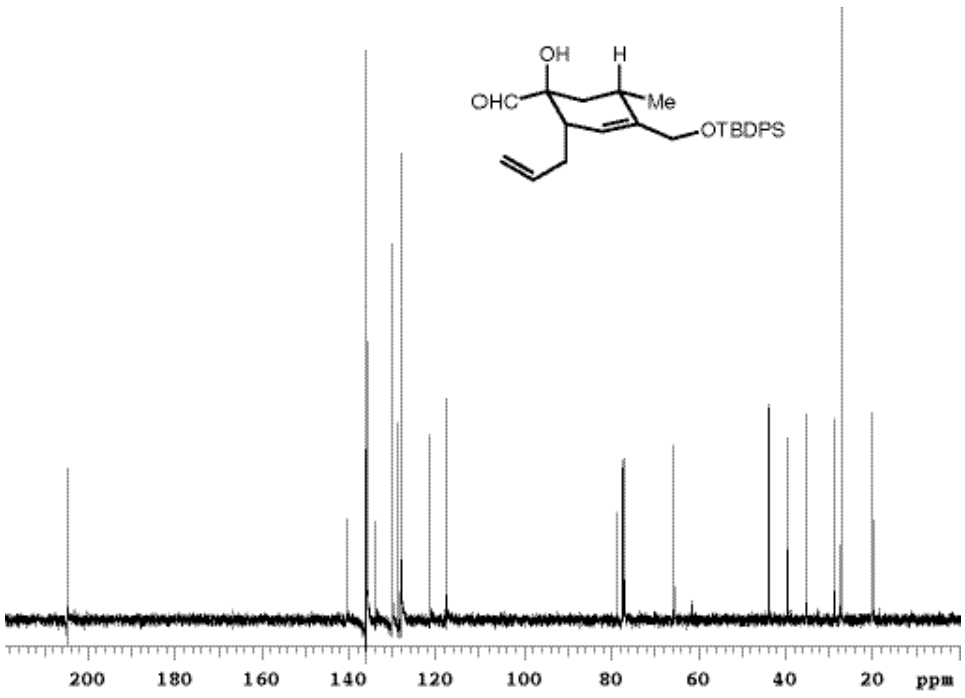
OH
H
OHC
Me
OTBDPS
200
180
160
140
120
100
80
60
40
20
ppm

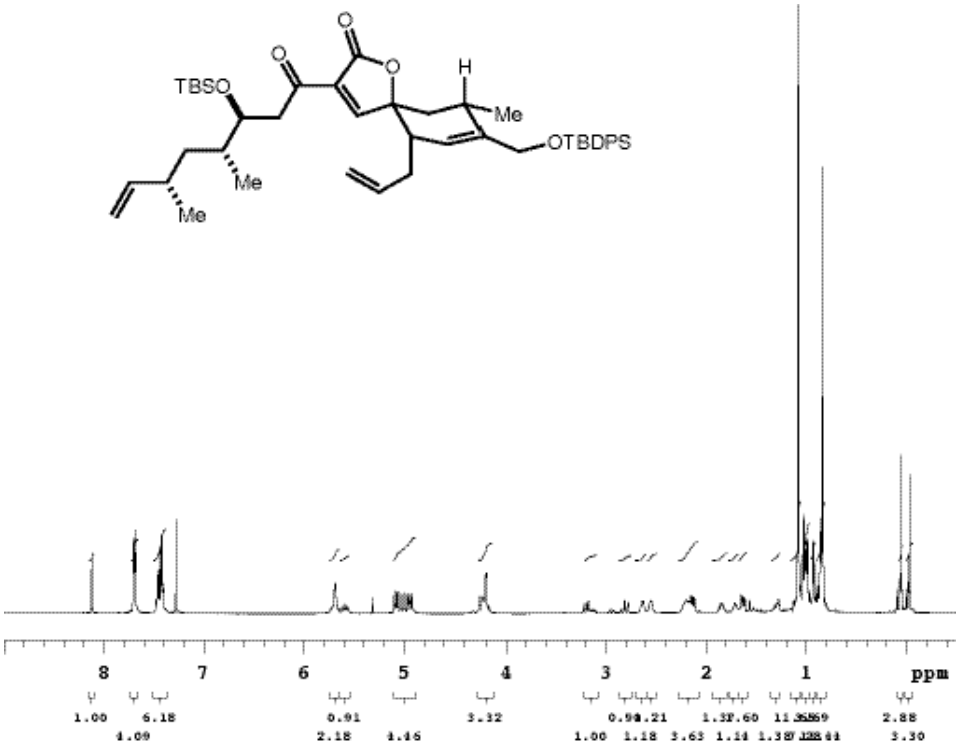
TBSO
O
O
O
H
Me
OTBDPS
Me
Me
8
7
6
5
4
3
2
1
ppm

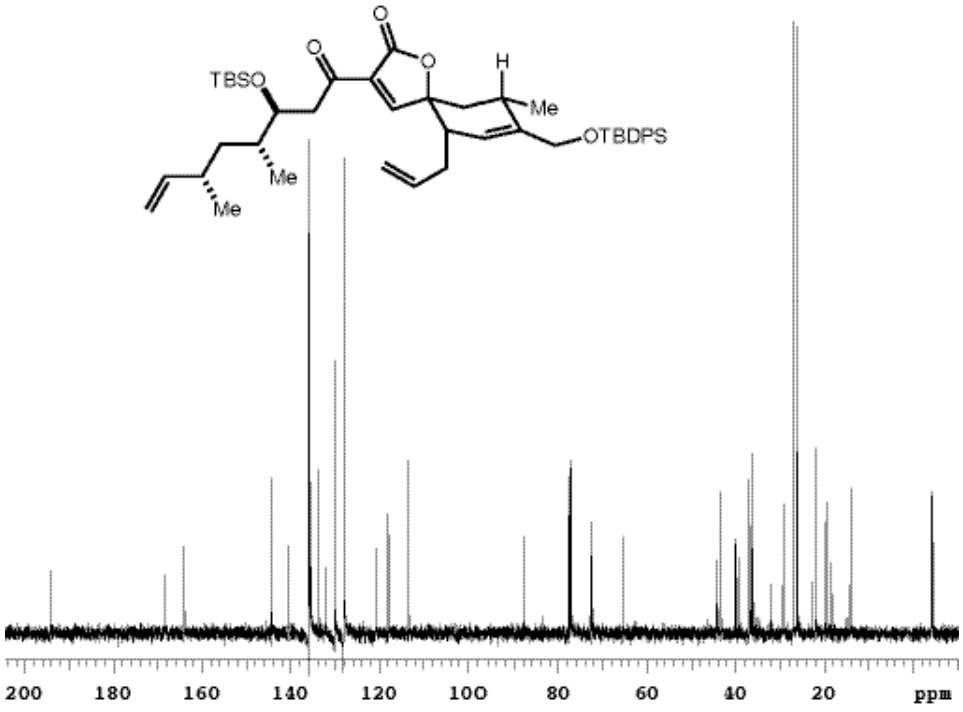
TBSO
O
O
O
H
Me
OTBDPS
Me
Me
200
180
160
140
120
100
80
60
40
20
ppm

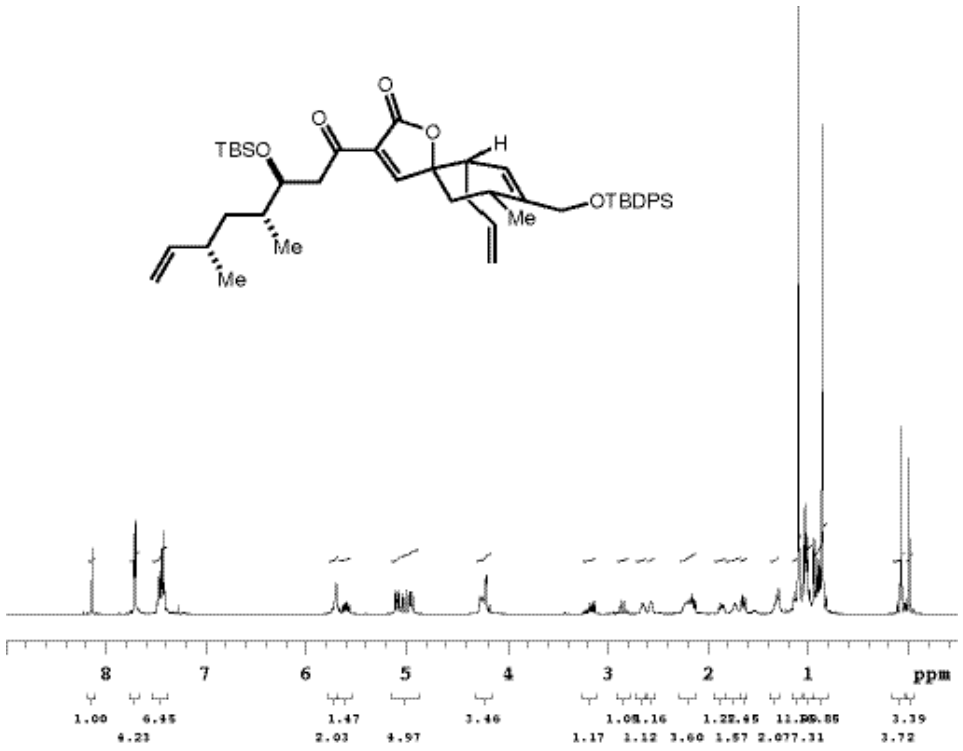
TBSO
O
O
O
H
Me
Me
Me
OTBDPS
8
7
6
5
4
3
2
1
ppm

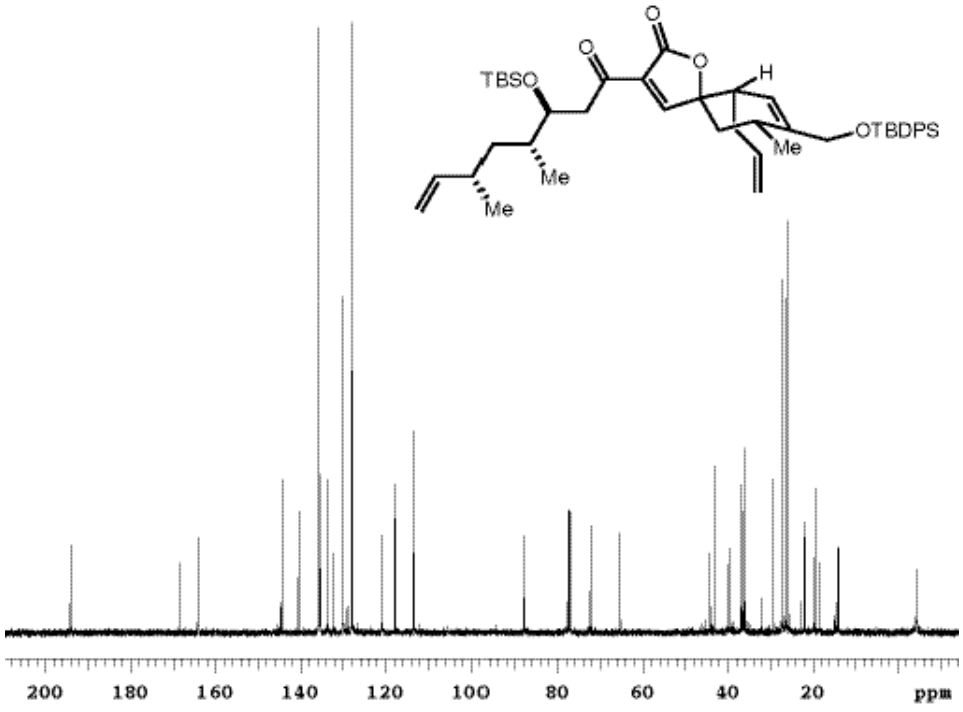
TBSO
O
O
O
H
Me
Me
Me
OTBDPS
200
180
160
140
120
100
80
60
40
20
ppm

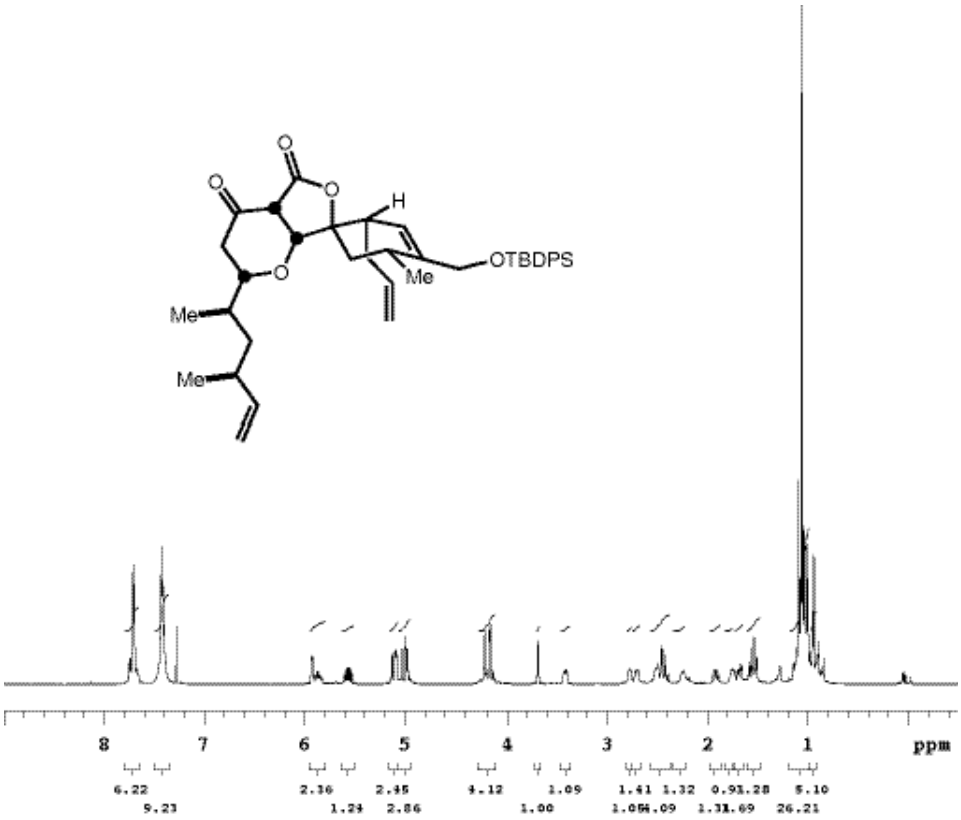
H
OTBDPS
Me
Me
Me
8
7
6
5
4
3
2
1
ppm
6.22
9.23
2.36
1.29
2.85
2.86
4.12
1.00
1.09
1.41
1.32
0.93
1.28
5.10
26.21

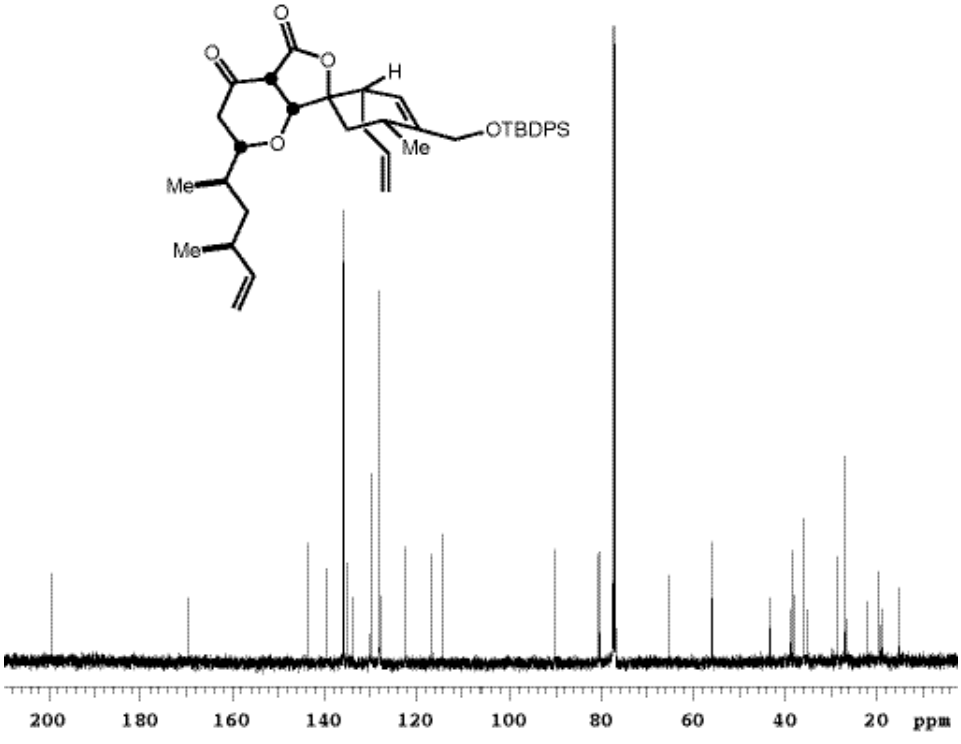
H
OTBDPS
Me
Me
Me
200
180
160
140
120
100
80
60
40
20
ppm

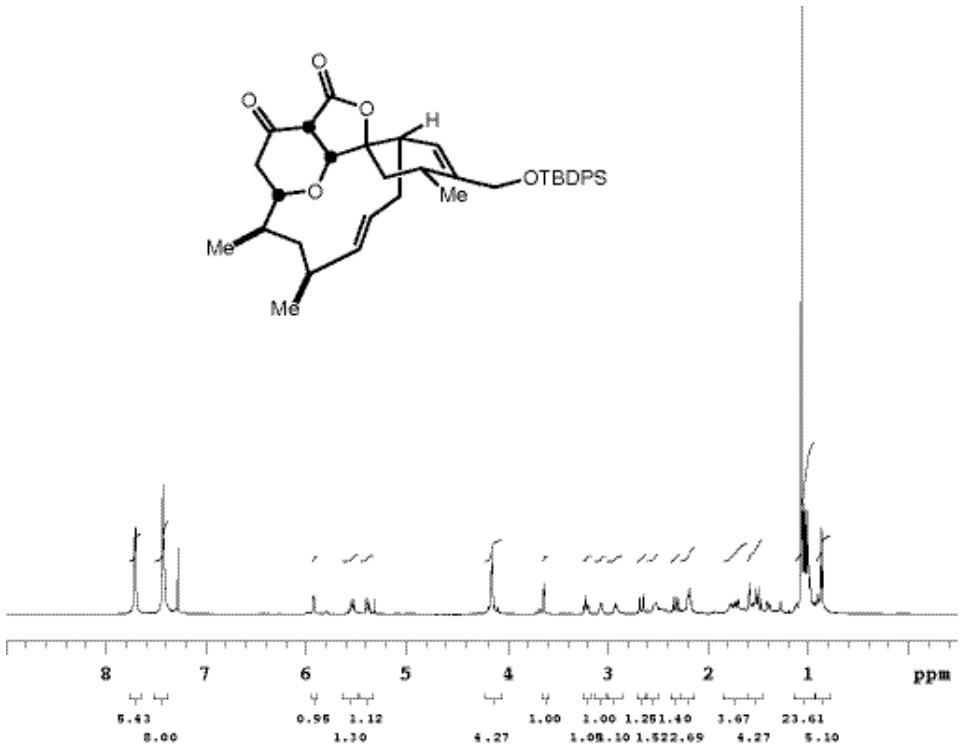
O
O
O
O
H
OTBDPS
Me
Me
Me
8
7
6
5
4
3
2
1
ppm
5.43
8.00
0.95
1.12
1.30
4.27
1.00
1.00
1.08
1.10
1.25
1.52
1.40
2.69
3.67
4.27
23.61
5.10

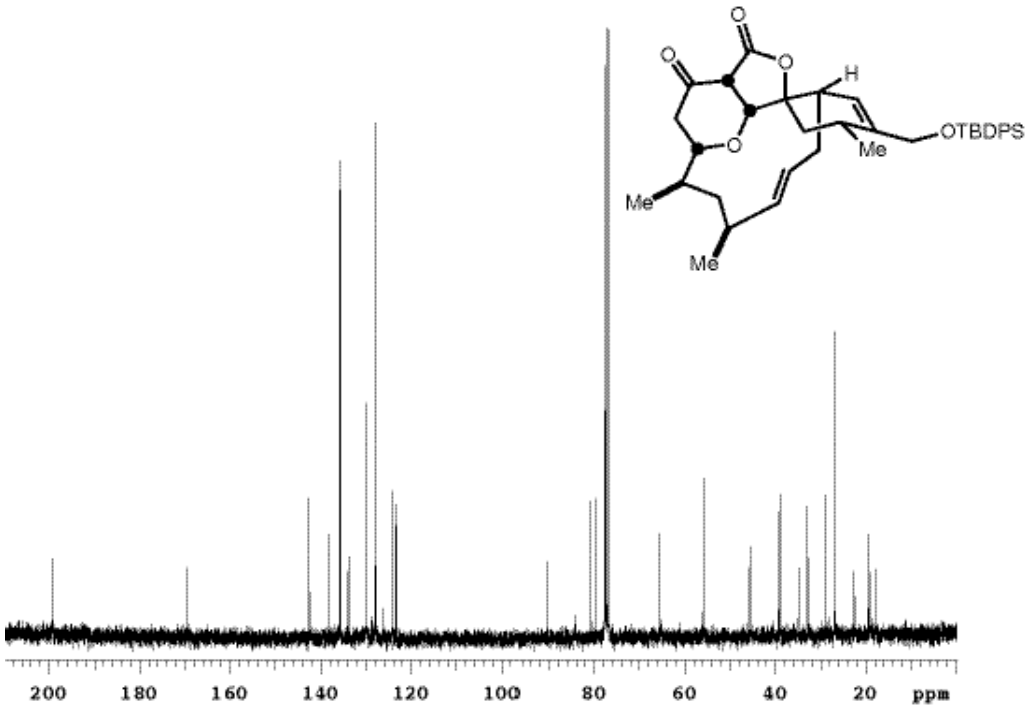
O
O
O
O
H
OTBDPS
Me
Me
Me
200
180
160
140
120
100
80
60
40
20
ppm

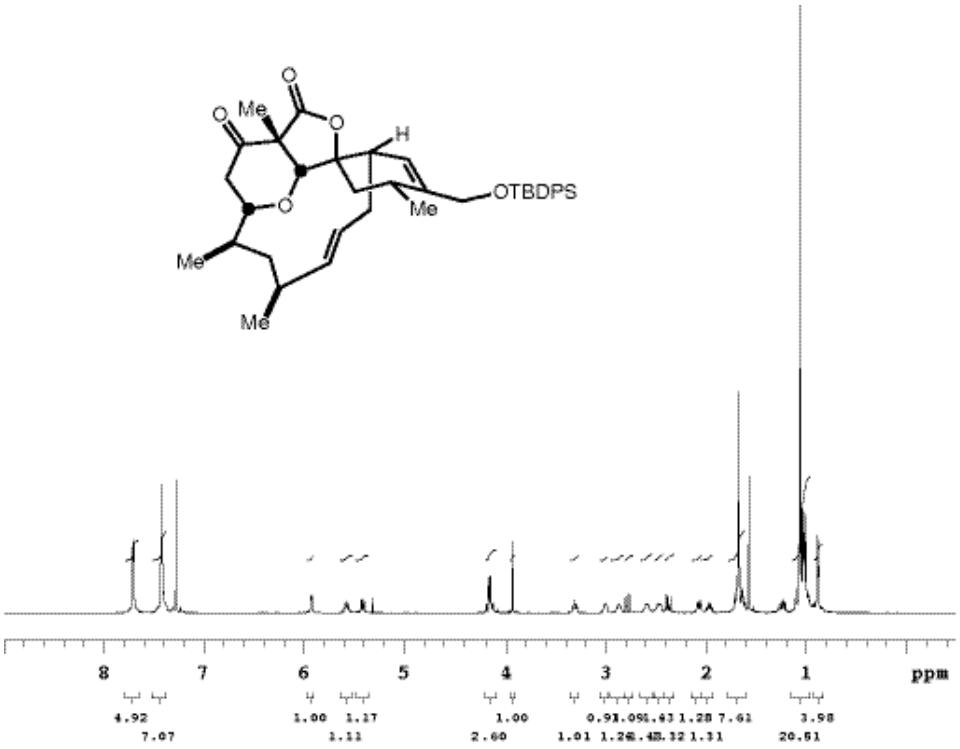
Me
O
O
O
H
OTBDPS
Me
Me
Me
8
7
6
5
4
3
2
1
ppm
4.92
7.07
1.00
1.17
1.11
1.00
2.60
0.91
0.95
1.01
1.28
1.43
1.32
1.28
1.31
7.61
3.98
20.61

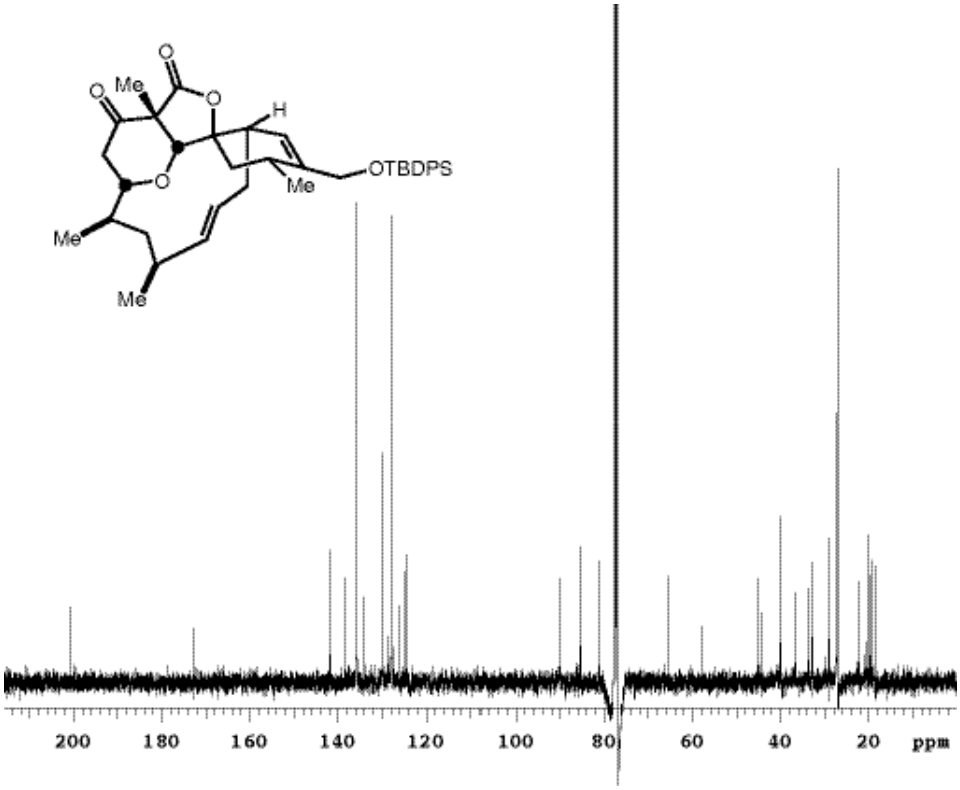
Me
O
O
O
H
OTBDPS
Me
Me
Me
200
180
160
140
120
100
80
60
40
20
ppm

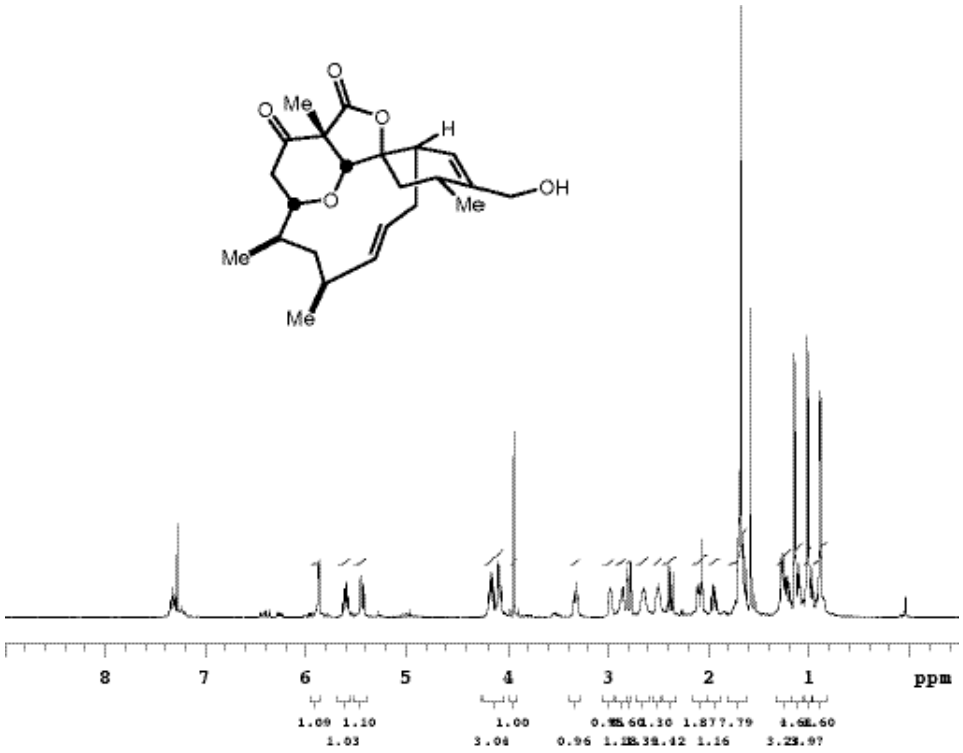
Me
O
O
O
H
OH
Me
Me
Me
8
7
6
5
4
3
2
1
ppm

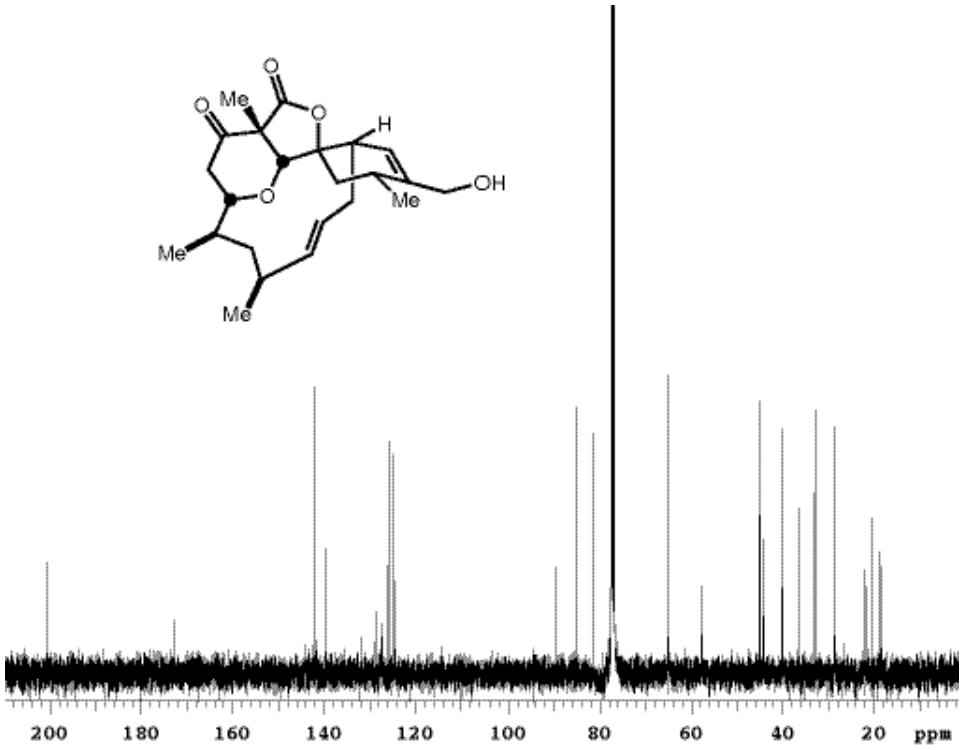
Me
O
O
O
H
OH
Me
Me
Me
200
180
160
140
120
100
80
60
40
20
ppm

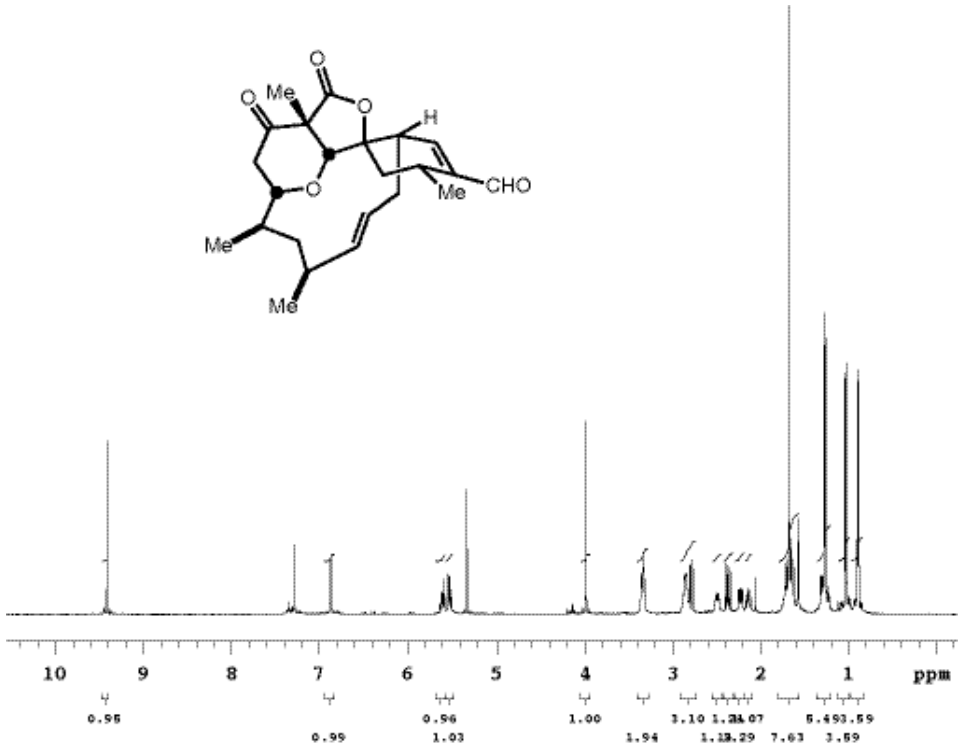
O
Me
O
O
H
O
Me
CHO
Me
Me
10
9
8
7
6
5
4
3
2
1
ppm
0.95
0.99
0.96
1.03
1.00
1.94
3.10
1.07
7.63
3.59

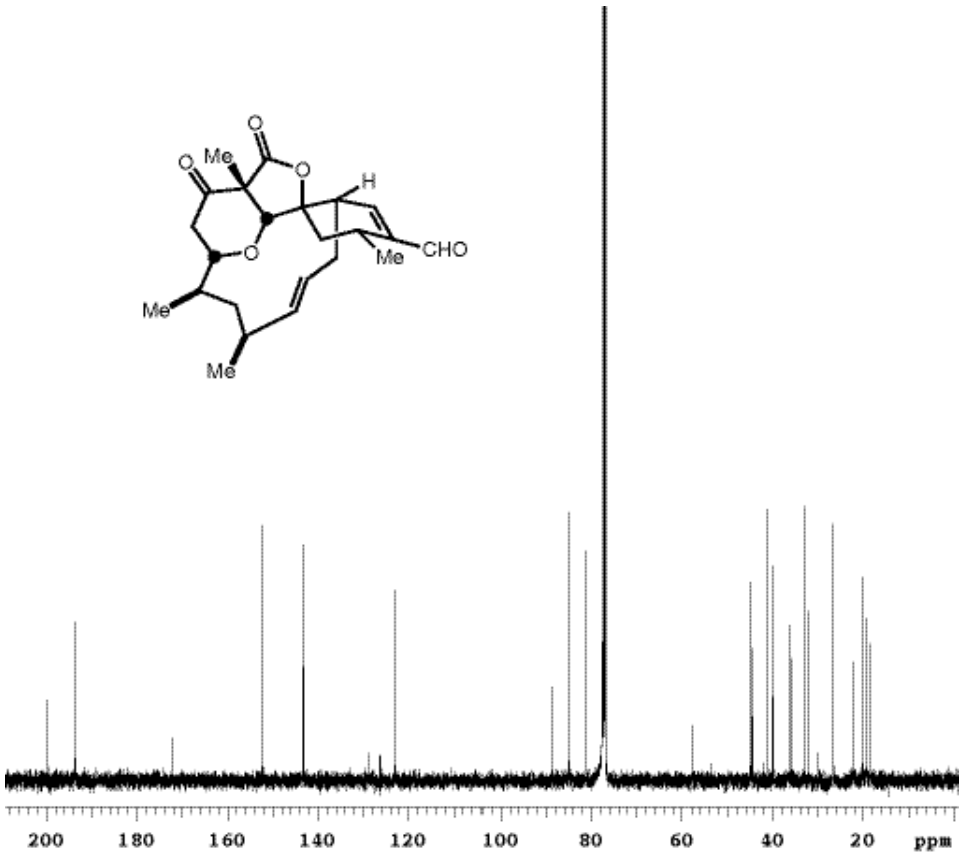
O
Me
O
O
H
O
Me
CHO
Me
Me
200
180
160
140
120
100
80
60
40
20
ppm

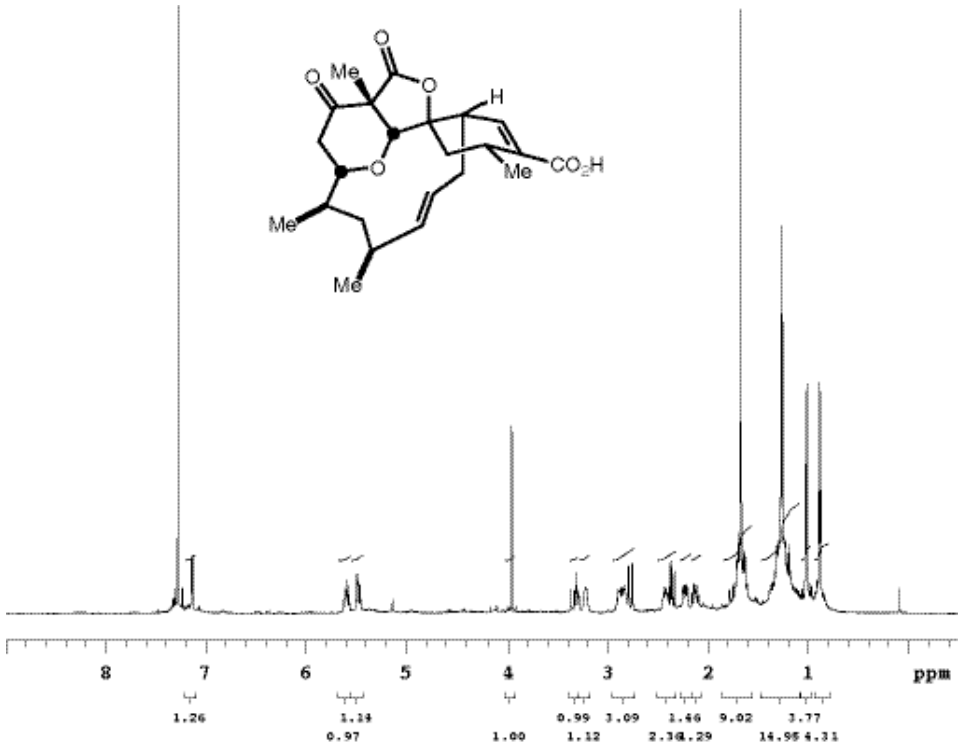
Me
O
O
O
H
O
Me
CO2H
Me
Me
8
7
6
5
4
3
2
1
ppm
1.26
1.14
0.97
1.00
0.99
3.09
1.12
1.46
9.02
3.77
14.95
4.31

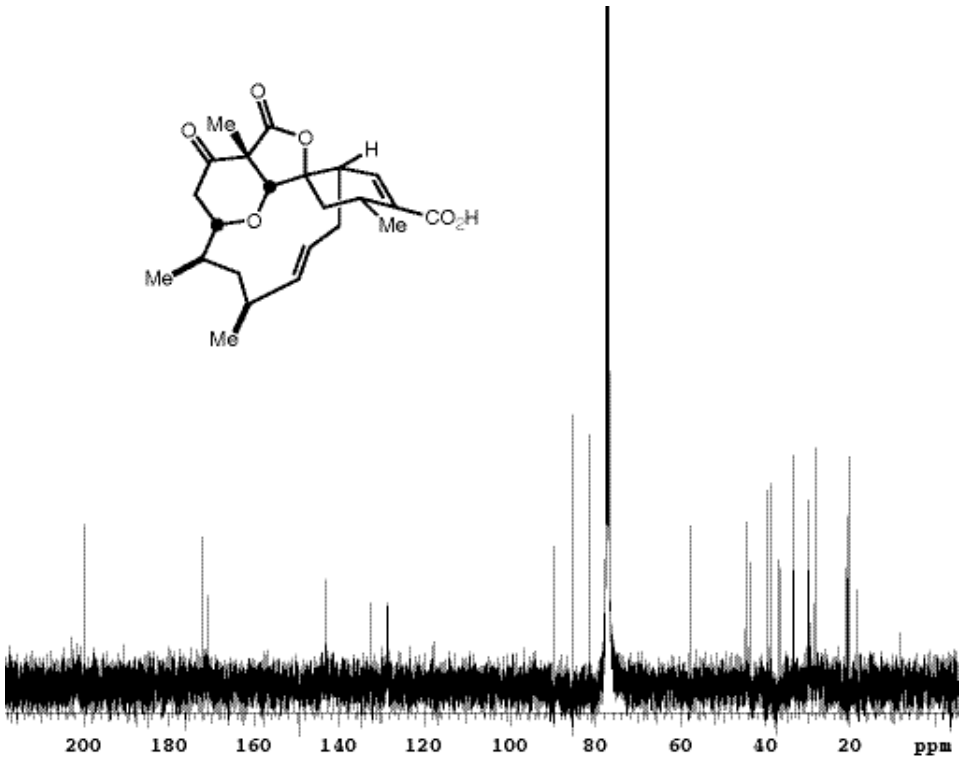
Me
O
O
O
H
O
Me
CO2H
Me
Me
200
180
160
140
120
100
80
60
40
20
ppm

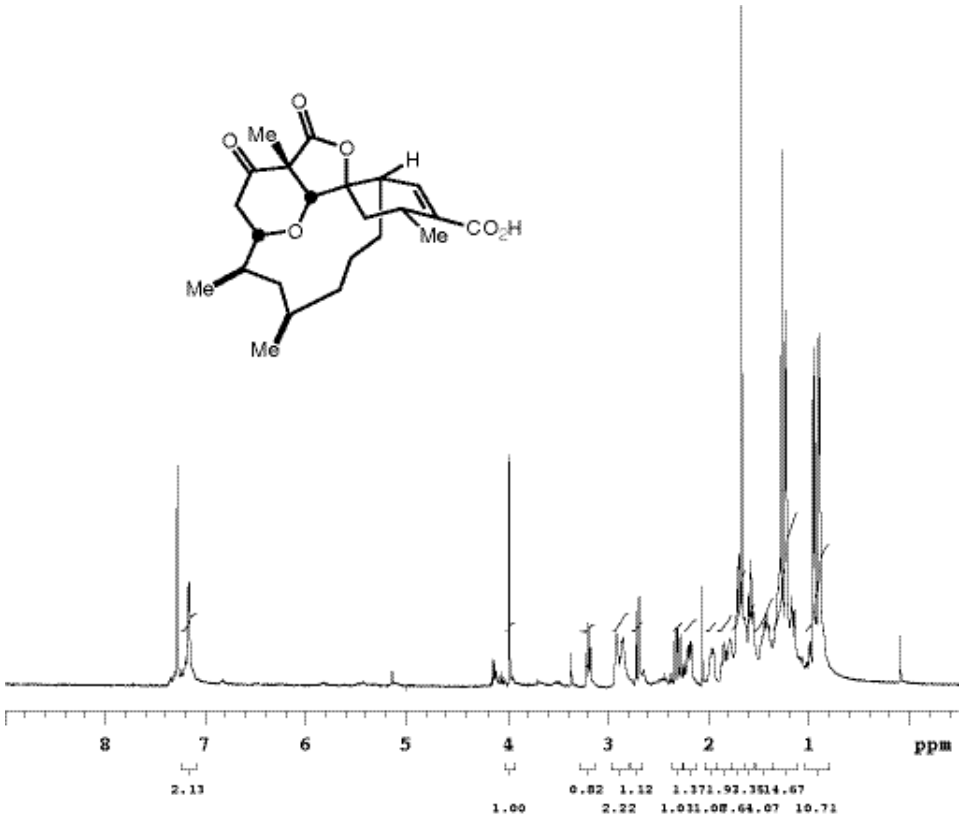
Me
O
O
O
H
Me
CO2H
Me
Me
8
7
6
5
4
3
2
1
ppm
2.13
1.00
0.82
1.12
2.22
1.37
1.93
3.61
4.67
1.03
1.08
4.64
4.07
10.71

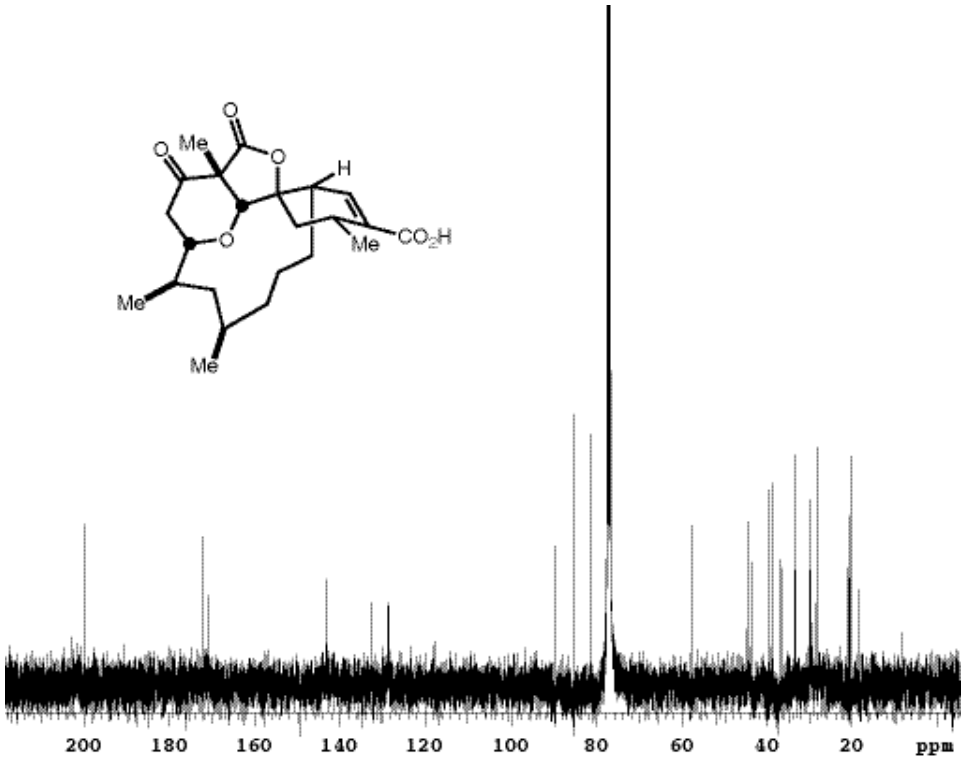
Me
O
O
O
H
Me
CO2H
Me
Me
200
180
160
140
120
100
80
60
40
20
ppm

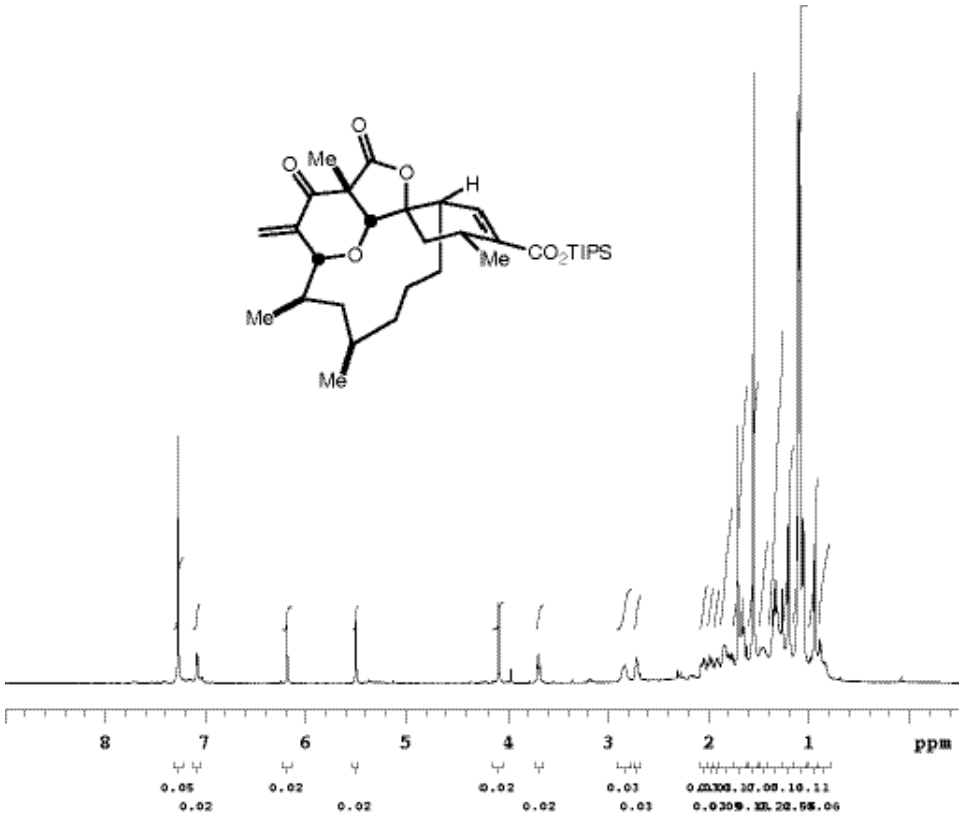
Me
H
Me
CO2TIPS
Me
Me
8
7
6
5
4
3
2
1
ppm

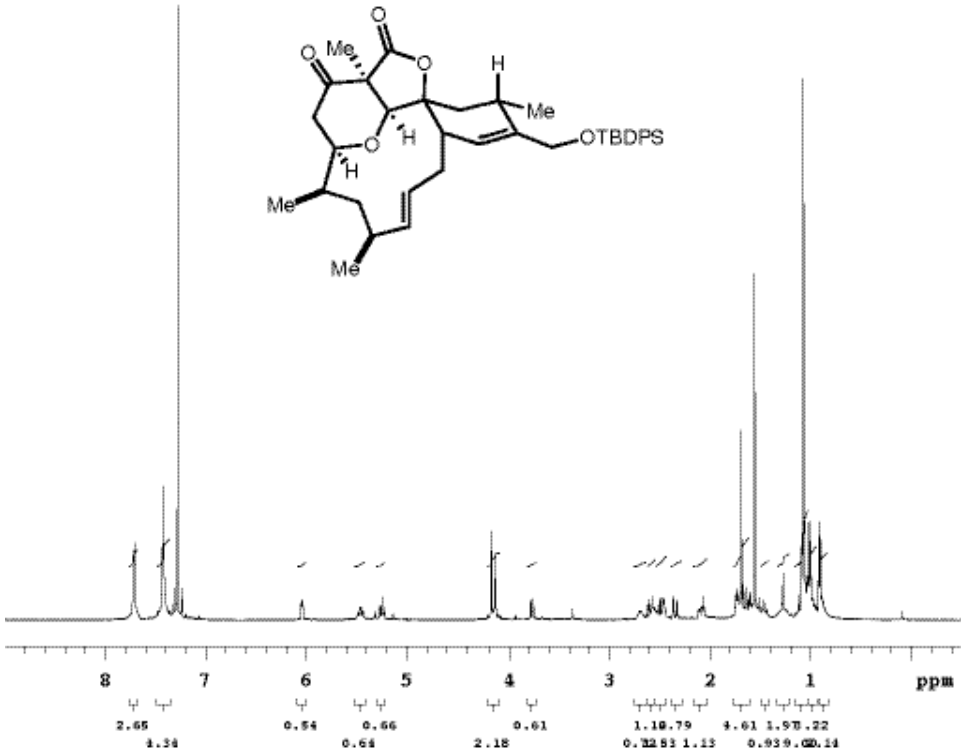
Me
H
Me
OTBDPS
H
Me
Me
8
7
6
5
4
3
2
1
ppm

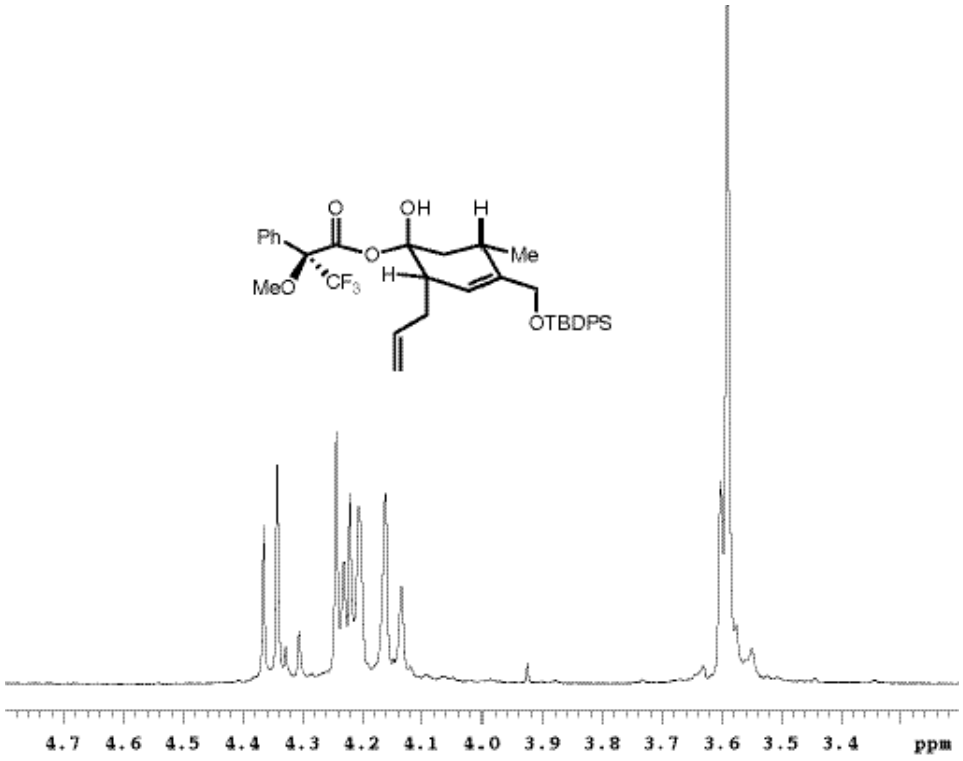
O
OH
H
Ph
O
Me
MeO
CF3
H
OTBDPS
4.7 4.6 4.5 4.4 4.3 4.2 4.1 4.0 3.9 3.8 3.7 3.6 3.5 3.4 ppm

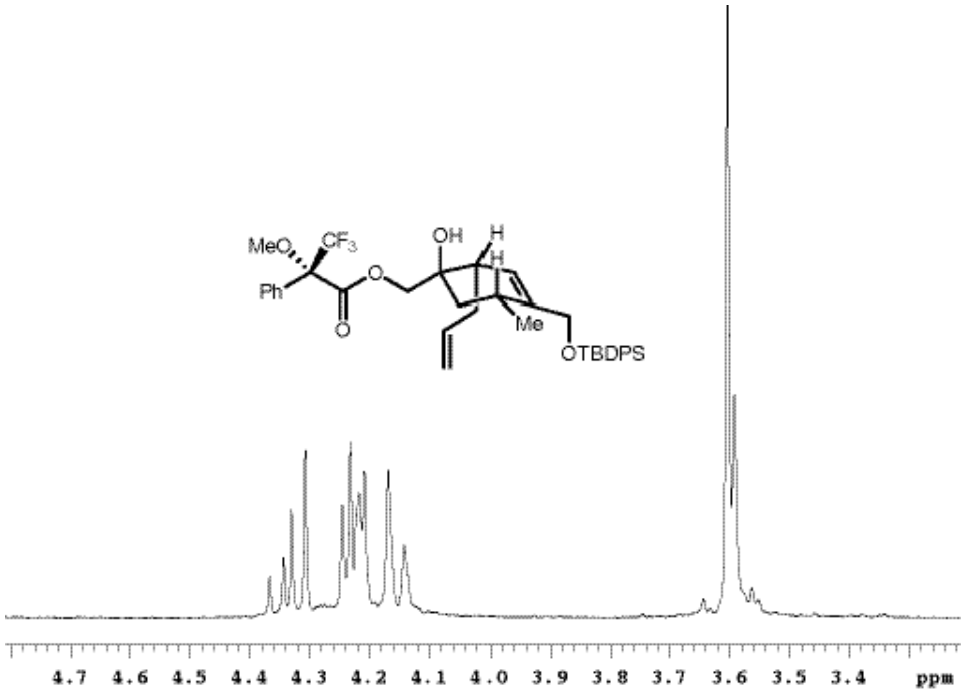
MeO
CF3
OH
H
H
Ph
O
O
Me
OTBDPS
4.7 4.6 4.5 4.4 4.3 4.2 4.1 4.0 3.9 3.8 3.7 3.6 3.5 3.4 ppm

References:

(1) Newman, D. J.; Cragg, G. M.; Snader, K. M. *Journal of Natural Products* **2003**, *66*, 1022-1037.

(2) Schreiber, S. L. *Bioorganic & Medicinal Chemistry* **1998**, *6*, 1127-1152.

(3) Hung, D. T.; Jamison, T. F.; Schreiber, S. L. *Chemistry & Biology* **1996**, *3*, 623-639.

(4) Imai, H.; Suzuki, K. I.; Morioka, M.; Numasaki, Y.; Kadota, S.; Nagai, K.; Sato, T.; Iwanami, M.; Saito, T. *Journal of Antibiotics* **1987**, *40*, 1475-1482.

(5) Imai, H.; Suzuki, K.; Morioka, M.; Numasaki, Y.; Kaniwa, H.; Fujita, S.; Iwanami, M.; Saito, T. *Journal of Pharmaceutical Sciences* **1987**, *76*, S199-S199.

(6) Nakai, R.; Kakita, S.; Asai, A.; Chiba, S.; Akinaga, S.; Mizukami, T.; Yamashita, Y. *Journal of Antibiotics* **2001**, *54*, 836-839.

(7) Zografos, A. L.; Georgiadis, D. *Synthesis-Stuttgart* **2006**, 3157-3188.

(8) Kellersc.W; Muntwyle.R; Pache, W.; Zahner, H. *Helv. Chim. Acta* **1969**, *52*, 127-&.

(9) Ireland, R. E.; Thompson, W. J. *J. Org. Chem.* **1979**, *44*, 3041-3052.

(10) Takeda, K.; Igarashi, Y.; Okazaki, K.; Yoshii, E.; Yamaguchi, K. *J. Org. Chem.* **1990**, *55*, 3431-3434.

(11) Roush, W. R.; Sciotti, R. J. *J. Am. Chem. Soc.* **1998**, *120*, 7411-7419.

(12) Kusumi, T.; Ichikawa, A.; Kakisawa, H.; Tsunakawa, M.; Konishi, M.; Oki, T. *J. Am. Chem. Soc.* **1991**, *113*, 8947-8948.

(13) Kusumi, T.; Ichikawa, A.; Kakisawa, H.; Tsunakawa, M.; Konishi, M.; Oki, T. *Abstracts of Papers of the American Chemical Society* **1992**, *203*, 370-ORGN.

(14) Roush, W. R.; Barda, D. A. *Tetrahedron Lett.* **1997**, *38*, 8781-8784.

(15) Roush, W. R.; Barda, D. A. *Tetrahedron Lett.* **1997**, *38*, 8785-8788.

(16) Roush, W. R.; Barda, D. A. *J. Am. Chem. Soc.* **1997**, *119*, 7402-7403.

(17) Roush, W. R.; Barda, D. A. *Org. Lett.* **2002**, *4*, 1539-1542.

(18) Roush, W. R.; Barda, D. A.; Limberakis, C.; Kunz, R. K. *Tetrahedron* **2002**, *58*, 6433-6454.

(19) Bister, B.; Bischoff, D.; Strobele, M.; Riedlinger, J.; Reicke, A.; Wolter, F.; Bull, A. T.; Zahner, H.; Fiedler, H. P.; Sussmuth, R. D. *Angew. Chem. Int. Ed.* **2004**, *43*, 2574-2576.

(20) Zapf, C. W.; Harrison, B. A.; Drahl, C.; Sorensen, E. J. *Angew. Chem. Int. Ed.* **2005**, *44*, 6533-6537.

(21) Zapf, C. W.; Harrison, B. A.; Drahl, C.; Sorensen, E. J. *Abstracts of Papers of the American Chemical Society* **2005**, *230*, U3149-U3150.

(22) Snider, B. B.; Zou, Y. F. *Org. Lett.* **2005**, *7*, 4939-4941.

(23) Couladouros, E. A.; Bouzas, E. A.; Magos, A. D. *Tetrahedron* **2006**, *62*, 5272-5279.

(24) Nicolaou, K. C.; Harrison, S. T. *J. Am. Chem. Soc.* **2007**, *129*, 429-440.

(25) Staunton, J.; Weissman, K. J. *Nat Prod Rep* **2001**, *18*, 380-416.

(26) Imai, H.; Nakagawa, A.; Omura, S. *Journal of Antibiotics* **1989**, *42*, 1321-1323.

(27) Jia, X. Y.; Tian, Z. H.; Shao, L.; Qu, X. D.; Zhao, Q. F.; Tang, J.; Tang, G. L.; Liu, W. *Chemistry & Biology* **2006**, *13*, 575-585.

(28) Oikawa, H. *Bulletin of the Chemical Society of Japan* **2005**, *78*, 537-554.

(29) Nakai, R.; Ishida, H.; Asai, A.; Ogawa, H.; Yamamoto, Y.; Kawasaki, H.; Akinaga, S.; Mizukami, T.; Yamashita, Y. *Chemistry & Biology* **2006**, *13*, 183-190.

(30) Drahl, C.; Cravatt, B. F.; Sorensen, E. J. *Angew. Chem. Int. Ed.* **2005**, *44*, 5788-5809.

(31) Hanahan, D.; Weinberg, R. A. *Cell* **2000**, *100*, 57-70.

(32) Rezler, E. M.; Bearss, D. J.; Hurley, L. H. *Current Opinion in Pharmacology* **2002**, *2*, 415-423.

(33) Shay, J. W.; Wright, W. E. *Nature Reviews Drug Discovery* **2006**, *5*, 577-584.

(34) White, L. K.; Wright, W. E.; Shay, J. W. *Trends in Biotechnology* **2001**, *19*, 114-120.

(35) Takeda, K.; Shimotani, A.; Yoshii, E.; Yamaguchi, K. *Heterocycles* **1992**, *34*, 2259-2261.

(36) Yamaguchi, K.; Takeda, K.; Shimotani, A.; Yoshii, E. *Acta Crystallogr C* **1993**, *49*, 1680-1683.

(37) Boulet, S. L.; Paquette, L. A. *Synthesis* **2002**, 895-900.

(38) Paquette, L. A.; Boulet, S. L. *Synthesis* **2002**, 888-894.

(39) Danishefsky, S. J.; Deninno, M. P. *Angew. Chem. Int. Ed.* **1987**, *26*, 15-23.

(40) Nicolaou, K. C.; Snyder, S. A.; Montagnon, T.; Vassilikogiannakis, G. *Angew. Chem. Int. Ed.* **2002**, *41*, 1668-1698.

(41) Elliott, M. C. *J. Chem. Soc., Perkins Trans. 1* **2002**, 2301-2323.

(42) Elliott, M. C.; Williams, E. *J. Chem. Soc., Perkins Trans. 1* **2001**, 2303-2340.

(43) Evans, D. A.; Starr, J. T. *Angew. Chem. Int. Ed.* **2002**, *41*, 1787-+.

(44) Evans, D. A.; Starr, J. T. *J. Am. Chem. Soc.* **2003**, *125*, 13531-13540.

(45) Vosburg, D. A.; Vanderwal, C. D.; Sorensen, E. J. *J. Am. Chem. Soc.* **2002**, *124*, 4552-4553.

(46) Liu, P.; Jacobsen, E. N. *J. Am. Chem. Soc.* **2001**, *123*, 10772-10773.

(47) Mikami, K.; Motoyama, Y.; Terada, M. *J. Am. Chem. Soc.* **1994**, *116*, 2812-2820.

(48) Keck, G. E.; Li, X. Y.; Krishnamurthy, D. *J. Org. Chem.* **1995**, *60*, 5998-5999.

(49) Joly, G. D.; Jacobsen, E. N. *Org. Lett.* **2002**, *4*, 1795-1798.

(50) Dossetter, A. G.; Jamison, T. F.; Jacobsen, E. N. *Angew. Chem. Int. Ed.* **1999**, *38*, 2398-2400.

(51) Yamashita, Y.; Saito, S.; Ishitani, H.; Kobayashi, S. *Org. Lett.* **2002**, *4*, 1221-1223.

(52) Doyle, M. P.; Phillips, I. M.; Hu, W. H. *J. Am. Chem. Soc.* **2001**, *123*, 5366-5367.

(53) Unni, A. K.; Takenaka, N.; Yamamoto, H.; Rawal, V. H. *J. Am. Chem. Soc.* **2005**, *127*, 1336-1337.

(54) Adams, D. R.; Bhatnagar, S. P. *Synthesis* **1977**, 661-672.

(55) Lolkema, L. D. M.; Semeyn, C.; Ashek, L.; Hiemstra, H.; Speckamp, W. N. *Tetrahedron* **1994**, *50*, 7129-7140.

(56) Crosby, S. R.; Harding, J. R.; King, C. D.; Parker, G. D.; Willis, C. L. *Org. Lett.* **2002**, *4*, 577-580.

(57) Rychnovsky, S. D.; Marumoto, S.; Jaber, J. J. *Org. Lett.* **2001**, *3*, 3815-3818.

(58) Roush, W. R.; Dilley, G. J. *Synlett* **2001**, 955-959.

(59) Cloninger, M. J.; Overman, L. E. *J. Am. Chem. Soc.* **1999**, *121*, 1092-1093.

(60) Semeyn, C.; Blaauw, R. H.; Hiemstra, H.; Speckamp, W. N. *J. Org. Chem.* **1997**, *62*, 3426-3427.

(61) Marko, I. E.; Dumeunier, R.; Leclercq, C.; Leroy, B.; Plancher, J. M.; Mekhalfia, A.; Bayston, D. J. *Synthesis* **2002**, 958-972.

(62) Keck, G. E.; Covel, J. A.; Schiff, T.; Yu, T. *Org. Lett.* **2002**, *4*, 1189-1192.

(63) Huang, H. B.; Panek, J. S. *Org. Lett.* **2001**, *3*, 1693-1696.

(64) Huang, H. B.; Panek, J. S. *J. Am. Chem. Soc.* **2000**, *122*, 9836-9837.

(65) Zhang, W. C.; Li, C. J. *Tetrahedron* **2000**, *56*, 2403-2411.

(66) Jaber, J. J.; Mitsui, K.; Rychnovsky, S. D. *J. Org. Chem.* **2001**, *66*, 4679-4686.

(67) Jasti, R.; Vitale, J.; Rychnovsky, S. D. *J. Am. Chem. Soc.* **2004**, *126*, 9904-9905.

(68) Kopecky, D. J.; Rychnovsky, S. D. *J. Am. Chem. Soc.* **2001**, *123*, 8420-8421.

(69) Aubele, D. L.; Wan, S. Y.; Floreancig, P. E. *Angew. Chem. Int. Ed.* **2005**, *44*, 3485-3488.

(70) Petasis, N. A.; Lu, S. P. *Tetrahedron Lett.* **1996**, *37*, 141-144.

(71) Smith, A. B.; Minbiole, K. P.; Verhoest, P. R.; Schelhaas, M. *J. Am. Chem. Soc.* **2001**, *123*, 10942-10953.

(72) Smith, A. B.; Safonov, I. G.; Corbett, R. M. *J. Am. Chem. Soc.* **2002**, *124*, 11102-11113.

(73) Smith, A. B.; Mesaros, E. F.; Meyer, E. A. *J. Am. Chem. Soc.* **2005**, *127*, 6948-6949.

(74) Kageyama, M.; Tamura, T.; Nantz, M. H.; Roberts, J. C.; Somfai, P.; Whritenour, D. C.; Masamune, S. *J. Am. Chem. Soc.* **1990**, *112*, 7407-7408.

(75) Evans, D. A.; Bender, S. L.; Morris, J. *J. Am. Chem. Soc.* **1988**, *110*, 2506-2526.

(76) Blakemore, P. R.; Browder, C. C.; Hong, J.; Lincoln, C. M.; Nagornyy, P. A.; Robarge, L. A.; Wardrop, D. J.; White, J. D. *J. Org. Chem.* **2005**, *70*, 5449-5460.

(77) Hilli, F.; White, J. M.; Rizzacasa, M. A. *Org. Lett.* **2004**, *6*, 1289-1292.

(78) Hilli, F.; White, J. M.; Rizzacasa, M. A. *Tetrahedron Lett.* **2002**, *43*, 8507-8510.

(79) Clemens, R. J.; Hyatt, J. A. *J. Org. Chem.* **1985**, *50*, 2431-2435.

(80) Boeckman, R. K.; Perni, R. B.; Macdonald, J. E.; Thomas, A. J. *Org. Syn.* **1988**, *66*, 194-202.

(81) Dess, D. B.; Martin, J. C. *J. Am. Chem. Soc.* **1991**, *113*, 7277-7287.

(82) Ley, S. V.; Norman, J.; Griffith, W. P.; Marsden, S. P. *Synthesis* **1994**, 639-666.

(83) Huang, S. L.; Omura, K.; Swern, D. *J. Org. Chem.* **1976**, *41*, 3329-3331.

(84) Parikh, J. R.; Doering, W. V. E. *J. Am. Chem. Soc.* **1967**, *89*, 5505-&.

(85) Hayashi, M.; Yoshiga, T.; Nakatani, K.; Ono, K.; Oguni, N. *Tetrahedron* **1994**, *50*, 2821-2830.

(86) Noyori, R.; Nishida, I.; Sakata, J.; Nishizawa, M. *J. Am. Chem. Soc.* **1980**, *102*, 1223-1225.

(87) Sabitha, G.; Reddy, G. S. K. K.; Rajkumar, M.; Yadav, J. S.; Ramakrishna, K. V. S.; Kunwar, A. C. *Tetrahedron Lett.* **2003**, *44*, 7455-7457.

(88) Clarke, P. A.; Martin, W. H. C. *Org. Lett.* **2002**, *4*, 4527-4529.

(89) Olah, G. A.; Narang, S. C. *Tetrahedron* **1982**, *38*, 2225-2277.

(90) Matsuda, T.; Tanino, K.; Kuwajima, I. *Tetrahedron Lett.* **1989**, *30*, 4267-4270.

(91) Kobayashi, S.; Hachiya, I. *J. Org. Chem.* **1994**, *59*, 3590-3596.

(92) Kobayashi, S.; Sugiura, M.; Kitagawa, H.; Lam, W. W. L. *Chem. Rev.* **2002**, *102*, 2227-2302.

(93) Kobayashi, S.; Hachiya, I.; Ishitani, H.; Araki, M. *Synlett* **1993**, 472-474.

(94) Kajiro, H.; Mitamura, S.; Mori, A.; Hiyama, T. *Bulletin of the Chemical Society of Japan* **1999**, *72*, 1553-1560.

(95) Ishihara, K.; Kubota, M.; Kurihara, H.; Yamamoto, H. *J. Am. Chem. Soc.* **1995**, *117*, 4413-4414.

(96) Teerhuis, N. M.; Hiemstra, H.; Speckamp, W. N. *Tetrahedron Lett.* **1997**, *38*, 159-162.

(97) Teerhuis, N. M.; Hiemstra, H.; Speckamp, W. N. *Tetrahedron Lett.* **1997**, *38*, 155-158.

(98) Morris, W. J.; Custar, D. W.; Scheidt, K. A. *Org. Lett.* **2005**, *7*, 1113-1116.

(99) Ben, A.; Yamauchi, T.; Matsumoto, T.; Suzuki, K. *Synlett* **2004**, 225-230.

(100) Orru, R. V. A.; de Greef, M. *Synthesis* **2003**, 1471-1499.

(101) Burke, M. D.; Schreiber, S. L. *Angew. Chem. Int. Ed.* **2004**, *43*, 46-58.

(102) Myers, A. G.; Yang, B. H.; Chen, H.; Kopecky, D. J. *Synlett* **1997**, 457-&.

(103) Myers, A. G.; Yang, B. H.; Chen, H.; McKinstry, L.; Kopecky, D. J.; Gleason, J. L. *J. Am. Chem. Soc.* **1997**, *119*, 6496-6511.

(104) Larcheveque, M.; Ignatova, E.; Cuvigny, T. *J. Organomet. Chem.* **1979**, *177*, 5-15.

(105) Larcheveque, M.; Ignatova, E.; Cuvigny, T. *Tetrahedron Lett.* **1978**, 3961-3964.

(106) Myers, A. G.; Yang, B. H.; Kopecky, D. J. *Tetrahedron Lett.* **1996**, *37*, 3623-3626.

(107) Kruger, J.; Carreira, E. M. *J. Am. Chem. Soc.* **1998**, *120*, 837-838.

(108) Zhang, W. J.; Robins, M. J. *Tetrahedron Lett.* **1992**, *33*, 1177-1180.

(109) Grieco, P. A.; Gilman, S.; Nishizawa, M. *J. Org. Chem.* **1976**, *41*, 1485-1486.

(110) Taber, D. F.; Christos, T. E.; Rahimizadeh, M.; Chen, B. *J. Org. Chem.* **2001**, *66*, 5911-5914.

(111) Taber, D. F.; Meagley, R. P. *Tetrahedron Lett.* **1994**, *35*, 7909-7910.

(112) Taber, D. F.; Meagley, R. P.; Doren, D. J. *J. Org. Chem.* **1996**, *61*, 5723-5728.

(113) Taber, D. F.; Walter, R.; Meagley, R. P. *J. Org. Chem.* **1994**, *59*, 6014-6017.

(114) Ohira, S.; Ida, T.; Moritani, M.; Hasegawa, T. *J. Chem. Soc., Perkins Trans. 1* **1998**, 293-297.

(115) Peterson, D. J. *J. Org. Chem.* **1968**, *33*, 780-&.

(116) Lipshutz, B. H.; Hackmann, C. *J. Org. Chem.* **1994**, *59*, 7437-7444.

(117) Cramer, R. *J. Am. Chem. Soc.* **1967**, *89*, 1633-&.

(118) Cramer, R. *J. Am. Chem. Soc.* **1966**, *88*, 2272-&.

(119) Barda, D. A.; Roush, W. R. *Abstracts of Papers of the American Chemical Society* **1996**, *211*, 441-ORGN.

(120) Qi, J.; Roush, W. R. *Org. Lett.* **2006**, *8*, 2795-2798.

(121) Roush, W. R.; Brown, B. B. *Tetrahedron Lett.* **1989**, *30*, 7309-7312.

(122) Rubottom, G. M.; Vazquez, M. A.; Pelegrin.Dr *Tetrahedron Lett.* **1974**, 4319-4322.

(123) Schwartz, J.; Labinger, J. A. *Angew. Chem. Int. Ed.* **1976**, *15*, 333-340.

(124) Williams, J. M.; Jobson, R. B.; Yasuda, N.; Marchesini, G.; Dolling, U. H.; Grabowski, E. J. J. *Tetrahedron Lett.* **1995**, *36*, 5461-5464.

(125) Maryanoff, B. E.; Reitz, A. B. *Chem. Rev.* **1989**, *89*, 863-927.

(126) Vedejs, E.; Cabaj, J.; Peterson, M. J. *J. Org. Chem.* **1993**, *58*, 6509-6512.

(127) Oppolzer, W.; Chapuis, C.; Bernardinelli, G. *Helv. Chim. Acta* **1984**, *67*, 1397-1401.

(128) Oppolzer, W.; Rodriguez, I.; Blagg, J.; Bernardinelli, G. *Helv. Chim. Acta* **1989**, *72*, 123-130.

(129) Witzeman, J. S.; Nottingham, W. D. *J. Org. Chem.* **1991**, *56*, 1713-1718.

(130) Witzeman, J. S. *Tetrahedron Lett.* **1990**, *31*, 1401-1404.

(131) Roush, W. R.; Brown, B. B. *J. Org. Chem.* **1993**, *58*, 2162-2172.

(132) Roush, W. R.; Brown, B. B. *J. Org. Chem.* **1993**, *58*, 2151-2161.

(133) Jacobsen, E. N.; Taylor, M. S. *Abstracts of Papers of the American Chemical Society* **2006**, *231*, -.

(134) Reiter, M.; Turner, H.; Gouverneur, V. *Chem. Eur. J.* **2006**, *12*, 7190-7203.

(135) Reiter, M.; Turner, H.; Mills-Webb, R.; Gouverneur, V. *J. Org. Chem.* **2005**, *70*, 8478-8485.

(136) Jung, H. H.; Floreancig, P. E. *Org. Lett.* **2006**, *8*, 1949-1951.

(137) Rendler, S.; Oestreich, M. *Synthesis* **2005**, 1727-1747.

(138) Chuit, C.; Corriu, R. J. P.; Reye, C.; Young, J. C. *Chem. Rev.* **1993**, *93*, 1371-1448.

(139) Scheidt, K. A.; Chen, H.; Follows, B. C.; Chemler, S. R.; Coffey, D. S.; Roush, W. R. *J. Org. Chem.* **1998**, *63*, 6436-6437.

(140) Noyori, R.; Nishida, I.; Sakata, J. *J. Am. Chem. Soc.* **1983**, *105*, 1598-1608.

(141) Noyori, R.; Nishida, I.; Sakata, J. *Tetrahedron Lett.* **1980**, *21*, 2085-2088.

(142) Grubbs, R. H. *Angew. Chem. Int. Ed.* **2006**, *45*, 3760-3765.

(143) Grubbs, R. H.; Chang, S. *Tetrahedron* **1998**, *54*, 4413-4450.

(144) Grubbs, R. H.; Miller, S. J.; Fu, G. C. *Acc. Chem. Res.* **1995**, *28*, 446-452.

(145) Kingsbury, J. S.; Harrity, J. P. A.; Bonitatebus, P. J.; Hoveyda, A. H. *J. Am. Chem. Soc.* **1999**, *121*, 791-799.

(146) Lindgren, B. O.; Nilsson, T. *Acta Chemica Scandinavica* **1973**, *27*, 888-890.

(147) Salomon, C. J.; Mata, E. G.; Mascaretti, O. A. *Tetrahedron* **1993**, *49*, 3691-3734.

(148) Schreibe.J; Maag, H.; Hashimot.N; Eschenmo.A *Angew. Chem. Int. Ed.* **1971**, *10*, 330-&.

(149) Chenard, B. L.; Laganis, E. D. *Abstracts of Papers of the American Chemical Society* **1985**, *189*, 221-ORGN.

(150) O'malley, S. J.; Tan, K. L.; Watzke, A.; Bergman, R. G.; Ellman, J. A. *J. Am. Chem. Soc.* **2005**, *127*, 13496-13497.

(151) Nicolaou, K. C.; Estrada, A. A.; Zak, M.; Lee, S. H.; Safina, B. S. *Angew. Chem. Int. Ed.* **2005**, *44*, 1378-1382.

(152) Jarowicki, K.; Kocienski, P. *J. Chem. Soc., Perkins Trans. 1* **1998**, 4005-4037.

(153) Knowles, W. S. *Adv. Synth. Catal.* **2003**, *345*, 3-13.

(154) Hornfeld.Ab; Gronowit.Js; Gronowit.S *Acta Chemica Scandinavica* **1968**, *22*, 2725-&.

(155) Ireland, R. E.; Bey, P. *Org. Syn.* **1988**, *50-9*, 459-460.

(156) Vandenheuvel, F. A. *Analytical Chemistry* **1956**, *28*, 362-365.

(157) Kitahara, T.; Kurata, H.; Matsuoka, T.; Mori, K. *Tetrahedron* **1985**, *41*, 5475-5485.

(158) Imada, Y.; Iida, H.; Naota, T. *J. Am. Chem. Soc.* **2005**, *127*, 14544-14545.

(159) Corey, E. J.; Pasto, D. J.; Mock, W. L. *J. Am. Chem. Soc.* **1961**, *83*, 2957-&.

(160) Corey, E. J.; Mock, W. L.; Pasto, D. J. *Tetrahedron Lett.* **1961**, 347-352.

(161) Danishefsky, S.; Kitahara, T.; Mckee, R.; Schuda, P. F. *J. Am. Chem. Soc.* **1976**, *98*, 6715-6717.

(162) Gras, J. L. *Org. Syn.* **1981**, *60*, 88-91.

(163) Harmon, A. D.; Hutchinson, C. R. *J. Org. Chem.* **1975**, *40*, 3474-3480.

(164) Hon, Y. S.; Hsieh, C. H. *Tetrahedron* **2006**, *62*, 9713-9717.

(165) Kraus, G. A.; Kim, J. *Synthesis* **2004**, 1737-1738.

(166) Nicolaou, K. C.; Rutjes, F. P. J. T.; Theodorakis, E. A.; Tiebes, J.; Sato, M.; Untersteller, E. *J. Am. Chem. Soc.* **1995**, *117*, 1173-1174.

(167) Peters, H. M.; Feigl, D. M.; Mosher, H. S. *J. Org. Chem.* **1968**, *33*, 4245-&.

(168) Denmark, S. E.; Beutner, G. L.; Wynn, T.; Eastgate, M. D. *J. Am. Chem. Soc.* **2005**, *127*, 3774-3789.